Physics Area - Ph.D. course in Astroparticle Physics

SISSA, Trieste

Beyond Lorentz invariance: a journey from Analogue to Hořava Gravity

SUPERVISOR:
Stefano Liberati

CANDIDATE:
Francesco Del Porro

ACADEMIC YEAR 2023/2024

If your theory is found to be against the second law of thermodynamics I can give you no hope; there is nothing for it but to collapse in deepest humiliation.

— Sir Arthur Eddington

Declaration

I hereby declare that, except where specific reference is made to the work of others, the contents of this thesis are original and have not been submitted in whole or in part for consideration for any other degree or qualification in this, or any other university.

The discussion is based on the following works:

- F. Del Porro, S. Liberati, M. Schneider, "Tunneling method for Hawking quanta in analogue gravity", ArXiv: 2406.14603 [gr-qc], (Jun 20, 2024)
- F. Del Porro, S. Liberati, M. Schneider, "Rescuing the Unruh Effect in Lorentz Violating Gravity", ArXiv: 2312.03070 [gr-qc], (Dec 5, 2023)
- F. Del Porro, M. Herrero-Valea, S. Liberati, M. Schneider, "Hawking Radiation in Lorentz Violating Gravity: A Tale of Two Horizons", *JHEP* 12 (2023) 094, ArXiv: 2310.01472 [gr-qc], (Oct 2, 2023)
- M. Schneider, F. Del Porro, M. Herrero-Valea, S. Liberati, "On the Resilience of Black Hole Evaporation: Gravitational Tunneling through Universal Horizons", *J.Phys.Conf.Ser.* 2531 (2023) 1, 012013, ArXiv: 2303.14235 [gr-qc], (Mar 24, 2023)
- F. Del Porro, M. Herrero-Valea, S. Liberati, M. Schneider, "Gravitational tunneling in Lorentz violating gravity", *Phys.Rev.D* 106 (2022) 6, 064055, ArXiv: 2207.08848 [gr-qc], (Jul 18, 2022)
- F. Del Porro, M. Herrero-Valea, S. Liberati, M. Schneider, "Time orientability and particle production from universal horizons", *Phys.Rev.D* 105 (2022) 10, 104009, ArXiv: 2201.03584 [gr-qc], (Jan 10, 2022)

Abstract

In this thesis, we explore a scenario in which local Lorentz invariance is broken at high energies. This approach is primarily motivated by the pursuit of a quantum gravity theory, specifically Hořava gravity, where Lorentz violation is introduced so to achieve power-counting renormalizability.

In laboratory settings, Lorentz invariance violations intersect with gravity through analogue models, where the breakdown of Lorentz symmetry is a common feature of quantum perturbations within analogue black hole geometries.

Analogue experiments have successfully measured Hawking radiation, which is anticipated and deserved to remain robust despite the breakdown of Lorentz symmetry.

We begin by revisiting the analogue framework, demonstrating the resilience of the Hawking effect in the presence of Lorentz symmetry breaking.

Subsequently, we apply these insights to Lorentz-violating gravity models, reexamining the concept of black holes and introducing the notion of the universal horizon, a Lorentz-breaking counterpart to the traditional Killing horizon. We investigate how the evaporation of a Hořava gravity black hole reflects an intriguing interplay between universal horizon and the relativistic Killing horizon, highlighting a deeper connection between thermodynamics and gravity that goes beyond Lorentz invariance.

This relationship is further explored in flat spacetimes by investigating the Unruh effect, where we employ a novel construction of the Rindler wedge to demonstrate that the duality between acceleration and gravity remains intact.

Finally, we focus on the ultraviolet aspects of Hořava gravity, assessing its potential as a viable quantum gravity candidate and reviewing the current status in essessing its perturbative renormalizability.

The overall picture that emerges is coherent: on one hand, the proposed quantum gravity theory offers a compelling theoretical appeal due to its renormalizability. On the other, the resulting phenomenology provides intriguing insights into the enduring connection between thermality and gravity.

Acknowledgments

Here we are, at the end of this journey. The time spent writing this thesis, the final act of my PhD, has been an opportunity to look back at the last four years of my life, giving me the chance to take stock of this experience in Trieste, both at the professional and at the personal level.

The acknowledgments, which recently someone (I will not say who) has defined as "the hardest part to write in a PhD thesis", are therefore mandatory. They unavoidably represent a glimpse of what these four years have meant to me, hence I will try to avoid the massive usage of chatGPT that is apparently becoming more and more popular among the community of physicists as a tool for improving the style of the presentations. So, let me apologize in advance with the reader if I yield to some Italian expressions along these few lines.

As a canonical starting point, I want to express my gratitude to my supervisor Stefano Liberati. It is not just about following the etiquette that I mention him first. On the professional side, his patience, guidance, and expertise have made me completely change my approach to physics and, in particular, he has served as a perfect example of how physics cannot be seen as a compartmentalized subject, despite the spread temptation to classify the research under one name or another. On the personal side, and maybe more importantly, I found an incredible person, who I enjoyed discussing with about everything, not always physics-related. Back to the end of the first year, I would redo the same choice all the times.

Then, I want to thank Marc. His support during these years has been fundamental and I think his patience is limitless, given the uncountable number of days that he spent with me at the blackboard (annoying all the people in the common room) trying to figure out how to solve the problems that, almost every day, I have been coming up with, especially in the afternoon, when every respectable German is at home for dinner. Beyond that, I have found an incredible person, and a friend, other than a collaborator.

A big thank goes also to Miriam, a great collaborator without whom my PhD experience would not have been the same. She gave me also the chance to experience Barcellona, in my opinion one of the best cities in the world.

Trieste has been a city that I learned to love, especially in summer, when Barcola offers one of the best sunset that I have ever got the chance to admire. However, my life there would not have been as it was without an amazing group of friends, that shared with me all the beautiful sides of this town. Before naming them, let me take the chance to mention the role of SISSA, a unique school in the world that, thanks to its great environment, gave me the chance to know those people.

So, thanks to my APP mates. Diego, my officemate for four years, has always

been down for stimulating discussions. He shared with me that incredible Follonica-Copertino trip, which memory is part of baggage of Trieste. Vale: now we know how it feels to spend the whole August in an empty city to write the thesis. Daniele, who has given me the honour to play the only well-tuned piano I have ever found in these four years. Vania, that has always been a step forward from me, last but not least in learning Danish.

Moving on, how not to mention Cri. Besides I am becoming more and more convinced that there must be a common root in the way roman people and tuscan ones interact with the others, the friendship between us goes far beyond and I am grateful for that. Thank you my friend, for everything.

Fabi asked me for "at least five lines" in the acknowledgements. I do not know if I will manage to achieve that number in the final version of these acknowledgements (that was, after all, a strongly font-dependent statement). However, if the first thing that comes to my mind while thinking what to type here is Barcola at the golden hour, I think this pictures exactly what memory I will keep with me. Thanks.

During these years, I also had the opportunity to enjoy the musical scene of Trieste. The main credit goes to Jack, incredible guitarist, that captured me and Lodo (romantic flute-player) with his version of "Spain", song that we agreed to play in one of the numerous jam session in Spazzacamino and Round Midnight we played at. Once, we made it: it was terrible[1]. However, that has given me the opportunity to meet Francesco and Federico, with whom we also invaded the music room of the PGT every Tuesday for almost one year. Thank you guys, it has been an honour to play with you.

On this side, I want to mention Max, a hidden musical talent with a musical taste incredibly similar to mine. Defining Max is anyway practically impossible, so let me just thank him reminding that we have still to apologize to the whole world for having destabilized the international equilibrium within a single night.

A big thank goes to Davide, probably the kindest person in the world. Besides being my officemate during the hardest period of a PhD, the postdoc applications, with his incredible experience he has made me discover the passion for exploring the mountains of Friuli. I still remember the first time, walking immersed into half meter of snow. This passion for hiking reminds me also to thank Daniel and Steph, with whom I explored the most emblematic peaks of Tenerife and Haute-Savoie, respectively: thank you, my friends.

Curiously, my acknowledgements for Giulio recall me an event about mountains for which I have no memory but that he remembers very well. Maybe it is worth saying: Giulio, thanks from Eddie.

Thanks to Fra, who shared with me, together with the name, the passion for Tuscany and for playing tennis, even if he is undoubtedly a way better player than I have ever been.

Giua, the biggest guy of Audace, thank you for any single pull-up: I greatly enjoyed.

And how not to mention Grizi, without whom the "wednesdinner" could not have been existed, Mavi, for the many vegan dinners at her place, Cristoforo, with his strange roman-english mixed vocabulary, Frago (but not for making me aware

[1] a big apology to the memory of Chick Corea

of the world “sfrastico”), Lorenzo, Diego2 and Morgana. Thank you guys.

I want to close this long list thanking Andre, with whom I shared the achievement of the second star of the best football team in the world, reminding him his promise to organize the big reunion of 2026.

The conclusion of these acknowledgements is reserved to my family. Their support during these years has been fundamental in every single step. They know how much I enjoyed this journey, but it is of great importance to me to make them aware that none of this could have been possible without them. Therefore thanks to mamma, babbo, nonna, Costi, Ernest, Leo, Franca and to our new-entry Berto. Vi voglio bene.

Notations and conventions

In this thesis we will use the following conventions, where not specified differently: we will adopt the "mostly plus" conventions for the signature of the metric, namely $\mathrm{diag}(-,+,+,+)$. We will use the conventions of [1] for the indices, namely the latin letters $\{a, b, c, \dots\}$ will run from 0 to 3.

In Chapter 7, and solely for that, we will use the "mostly minus" signature $(\mathrm{diag}(+,-,-,-))$, often used in high energy physics and the latin indices $\{i, j, k, l, \dots\}$ will run from 1 to 3. In the whole treatment we will adopt the so-called natural units $\hbar = c = G = k_B = 1$.

Acronyms

ADM Arnowitt– Deser–Misner

AG Analogue Gravity

BEC Bose-Einstein condensates

BFV Batalin-Fradkin-Vilkovisky

BL Boyer-Lindquist

EA Einstein-aether

EFB Eddington-Finkelstein-Bardeen

EFH effective horizon

EFT Effetive Field Theory

ETF Effective Temperature Function

GR General Relativity

HG Hořava Gravity

KMS Kubo-Martin-Schwinger

LLI Local Lorentz Invariance

LV Lorentz Violating

MDR modified dispersion relation

QFT Quantum Field Theory

QG Quantum Gravity

QUH quasi-universal horizon

SR Special Relativity

UH universal horizon

UV ultraviolet

WKB Wentzel-Kramers-Brillouin

Contents

List of Figures

Chapter 1

Introduction

The search for Quantum Gravity (QG) has been – and still is – one of the main goals of contemporary physics. Although General Relativity (GR), our current description of gravity, has passed an incredible number of experimental tests [2, 3], a quantum description of gravity arises as a strong theoretical necessity. Interestingly, it turns out that the theory predicts its own limits that in their mathematical form are the so-called singularity theorems [1, 4–6].

The (unavoidable) presence of singularities – such as those encountered in black holes or cosmology – strongly suggests that we need to look beyond a classical formulation and find a way to incorporate the quantum world into the game.

Unfortunately, the same tools that have been used to unify the other three fundamental forces into the Standard Model of particle physics cannot be directly applied to GR in order to render it a quantum theory. Indeed, within a Quantum Field Theory (QFT) perspective, GR represents a non-renormalizable theory [7, 8], therefore at most it has to be taken as an Effetive Field Theory (EFT) predictive only up to some energy scale.

Experimentally, the main issue in trying to investigate the quantum aspects of gravity, is encoded in the separation of energy scales that exists between particle physics and the gravitational world. GR is intrinsically endowed with an energy scale – the Planck energy $E_p \sim 10^{19}$GeV – at which one expects quantum gravitational effects to become important. This energy scale lies way above any other scale at which particle physics experiments are currently performed [9]. Therefore, trying to find a hint for QG by lab-based experiments is an incredibly hard task.

On the other hand, the huge gap separating Standard Model and Planck scales suggests a broad range of energies where gravity can be still considered a classical entity while matter follows quantum rules. Since classical gravity can be interpreted as the spacetime geometry, that *tells matter how to move*, in this regime it is possible to examine the behaviour of quantum fields on a curved background. Probing QFT in curved spacetime has led to unexpected and fascinating results regarding black holes and cosmology, pointing out the role that different observers play in defining the local QFT. Let us dig this topic a bit more.

Quantum field theory in curved spacetime

Among the aforementioned results the discovery that black holes radiate as black bodies shines [10, 11]: Hawking found that these objects are characterized by a temperature $T_{\rm H}$ and entropy $S_{\rm BH}$ given by

$$k_B T_{\rm H} = \frac{\kappa_{\rm H}\hbar}{2\pi c}\,, \qquad S_{\rm BH} = \frac{A_{\rm H}}{4l_p^2}\,,$$

where k_B is the Boltzmann's constant, $\kappa_{\rm H}$ is the surface gravity of the horizon and $A_{\rm H}$ is its area, while $l_p = \sqrt{\hbar G c^{-3}}$ is the Planck length. This result shows that black holes are in fact thermodynamical systems. The so-called "Black Hole Thermodynamics" – which describes the mechanics of a black hole in a complete analogy with the 4 laws of classical thermodynamics – is an anchor for the QG investigation.

Moreover, Hawking's calculations demonstrate that when one attempts to formulate quantum field theory (QFT) within the context of a classical black hole geometry, these black holes must inevitably radiate, leading to their gradual evaporation. This outcome aligns with predictions made by standard thermodynamic principles, thereby resolving a potential classical paradox. Specifically, a non-radiating black hole immersed in a thermal bath at a lower temperature would paradoxically decrease the total entropy of the system simply by absorbing energy from its surroundings [12].

Immediately after Hawking's discovery, QFT in curved spacetime started to emphasize the strong connection that spacetime seems to have with thermodynamics. The equivalence principle tells us that acceleration and gravity are two sides of the same coin. Thus, an uniformly accelerated observer has been shown to describe the Minkowski vacuum as a thermal state, with a temperature proportional to his own proper acceleration a_p

$$k_B T_{\rm U} = \frac{a_p \hbar}{2\pi c}\,,$$

a result that dates back to Unruh in the 70s [13]. This phenomenon, known as the Unruh effect, serves as a striking example of how different observers – in this case, a geodesic observer and a uniformly accelerated one – can have fundamentally different experiences of the same quantum field, despite both existing within the same spacetime.

A big step forward in the direction of unveiling how intimate is the relation between gravity and thermality has been performed when, for the first time in 1995, Jacobson realized that the discussion can go beyond the black hole framework [14]. The equivalence principle allows to cast every geometry as locally flat, thus associating a temperature to the local Rindler patch. Spacetime dynamics can then be derived simply requiring thermodynamical equilibrium, where the geometrical deformation is induced by the heat flux δQ that flows across the Rindler horizon. The shape of the horizon – which determines its entropy S – is adjusted in order to preserve the thermodynamical equilibrium for which:

$$T\, dS = \delta Q\,.$$

It turns out that the imposition of the Clausius relation implies the Einstein equations, without knowing anything about the gravitational Lagrangian. In this way, it is possible to interpret the Einstein field equations as *equations of state*.

This point of view is quite revolutionary and opens up the possibility that spacetime could be not a fundamental entity but an emergent phenomenon instead. The principle "if you can heat something, it must have a microstructure", which led Boltzmann to infer the existence of atoms before their experimental necessity, is adopted to describe geometry as some effective description of a given microphysics. In fact, a lot of work has been done in this direction, and the emergence of a classical spacetime and its dynamics is a building block of several QG approaches. Frameworks like Loop Quantum Gravity, String theory, Group field theory and Lattice theories are just a few examples [15].

Let us stress that, even though QFT in curved spacetime has direct implications in the phenomenology of gravity, it is important to realize that, strictly speaking, it shares no link with general relativistic settings: a quantized field on top of a curved geometry will not be sensitive to the origin of the background. In other words, it does not matter if the effective spacetime comes as a solution of the Einstein field equations (as it does in GR) or from other conditions. Viewed in this way, an effect such as Hawking radiation is insensitive to the dynamics of the geometry, being rather a description of the fields kinematics on a curved Lorentzian manifold.

This allows us to try and look for these effects also in completely different contexts than gravitational black holes. Of particular interest are the so-called *analogue models* for gravity. Playing by analogies, in the 80s it was realized that the analysis of perturbations (phonons) of a perfect fluid can be mapped into a case of field theory on curved background [16]. Indeed a perturbative treatment of the equations governing the fluid behaviour – the continuity equation and the Euler equation – describes phonons moving onto a curved acoustic metric. This metric, being a solution of fluid-dynamic equations, has no knowledge of GR but it shows up to be a surprisingly useful tool to investigate curved spacetime effects on fields. These geometries can be used to build objects with (acoustic) horizons, which play the role of the analogue of a black hole, and their evaporation can be studied, both theoretically and experimentally. However, as already mentioned, these kind of spacetimes have nothing to do with GR and they know nothing about the Einstein field equations, which confirms that curved background effects in QFT are purely kinematics.

Beside reproducing relativistic phenomena, analogue models are also a way to probe the open question that arises once one accepts Hawking's result. The fact that the final state after the black hole complete evaporation looks as a thermal state, seems to suggest a non-unitary evolution between the initial pure state from which the black hole itself was formed. That implies a loss of information between the future and the past state, giving rise to the "information-loss paradox". This problem has been adressed in the context of analogue models, in a cosmological-analogue setting, showing how the knowledge about the microstructure allows to keep trace of the information, not only in the form the correlations between the pairs of quanta produced in the process, but also by taking into account the correlation of those quanta with the atoms of the background [17].

Another example is given by the so-called "trans-Planckian problem". In a rela-

tivistic setting, if one traces back an Hawking quantum from infinity to the horizon, that particle seems to experience and infinite peel-out from the black hole horizon, together with an infinite blueshift in energy. This brings the particle to experience trans-Planckian energies $\omega \gg E_p$, exceeding the range of validity of our semiclassical approximation of QFT in curved spacetime. Analogue models naturally provide a way to study Hawking radiation without transplanckian frequencies. It is actually quite common that, in systems where it is experimentally possible to simulate Hawking radiation – for instance, in superfluids or Bose-Einstein condensates, where the coherence time is longer than in a standard fluid – perturbations obey a modified dispersion relation, like

$$\omega^2(k) = c_s^2 \left(k^2 + \frac{k^4}{\Lambda^2} + \cdots \right) ,$$

where Λ is a cutoff, that is the characteristic scale of the microphysics, c_s is the speed of sound and the dots can be seen as further terms in an expansion in k/Λ [18]. In this case, no perfect exponential peeling occurs at the horizon and the blueshift is cut off at energy Λ. However, this regularization comes at the price of introducing a Lorentz violating part in the dispersion relation, for which the Lorentz invariant behaviour is approximately recovered when $k^2 \ll \Lambda^2$. It has been shown that the Hawking effect is incredibly robust to these modifications: the analogue black hole radiates and in the regime when $\kappa_{\rm H} \ll \Lambda$ this radiation is thermal, with a temperature $T_{\rm H}$ [19].

The robustness of Hawking radiation is a remarkable observation because it makes us to rethink the hierarchy of our assumptions and may conclude that such an effect may be, if not universal, at least quite insensitive to the ultraviolet (UV) completion of the theory which generated the curved background. In particular, Lorentz invariance and horizons seem less strict requirements than one may think in order for such an effect to take place. Actually, besides Lorentz invariance violation, the presence of Hawking radiation also for horizonless objects has already been pointed out in the literature [20].

Thus, even though not strictly speaking quantum-gravitational, the effects of quantum fields in curved space represent an incredibly good playground for testing properties of gravity beyond the classical regime. As mentioned above, these may help guide the search for QG towards the right direction, unveiling the layers of assumptions which constitute GR. Moreover, the possibility of testing these features in the lab makes them very appealing for contemporary research.

The need for quantum gravity

In summary, the formulation of a QFT with a classical curved spacetime represents the first step toward the inclusion of quantum effects in gravity. However, this treatment raises other puzzles, such as the information-loss paradox or the trans-Planckian problem, where the approximation breaks down. In principle, this does not directly tell us that gravity must be quantized, but rather that the backreaction of the field onto the geometry must be taken into account at some point. One can imagine that the solution to these new theoretical questions can also come from

a complete semiclassical treatment, where a gravity-matter system is defined by solving the semiclassical Einstein equations:

$$G_{ab} = \frac{8\pi G}{c^4}\langle\psi|\hat{T}_{ab}|\psi\rangle\,.$$

Here, the matter stress-energy tensor $\hat{T}_{ab}$ is an operator acting on the quantum state of matter $|\psi\rangle$. This equation contains the backreaction that matter has on the geometry and, in principle, solving it consistently should provide us with a full semiclassical matter-gravity theory, of which the test-field limit represents the QFT in curved spacetime formalism. This idea is quite appealing because, even if technically involved, there would solve the problem of incorporating our (quantum) treatment of matter into our (classical) description of gravity without invoking QG. This kind of hypothesis has been considered in the past (see e.g. [21] and references therein), which unfortunately shows up to be inconsistent, since a classical gravitational setting can in principle lead to a violation of the uncertainty principle in the matter quantum world [21].

On the experimental side, investigations are currently being carried on this direction. The idea is to apply quantum information techniques to gravitational interaction in the lab and try to entangle gravitons: this would confirm the intrinsic quantum nature of gravity [22].

Additionally, a purely semiclassical approach has been shown not to answer the original questions about where classical GR loses his predictivity: singularities are still there and they cannot be prevented by a semiclassical treatment[1]. Therefore, we have no other choice than moving beyond.

Many different approaches

Physics is facts, not theory. Quoting Feynman: *if the facts are right, then the proofs are a matter of playing around with the algebra correctly.* This summarizes once again the main issue concerning the QG program. Without any experimental insight to drive theoreticians, nowadays we are left with an incredible amount of proposals, all of them based on a different approach, and for each of them quantizing gravity can mean a completely different thing. One can formally divide this huge set between theories where spacetime is emergent and theories where that represents the fundamental entity.

The former subset is, in general, conceptually more involved, trying to describe structures that, after some coarse-graining procedure, effectively generate the spacetime. Typical examples are [15, 24]:

- Superstring theory (or M-theory): a higher-dimensional, supersymmetric theory, where the fundamental entities are given by branes. After a compactification procedure, our 4-dimensional spacetime emerges [25].

[1]Purely speaking, a violation of the standard energy conditions in $\langle T_{ab}\rangle$ can provides nonsingular models. However, usually, this violation is phenomenologically introduced and justified by invoking some QG-mechanism, as in regular black hole models (see [23] and references therein)

- Loop quantum gravity: derived as an improvement of the canonical quantisation approach, loop quantum gravity interprets the spacetime as a fabric of a finite length loops, enjoying a non-abelian gauge symmetry similar to the one of the Standard Model [26].

- Group field theory: inspired by the loop quantum gravity approach, the constituents are chunks of spacetimes, defined on a group manifold. In some applications, the coarse-graining procedure, spacetime arises in a very similar fashion as the analogue models [27, 28].

- Causal dynamical triangulations: this is a lattice theory, where the spacetime manifold is described by a lattice and recovered in the continuum limit [29].

The one above is a non-exhaustive list, but just an example of how diverse the specific theoretical framework can be when we talk about quantum gravity.

Besides these emergent-spacetime theories[2], there is a whole set of approaches where the metric is the building block. This point of view is indubitably more conservative, since it does not require to create different structures other than the geometry itself. The principal ones are [24]

- Asymptotically safe gravity: the Lagrangian formulation is the same as in GR, but the Newton's constant G and the cosmological constant Λ run with the energy scale, eventually reaching a finite value in the far UV, thus rendering the theory under control at all energies [30].

- Higher-derivative gravity: higher curvature terms – like R^2, $R_{ab}R^{ab}$ and so on – are considered in the gravitational sector. The theory become perturbatively renormalizable but it is affected by the presence of ghosts due to higher time-derivatives (see Chapter 4) [31].

- Lorentz violating gravity: local Lorentz symmetry is dropped in first place, in order to formulate a theory which is power-counting renormalizable and not affected by instabilities, as it entails higher derivatives only in space [32].

All of those proposals have different guiding ideas and weak points, but none of them can currently be considered definitive. However, based on the discussion we have made in the previous sections, it is possible to outline some guidelines to make our choice.

Removing the inessential

In the axiomatic derivation of Special Relativity (SR) a cornerstone is represented by the so-called *von Ignatowski theorem* (1911). It states that once we assume [33]:

- Spatial homogeneity and isotropy

- Temporal homogeneity

[2]To be precise, in the causal dynamical triangulation approach the spacetime is not emergent from a more fundamental theory but as a continuum limit procedure, as in lattice QCD

- Relativity Principle (i.e. the equivalence of all the inertial frames)
- Pre-causality (i.e. the order of two events on a worldline is the same in any reference frame)

then we must have SR. Interestingly, the special theory of relativity can be uniquely derived as a theorem by a set of reasonable physical assumption and, with the addition of the strong equivalence principle – which implies that all the local physics, included SR, holds as without gravity – we can infer GR. Therefore, general relativity seems to be quite a unique conclusion, once we have set the assumptions as above.

Very often those assumptions are taken to be valid also in the QG proposals up to the far UV. Superstring theory is an example of Lorentz-invariant theory at all energies, and the same happens in the Asymptotic safety scenario. However, in both cases, the formulation of the theory is radically different from the one that we use to describe the Standard Model. While the latter is perturbatively-renormalizable, those QG candidates treat the problem either in a non-perturbative way, or invoking completely different settings.

Another possibility to go beyond GR is to take a step back to the fundamental assumptions and try to generalize the theory looking for the inessential. Adopting an approach that removes assumptions rather than adding complex layers is a healthy way to look at problems. Anytime we try to generalize a problem by reducing the constraints, we may discover hidden degeneracies and, most importantly, we learn that whatever physics we are left with, it is independent from – thus more fundamental than – that assumption.

In the case of gravity we can ask ourselves what happens when we try to drop one of the assumptions that lead to SR. In this, very conservative, procedure the sensible possibilities reduce to two: taking away spatial isotropy returns us Finsler geometries, where the metric is defined both in the tangent and in the co-tangent space of the the spacetime manifold [34]; the other possibility is to drop the relativity principle, thus the equivalence of all the local inertial frames. This builds a theory with a preferred frame, explicitly violating the Local Lorentz Invariance (LLI).

While it may seem quite scaring at first sight, Lorentz Violating (LV) gravity seems to show the nice features we demand to a QG candidate in three different aspects.

Within a QFT framework, dropping LLI has been shown to produce a power-counting renormalizable theory, known as "Hořava Gravity (HG)". There are strong hints for HG to be a perturbatively renormalizable theory, that would make it treatable with the same QFT techniques that we already know from the usual Standard Model physics.

On the other hand, the low-energy implications of LV gravity can be as interesting as their counterparts in the UV. Analogue models – where Lorentz breaking phenomena arise spontaneously – already have provided us with an example where the LV character of the perturbations does not spoil one of the main results of QFT in curved spacetime, that is the Hawking radiation. It is then obvious that studying LV models of gravity can also help us to understand better if the close relation that in relativistic physics holds between spacetime and thermodynamics, is actually based on Lorentz symmetry or represents something more fundamental.

In addition, at current times, LV physics is one of the most experimentally viable setting. In the gravitational sector, it has been shown that the Lorentz breaking scale has to be sub-Planckian for several orders of magnitude, therefore requiring much less effort to reach that energy [33].

These three motivations will be the guidelines that will accompany us throughout the present work. Armed with them, we will adopt this reductive approach and investigate a world where gravity is no longer Lorentz invariant.

Plan of the thesis

This work is organized as follows: the first Chapter (2) will be used to revise the basic technical toolkit that is used when dealing with black hole radiation, such as the quantum tunneling method or the Bogolyubov coefficient approach. This will give us the chance to stress some useful point of view that will be adopted in the rest of the work.

Then, we will start our journey in the lab: in Chapter 3 we will review in grater detail the analogue models and their role as a tool for studying QFT in curved spacetime both in the relativistic and non-Lorentz invariant cases. This will give us the chance to clarify some open questions in the literature, showing the robustness of the Hawking effect in a context where LV physics is built-in.

In Chapter 4 we will introduce some actual models of LV gravity. In a spirit of semiclassical gravity, here we will focus on the low energy, classical approximation of Lorentz braking gravity, such as Einstein-Aether and khronometric gravity. We will analyze the new causal structure, explaining how black holes arise in a different fashion with respect to their relativistics counterpart. A new notion of horizon – the universal horizon – is introduced, and we will speculate on the existence of rotating solutions.

In Chapter 5, quantum fields are introduced in these geometries. We will describe the kinematics of particles in LV-black hole scenarios and, after a review of the previous result, we will provide a novel treatment for describing the radiation of these objects, concluding with an analysis on the quantum states compatible with our result.

Chapter 6 will be devoted to dig more into the LV-spacetime thermodynamics, through the analysis of the Unruh effect. After a first part of revision, where it will be clear that this is an open issue in the literature, we will give a novel notion of Rindler wedge, adapted to the presence of LV. We will show that the Unruh effect is preserved and that thermality is ensured by the Kubo-Martin-Schwinger (KMS) condition of the quantum state, fixed by the universal horizon. In the same Chapter, we will also analyze the role of an accelerated detector, discussing its response function.

Finally in Chapter 7 we will discuss the Hořava proposal as a QG candidate. What has been done and what is left to do will be analyzed together with some preliminary results.

Chapter 8 will contain the conclusions: we will review the work done, commenting on the possible future perspective on the field.

Chapter 2

Hawking radiation: a primer for QFT in curved spacetime

As mentioned in the previous Chapter, Hawking radiation is one of the most fascinating and unexpected result of QFT in curved spacetime [11]. It has posed the basis for the study of quantum effect in GR and it represents a cornerstone of the spacetime thermodynamics. Being the first, most-investigated, example of quantum fields behaviour on curved background, it is often taken as a primer for the field. In this Chapter we will briefly revise its derivations and use it to introduce concepts and techniques that will be useful in the following of this thesis. In particular, we will describe two well-known derivations, namely the Bogolyubov coefficients and the tunneling method, which are the basic toolkit for the contents of the main references of this work [35–40].

In the last part of this Chapter, we will also review an alternative derivation of the same effect involving the Euclidean path integral, which will be useful in Chapter 5 and 6.

2.1 Inequivalence of vacua: Hawking radiation as a Bogolyubov transformation

One of the main features of QFT in curved spacetime effects is based on the following observation: while in a flat spacetime treatment the notion of vacuum state for a quantum field $\hat{\phi}$ represents a unique, Lorentz-invariant, physical state – so any inertial observer will describe the same vacuum – the same is not valid in a generic curved spacetime [41, 42]. This is quite obvious: since the definition of vacuum state is based on the construction of the Fock space, that relies on a choice of a concept of energy in order to build the modes, it has to be a coordinate-dependent (or, equivalently, observer-dependent) statement. Since two different observers will perceive time differently, the same quantum state can be simultaneously vacuum for one of them and a populated state for the other. Let us see how.

2.1.1 Bogolyubov coefficients

Let us consider, as a starting point, a simple model for a minimally coupled real scalar field ϕ with mass m on a curved background g_{ab} [41]:

$$\mathcal{L} = -\frac{1}{2}\sqrt{-g}\left[g^{ab}\phi\nabla_a\nabla_b\phi - m^2\phi^2\right] . \tag{2.1}$$

The canonical quantization procedure of ϕ goes as follows: we consider a spatial foliation for our Lorentzian manifold $\mathcal{M}$, through the choice of a time coordinate t and define the conjugate momentum π:

$$\pi = \frac{\delta\mathcal{L}}{\delta\partial_t\phi} = \sqrt{-g}g^{at}\nabla_a\phi\,. \tag{2.2}$$

The quantization can be performed by promoting ϕ and π to operator-valued object which satisfy the canonical commutation relations at equal times

$$\begin{aligned}[\hat{\phi}(t,\mathbf{x}),\hat{\pi}(t,\mathbf{y})] &= \frac{i}{\sqrt{-g}}\delta(\mathbf{x}-\mathbf{y})\,,\\ [\hat{\phi}(t,\mathbf{x}),\hat{\phi}(t,\mathbf{y})] &= [\hat{\pi}(t,\mathbf{x}),\hat{\pi}(t,\mathbf{y})] = 0\,.\end{aligned} \tag{2.3}$$

where the "hatted" quantities have the usual notational meaning as indicating an operator. The Fock space can be built as follows: let us take a constant time leaf $\Sigma_t = \{t = \text{const.}\}$ and define the following *inner product*

$$\langle\phi_1,\phi_2\rangle_{\Sigma_t} = -i\int_{\Sigma_t} n^a\left(\phi_1\nabla_a\phi_2^* - \phi_2^*\nabla_a\phi_1\right) \tag{2.4}$$

where n^a is the normal vector to Σ_t. This product, known also as Klein-Gordon product determines the simplectic structure of the space of solutions of the field equation for ϕ, that is, from (2.1)

$$\frac{\delta\mathcal{L}}{\delta\phi} = (\Box - m^2)\phi = 0\,. \tag{2.5}$$

Within the space of solution of (2.5), the inner product $\langle\phi_1,\phi_2\rangle_{\Sigma_t}$ can be easily shown to be independent of the specific leaf Σ_t that is chosen for computing the integral.

Armed with this inner product, it is possible to define an orthonormal basis $\{f_\Omega\}$, where f_Ω solves (2.5) and satisfies the eigenvalue relation $\partial_t f_\Omega = -i\Omega f_\Omega$; similarly it happens for their complex-conjugated version $\partial_t f_\Omega^* = i\Omega f_\Omega^*$. Intuitively, Ω is the energy defined with respect to the time t. Considering only $\Omega > 0$, we have a complete set of solutions that satisfy:

$$\langle f_\Omega, f_{\bar{\Omega}}\rangle = -\langle f_\Omega^*, f_{\bar{\Omega}}^*\rangle = \delta(\Omega-\bar{\Omega})\,, \qquad \langle f_\Omega, f_{\bar{\Omega}}^*\rangle = 0\,. \tag{2.6}$$

Due to this relations, f_Ω is often called a positive-normed mode, while f_Ω^* is negative-normed. Since $\{f_\Omega\}$ form a basis of solutions, any operator $\hat{\phi}$ can be expanded in this basis

$$\hat{\phi} = \int_0^\infty \frac{\mathrm{d}\Omega}{2\pi}\left[\hat{a}_\Omega f_\Omega + \hat{a}_\Omega^\dagger f_\Omega^*\right] . \tag{2.7}$$

The operators $\hat{a}_\Omega$ and $\hat{a}^\dagger_\Omega$ are the (position-independent) annihilation and creation operator for a single mode of energy Ω. They satisfy the canonical commutation relations:

$$[\hat{a}_\Omega,\, \hat{a}^\dagger_{\bar{\Omega}}] = \delta(\Omega - \bar{\Omega})\,, \qquad [\hat{a}_\Omega,\, \hat{a}_{\bar{\Omega}}] = [\hat{a}^\dagger_\Omega,\, \hat{a}^\dagger_{\bar{\Omega}}] = 0\,. \tag{2.8}$$

Most importantly, these operators define the vacuum state $|0\rangle_f$ through the relation

$$\hat{a}_\Omega |0\rangle_f = 0\,. \tag{2.9}$$

From this construction, it is crystal clear how the definition of the vacuum must depend on the choice of time (or energy) that we have made at the beginning. The state $|0\rangle_f$ is Poincarè-invariant, but it is not under generic coordinate transformation. Let us imagine to start again from (2.1) and repeat the construction but with a different choice of time: this will lead to describe the space of solution with a different basis $\{g_\omega\}$, where ω is the eneregy defined with the help of the "new" time. This implies

$$\hat{\phi} = \int_0^\infty \frac{\mathrm{d}\omega}{2\pi} \left[\hat{b}_\omega g_\omega + \hat{b}^\dagger_\omega g^*_\omega\right] \tag{2.10}$$

for a new set of operators $\hat{b}_\omega$ and $\hat{b}^\dagger_\omega$ satisfying the canonical commutation relations and defining a different vacuum state through

$$\hat{b}_\omega |0\rangle_g = 0\,. \tag{2.11}$$

Since the two basis formed by f_Ω and g_ω describe the same field linearly, the transformation that relates the two sets will be linear as well, that is to say:

$$g_\omega = \int_0^\infty \frac{\mathrm{d}\Omega}{2\pi} \left[\alpha_{\omega\Omega} f_\Omega + \beta_{\omega\Omega} f^*_\Omega\right]\,. \tag{2.12}$$

The coefficients $\alpha_{\omega\Omega} = \langle g_\omega, f_\Omega\rangle$ and $\beta_{\omega\Omega} = -\langle g_\omega, f^*_\Omega\rangle$ are called *Bogolyubov coefficients*. From the normalization of g_ω one infers the completeness relations

$$\int_0^\infty \frac{\mathrm{d}\Omega}{2\pi} \left[\alpha_{\omega\Omega}\alpha^*_{\bar{\omega}\Omega} - \beta_{\omega\Omega}\beta^*_{\bar{\omega}\Omega}\right] = \delta(\omega - \bar{\omega})\,, \tag{2.13}$$

$$\int_0^\infty \frac{\mathrm{d}\Omega}{2\pi} \left[\alpha_{\omega\Omega}\beta_{\bar{\omega}\Omega} - \beta_{\omega\Omega}\alpha_{\bar{\omega}\Omega}\right] = 0\,. \tag{2.14}$$

Let us note that equation (2.12) translates into a linear map between the annihilation and creation operators:

$$\hat{b}_\omega = \int_0^\infty \frac{\mathrm{d}\Omega}{2\pi} \left[\alpha^*_{\omega\Omega}\hat{a}_\Omega - \beta_{\omega\Omega}\hat{a}^\dagger_\Omega\right]\,. \tag{2.15}$$

This relation can be used to highlight the inequivalence between $|0\rangle_f$ and $|0\rangle_g$. A standard result, which comes directly from equation (2.15) regards the population of $|0\rangle_f$ in terms of the modes g_ω. Indeed, taking the expectation value for the number operator $\hat{N}_\omega = \hat{b}^\dagger_\omega \hat{b}_\omega$ we obtain, after some simple manipulation [41]

$$\langle \hat{N}_\omega\rangle_f =_f \langle 0|\hat{b}^\dagger_\omega \hat{b}_\omega|0\rangle_f = \int_0^\infty \frac{\mathrm{d}\Omega}{2\pi} |\beta_{\omega\Omega}|^2\,. \tag{2.16}$$

This is an extremely interesting result of QFT in curved spacetime. As anticipated, we discover that two different observers, which experience two different notion of time, thus defining two different vacua, experience the same state differently. In particular, we can see that the vacuum $|0\rangle_f$ is seen as a populated state in terms of the basis $\{g_\omega\}$ if the Bogolyubov transformation contains some non-zero β coefficients. That is to say that a single mode g_ω must be a superposition of positive energy modes f_Ω *and* negative-energy modes f^*_Ω. Without that mode-mixing, no particle production happens (namely $\langle \hat{N}_\omega \rangle_f = 0$). In the following, we will apply this formalism to describe black hole radiation.

2.1.2 Black hole radiation: a Bogolyubov approach

For definiteness, in what follows we will consider a static, spherically symmetric, black hole geometry. This, as a vacuum solution of the Einstein equations, takes the form of the Schwarzschild metric [1, 43]:

$$\mathrm{d}s^2 = g_{ab}\mathrm{d}x^a\mathrm{d}x^b = -F(r)\mathrm{d}t^2 + \frac{\mathrm{d}r^2}{F(r)} + r^2\mathrm{d}\mathbb{S}_2, \qquad F(r) = 1 - \frac{r_s}{r}\,, \tag{2.17}$$

where $\mathrm{d}\mathbb{S}_2$ denotes the two-sphere, labelled by the angular coordinates θ and φ, and $r_s = 2M$ is the Schwarzschild radius for a black hole of mass M. As usual in static spacetimes, the black hole region is defined by a Killing horizon, that in this case is the surface at which the norm of $\chi^a\partial_a = \partial_t$ vanishes. In other words

$$|\chi|^2 = g_{00} = -F(r) = 0 \iff r = r_s\,. \tag{2.18}$$

A minimally coupled scalar field ϕ is described by (2.1). Let us take the massless case $m = 0$ for simplicity, but an equivalent treatment is valid for the massive case [42]. Its equation of motion is

$$\Box\phi = 0\,. \tag{2.19}$$

Due to the symmetry of the background, the solutions of the Klein-Gordon equation are separable in the radial and angular variables:

$$\phi(t, r, \theta, \varphi) = \sum_{l,m} \frac{\psi_l(t, r)}{r} Y_{lm}(\theta, \varphi)\,. \tag{2.20}$$

With this parametrization, the massless Klein-Gordon equation assumes a particularly simple form in the the Regge-Wheeler coordinate r_*

$$\mathrm{d}r_* = \frac{\mathrm{d}r}{F(r)}\,, \qquad r_* = r + r_s \log\left(\frac{r - r_s}{r_s}\right)\,, \tag{2.21}$$

that is [43]

$$-\frac{\partial^2\psi_l}{\partial t^2} + \frac{\partial^2\psi_l}{\partial r_*^2} + V_l(r)\psi_l = 0\,, \tag{2.22}$$

where the potential V_l is

$$V_l(r) = -F(r)\left[\frac{F'(r)}{r} + \frac{l(l+1)}{r^2}\right] . \tag{2.23}$$

This potential is the energy barrier that a particle has to climb in order to escape from the gravitational attraction of the black hole. The main feature is that V_l vanishes both asymptotically, for $r \to +\infty$ (equivalently $r_* \to +\infty$), and for $r = r_s$ (equivalently for $r_* \to -\infty$). It is therefore useful to define the two null coordinates $u = t - r_*$ and $v = t + r_*$. When the potential vanishes the field equations simplifies to

$$-\frac{\partial^2\psi_l}{\partial t^2} + \frac{\partial^2\psi_l}{\partial r_*^2} = -\frac{\partial^2\psi_l}{\partial u \partial v} = 0 . \tag{2.24}$$

Thus, both asymptotically and near the horizon the solution of the field equation, splits into an ingoing (only v-dependent) and an outgoing (only u-dependent) contribution $\psi_l(r,t) = g_l(v) + f_l(u)$. For the purpose of this calculation, only the outgoing sector will be important. In fact, our goal is to study the radiation emitted by the black hole, that reaches infinity in the null far future, at $\mathscr{I}^+$, that is purely outgoing.

The explanation of the Hawking effect as an effect of inequivalence of vacua comes once we consider the following two physical observers: the first will be sitting at $r \to \infty$, where the metric is flat (and $r_* = r$), and will define its time with the Schwarzschild time t. Hence, one basis will be formed by (up to a normalization factor)

$$f_\Omega^\infty = e^{-i\Omega(t-r)} = e^{-i\Omega(v-2r)} , \qquad \partial_t f_\Omega^\infty = -i\Omega f_\Omega^\infty , \tag{2.25}$$

together with their complex conjugated negative-normed modes. Let us note that the definition of energy with respect to t is tantamount to say that the observer sitting at infinity describes the energy using its own proper time. This observer is not moving spatially and it is geodesics, thus follow the integral lines of χ. Since $|\chi|^2(r=\infty) = -1$, t describes exactly the proper time of someone staying still on $\mathfrak{i}^0$.

The second basis will be constituted by the near-horizon modes from the point of view of a freely-falling observer crossing the horizon. In order to better describe this physical frame, it is convenient to make a coordinate change and describe our geometry in some coordinate, which are regular at the horizon. For an infalling trajectory, this is the case of the $\{v, r\}$ set of coordinates, which takes the name of Eddington-Finkelstein-Bardeen (EFB) coordinates, for which the line element looks like [43]

$$\mathrm{d}s^2 = -F(r)\mathrm{d}v^2 + 2\mathrm{d}v\mathrm{d}r + r^2\mathrm{d}\mathbb{S}_2 . \tag{2.26}$$

We can immediately see that, from the above equation, the apparent singularity at the Schwarzschild radius disappears. Since a freely falling observer will regularly cross the horizon at some finite retarded time v_{KH}, we can take again the Killing vector field – which in EFB coordinates looks like $\chi^a\partial_a = \partial_v$ – to define our time[1].

[1]Since v_{KH} and $\partial_\tau v_{\mathrm{KH}}$, where τ is the proper time of the free-falling observer, are well defined, making $v(\tau)$ locally invertible, the choice of v as a time is coherent with the choice of the observer.

Besides the presence of the – regular at $r = r_s$ – ingoing sets of modes, the outgoing ones will take the form:

$$f_\Omega^{\rm KH} = e^{-i\Omega(v-2r_*)}\,, \qquad \chi^a\partial_a f_\Omega^{\rm KH} = \partial_v f_\Omega^{\rm KH} = -i\Omega f_\Omega^{\rm KH}\,. \tag{2.27}$$

Note that for both observers the energy is defined with respect to the Killing vector.

At this point, the only thing which is left to do is to compare the two basis $\{f_\Omega^{\rm KH}\}$ and $\{f_\Omega^{\infty}\}$ to evaluate the Bogolyubov coefficients. Let us take a closer look to the (outside) near-horizon set of modes:

$$f_\Omega^{\rm KH} = e^{-i\Omega(v-2r_*)} = \exp\left[-i\Omega\left(v - 2r_s\log(r-r_s)\right)\right]\,. \tag{2.28}$$

Due to the logarithmic divergence of r_* at the horizon, these mode are not analytical at the horizon [42]. Actually, in (2.21), the formula for r_* is given for the exterior of the black hole. The integration of r_* on interior is different and leads to an opposite sign in the argument of the logarithm. Therefore, in principle, outgoing solutions in the near-horizon limit, have supports only on one of the two sides of the horizon. We thus have that $f_\Omega^{\rm KH}$ divides into

$$\begin{aligned} f_\Omega^{\rm KH,out} &= \Theta(r-r_s)\exp\left[-i\Omega\left(v - 2r_s\log\left(\frac{r-r_s}{r_s}\right)\right)\right]\,,\\ \left(f_\Omega^{\rm KH,in}\right)^* &= \Theta(r_s-r)\exp\left[-i\Omega\left(v - 2r_s\log\left(\frac{r-r_s}{r_s}\right)\right)\right]\,. \end{aligned} \tag{2.29}$$

Here Θ is the Heaviside function, that highlights the single-side support of the $f_\Omega^{\rm KH}$'s. Let us point out that the modes inside have been written as conjugated modes because in this form they have negative norm. Let $x = r - r_s$ and h_{ab} be the induced metric in the orthogonal of ∂_v:

$$\begin{aligned} &\langle\left(f_\Omega^{\rm KH,in}\right)^*, \left(f_\Omega^{\rm KH,in}\right)^*\rangle = \\ &-i\int_{v=\rm const}\sqrt{h}\,{\rm d}x\,{\rm d}\varphi\,{\rm d}\theta\,\Theta(-x)\left[\left(f_\Omega^{\rm KH,in}\right)^*(v,-x)\overset{\leftrightarrow}{\partial}_v f_\Omega^{\rm KH,in}(v,-x)\right] = \\ &i\int_{v=\rm const}\sqrt{h}\,{\rm d}x\,{\rm d}\varphi\,{\rm d}\theta\,\Theta(x)\left[f_\Omega^{\rm KH,in}(v,x)\overset{\leftrightarrow}{\partial}_v\left(f_\Omega^{\rm KH,out}\right)^*(v,x)\right] = \\ &-\langle f_\Omega^{\rm KH,out}, f_\Omega^{\rm KH,out}\rangle\,. \end{aligned} \tag{2.30}$$

The Bogolyubov coefficients that interest us are the ones between $\{f_\Omega^{\rm KH,out}\}$ and $\{f_\Omega^{\infty}\}$. These coefficients will tell us how the outgoing mode, right outside the horizon, will be read in terms of the basis at infinity.

The computation of the Bogolyubov coefficient can be easily done following Unruh in [13]. He observed that, the non-analytical modes of (2.29) can be combined in such a way that their combination is analytical in the upper (lower) branch of the r-complex plane. Basically, this makes use of the continuation of the complex logarithm. For $z \in \mathbb{C}$, so $z = |z|e^{i\theta}$, we have that the principal branch of $\log(z)$ behaves as:

$$\log(z) = \log(|z|) + i\theta\,. \tag{2.31}$$

This allows us to write down two sets of modes $\Phi^{\pm}_{\Omega}$ at fixed energy Ω:

$$\Phi^{\pm}_{\Omega} = \mathcal{C}^{\pm}\left[f^{\mathrm{KH,out}}_{\Omega} + e^{\mp\frac{\pi\Omega}{\kappa_{\mathrm{KH}}}}\left(f^{\mathrm{KH,in}}_{\Omega}\right)^{*}\right], \tag{2.32}$$

where we have set $\kappa_{\mathrm{KH}} = (2r_s)^{-1}$ being the surface gravity of the horizon [43] and $\mathcal{C}^{\pm}$ are normalization constants. The sign $\pm$ corresponds to the two continuations of the logarithm on the upper and lower half-complex planes. Thus, we have:

$$\langle\Phi^{+}_{\Omega},\Phi^{+}_{\bar{\Omega}}\rangle = -\langle\Phi^{-}_{\Omega},\Phi^{-}_{\bar{\Omega}}\rangle = \delta(\Omega-\bar{\Omega}), \quad \langle\Phi^{+}_{\Omega},\Phi^{-}_{\bar{\Omega}}\rangle = 0. \tag{2.33}$$

This implies

$$\mathcal{C}^{\pm} = \frac{1}{1-e^{\mp\frac{2\Omega\pi}{\kappa_{\mathrm{KH}}}}}. \tag{2.34}$$

Moreover, with these normalization coefficients, one can directly check that

$$f^{\mathrm{KH},out}_{\Omega} = \Phi^{+}_{\Omega} + \Phi^{-}_{\Omega}. \tag{2.35}$$

Hence, since Φ^{+}_{Ω} (Φ^{-}_{Ω}) is analytical in r, it can be described with a superposition of only positive- (negative-) normed modes f^{∞}_{Ω} ($f^{\infty,*}_{\Omega}$), and the relation (2.12) reads

$$\Phi^{+}_{\Omega} = \int_0^{+\infty}\frac{\mathrm{d}\bar{\Omega}}{2\pi}\alpha_{\Omega\bar{\Omega}}f^{\infty}_{\bar{\Omega}}, \qquad \Phi^{-}_{\Omega} = \int_0^{+\infty}\frac{\mathrm{d}\bar{\Omega}}{2\pi}\beta_{\Omega\bar{\Omega}}\left(f^{\infty}_{\bar{\Omega}}\right)^{*}. \tag{2.36}$$

This, together with the definition of the Bogolyubov coefficients (2.12) leads to the direct computation of $|\beta_{\Omega\bar{\Omega}}|^2$, since, instead of $\langle(f^{\infty})^{*}, f^{\mathrm{KH,out}}\rangle$, we can compute:

$$\begin{aligned}\mathcal{C}^{-} = \langle\Phi^{-}_{\Omega}, f^{\mathrm{KH},out}_{\Omega}\rangle = \int\frac{\mathrm{d}\bar{\Omega}}{2\pi}\beta_{\Omega\bar{\Omega}}\langle\left(f^{\infty}_{\bar{\Omega}}\right)^{*}, f^{\mathrm{KH},out}_{\Omega}\rangle = \\ -\int\frac{\mathrm{d}\bar{\Omega}}{2\pi}\beta_{\Omega\bar{\Omega}}\beta^{*}_{\Omega\bar{\Omega}} = -\int\frac{\mathrm{d}\bar{\Omega}}{2\pi}|\beta_{\Omega\bar{\Omega}}|^2.\end{aligned} \tag{2.37}$$

The derivation of the Hawking effect can now be stated in this way: let us take the free-falling observer. If we assume that, while crossing the horizon, no particles are observed by him, then the vacuum will be set through the basis f^{KH}_{Ω}, we can evaluate the particle content of that state in terms of the modes detected by the asymptotic observer:

$$\langle\hat{N}_{\Omega}\rangle_{\mathrm{ff}} = \int\frac{\mathrm{d}\bar{\Omega}}{2\pi}|\beta_{\Omega\bar{\Omega}}|^2 = -\mathcal{C}^{-} = \frac{1}{e^{2\pi\Omega/\kappa_{\mathrm{KH}}}-1}, \tag{2.38}$$

where "ff" denotes that the mean value has taken on the vacuum for the free falling observer. The obtained spectrum represents a Bose-Einstein distribution in Ω, from which we can read a temperature temperature T_{H} (the so-called *Hawking temperature*)

$$T_{\mathrm{H}} = \frac{\kappa_{\mathrm{KH}}}{2\pi}. \tag{2.39}$$

This tells us that, if the free-falling observer is in vacuum, there is a particle production in terms of modes at infinity. Note that the spectrum at infinity will be also affected by the probability for each one of these modes, produced nearby the horizon, to climb the potential $V_l(r)$. The resulting distribution at infinity is thus modulated by this probability $\Gamma(l,\Omega)$, which is called *greybody factor* [42]:

$$n(\Omega,l)=\frac{\Gamma(l,\Omega)}{e^{2\pi\Omega/\kappa_{\rm KH}}-1}\,. \tag{2.40}$$

The presence of a greybody factor, however, does not change the thermal nature of the distribution, which is always peaked at $T_{\rm H}$.

2.2 A local approach: Hawking radiation as a tunneling

Let us now describe a second method for deriving Hawking radiation. This approach is based on the quantum tunneling technique [44], for which we will discuss the static, spherically symmetric case. More general cases, such as non-static situations and dynamical horizons treatment are extensively discussed, e.g. in [45, 46].

2.2.1 Quantum tunneling: from non-relativistic quantum mechanics to QFT

The tunneling process is a purely quantum-mechanical effect, which tells us that particles, being non-localized objects, can go through classically forbidden paths, with a non-zero probability. Let us make a brief example on how it should work.

Non-relativistic quantum mechanics

Suppose that we have a bounded one-dimensional $\mathbb{L}^1$-integrable classical potential $V(x)$, such that

$$\lim_{x\to\pm\infty}V(x)=0 \tag{2.41}$$

The probability for a quantum mechanical wave function $\Psi(x)$ with energy $E<\max\left(V(x)\right)$ to tunnel through (sometimes called *transmission coefficient*) it is given by the ratio of the norm of the transmitted wave $\Psi_>$ divided by the norm of the incident wave $\Psi_<$ before hitting the wall [47]

$$|T|^2=\frac{\|\Psi_>\|^2}{\|\Psi_<\|^2}. \tag{2.42}$$

For any shape of the potential, as long as the potential itself is only mildly time-dependent, this can be described by using a Wentzel-Kramers-Brillouin (WKB) approximation for the wave function. Here, restoring $\hbar$ in physical units

$$\Psi(x)=\Psi_0\exp\left(\tfrac{i}{\hbar}\sum_i\mathcal{S}_i(x)\hbar^i\right), \tag{2.43}$$

where we expanded $\mathcal{S}$ in powers of $\hbar$.

To leading order in $\hbar$, and considering the Schrödinger equation, the solution for ingoing and outgoing waves is determined by the classical action

$$\mathcal{S}_0 = \pm \int \mathrm{d}x \, \sqrt{2m(E - V(x))} \tag{2.44}$$

with E being the energy of the incident wave and m its mass. Thus, one can understand the tunneling process as occurring through a classically forbidden path where the exponent becomes complex – since inside the potential $E < V(x)$. This has some similarities with the case of gravitational paths, as we see below.

QFT in curved spacetime

Within a particle point of view, the Hawking effect can be intuitively described by the same cartoon picture already suggested by Hawking himself [11]. Close to but still outside the horizon, a Hawking pair consisting of a positive and a negative energy particle, can be created. The positive energy particle escapes the gravitational well and it is measured by an asymptotic observer, while the negative energy one falls into the black hole, where its existence on-shell is allowed by the spacelike nature of the Killing vector associated to stationarity in time of this geometry.

Courtesy of the energy budget provided by the black hole, we can describe this from a different perspective. Instead of a pair creation, we interpret the same process as a single particle coming from the interior and tunneling outwards in a quantum mechanical way. In fact, it is always possible to trade an inward-pointing negative Killing energy particle with a positive energy, outward-pointing one, just reversing the sign of time.

Similarly to what we have done for the non-relativistic particle, since our spacetime is static, we can make a WKB ansatz for the field, which obeys (2.5), having

$$\phi = \phi_0 e^{\frac{i}{\hbar}\sum_n \hbar^n \mathcal{S}_n(x)} = \phi_0 e^{\frac{i}{\hbar}\mathcal{S}_0 + \mathcal{O}(1)} \tag{2.45}$$

with $\mathcal{S}_0(x)$ the classical (or point-particle) action. The amplitude ϕ_0 is allowed to have a mild coordinate dependence, but it is usually treated as effectively constant. With our ansatz, the Klein-Gordon equation becomes the Hamilton–Jacobi equation to lowest order[2] in $\hbar$

$$\partial_a \mathcal{S}_0 \partial^a \mathcal{S}_0 = 0. \tag{2.46}$$

The interpretation of $\mathcal{S}_0$ as a point particle action is coherent with a definition of a notion of four-momentum k_a for a particle described by that action

$$k_a \equiv -\partial_a \mathcal{S}_0 \, . \tag{2.47}$$

Let us note that, with this definition, (2.46) becomes the dispersion relation for a massless particle. Within the geometry (2.17), it is convenient to define the Killing

[2]In principle we could also consider the sub-leading term $\mathcal{S}_1$. However, this does not contribute to the tunneling probability.

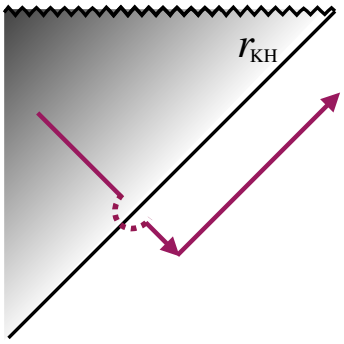

Figure 2.1: The Killing horizon is displayed as a null-line that separates the normal (unshaded) from the trapped region (grayshaded). The tunneling path shows a positive energy particle that starts in the interior on a past-directed outgoing null path, crosses the horizon on a complex path (dashed), and scatters into a future-directed outgoing null path, once it has crossed the horizon. This is equivalent to the negative energy particle tunneling inwards.

energy $\Omega = \chi^a k_a$, thus getting

$$\mathcal{S}_0 = -\Omega v + \int^r k_r(r)\,\mathrm{d}r\,. \tag{2.48}$$

Let us note that here, for simplicity, we have dropped the angular direction. So, in principle, we are restricting our study of ϕ to s-waves. However, due to the background symmetries, we will see that the angular directions do not play any role in the tunneling analysis.

Coming back to our discussion on the quantum-mechanical tunneling, in a system with gravitational tunneling the probability to reach a classically inaccessible region is given through complex paths, which is reminiscent to the case of the one-dimensional potential barrier. The positive energy particle inside a black hole is now interpreted to take a generically complex path across the horizon determined by $\mathcal{S}_0$, as shown in figure 2.1.

Finally, we can define the tunneling rate as the ratio between the transmitted fraction and the incident wave [48]

$$\Gamma = \frac{\|\phi_{>}\|^2}{\|\phi_{<}\|^2} = e^{-\frac{2}{\hbar}\mathrm{Im}(\mathcal{S}_0)}, \tag{2.49}$$

which is 1 along classical paths $\mathrm{Im}(\mathcal{S}_0) = 0$. This is connected to thermodynamics by following [49, 50]. Comparing the probability for a detector to absorb a particle P_{abs} with its probability to emit one P_{em} at a fixed energy Ω we get

$$\Gamma \equiv \frac{P_{\mathrm{em}}}{P_{\mathrm{abs}}} = e^{-\Omega/T_{\mathrm{H}}}, \tag{2.50}$$

thus finding that the detector is in a thermal equilibrium at (horizon) temperature T_{H}. So, the statistical interpretation, given by the rate of particle produced matches with the probabilistic interpretation for a single particle of being produced.

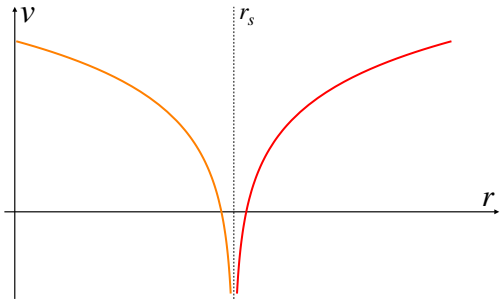

Figure 2.2: Trajectory of a particle with action (2.52) in the (v, r) plane. The particle infinitely peels out at the KH ($r = r_s$) both inside (orange line) and outside (red line).

Thus, whenever $\mathrm{Im}(\mathcal{S}_0) \propto \Omega$, we can read off a horizon temperature from the tunneling rate. However, the thermodynamics is only well-defined whenever the imaginary part is positive definite [46]

$$\mathrm{Im}(\mathcal{S}_0) > 0, \tag{2.51}$$

otherwise the process leads to inconsistencies such as the violation of the probabilistic interpretation.

2.2.2 Tunneling on a Schwarzschild background

Now we are ready to apply the tunneling machinery to the Schwarzschild geometry (2.17). In this case we already know how modes of a fixed Killing energy behave on the two sides of the horizon (2.29), in the EFB frame. We can read the particle action $\mathcal{S}_0$

$$\mathcal{S}_0 = -\Omega v + \Omega \int^r \mathrm{d}r \frac{2r_s}{r - r_s} \tag{2.52}$$

and consider a tunneling path which crosses the horizon. In figure 2.2 we give a plot of a constant $\mathcal{S}_0$ contour (i.e. the classical trajectory of the particle).

It is clear that in (2.52) any regular (so that crosses the horizon smoothly) tunneling path $v(r)$ does not rise any imaginary part from the first term on the L.H.S. of the equation. However, the r-dependent part of the integral develops a simple pole at the Killing horizon. Therefore we can, without any loss of generality take $v = \text{const.}$ and get

$$\mathrm{Im}(\mathcal{S}_0) = \mathrm{Im}\left[\Omega \int_{r_1}^{r_2} \mathrm{d}r \frac{2r_s}{r - r_s}\right] . \tag{2.53}$$

where $r_1 < r_s < r_2$. The imaginary part is given computing the integral in the r-complex plane. The simplest method is to add an $i\varepsilon$-prescription, shifting the pole in the imaginary axis $(r - r_s) \to (r - r_s - i\varepsilon)$, and then take the limit $\varepsilon \to 0^+$. Putting all together, we have, after some manipulations (cf. [46] for details)

$$\mathrm{Im}(\mathcal{S}_0) = \lim_{\varepsilon \to 0^+} \mathrm{Im}\left[\int_{r_1}^{r_2} \frac{\Omega \mathrm{d}r}{\kappa_{\mathrm{KH}}\,(r - r_s - i\varepsilon)}\right] = \frac{\pi\Omega}{\kappa_{\mathrm{KH}}} . \tag{2.54}$$

Finally, inserting (2.54) into (2.49) we get a Boltzmann factor, from which we can read the temperature, which turns out to be exactly $T_{\rm H}$:

$$\Gamma = e^{-\Omega/T_{\rm H}}\,, \qquad T_{\rm H} = \frac{\kappa_{\rm KH}}{2\pi}\,. \tag{2.55}$$

2.3 Tunneling vs Bogolyubov: equivalence of two methods

So far, throughout all this Chapter, we have shown two different derivations of the Hawking effect for a static, spherically symmetric, black hole geometry: the Bogolyubov coefficient calculation relates the modes at infinity with the near-horizon ones, thus relying on a global knowledge of the spacetime and on a choice of the vacuum state. The other, based on the quantum-tunneling formalism, tackles the same problem in a local way, interpreting the particle-production at the horizon as a tunnel-out of a particle – a WKB solution of the field equation – through a classically forbidden path across the horizon itself.

At first glance, these are two conceptually different methods. Within the tunneling approach, no knowledge of the observer at infinity is required and it is not clear where the choice of vacuum is actually performed. So, why do they give the same result?

Actually, at a closer look, one may note that, within the two methods, there are more similarities with respect to what we have just observed. Let us start from the formula of the tunneling rate (2.49). This equation interprets the probability of tunneling out of a single particle a the ratio of the "ratio between the transmitted fraction over the incident wave". Within a point-particle viewpoint, this is the ratio between the probability for a particle to tunnel-out across the horizon, over the probability of doing the reverse path. For concreteness, let us take equation (2.48) as an example of our point-particle action.

If $k_r(r)$ presents a simple pole, we have a non-analiticity on the WKB solution $\phi = \phi_0 e^{i\mathcal{S}_0}$ of the log-type in the exponential. The imaginary part of the action for the tunnel-out process and for the revers process are opposite in sign:

$$\mathrm{Im}(\mathcal{S}_0)|_{\rightarrow} = \mathrm{Im}\left[\Omega\int_{r_1}^{r_2}\mathrm{d}r\frac{2r_s}{r-r_s}\right] = -\mathrm{Im}\left[\Omega\int_{r_2}^{r_1}\mathrm{d}r\frac{2r_s}{r-r_s}\right] = -\mathrm{Im}(\mathcal{S}_0)|_{\leftarrow}. \tag{2.56}$$

This two imaginary parts correspond exactly to the coefficents that appear in (2.32) in between the in- and out-modes, therefore they match the two possible analytical continuation of the logarithmic singularity in the action. Thus, in equation (2.32), the combination $\Phi^{\pm}_{\Omega}$ correspond exactly to the two processes of out- and in-tunneling of our particle.

An important remark consists in noticing that the equivalence between a WKB solution like the one in (2.45), used for the tunneling, and a full solution in the near horizon region, such as (2.32) holds because of the infinite blueshift of the mode. The pole that is present within $k_r(r)$ makes the WKB mode to fullfil exactly the adiabaticity condition

$$\left|\frac{\dot{k_r}}{k_r^2}\right| \xrightarrow{r\to r_s} 0\,, \tag{2.57}$$

where the "dot" is the derivative with respect to the proper time of the free falling observer, which defines the vacuum state [38, 51] (we shall discuss this issue in Chapter 5). So, in the case of exponential peeling, there is no difference between the WKB-approximated solution and the full one at the horizon; therefore it is not surprising that $\Phi^{\pm}$ coincide with $\phi^{\rm WKB}$.

The probability of having an outgoing particle just outside the horizon is given by the sum of these two processes weighted with some probability P:

$$f_{\Omega}^{\rm KH,out} = P\Phi_{\Omega}^{-} + (1-P)\Phi_{\Omega}^{+}\,, \tag{2.58}$$

which tells us that a particle $f_{\Omega}^{\rm KH,out}$ can be originated by a emission with probability $P = P_{\rm em}$ and by the reverse process with probability $(1-P) = P_{\rm abs}$. From (2.32) we can derive:

$$P = \mathcal{C}^{-} = -\int \frac{{\rm d}\bar{\Omega}}{2\pi}|\beta_{\Omega\bar{\Omega}}|^2\,, \qquad 1-P = \mathcal{C}^{+} = \int \frac{{\rm d}\bar{\Omega}}{2\pi}|\alpha_{\Omega\bar{\Omega}}|^2\,. \tag{2.59}$$

Note that, by definition,

$$1 = \mathcal{C}^{+} + \mathcal{C}^{-} = \int \frac{{\rm d}\bar{\Omega}}{2\pi}\left(|\alpha_{\Omega\bar{\Omega}}|^2 - |\beta_{\Omega\bar{\Omega}}|^2\right), \tag{2.60}$$

which recovers the completeness relation for the Bogolyubov coefficients (2.13). From the tunneling amplitude (2.49) we have the rate, connected with $\mathrm{Im}(\mathcal{S}_0)|_{\rightarrow}$:

$$\Gamma = \frac{\|\phi_{>}\|^2}{\|\phi_{<}\|^2} = \frac{\langle f_{\Omega}^{\rm KH,out}, \Phi_{\Omega}^{-}\rangle}{\langle f_{\Omega}^{\rm KH,out}, \Phi_{\Omega}^{+}\rangle} = -\frac{P}{1-P} = e^{-2\pi\Omega/\kappa_{\rm KH}}\,. \tag{2.61}$$

This leads to:

$$\frac{\int \frac{{\rm d}\bar{\Omega}}{2\pi}|\beta_{\Omega\bar{\Omega}}|^2}{\int \frac{{\rm d}\bar{\Omega}}{2\pi}|\alpha_{\Omega\bar{\Omega}}|^2} = e^{-2\pi\Omega/\kappa_{\rm KH}}\,. \tag{2.62}$$

Putting altogether with the completeness relation one has:

$$\int \frac{{\rm d}\bar{\Omega}}{2\pi}|\beta_{\Omega\bar{\Omega}}|^2 = \int \frac{{\rm d}\bar{\Omega}}{2\pi}|\alpha_{\Omega\bar{\Omega}}|^2 e^{-2\pi\Omega/\kappa_{\rm KH}} = \left(1 + \int \frac{{\rm d}\bar{\Omega}}{2\pi}|\beta_{\Omega\bar{\Omega}}|^2\right) e^{-2\pi\Omega/\kappa_{\rm KH}}\,, \tag{2.63}$$

therefore we get

$$\int \frac{{\rm d}\bar{\Omega}}{2\pi}|\beta_{\Omega\bar{\Omega}}|^2 = \frac{1}{e^{\Omega/T_{\rm H}} - 1}\,, \tag{2.64}$$

obtaining the same result. Let us stress that $P < 0$, so it does not define, purely speaking, a probability distribution. The sign of P, however, points out precisely the role of the negative-norm modes in the process.

The compatibility of the two derivations allows us to point out a few things. First of all, both approaches are, in a spherically symmetric case, independent from the angles θ and φ: the rate of production of particles by the horizon is given only in terms of the produced particle's energy. As a tunneling calculation, this is obvious

from the fact that the non-analiticity of the action lies on the radial direction. For the Bogolyubov coefficients, we see that the potential – and so the $l-$dependence of the mode – drops when approaching both the Horizon and the asymptotic region. The angular dependence appears only in the greybody factor

We have shown that, considering the rate of tunneling of a point particle leads us to evaluate the single absorption and emission probability of the black hole. These quantities, in terms of the Bogolyubov transformation, match the integral of the modoulus squared of the α and β coefficients. Let us stress that, in principle, no vacuum state has been invoked so far. The role of the vacuum choice, in the Bogolyubov approach, tells us that the spectrum measured by an observer at infinity is proportional to the integral of $|\beta|^2$, because the observer in free-falling detects no particles. However, it is important to understand that the computation of the Bogolyubov coefficients – that relates two basis – and the definition of vacuum are two separated procedures. Here we have shown that the former computation can equivalently be done with the tunneling method, but the choice of the vacuum state remains something additional to both this calculations.

Within our treatment, we have considered vacuum for the freely-falling observer, since it is possible to show that this is the state described at late times after the formation of a black hole by collapsing matter [52]. This state is usually called *Unruh state*.

However, even if the choice of Unruh state is physically sensible, here we want to point out that another choice of vacuum would have produced a different outcome on the particle content on $\mathscr{I}^+$. For instance, a black hole in equilibrium with an external thermal bath, in the Hartle-Hawking state, would not evaporate [3].

The main conclusion is: the Bogolyubov relation between the analytical basis (2.32) and the non-analytical one (2.29) is always the same and it is equivalent to the tunneling rate (2.49). Everything is local at this level, since it has been worked out near horizon. The analysis become global once one introduces a notion of asymptotic basis (at $r \to \infty$) that, in the asymptotically-flat case, is equivalent to $\Phi^{\pm}_{\Omega}$, and imposes the Unruh vacuum. So, in this sense, the tunneling method and the Bogolyubov approach are equivalent.

2.4 Hawking temperature in Euclidean quantum gravity

While the Bogolyubov approach and the tunneling method turn out to be closely related (if not the same thing), an alternative derivation is given by the Euclidean path integral approach to QG [54]. The approach is based on considering the Eucledan gravitational path integral:

$$Z = \int [\mathcal{D}g]\, e^{-S[g]}\,, \tag{2.65}$$

[3] Actually, recent works have shown that it is possible to tune the future state on $\mathscr{I}^+$ by choosing appropriately the initial state on $\mathscr{I}^-$ [53]

where the integral runs over all the regular Euclidean metrics g_{ab} [4]. The classical action $S[g]$ contains the Einsten-Hilbert term R plus the Gibbons-Hawking boundary term $K_{\rm GH}$ [43]. The analysis performed by Hawking and Gibbons in [54] considers a saddle point approximation of Z, namely a gravitational instanton.

It turns out that objects with horizons are gravitational instantons only if the rotated time variable is taken with the right periodicity to avoid conical singularities. For example, let us consider the metric (2.17) in its Euclidean version $t \to \tau = it$:

$$\mathrm{d}s^2 = F(r)\mathrm{d}\tau^2 + \frac{\mathrm{d}r^2}{F(r)} + r^2\mathrm{d}\mathbb{S}_2\,. \tag{2.66}$$

The near-horizon limit of this metric is given by

$$\mathrm{d}s^2 = 2\kappa_{\rm KH}(r-r_s)\mathrm{d}\tau^2 + \frac{\mathrm{d}r^2}{2\kappa_{\rm KH}(r-r_s)} + r_s^2\mathrm{d}\mathbb{S}_2\,, \tag{2.67}$$

where $F(r) = 2\kappa_{\rm KH}(r-r_s) + \mathcal{O}((r-r_s)^2)$ as in the previous sections. Let us now define $\rho(r)$:

$$d\rho = \frac{\mathrm{d}r}{\sqrt{2\kappa_{\rm KH}(r-r_s)}}\,, \tag{2.68}$$

obtaining

$$\mathrm{d}s^2 = \rho^2\mathrm{d}(\kappa_{\rm KH}\tau)^2 + \mathrm{d}\rho^2 + r_s^2\mathrm{d}\mathbb{S}_2\,. \tag{2.69}$$

therefore the near-horizon metric is non-singular at $\rho = 0$ if we have a periodicity in the termal time:

$$\kappa_{\rm KH}\tau \to \kappa_{\rm KH}\tau + 2\pi n\,. \tag{2.70}$$

with $n \in \mathbb{Z}$. So, the period β to assign to τ is given by:

$$\beta = \frac{2\pi}{\kappa_{\rm KH}} = \frac{1}{T_{\rm H}}\,. \tag{2.71}$$

So, the periodicity in the Euclidean time is exactly the inverse of the Hawking temperature. The periodicity in the Euclidean metric, dramatically reflects into the quantum state defined onto it.

Let us consider a field $\hat{\phi}$ defined on the (Lorentzian) background (2.17). If the two-point function $\langle\hat{\phi}(0,\mathbf{y})\hat{\phi}(t,\mathbf{x})\rangle$ satisfy the so-called KMS condition [41, 56]:

$$\langle\hat{\phi}(0,\mathbf{y})\hat{\phi}(t,\mathbf{x})\rangle = \langle\hat{\phi}(t+i\beta,\mathbf{x})\hat{\phi}(0,\mathbf{y})\rangle \tag{2.72}$$

[4] The Wick rotation from Lorenzian to Euclidean spacetimes is not every time well defined. The main reason is that the notion of time is coordinate dependent and, if one starts directly studying the Euclidean path integral, rotating back from Euclidean to Lorentzian is not always possible. It has been shown that the procedure is well defined if the spacetime manifold $\mathcal{M}$ admits a well-defined timelike vector field [55]. In that context, the Wick rotation can be seen as taking two real section (a Euclidean version and its Lorentzian counterparts) of the same complex manifold.

then the state for the field $\hat{\phi}$ is thermal (in particular, the particle number reads as (2.38)).

If we define the evolution operator for the field $\hat{\phi}$ with respect to the time t felt by the asymptotic observer, then the evolution is determined by $\alpha_t = e^{i\hat{H}t}$, where $\hat{H}$ is the associated Hamiltonian operator. The periodicity in the thermal time tells us that the KMS condition (2.72) is satisfied if the metric enjoys the periodicity found in (2.71).

With this point of view, the thermality of the state is a matter of consistency in the gravitational background that has little to do with the specifics of the matter that we consider to live there.

Chapter 3

Hawking radiation in the lab: an analogue gravity perspective

Analogue Gravity (AG) models were developed, beginning in 1981 with William Unruh's seminal paper [16] with the aim to explore open questions that the discovery of black hole radiations left open, such as the trans-Planckian problem and the information-loss paradox. These models simulate QFT phenomena in curved spacetime within laboratory settings. In addition, they offer a concrete example in which the UV completion of the theory is explicitly known.

Regarding the information-loss paradox, this knowledge turns out to be particularly useful: taking into account the full Hilbert space of the system – made by the quantum perturbations and the UV degrees of freedom –, it is possible to show that no information-loss happens [17].

Interestingly, ten years after Unruh's first paper, it was realised that analogue gravity could provide a physical model for the trans-Planckian modes, believed to be relevant for the Hawking effect and the investigation of Hawking radiation in the presence of modified dispersion relations was further explored [18, 57, 58]. It was soon recognised that analogue gravity systems (see [59] for an extensive review) provide an ideal testing ground for the robustness of Hawking radiation against high-energy modifications. This is due to their theoretical simplicity and versatility as well as their capability to offer explicit tabletop experimental settings to test such predictions.

The natural presence of quantum fields with modified dispersion relations, which is a consequence of LV terms in the equation of motions, renders the analogue setting a perfect starting point for this work.

In this Chapter, which results are based on [40], we will briefly review how QFT in curved spacetime can be derived starting from the fluid dynamics and how analogue black holes arise as solutions of the hydrodynamical equations. We will then review the main results presented in the literature concerning Hawking radiation of analogue black holes. Finally, with the help of the tunneling approach – never used before in this framework – we will revise some known result, shedding some light onto questions left open in previous works.

3.1 Analogue gravity in a nutshell: from fluid dynamics to curved spacetime

The idea that a fluid can behave as a curved background is based on a very simple physical intuition: a moving fluid will drag its own perturbations (sound waves) along with its flow. Therefore, if the flow is non-trivial, the sound waves trajectories will be bent accordingly with the velocity of the background, analogously to what happens to light rays when the spacetime is curved. In a situation where the fluid velocity overcomes the speed of sound for the perturbations, then we have a region that traps any sound wave, namely a black hole analogue (or "sonic hole", or "dumb hole", as commonly named in the literature).

Mathematically speaking, the equivalence can be shown as follows. Without external forces, a perfect fluid – therefore irrotational and non-viscous – fulfills the continuity and the Euler equations [60]:

$$\frac{\partial \rho}{\partial t} + \nabla \cdot (\rho \mathbf{v}) = 0 \,, \qquad \nabla p = -\rho \left[\frac{\partial \mathbf{v}}{\partial t} + (\mathbf{v} \cdot \nabla)\mathbf{v} \right] \,, \tag{3.1}$$

where ρ is the density, p the pressure and $\mathbf{v}$ is the velocity of the fluid. Being irrotational, the velocity vector satisfy $\nabla \times \mathbf{v} = 0$, thus allows for the introduction of a potential ϕ such that $\mathbf{v} = \nabla\phi$. Let us consider a barotropic fluid, that is endowed with an equation of state $\rho = \rho(p)$. If we now define:

$$\phi = \phi_0 + \phi_1 \,, \quad \rho = \rho_0 + \rho_1 \,, \quad p = p_0 + p_1 \,, \quad \mathbf{v} = \mathbf{v}_0 + \mathbf{v}_1 \,, \tag{3.2}$$

where the fields with subscript "1" are considered perturbations with respect to the background quantities with subscript "0", we can show that the linearized version of equations (3.1) become a Klein-Gordon equation for the perturbation ϕ_1 [16, 59]

$$\Box_g \phi_1 = 0 \,. \tag{3.3}$$

Here the the operator $\Box_g$ is the D'Alambert operator, built with the so-called "acoustic metric" g_{ab}:

$$g_{ab} = \frac{\rho_0}{c_s^2} \begin{pmatrix} -(c_s^2 - \mathbf{v_0} \cdot \mathbf{v_0}) & -\mathbf{v}_0^{\mathbf{T}} \\ -\mathbf{v}_0 & \mathbb{I}_{3\times 3} \end{pmatrix} \,. \tag{3.4}$$

The speed of sound c_s is given by the equation of state $c_s^2 = \partial p / \partial \rho$. The derivation of this result involves simple algebra (see [59] for details) and we will not report the calculations, which are not instructive for the aim of this Chapter.

Here we stress the following: equation (3.2) tells us that phonons – sound perturbation in a fluid – behave as a massless scalar field in an acoustic geometry (3.4), determined by the background value of the fluid flow. Let us emphasize that, even if geometry corresponds to a relativistic $(3+1)$-dimensional Lorentzian metric, the tensor g_{ab} comes out as an effective combination of the background solution of the system (3.1) and has nothing to do with the Einstein field equations. Therefore, beside being quite tempting, we have to keep in mind that it is not possible to study the gravitational dynamics in analogue settings. Instead, as we shall see, analogue spacetimes are very useful in probing the kinematics of – classical or quantum – fields in curved spacetimes.

3.1.1 Black holes analogues

Let us now see how analogue black holes geometries arise in the case of acoustic metrics. In the following, in order to simplify the notation, we shall drop the subscript "0" from the background geometry. This will be no source of confusion, since the linearized hydrodynamics reduce to a Klein-Gordon equation only for the perturbation ϕ (for which we are going to drop the subscript "1") and no other equation for the other physical perturbations is given.

Heuristically speaking, a sound ray living on top of the flowing fluid moves with speed c_s along some direction $\mathbf{n}$ with respect to the flow. The total speed with respect to the laboratory frame is:

$$\frac{\mathrm{d}\mathbf{x}}{\mathrm{d}t} = \pm c_s \mathbf{n} + \mathbf{v}\,. \tag{3.5}$$

Since $\mathbf{n}$ is a spatial normalized vector ($\mathbf{n}\cdot\mathbf{n}$=1) we can rewrite the trajectory in terms of a null curve of the effective geometry [59]

$$0 = \mathrm{d}s^2 = -c_s \mathrm{d}t^2 + (\mathrm{d}\mathbf{x} - \mathbf{v}\mathrm{d}t)^2 = -[c_s^2 - \mathbf{v}^2]\mathrm{d}t^2 - 2\mathbf{v}\cdot\mathrm{d}\mathbf{x}\mathrm{d}t + \mathrm{d}\mathbf{x}\cdot\mathrm{d}\mathbf{x}\,, \tag{3.6}$$

which are precisely the null curves of the metric (3.4). Let us observe that, any particle following (3.5), for a fixed flow $\mathbf{v}$, cannot travel against the flow whenever $|c_s| \leq |\mathbf{v}|$. This tells us that the region of the spacetime defined by the metric (3.4) in which the flow velocity overcomes the speed of sound is a special region for sound rays: any wave propagating in that region is obliged to follow the flow direction.

At the level of the effective geometry, this can be determined by the metric, just looking at the component g_{00}. The spacetime position in which the flow equates c_s is given by the equation $g_{00} = 0$. Therefore it is extremely useful the definition of the vector:

$$\chi^a \partial_a = \partial_t \implies g_{00} = \frac{c_s^2}{\rho} g_{ab}\chi^a\chi^b = \frac{c_s^2}{\rho}|\chi|^2\,. \tag{3.7}$$

Wherever the norm of χ vanishes, we have that the null rays of g_{ab} are dragged by the flow. In this sense $g_{00} = 0$ defines the boundary of an ergoregion, namely a portion of spacetime where even sound waves must move accordingly with $\mathbf{v}$.

Let us now take an inward-pointing flow. Every time that the normal component of the fluid velocity $v_\perp$ overcomes the speed of sound, this defines a trapping region, namely a point where the normal component of (3.5) has the same sign of $v_\perp$, and a sound wave must move inward. As in GR, the union of all the trapping surface gives an apparent horizon.

However, in order to define a black hole region for these geometries, we need to specify the event horizon. Within a gravitational setting, the definition of an event horizon is a global concept: one must take trace of the whole history of the universe and characterize the portion that does not allow the null rays to escape [61].

In case of stationary spacetimes the definition becomes easier, because the position of the outermost trapping surface is invariant under time translation (where with "time" we mean the time direction defining the isometry). In that case the event horizon, which coincides with the apparent horizon, becomes a Killing horizon, defined as the null hypersurface where the norm of the Killing vector goes to 0.

Here, the analogous of stationary spacetimes are the ones where the flow is "steady", namely when the vector χ is a symmetry, thus a Killing vector for the metric (3.4). If this is the case, the Killing horizon is given by:

$$|\chi|^2 = g_{00} = c_s^2 - \mathbf{v}^2 = 0\,. \tag{3.8}$$

This equation defines the boundary of a black hole region, to which we can associate a geometrical notion surface gravity $\kappa_{\rm KH}$ through the normal derivative computed at the horizon:

$$\kappa_{\rm KH} = \frac{1}{2}\nabla_n(c_s^2 - \mathbf{v}^2)\Big|_{c_s^2=\mathbf{v}^2}\,, \tag{3.9}$$

where the derivative ∇_n is taken to be along the direction normal to the surface $c_s^2 - \mathbf{v}^2 = 0$.

Although the definition of a black hole region and horizon's surface gravity has been presented in the steady-flow case, it is worth mentioning that it is possible to give a similar definition in the case of non-steady flows, for more details see [59].

3.1.2 Laboratory frame vs preferred frame

In the previous section we have seen how to introduce the concept of a sonic black hole, trapping the sound waves which enters the horizon. Before studying of the quantum properties of these object, let us take some time to introduce some geometrical definitions, which will be useful in the rest of the present Chapter.

The description of analogue systems in terms of an effective metric, makes these systems taste very much likely gravitational spacetimes. However, it is important to make a crucial disclaimer. In equation (3.8) we made use of the stationarity of the metric to define the Killing horizon. Unlike relativistic settings, here the meaning of the Killing time has a precise definition in physical terms. In fact, any analogue experiment is automatically endowed with a special notion of time. The fact is that these systems corresponds to a specific experimental settings that take place in a laboratory. The appearance of an effective geometry for the fluid perturbation is nothing else than an artifact and no real curved geometry is present. Instead they are endowed with a notion of time that recalls more a Newtonian definition instead of a relativistic one. If one looks to our starting point (3.1), there is no ambiguity in what is the time coordinate that define the evolution of the phyisical quantities characterizing the fluid. Actually, an observer sitting down in the lab, will be able to describe the whole evolution through the coordinate time t, which corresponds to the so-called *laboratory frame*. Within this frame, the role of time is played by the vector χ and a steady-flow represents a fluid which velocity $\mathbf{v}$ is only space-dependent, that is $\mathbf{v} = \mathbf{v}(\mathbf{x})$. Indeed, that observer experiences a (almost) flat spacetime given by

$$\eta_{ab} = \mathrm{diag}(-c^2, 1, 1, 1) \tag{3.10}$$

for which the (flat) time coordinate is given precisely by χ and c is the speed of light.

In contrast, a ray traveling inside the fluid is dragged by it. That allows us to define the so-called *preferred frame*, in which the fluid is at rest:

$$u^a \partial_a = \frac{1}{c_s}\left(\partial_t + \mathbf{v}\cdot\nabla\right). \tag{3.11}$$

This is a natural description for someone moving with respect to the fluid, which will be useful in the following sections.

3.2 Quantum phonons

Now that we have our geometry, let us see how to simulate quantum fields, on analogue systems. To this aim, the best candidates are quantum fluids – such as superfluids or Bose-Einstein condensates (BEC) – because the offer features which better adapts to quantum effects, for instance Hawking radiation. They show a high degree of quantum coherence and low speed of sound – therefore suitable for the formation of black hole gemoetries – and are characterized by very low temperatures, which reduces the noise. This last aspect is crucial, since the correspondent astrophysical case renders the Hawking flux practically impossible to measure, due to the difference between an astrophysical-black hole temperature and the enviromental one. If the enviroment and the radiation are of the same order, then experiments are possible.

BECs have been proposed as a possible way towards analogue Hawking radiation in the early 2000s [62, 63] and they are still today one of the most studied systems for simulating quantum fields in curved spacetimes.

3.2.1 Quantum fields from BECs: a proxy for Lorentz violation

Let us take a diluted gas of bosons, described by a bosonic quantum field $\hat{\Psi}$, obeying the following equation of motion [59, 63, 64]

$$i\hbar\partial_t\hat{\Psi} = \left[-\frac{\hbar^2}{2m}\nabla^2 + V(\mathbf{x}) + g\hat{\Psi}^\dagger\hat{\Psi}\right]\hat{\Psi}\,, \tag{3.12}$$

where m is the atomic mass, g is the effective coupling and V is an external potential. The ground state of the field $\hat{\Psi}$ describes a condensate. So, if $\Psi_0 = \langle\hat{\Psi}\rangle$ is the expectation value of the field operator, the condensate is defined as a solution of the Gross-Pitaevskii equation:

$$i\hbar\partial_t\Psi_0 = \left[-\frac{\hbar^2}{2m}\nabla^2 + V(\mathbf{x}) + g\rho_0\right]\Psi_0\,, \tag{3.13}$$

with $\rho_0 = |\Psi_0|^2$ being the particle density. Within the so-called Madelung representation, we can write the wave function for the ground state as:

$$\Psi_0 = \sqrt{\rho_0}e^{-i\theta/\hbar} \tag{3.14}$$

with θ being the function defining the phase. The background velocity will be given by [59]

$$\mathbf{v} = \frac{\nabla\theta}{m}\,. \tag{3.15}$$

QFT arises once one considers a perturbative treatment of $\hat{\Psi}$ around its expectation value Ψ_0:

$$\hat{\psi} = \frac{\hat{\Psi} - \Psi_0}{\Psi_0}\,. \tag{3.16}$$

The linearization of equation (3.12) in terms of $\hat{\psi}$ returns the Bogolyubov-de Gennes equation

$$i\hbar\partial_t\hat{\psi} = \left[-\frac{\hbar^2}{2m\rho_0}\nabla\cdot(\rho_0\nabla) - i\hbar\mathbf{v}\cdot\nabla + mc_s^2\right]\hat{\psi} + mc_s^2\hat{\psi}^\dagger\,, \tag{3.17}$$

where $c_s = \sqrt{g\rho_0/m}$ is the speed of sound. This equation couples $\hat{\psi}$ and $\hat{\psi}^\dagger$ and contains only first derivatives apart from the first term on the right-hand-side. One can go to Fourier space, defining

$$\Omega\hat{\psi} = i\hbar\partial_t\hat{\psi}\,, \quad \mathbf{k}\hat{\psi} = i\hbar\nabla\hat{\psi} \tag{3.18}$$

and, combining (3.17) with its complex conjugate, one obtains that $\hat{\psi}$ behaves as a particle obeying a supersonic dispersion relation in the eikonal approximation (see [59] for details):

$$(\Omega - \mathbf{v}\cdot\mathbf{k})^2 = \omega(k)^2 = c_s^2k^2\left(1 + \frac{c_s^2k^2}{\Lambda^2}\right)\,, \tag{3.19}$$

where $\Lambda = 2mc_s^2/\hbar$ is called "healing frequency". Equation (3.19) describes a modified dispersion relation (MDR) for a fluctuation of the bosonic field $\hat{\Psi}$, moving onto a geometric background of the type (3.4) with flow velocity $\mathbf{v}$ and speed of sound c_s.

Within the background geometry, that dispersion relation describes an example of Lorentz-violating behaviour. The sound-relativistic behaviour is recovered at low frequencies ($k^2 \ll \Lambda^2$), while at high frequencies the behaviour resembles the one of an individual gas particle, for which $\omega = \hbar^2k^2/(2m)$.

Let us point out that (3.19) highlights the role of the two frames described in section 3.1.2. Here the energy Ω is the energy defined with respect to the laboratory frame, while the combination

$$\omega = \Omega - \mathbf{k}\cdot\mathbf{v} \tag{3.20}$$

represents the energy defined with respect to the preferred frame u given in (3.11). We can immediately see that the form of the dispersion relation (3.19) takes a particularly easy form only if expressed in the preferred frame.

3.2.2 Analogue black hole radiation

The possibility to study quantum fluctuation onto a curved background allows the investigation of radiative properties by black hole horizon. Hawking radiation seems to be an extremely robust effect, both theoretically (see e.g. [58, 65–70]) and, most importantly, at the experimental level, in the context of Bose-Einstein condensates [71–74] (see also [75] for a review and other references).

The experimental approach is based on the analysis of the correlation function between the Hawking quanta and its partner. In gravitational physics, the region inside the horizon is not accessible, while in analogue models one has complete control on the whole system, thus making possible to probe both the particles. The evaluation of the correlation function between those two modes can be done in the momentum space, thus giving the k-space correlation spectrum $\langle \hat{b}_{k,\mathrm{HR}} \hat{b}_{k,\mathrm{HP}} \rangle$[1]. This quantity is linked to the Bogolyubov coefficients (2.12) through [71, 72]:

$$|\langle \hat{b}_{k,\mathrm{HR}} \hat{b}_{k,\mathrm{HP}} \rangle|^2 = |\beta|_k^2 |\alpha|_k^2 \tag{3.21}$$

where we have set

$$|\beta|_k^2 = \int \frac{\mathrm{d}\bar{k}}{2\pi} |\beta_{k\bar{k}}|^2 \,, \quad |\alpha|_k^2 = \int \frac{\mathrm{d}\bar{k}}{2\pi} |\alpha_{k\bar{k}}|^2 \,. \tag{3.22}$$

Employing the completeness relation $1 = |\alpha|_k^2 - |\beta|_k^2$, one can deduce

$$|\langle \hat{b}_{k,\mathrm{HR}} \hat{b}_{k,\mathrm{HP}} \rangle|^2 = |\beta|_k^2 (1 + |\beta|_k^2) \tag{3.23}$$

and extract the shape of $|\beta|_k^2$. This approach is then strongly based on a Bogolyubov analysis, which has been the main tool also at theoretical level.

Modified dispersion relations

Interestingly, the presence of modified dispersion in analogue system has been shown to not drastically modify the effect of particle production by the horizon. This was confirmed both at theoretical and at experimental levels [76–79]. Whenever the surface gravity of the horizon κ_{H} is much smaller than the healing frequency $\kappa_{\mathrm{H}} \ll \Lambda$ the thermal spectrum, peaked at the Hawking temperature, is recovered [19].

However, the presence of dispersion, makes the sonic horizon not to represent anymore a causal boundary (in the sense of the sonic causal cone). Therefore, deviation from thermality is expected [80].

In this context, the Bogolyubov method, even if extremely useful in an experimental setting, does not allow an easy analytical treatment. The analytical procedures developed in this regard [19] are technically quite involved and stop to the 0th order in the $\kappa_{\mathrm{H}}/\Lambda$ analysis.

On the other hand, the tunneling method presented in Chapter 2 has the advantage to study the problem in a point particle picture, thus being technically very affordable and does not require any notion of the asymptotics to be applied.

In the following section we aim to study the analogue Hawking effect in presence of dispersion, with the help of the tunneling picture. We will show that this

[1] where "HR" states for the Hawking quanta and "HP" for the partner

derivation is able to capture the deviation from thermality induced by the dispersive character of the particles we will consider. This fact will lead to interesting considerations.

3.3 Analogue Hawking radiation: tunneling particles with dispersion

Let us consider a $(1+1)$-dimensional stationary geometry, in which the background acoustic metric is given by the line-element

$$\mathrm{d}s^2 = -\mathrm{d}t^2 + (\mathrm{d}x - v(x)\mathrm{d}t)^2 = -(1-v^2(x))\mathrm{d}t^2 - 2v(x)\mathrm{d}x\mathrm{d}t + \mathrm{d}x^2\,, \tag{3.24}$$

which corresponds to (3.4), where the flow velocity is completely given by its x-component and it does not depend on time. Additionally, we have set $c_s^2 = 1$, in order to further simplify the system.

It is possible to show that the sign of $v(x)$ determines the nature of this spacetime. This line-element describes the Painlevé-Gullstrand coordinates of a sonic black hole if $v(x) \leq 0$ and of a sonic white hole if $v(x) \geq 0$ [81]. In the following we are going to focus on the former case. Hereinafter, we will omit to write the $x-$dependence explicitly, unless necessary. Since the metric is stationary, it enjoys the time translation invariance in the laboratory frame, given by $\chi^a\partial_a = \partial_t$.

The preferred frame (3.11) takes the form

$$u^a\partial_a \equiv (\partial_t + v\partial_x)\,, \qquad s^a\partial_a \equiv \partial_x\,. \tag{3.25}$$

Here, we introduced s^a as the orthonormal vector to u^a. The sonic horizon (3.2) of this geometry is located at

$$|\chi|^2 = v^2 - 1 = 0\,. \tag{3.26}$$

Let us emphasize that, depending on the value that $v(x)$ assumes, this object does/does not describe a sonic hole. In particular we will talk about *supercritical flow* if $|v| > 1$ in some region of the acoustic spacetime, instead we will name *subcritical* the flow which never overcomes the speed of sound and as *critical* the case at which $\sup_x |v(x)| = 1$.

In the following discussion, we will focus in objects with at most a single horizon, therefore, no particular restriction will be made on the profile of $v(x)$ apart from the request of being a monotonous function everywhere.

3.3.1 Particles with MDR

In section 3.2.1 we have seen that quantum perturbation can arise with MDRs. Here we will not specify the microscopic model that originate the dispersion, but, keeping in mind the BEC case, we will generically consider a scalar perturbation ϕ living on this geometry and obeying a generic field equation with dispersion [82]:

$$-(\partial_t + \partial_x v)(\partial_t + v\partial_x)\phi + F(\partial_x^2, \Lambda)\phi = 0. \tag{3.27}$$

The function F is in principle free and it is the origin of the dispersion in our simple model. However, in order to detect the effects of dispersion, we will consider F to be expanded in powers of ∂_x/Λ, being Λ the cut-off energy scale. Taking the first nonrelativistic correction, we generically can write:

$$\left(\Box + \xi\frac{\Delta^2}{\Lambda^2}\right)\phi = 0\,. \tag{3.28}$$

Here $\Delta = (g^{ab} + u^a u^b)\nabla_a\nabla_b$ is a purely spatial operator in the preferred frame provided via the flow four-velocity u^a. The parameter $\xi = \pm 1$ – which can be always set to $|\xi| = 1$ up to a rescaling of Λ – determines the sign of the higher derivative operators. Let us stress that different analogue systems predict different values for such parameters [76, 78].

In what follows, we shall call the dispersion relations with $\xi = \pm 1$ superluminal (upper sign) and subluminal (lower sign) respectively, as they correspond to cases for which the group velocity of perturbations is always larger/smaller than the speed of sound.

WKB ansatz

As required by the tunneling treatment, we need to provide a particle interpretation to the field ϕ. To this aim, we adopt a WKB approximation (2.45)

$$\phi = \phi_0 e^{i\mathcal{S}} \quad \text{and} \quad k_a = -\partial_a\mathcal{S} \tag{3.29}$$

where ϕ_0 is a slowly varying amplitude and S is a phase that represents the point-particle action.

The constant phase contours of ϕ yield the trajectory of the associated ray. Introducing the four-momentum k_a enables us to rewrite the field equation as a dispersion relation for a point particle, at the leading order in the WKB formalism

$$\omega^2 = \left(k^2 + \xi\frac{k^4}{\Lambda^2}\right)\,. \tag{3.30}$$

The relation for $\omega(k)$ given in (3.30) has been written in the preferred frame, such that $\omega = k_a u^a$ becomes the preferred notion of energy and $k = k_a s^a$ the preferred (spatial) momentum. For $\xi = 1$ this coincides exactly with (3.19).

Due to the stationarity of our flow, the system provides a notion of Killing energy $\Omega = k_a\chi^a$ for the particle. This can be linked to the preferred frame's energy ω in the very simple way, analogously to what we did in (3.19)[2]

$$\Omega = \omega - vk\,. \tag{3.31}$$

Since Ω is associated to a translational symmetry, the idea is to find mode solutions ϕ_Ω of (3.30) at fixed Killing energy, which can be proven to be a conserved quantity even for MDR [83]. This, together with the dependence of our modified dispersion relation on Λ, strongly suggest the introduction of a dimensionless parameter

$$\alpha \equiv \Omega/\Lambda \tag{3.32}$$

[2]Note that here we have defined k with the opposite sign

that controls the deviations from the relativistic behaviour – recovered in the limit $\alpha \to 0$ ($\Lambda \to \infty$). We will see the importance of this parameter every time a modification to the relativistic dispersion relation arises.

Characteristics and turning point

In order to deal with a point particle we shall consider a superposition of monochromatic modes ϕ_Ω, peaked around some energy Ω, which trajectory is identified with the group velocity c_g:

$$c_g = \frac{\partial \omega}{\partial k} = \frac{k}{\omega}\left(1 + 2\xi\frac{k^2}{\Lambda^2}\right) . \tag{3.33}$$

Let us point out that, as anticipated, from the above expression follows immediately that for any k one has $|c_g| \geq 1$ for $\xi > 0$ and $|c_g| \leq 1$ for $\xi < 0$. The corresponding trajectory is locally given by

$$(c_g u_a + s_a)\mathrm{d}x^a = 0 \iff \frac{\mathrm{d}t}{\mathrm{d}x} = \frac{1}{c_g + v}\,, \tag{3.34}$$

where the dual vectors $u_a = (-1, 0)$ and $s_a = (-v, 1)$ are deduced from (3.25). The above expression also implies that the action for such point particle will take the form

$$\mathcal{S} = -\Omega \int \frac{(c_g u_a + s_a)}{(c_g u_t + s_t)}\mathrm{d}x^a = -\Omega\left(t + \int \frac{\mathrm{d}x}{c_g + v}\right) \tag{3.35}$$

The last expression can be formally integrated, to obtain the shape of the trajectory $t(x, \alpha)$ in the (x, t)-plane, which, as we shall see, is a function that depends on the Killing energy of the particle through α. For a relativistic particle, $c_g = \pm 1$ which exhibits that (3.34) describes an everywhere regular, ingoing mode as well as an outgoing mode with a simple pole at the Killing horizon, where $1 + v = 0$.

However, for modified dispersion relations the solution space is larger [38]: analysing (3.30), while keeping Ω fixed, amounts to solving a 4^{th} order algebraic equation. Nonetheless, the number of solutions at any given point x is not always the same, and in particular it depends on the norm of the Killing vector. This becomes clear when plugging equation (3.31) into the dispersion relation (3.30) so to obtain

$$\xi\frac{k^4}{\Lambda^2} - \left(v^2 - 1\right)k^2 - 2v\Omega k - \Omega^2 = 0\,. \tag{3.36}$$

Let us consider a supercritical flow describing a black hole, so that $v(x) < 0$ everywhere and the black hole region defined by $|v| > 1$. We find that all the coefficients in front of the various k^n-terms are of fixed-sign, with the exception of the coefficient in front of k^2. This particular one is proportional to $|\chi|^2$ and thus changes sign at the Killing horizon. Therefore, there will always be a region of spacetime with four real solutions for k and another one where this number reduces to two.

The boundary between these two regions depends on the energy and is located at the point $x_{\text{TP}}(\alpha)$ (with TP standing for "turning point") where two out of the four solutions become degenerate. In terms of trajectories, this represents two smoothly

merging trajectories at $x_{\text{TP}}(\alpha)$. The name turning point can be understood graphically in the (t, x)-plane. The curves at the meeting point can always be interpreted as two branches of a single trajectory that, in the (t, x)-plane, turns back at $x_{\text{TP}}(\alpha)$. Additionally, the position of $x_{\text{TP}}(\alpha)$ depends crucially on the sign of ξ. In the superluminal case, $x_{\text{TP}}(\alpha)$ can always be found inside the horizon, where $|\chi|^2 > 0$, while in the subluminal case $x_{\text{TP}}(\alpha)$ lies outside. This follows directly from the discriminant of (3.36). The shape of the trajectories is sketched for both cases in figure 3.1.

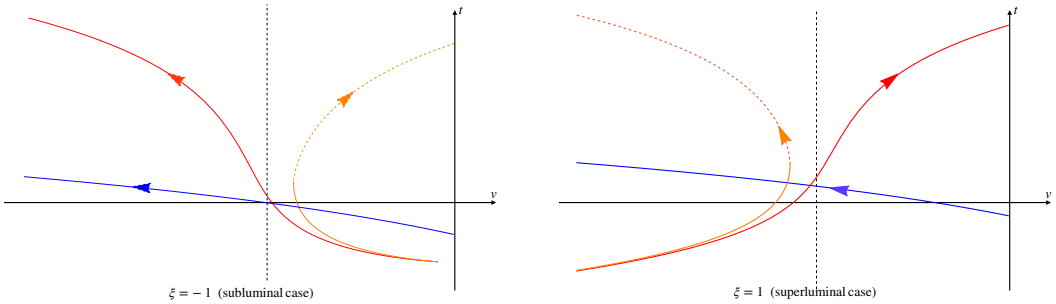

Figure 3.1: Example of the four different solution of (3.36) at fixed Ω. The horizontal axis shows v, without specifying any profile $v(x)$ yet. The dashed black vertical line is the Killing horizon $v = -1$ in both figures. In all plots, we have taken $\alpha = 0.02$ for each ray. Left panel: subluminal case ($\xi = -1$); we see that the turning point, where the dashed and the solid orange lines meet, lies outside the Killing horizon. Right panel: superluminal case ($\xi = 1$) for which we find turning point to be inside the Killing horizon. Both cases share a regular mode (in blue) which travels inwards and a mode (in red) which lingers at the horizon. The latter changes its direction depending on the sign of ξ, while the blue one remains qualitatively unchanged.

In the limit for which $\alpha \to 0$ ($\Lambda \to \infty$), the sub- and superluminal cases degenerate and we recover the relativistic behaviour, that is, two of the four solutions cease to exist, leaving us only with the upper branch of the turning mode (the dashed part of figure 3.1), on one side of the Killing horizon, and with half of the lingering mode on the other side. These two represent the usual outgoing-ingoing relativistic particles (the would-be Hawking pairs) that peel infinitely at the horizon.

3.3.2 Mimicking an horizon: the approximant

Technically speaking, the application of the tunneling method requires the presence of a simple pole in the particle action $\mathcal{S}$. This is clear from the definition of the rate (2.49), which needs the action to enjoy an imaginary part. The only way to have a nonvanishing imaginary part in the real axis is then to have a divergence with nonzero residue, i.e. a simple pole.

However, in a non relativistic scenario, nothing comparable will ever occur, given that the modified dispersion relation, never produces an exact peeling (see the qualitative difference between figures 3.1 and 2.2) and therefore the particle trajectories at the Killing horizon remain analytic. In turn, one would expect an absence of Hawking radiation in this settings – or at the least that this effect cannot be described via the tunneling method. On the other hand, we know that that Hawking

effect must be there also with MDRs and that the tunneling method fits its description in the relativistic limit. Therefore, there must be a way to implement that technique to recover the horizon radiation, at least perturbatively around $\alpha = 0$.

Actually, in a naive α-expansion of the group velocity

$$c_g = 1 + \delta c_g(x, \alpha) + \dots \,, \tag{3.37}$$

with $|\delta c_g(x, \alpha)| \ll 1$, one can compute the correction to the tunneling rate. In the case of a dispersion relation like (3.30), the correction assumes the form $\delta c_g(x, \alpha) = \alpha^2 f(x)$, with $f(x)$ depending on the geometry and on the sign of ξ. Hence

$$\frac{\mathrm{d}t}{\mathrm{d}x} = \frac{1}{c_g + v} = \frac{1}{1+v} - \frac{\alpha^2 f(x)}{(1+v)^2} + \cdots \,, \tag{3.38}$$

that causes a non-zero contribution when plugged into $\mathrm{Im}(\mathcal{S})$ as in equation (2.49), thus giving a non-trivial tunneling amplitude

$$\Gamma = e^{-\Omega/T(\alpha)} \,. \tag{3.39}$$

The associated "effective temperature" $T(\alpha)$ (as it stems *per se* from an approximated trajectory) will then receive corrections of order α^2. This will be given by the residue of the correction

$$T(\alpha) = \frac{\kappa_{\mathrm{KH}}}{2\pi} \left[1 + \alpha^2 \mathrm{Res} \left(\frac{f(x)}{(1+v(x))^2}, \, x_{\mathrm{KH}} \right) + \cdots \right] \,, \tag{3.40}$$

that coincides with T_{H} for $\alpha \to 0^+$. Let us emphasize that the tunneling calculations is sensitive only to the logarithmic divergence of the point-particle action (i.e. the residue of (3.34)). Higher-order poles may appear, but they give only real contributions to $\mathcal{S}$ (see, cf. [84, 85]) and do not play any role in the tunneling rate Γ.

This is an example about how to capture the correction to the thermal behaviour, for $\alpha \ll 1$. Those correction, makes $T(\alpha)$ not to be energy-independent, thus represents a deviation from thermality. Those deviations, as we shall see, are anyway very mild since they arise at the next-to-leading order in the perturbative parameter α.

The perturbative analysis for small α tells us something about the capability of the tunneling method to capture the dispersive character of the perturbation. However, this treatment can be improved, going beyond such an approximation. Let us see how.

Approximating the modes: outside the horizon

From the perturbative analysis, it becomes clear that the main protagonists in this computation are given by the upper branch of the turning mode and the lingering mode. These two branches are the only ones, together with the ingoing mode, that can reach the region $|v| \ll 1$. Quite interestingly, we can show that their lower branches are never defined in $v = 0$ (which is the asymptotically flat region of (3.24)). In fact, setting $v = 0$ in (3.31) and (3.30), we get:

$$\omega = \Omega + O(v) \,, \qquad \Omega^2 = k^2 + \xi \frac{k^4}{\Lambda^2} + O(v) \,. \tag{3.41}$$

Since for $v = 0$ the dispersion relation becomes an equation for k^2 we obtain only two real solutions with opposite signs that we name $k_0^{\pm}(\Omega)$, with $k_0^+ = -k_0^-$. Only these solutions will reach the $v = 0$ line for both superluminal and subluminal dispersion relations.

Specifically, with reference to figure 3.1, such solutions describe either the regular ingoing mode and the upper branch of the turning mode for the subluminal dispersion relation, or the regular ingoing one and the outside branch of the lingering one for the superluminal case.

In the superluminal case, it is clear from (3.36) that more than two real solution for k are allowed only inside the Killing horizon, thus the lower branches of the turning and lingering mode do not exist outside.

For what regards subluminal dispersion relations, in principle, (3.36) would tell us that these lower branches stays outside of the horizon. This is true, however we do not see it in equation (3.41). This can be explained by the fact that k does not share a smooth behaviour – for which the only two solution are given by (3.41) – on the lower branches while approaching $v \to 0^-$. In other words, k diverges as v decreases in modulus. However, k has a cutoff given by the dispersion relation (3.30): when $k^2 > \Lambda^2$, the preferred energy ω becomes imaginary and no real solution of the equations for the trajectories exists anymore.

Therefore, the asymptotic solutions outside the horizon can be described as follows: naming the three group velocities associated to the regular ingoing, turning and lingering modes respectively c_g^{reg}, c_g^{turn} and c_g^{ling}, we find at $v = 0$ that

$$c_g^{\text{reg}} = \begin{cases} -c_g^{\text{turn}} & \text{if} \quad \xi = -1 \\ -c_g^{\text{ling}} & \text{if} \quad \xi = 1 \end{cases} . \tag{3.42}$$

In both, the subluminal and the superluminal case, $-c_g^{\text{reg}}$ describes the trajectory of our Hawking quanta in the $|v| \ll 1$ region. Looking back at (3.41), we can easily see that this approximation, which is exact at $v = 0$, can be extended beyond this region, and is valid whenever $\Omega \gg kv$, thus

$$v^2 \ll \frac{1 + \sqrt{1 + 4\xi\alpha^2}}{2} . \tag{3.43}$$

Inside the horizon

Let us now assume that for some intermediate value of x our flow admits an unique acoustic horizon. Inside the latter, the asymptotic region will be described by the regime $|v| \gg 1$. If we solve (3.36) in this limit, we have again two solutions with opposite group velocities such that

$$k_\infty = -\frac{\Omega}{v+1} , \qquad \omega_\infty^{\pm} = \pm\frac{\Omega}{v+1} . \tag{3.44}$$

These two solution are as well associated to the regular mode and to the Hawking partner of figure 3.1. For the choice $\xi = 1$ the latter is represented by the upper branch of the turning mode, while for $\xi = -1$ this role is taken by the lingering

mode. In summary, at the leading order we have

$$c_g^{\text{reg}} = \begin{cases} -c_g^{\text{turn}} & \text{if} \quad \xi = 1 \\ -c_g^{\text{ling}} & \text{if} \quad \xi = -1 \end{cases} \tag{3.45}$$

Again, looking at equations (3.30) and (3.31) one can realize that the above approximation is still valid whenever $k^2 \ll \Lambda^2$ which translates into the following condition for the flow velocity.

$$(v+1)^2 \gg \alpha^2 \,. \tag{3.46}$$

The approximant trajectory

Putting all of the previous analysis together, we realise that (3.42) and (3.45) tell us that the trajectory defined through $-c_g^{\text{reg}}$ describes always the modes associated to the "effective Hawking pair" in both the regions $|v| \ll 1$ and $|v| \gg 1$, independently from the nature of the dispersion relation. In other words, this path effectively interpolates between these two different solutions. Hence, we call such an effective trajectory the "approximant".

We shall return to this later when we assert the range of validity of such an approximation as well as the question why it is sufficient to reproduce the Hawking radiation derived via a full Bogoliubov approach. For the moment let us see how the adoption of the approximant as a proxy for the trajectory of the Hawking pairs enables the emergence of a simple pole structure. Figure 3.2 provides a plot of this trajectory for both subcritical and supercritical flows and shows clearly the capacity of the approximant to uncover the presence of the effective horizon experienced by the modes associated to the Hawking process. Consequently, we can apply the tunneling method even though α is not perturbatively close to zero.

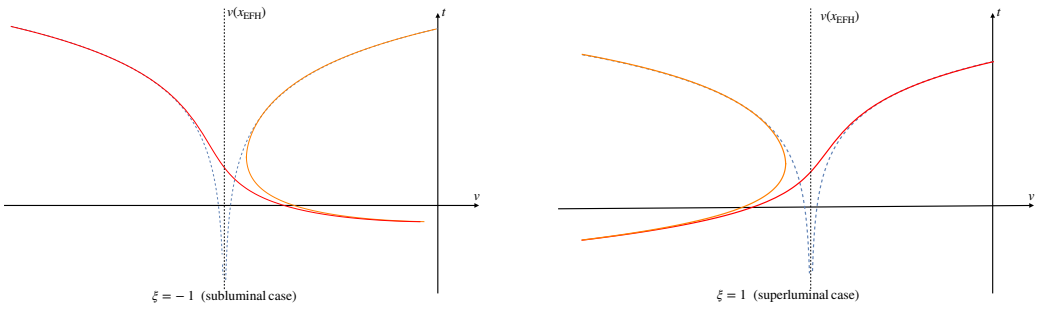

Figure 3.2: Approximant trajectory (dashed blue) versus actual solutions. The dashed trajectories mimic the branches responsible for the particle production in the subluminal (left) and superluminal (right) case asymptotically. Here again $\alpha = 2 \times 10^{-2}$. The dashed black vertical line is the point where the approximant peels, i.e. the effective horizon $v(x_{\text{EFH}})$.

3.3.3 Tunneling the approximant

Let us now apply the ideas from the previous section to the calculation of the tunneling rate. To do so, we consider modes with energies $\Omega = \alpha\Lambda$, such that the

trajectories of the Hawking partners are effectively estimated by our approximant. In particular, we take the outgoing ray to travel with speed $-c_g^{\rm reg}(x,\alpha)$ in the preferred frame. For this trajectory we find

$$\frac{\mathrm{d}t}{\mathrm{d}x} = \frac{1}{-c_g^{\rm reg}+v}\,. \tag{3.47}$$

The position of the simple pole associated to this expression localises $x_{\rm EFH}(\alpha)$ of the "effective horizon (EFH)" for a particle of energy α, so that

$$c_g^{\rm reg}(x_{\rm EFH},\alpha) = v(x_{\rm EFH})\,. \tag{3.48}$$

Please note, that the solution of this equation depends on α, on the range of values of $v(x)$, and on ξ. If a solution to (3.48) exists, it will allow us to define the trajectory outside of the EFH as

$$t(x) = \frac{1}{v'(x_{\rm EFH})(1-\partial_v c_g^{\rm reg})|_{\rm EFH}}\ln[x-x_{\rm EFH}(\alpha)]\,. \tag{3.49}$$

In analogy to our calculations in (2.49), we use (3.49) to calculate the tunneling rate as

$$\Gamma = \exp\left[-\frac{\Omega}{T(\alpha)}\right] \quad \text{where} \quad T(\alpha) = \frac{v'(x_{\rm EFH})(1-\partial_v c_g^{\rm reg})|_{\rm EFH}}{2\pi} \equiv \frac{\kappa(\alpha)}{2\pi}\,, \tag{3.50}$$

where we have defined $\kappa(\alpha)$ as the peeling factor of the EFH and $T(\alpha)$ as the associated "effective temperature". Let us stress that, despite the name, $T(\alpha)$ is energy dependent, and so the rate Γ cannot be considered as a true Boltzmann factor; thus the emission is not purely thermal.

3.4 Application: subcritical vs supercritical flows

After this general treatment, we are going to discuss next the tunneling rate of our effective trajectory. In doing so, we address the subluminal and superluminal dispersion relations individually and specifically distinguish further between subcritical ($|v|<1$, without a horizon) and supercritical (with a horizon) flow (in doing so we also comment on the critical flow). As we shall see soon, the resulting cases have remarkable similarities but also striking differences.

3.4.1 Particle production with an horizon: supercritical flows

Our starting point will be the supercritical flow, that is to say, the permitted range for $v(x)$ supports the presence of a horizon, i.e. $|v(x)|>1$ for some x. For now, we keep our treatment as general as possible without particularising to a specific profile for $v(x)$. We demand:

- $v(x)$ to be monotonous to avoid inner Killing horizons (namely, $v(x)=-1$ has a single root)
- $v\to 0$ for $x\to-\infty$, so that we have an asymptotically flat region

- conditions (3.43) and (3.46) hold almost everywhere apart from a small region around the effective horizon (we shall analyze this point later on)

A typical example of such flow is the one considered in [86]

$$v(x) = \tanh(\kappa_{\rm KH} x) - 1\,. \tag{3.51}$$

This profile interpolates between $v(-\infty) := v_{-\infty} = -2$ and $v(\infty) := v_\infty = 0$ while the Killing horizon is located at $x_{\rm KH} = 0$, such that $\kappa_{\rm KH} = v'(x_{\rm KH})$ denotes the horizon's surface gravity. As long as the surface gravity – the profile steepness at the KH – is large, the region around the horizon, where the approximant will deviate from the real trajectory of the Hawking pair, will be small.

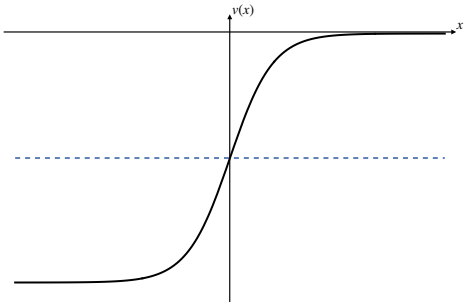

Figure 3.3: Supercritical velocity profile (3.51) for a left-going flow with one subsonic region ($x > 0$) and one supersonic region ($x < 0$). The dashed line marks the location of the sonic/Killing horizon, for which $x_{\rm KH} = 0$ and $v(x_{\rm KH}) = -1$.

As a general feature, the supercritical flow connects our calculation with the relativistic limit in both, the subluminal and in the superluminal case, because the particle production for relativistic fields happens only in the presence of a horizon. As already mentioned, the relativistic behaviour appears when the higher order of the dispersion relation can be neglected, or, in other words, when $\alpha \to 0$. Furthermore, when the lowest order corrections in $\alpha \ll 1$ are taken into account we saw from (3.40) how the relativistic Hawking temperature gets generically corrected. Now we explore such corrections for our specific dispersion relation and flow further; in doing so, we extend our investigation to a broader range of α.

Superluminal behaviour

If we choose $\xi = 1$ in (3.30), we will get $|c_g^{\rm reg}| \geq 1$ everywhere. Hence, in this case, the solutions of (3.48) must always be located inside the Killing horizon (i.e. for negative x), where $v \leq -1$ (with the equality valid for $\alpha = 0$).

Nominally, the allowed range for α spans from $\alpha = 0$, solving $c_g^{\rm reg} = -1$ up to $\alpha = \alpha_{\rm max}$, which is when the group velocity reaches the lower bound of $v(x)$, namely, $c_g^{\rm reg} = v_{-\infty}$. In the case at hand, that is, $v_{-\infty} = -2$, we find $\alpha_{\rm max} \simeq 3$. This is clearly in conflict with the effective meaning given to (3.30). Hence, we limit ourselves to values of $\alpha \leq 0.5$. In the left panel of figure 3.4, we show the location of the effective horizon, determined numerically by equation (3.48), for different values of α within the allowed range.

Similarly, once we know the shape of $x_{\rm EFH}(\alpha)$, one can evaluate $\kappa(\alpha)$ via equation (3.50) and contrast it with $\kappa_{\rm KH}$ of (3.51). The ratio $\kappa(\alpha)/\kappa_{\rm KH}$ is plotted in the left panel of figure 3.4: its deviation from unity and constancy can be taken as a measure of the deviation from thermality induced by the dispersive behaviour. As we can see, in agreement with the previous studies, the Hawking effect displays a remarkable robustness given that values of α of order or larger than 0.1 would have to be considered already in the far UV, as they corresponds to energies close to the cut-off Λ.

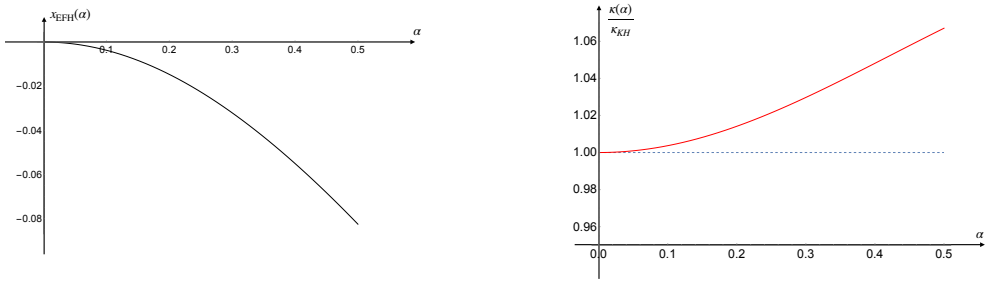

Figure 3.4: On the left: shape of $x_{\rm EFH}(\alpha)$ for the profile (3.51) up to $\alpha = 1/2$. On the right: shape of the ratio $\kappa(\alpha)/\kappa_{\rm KH}$. We see that, since $|x_{\rm EFH}(\alpha)| \geq |x_{\rm KH}|$, so the EFH is inside the KH, the temperature of it appears to be slightly hotter than $T_{\rm H}$ at low α and then showing a $O(5\%)$ deviation from thermality for $\alpha \sim 0.5$

Low-energy regime Here, we connect our result with the general formula provided in Eq. (3.40), by focusing on the low energy regime where an analytical treatment is possible. Let us start by solving (3.48) perturbatively in α, one obtains

$$v(x_{\rm EFH}(\alpha)) = -1 - \frac{3}{8}\alpha^2 + O(\alpha^3)\,, \tag{3.52}$$

or, if (3.51) is taken into account

$$x_{\rm EFH}(\alpha) = -\frac{3\alpha^2}{8\kappa_{\rm KH}} + O(\alpha^3)\,. \tag{3.53}$$

In both cases we find $x_{\rm EFH}$ to be perturbatively close to $x_{\rm KH}$ with corrections starting at $O(\alpha^2)$. As already mentioned, for the superluminal case $|x_{\rm EFH}| > |x_{\rm KH}|$. Given (3.52), we can compute the correction to $\kappa(\alpha)$. Since

$$1 - \partial_v c_g^{\rm reg} = 1 + \frac{3}{8}\alpha^2 + O(\alpha^3)\,, \quad \text{and} \quad v'(x_{\rm EFH}) = \kappa_{\rm KH} + O(\alpha^4)\,, \tag{3.54}$$

we get

$$\kappa(\alpha) = \kappa_{\rm KH}\left(1 + \frac{3}{8}\alpha^2\right) + O(\alpha^3)\,. \tag{3.55}$$

So, the first correction arises at order $O(\alpha^2)$, reproducing what we have found in (3.40). This highlights how the emission still remains quasi-thermal for low-energy particles.

Subluminal behaviour

For what regards the subluminal case, $\xi = -1$, we have $|c_g^{\rm reg}| \leq 1$ always, as such, (3.48) admits possible solutions only outside the Killing horizon – i.e. for positive x – where $|v| \leq 1$. Again, the equality is valid for $\alpha = 0$, but for values close to this minimum, perturbative analysis around the Killing horizon can be safely performed. For what concerns the upper bound in the α-range we can scrutinise (3.36) evaluated at $v = 0$. The solutions are given by (3.41) with $\xi = -1$. As anticipated, we find real solutions exclusively for $\alpha \leq 1/2$. Once again, we compute the position of $x_{\rm EFH}(\alpha)$ as well as the value of the ratio $\kappa(\alpha)/\kappa_{\rm KH}$ numerically so to test the robustness of Hawking radiation. The results are collected in figure 3.5 for the allowed range. We can see again that for $\alpha \ll 0.1$ the spectrum is basically thermal with small deviations from the relativistic result.

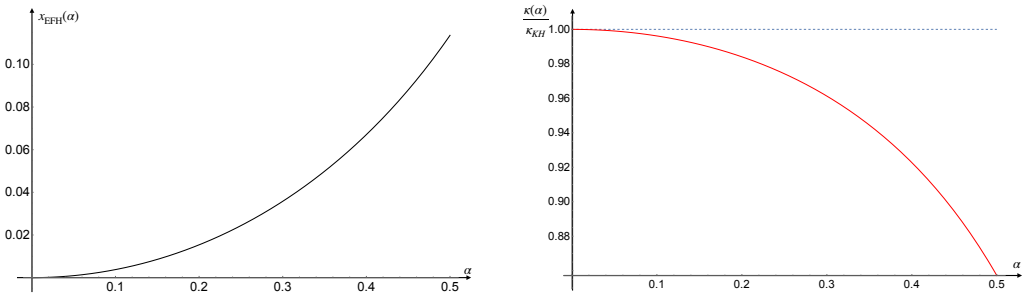

Figure 3.5: On the left: shape of $x_{\rm EFH}(\alpha)$ for the profile (3.51) up to $\alpha = 1/2$. On the right: shape of the ratio $\kappa(\alpha)/\kappa_{\rm KH}$. We see that, since $|x_{\rm EFH}(\alpha)| \leq |x_{\rm KH}|$, the effective horizon is inside the Killing one, the temperature of it being slightly colder than $T_{\rm H}$ at low α and then showing a $O(10\%)$ deviation from thermality for $\alpha \gtrsim 0.4$.

Low energy regime Similarly to the treatment in previous section, we can now analyze the low-energy regime for the subluminal case. Effectively the calculations change only for the sign of ξ, hence we find

$$v(x_{\rm EFH}(\alpha)) = -1 + \frac{3}{8}\alpha^2 + O(\alpha^3)\,, \tag{3.56}$$

suggesting an effective horizon that lies outside the Killing horizon. Recalling the velocity profile (3.51) we get

$$x_{\rm EFH}(\alpha) = \frac{3\alpha^2}{8\kappa_{\rm KH}} + O(\alpha^3)\,. \tag{3.57}$$

which consequently leads to

$$\kappa(\alpha) = \kappa_{\rm KH}\left(1 - \frac{3}{8}\alpha^2\right) + O(\alpha^3)\,. \tag{3.58}$$

showing a similar correction but with the opposite sign with respect to the superluminal case. Once again, we discover that the low-energy regime admits a quasi-thermal behaviour, as expected.

3.4.2 Extremal case: critical flow

This section discusses a second possible regime for the fluid velocity: the critical flow for which $v_{-\infty} = -1$ and $|v| < 1$ otherwise. An exemplary profile could be

$$v(x) = \frac{1}{2}[\tanh(\kappa_\circ x) - 1]\,, \tag{3.59}$$

which we plot in figure 3.6. Note, $\kappa_\circ$ is a fiducial scale to compensate the dimension of x.

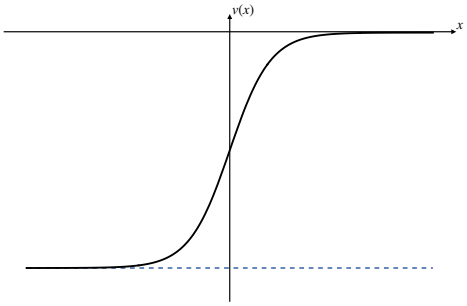

Figure 3.6: Critical velocity profile (3.51) for a left-going flow with one subsonic region ($x > -\infty$) and one sonic point at ($x_{\rm KH} = -\infty$). The dashed line marks the location of the sonic/Killing extremal horizon, for which $x_{\rm KH} = -\infty$ and $v(x_{\rm KH}) = 0$.

Here, the Killing horizon moved to $x_{\rm KH} = -\infty$ where the surface gravity vanishes $\kappa_{\rm KH} = v'_{-\infty} = 0$, thus reproducing the behaviour of an extremal analogue black hole. The analysis of (3.48) can be split into various cases based on the type of dispersion relation as follows:

- superluminal case: the only solution to (3.48) is found for $\alpha \to 0$. However, since $v'_\infty = 0$, $\kappa(\alpha) = 0$ and no particle production takes place, whatsoever.
- subluminal case: we instead solve (3.48) for $0 \leq \alpha \leq 1/2$ and numerically compute $x_{\rm EFH}(\alpha)$ and $\kappa(\alpha)$ (see figure 3.7).

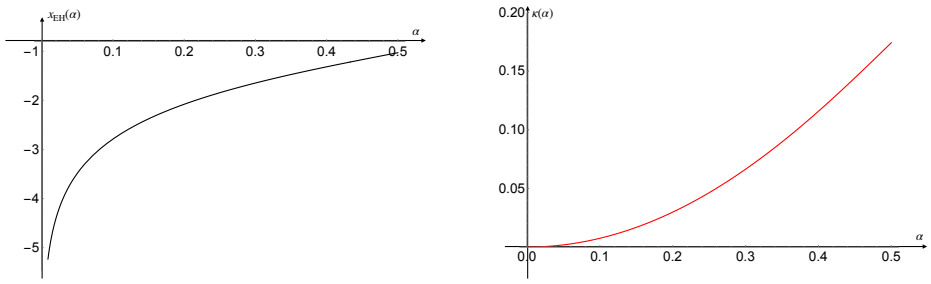

Figure 3.7: On the left: shape of $x_{\rm EH}(\alpha)$ for the profile (3.59) up to $\alpha = 1/2$. One can see that $x_{\rm EFH} \to -\infty$ when $\alpha \to 0$. On the right: shape of the ratio $\kappa(\alpha)$. This quantity goes to 0 (which is the relativistic value) for very low energies but it still shows some nonzero value for $\alpha > 0$.

Interestingly, the subluminal case still supports particle production processes even when the relativistic mechanism has ceased. Let us point out that both setups, subluminal and superluminal, resonate with what we have found in the perturbative analysis of (3.55) and (3.58) around $\alpha = 0$ which returned $\kappa(\alpha) = O(\alpha^3)$.

3.4.3 Particle production without an horizon: subcritical flows

Now, we complete our analysis by investigating a subcritical flow for which $|v| < 1$ besides $|v_{\max}| \sim O(1)$. Then, no sonic horizon exists, hence such a flow mimics a very compact star rather than a black hole, cf. [87, 88] for further references. This is a quite interesting case, given that experimental problems in shallow water waves experiments concerning the stability of horizons led to the prevalent realisation of such "near-critical" flows [74, 77, 89, 90]. Experiments that nonetheless observed particle production. This led to several numerical [91, 92] and analytical investigations [76] which verified the presence of a particle flux albeit generically characterised by substantial deviations from thermality.

Here we shall re-analyze this phenomenon using the tunneling method with the above introduced approximant trajectory. Doing so we shall recover the qualitative behaviour of the aforementioned results and at the same time clarify the basic physics behind this "at first sight puzzling" particle production. Let us start with the EFH condition (3.48).

- superluminal dispersion relation ($\xi = 1$): particles fail to see any effective horizon, in fact, (3.48) can never be fulfilled, since $|c_g^{\rm reg}| \geq 1$ always and $|v| < 1$ everywhere,
- subluminal dispersion relation ($\xi = -1$): $|c_g^{\rm reg}| \leq 1$ always, hence, there can be solutions of (3.48), even if $|v| < 1$ everywhere.

Before particularising to a specific profile of $v(x)$, we quantify first how far from the sonic point $v = -1$ can the flow most negative value be so to still admit some solution to (3.48) for our subluminal dispersion relation. Within our setting this yields numerically the upper bound (namely, the solution of (3.48) for $\alpha = 1/2$)

$$v_{\min} \simeq -0.88\,. \tag{3.60}$$

For flows for which the maximally negative value remains smaller in norm than this $|v_{\min}|$ there cannot be any particle production, at least within the here considered formalism. Actually, particle creation will take place for a subluminal dispersion relation only if $|v_{-\infty}| > |v_{\min}|$. Indeed, the set of solutions to (3.48) is consequently limited to the range of x in which $|v_{-\infty}| \geq |v| \geq |v_{\min}|$ instead of $1 > |v| > |v_{\min}|$.

In order to proceed further in our investigation, let us now assume a velocity profile of the form

$$v_\varepsilon(x) = \frac{1}{2+\varepsilon}[\tanh(\kappa_\circ x) - 1]\,, \tag{3.61}$$

where $\varepsilon > 0$ and $\kappa_\circ$ is again a fiducial scale to compensate the dimension of x. Note, (3.61) shows a similar shape than the critical one shown in Figure 3.7, however

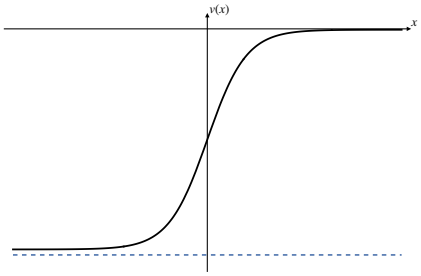

Figure 3.8: Profile for $v_\varepsilon(x)$ of eq. (3.61) with $\varepsilon = 5 \times 10^{-2}$. The dashed line represents $v(x) = -1$.

$|v_{-\infty}| < 1$. Indeed, we have

$$\lim_{x\to-\infty} v_\varepsilon(x) = -\frac{2}{2+\varepsilon} > -1\,. \tag{3.62}$$

In order to achieve somewhere $|v| > |v_{\min}|$, we need $\varepsilon \leq 0.27$. In figure 3.9 we have plotted $\kappa(\alpha)$ for different values of ε.

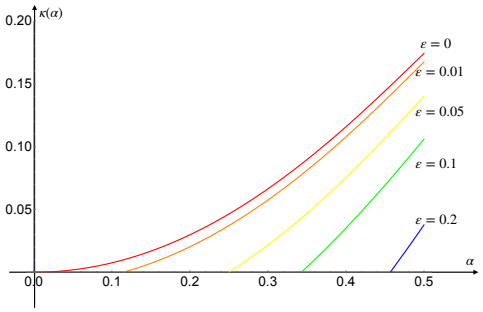

Figure 3.9: $\kappa(\alpha)$ for different values of ε: increasing ε reduces the range of α for which (3.48) has a solution. Moreover, $\kappa(\alpha)$ starts from 0 with a nonvanishing derivative (apart from the critical case $\varepsilon = 0$) which implies a deviation from thermality in the emission that will be the topic of the last section

As a final remark, we stress that the presence of particle production in absence of a Killing horizon has been noticed also in the "dual" case for which the flow is everywhere supercritical and the dispersion relation is superluminal [79]. Remarkably, it is easy to see that within our framework, this case is analogous to the just considered subluminal-subcritical case.

Indeed, for $|v| > 1$ everywhere, one still obtains roots for (3.48) only when $\xi = 1$ and, if the flow is not "too much" supercritical (a dual condition of that implied by Eq. (3.60)), this effect can be detected in the range $\alpha \leq 0.5$, obtaining a behaviour which resembles closely the one found in figure 3.9 for subluminal-subcritical case. This correspondence in behaviour is indeed just another manifestation of the duality between supercritical-superluminal and subcritical-subluminal settings already noticed in previous analogue gravity investigations.

3.5 Analogue tunneling: phenomenological considerations

With the light shed by our tunneling calculations, we can now move to some less technical considerations, which will help us to provide a complete and comprehensive picture of our results.

3.5.1 Deviation from thermality

The first question addresses the problem whether the predicted particle production leads to a thermal – or approximately thermal – spectrum or not. To answer this, we define the quantity

$$\delta(\alpha) = \left| \frac{\partial_\alpha \kappa(\alpha)}{\kappa(\alpha)} \right| . \tag{3.63}$$

Whenever $\delta(\alpha) \ll 1$, the change in $\kappa(\alpha)$ remains negligible with respect to $\kappa(\alpha)$ itself; therefore the emission will be considered as thermal.

Supercritical flow

For the supercritical regime, we can see, from (3.58) and (3.55) that within the low energy region, the surface gravity behaves as

$$\kappa(\alpha) = \kappa_{\text{KH}} + O(\alpha^2) \quad \text{and} \quad \partial_\alpha \kappa(\alpha) = \frac{3}{4}\xi \alpha \kappa_{\text{KH}} + O(\alpha^3) . \tag{3.64}$$

As a consequence, for $\alpha \simeq 0$, $\delta(\alpha) = O(\alpha)$ implying that the emitted spectrum shows perturbatively thermal features. This can be also extracted from figure 3.10.

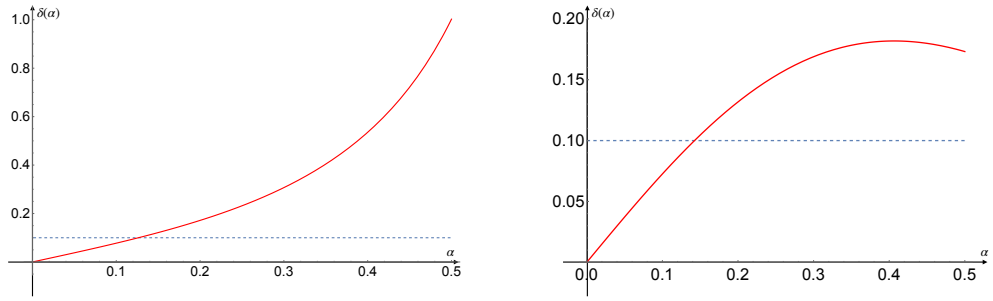

Figure 3.10: Deviation from thermatity in a supercritical flow. On the left: $\delta(\alpha)$ for the subluminal case. On the right: $\delta(\alpha)$ for the superluminal case. The dashed line is $f(\alpha) = 0.1$.

Subcritical flow

While we perturbatively recover thermality in the supercritical case, we see that a subcritical (and subluminal) setup displays the complete opposite behaviour. Albeit having generically $\partial_\alpha \kappa(\alpha) \neq 0$ for $\alpha \neq 0$, we find that $\kappa(\alpha) = 0$ at the minimum

value of the subcritical profile $v = -2/(2+\varepsilon)$. This, in turn, means that $\delta(\alpha)$ diverges, thus maximising the deviation from thermality. This should come as no surprise given the essential role of the presence of a Killing/sonic horizon to which the EFH has to be close, in order to assure the approximate constancy of $T(\alpha)$.

3.5.2 Spectrum

Whether or not thermal, the emission spectrum is determined by the tunneling rate (3.50). In figure 3.11, we plotted Γ for the supercritical regime, while the subcritical case (subluminal dispersion relation) is shown in figure 3.12.

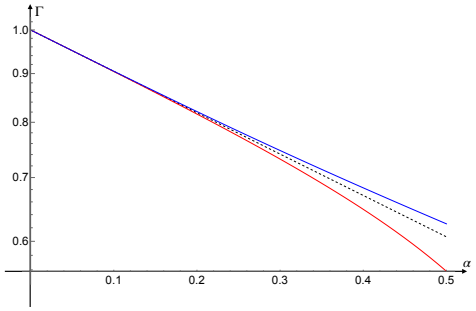

Figure 3.11: Plot (the vertical axis is displayed in a logarithmic scaling) of Γ for a supercritical flow. The dashed black line depicts the relativistic rate, while the blue solid line represents the superluminal and the red the subluminal case. For convenience, here we have set $2\pi\Lambda = 1$, such that $\Gamma = e^{-\alpha/\kappa(\alpha)}$ and $\kappa_{\text{KH}} = 1$.

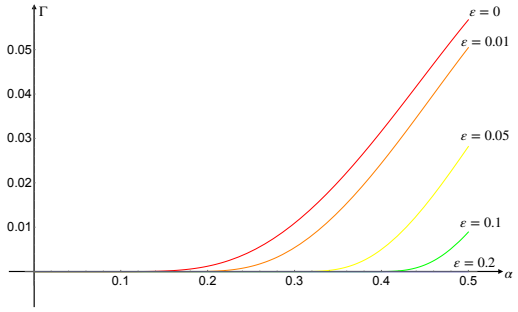

Figure 3.12: Plot of Γ in the subluminal case for some values of ε. The case $\varepsilon = 0$ represents the critical regime. Again we have set $2\pi\Lambda = 1$.

Comparing both spectra, we observe that Γ stays close to the relativistic tunneling rate – at low energies in the supercritical phase independently from the nature of the dispersion relation. However, when increasing α, the subluminal as well as the superluminal scenarios depart further and further from the relativistic behaviour, describing respectively a colder and a hotter object, respectively.

Finally, let us stress that even if subluminal dispersion relations predict particle production for super- as well as subcritical flows, it remains true that

$$|\Gamma_{\text{subcrit}}| \ll |\Gamma_{\text{supercrit}}| \,. \tag{3.65}$$

I.e. even if subluminal dispersion allows for an in-principle particle production in the absence of a Killing horizon, this effect is strongly suppressed with respect to the particle production in the presence of an horizon.

3.5.3 Energy conservation: subcritical particle production

The particle creation found in section 3.4.3 confirms previous results based on Bogoliubov coefficients [76, 91, 92]. However, given that in stationary geometries the spontaneous particle creation from the vacuum always requires the presence of an ergoregion to ensure energy conservation, this result might seem puzzling at first sight. Indeed, for this production to be consistent, the ingoing Hawking partner must carry a negative Killing energy to compensate for the positive one carried to infinity by the Hawking quantum. However, this can happen only within an ergoregion apparently absent in the considered subcritical flow. In what follows, we shall explain how this apparent paradox is resolved by the peculiar nature of subluminal dispersion relations.

Starting with Eq. (3.30), the requirement for the existence of a quantum with $\Omega < 0$ can be recast into the condition $\omega < kv$ (considering positive preferred energies amounts to $k < 0$) which in turn means

$$0 > c_{\rm ph} = \frac{\omega}{k} > v\,, \tag{3.66}$$

that is, the phase velocity's absolute value must be smaller than the fluid velocity.

For superluminal dispersion relations this requires $|v| > 1$ which implies the necessity of the presence of a Killing horizon. However, for subluminal dispersion relations we can write

$$c_{\rm ph}^2 = \frac{\omega^2}{k^2} = 1 - \frac{k^2}{\Lambda^2} < v^2\,. \tag{3.67}$$

This inequality is satisfied whenever

$$\Lambda^2 > k^2 > \Lambda^2(1 - v^2)\,, \tag{3.68}$$

where the upper bound $\Lambda^2 > k^2$ was added to respect the perturbative interpretation of the dispersion relation as well as to ensure $\omega^2(k) \geq 0$. Equation (3.68) then reveals an important feature: the energy balance can be satisfied in the subluminal case regardless of the presence of any Killing horizon. In particular, if $|v_{\rm max}|$ is close to the speed of sound, the window of opportunity described by (3.68) may allow for the presence of an EFH for $k < \Lambda$. While for deeply subcritical flows, such window rapidly closes and only for $k \simeq \Lambda$ some mode can be excited[3].

Let us notice that the possibility of having negative-energy modes only when $|v| > |c_{\rm ph}|$ is an established, well-known fact, see cf. [93, 94].

3.5.4 Tunneling the approximant: validity of the calculation

As a last topic we would like to quantify the validity of our approximation. All calculations are based on finding an approximant trajectory to our non-relativistic

[3]However, one should study the non-perturbative structure of the dispersion relation, to verify the reasoning in such regimes.

particle. Since this fiducial curve experiences an effective horizon, it allows us to perform a tunneling calculation as it is associated with a simple pole which is instead is absent in the true trajectory. Nonetheless our results confirm the expectations based on the Bogoliubov methods. How can this be?

The crucial issue here is that the actual particle creation process does not happen arbitrarily close to the horizon, but rather when the partners of the Hawking pair are sufficiently stripped apart from tidal forces for them to be distinguishable "on-shell" particles. Such critical distance is usually identified with the de Broglie wavelength (or Compton, if they are massive) of the particles [51, 95, 96]. Thus, in turn, we assume that if our process happens within a de Broglie wavelength, the calculation can be considered as trustworthy.

In an analogue setting, the de Broglie wavelength of an acoustic excitation has to be defined using the speed of sound c_s explicitly [59]. After restoring all relevant physical quantities, we can write

$$\lambda_s = \frac{hc_s}{\Omega}\,. \tag{3.69}$$

The idea is the following: since λ_s denotes the characteristic distance between the Hawking partners at which they go on-shell, we must require that the approximant trajectory fails to mimic the physical trajectories only when these are separated by a distance smaller than λ_s, in order for our method to apply. This is tantamount to say that the physical trajectories and the approximant are indistinguishable from the point of the particle creation process. In other words, if we define $x_1(\alpha)$ as the point where we violate (3.43) (the approximant fails to trace the ray outside the effective horizon) and $x_2(\alpha)$ as the point where (3.46) is violated (the approximant digresses strongly from the inside ray), then their distance $\Delta x(\alpha)$ has to be smaller than λ_s:

$$|\Delta x(\alpha)| = |x_2(\alpha) - x_1(\alpha)| \leq \lambda_s = \frac{hc_s}{\alpha\Lambda}\,. \tag{3.70}$$

Since (3.46) and (3.43) involve $v(x)$, we have to specify a profile for the flow velocity to determine actual values for Δx. Let us then take the following profile

$$v(a,b;x) = \frac{a}{2}\left[\tanh(bx) - 1\right]\,. \tag{3.71}$$

controlled by the two parameters a and b which are associated to alternative features of the flow:

- $a = -\lim_{x\to-\infty} v(a,b;x)$ controls the lower limit of v and can be identified as $a = |v_{-\infty}|$.
- b controls the slope, i.e. the bigger b is, the steeper v becomes in passing from 0 to $-a$.

This profile for v allows us to include all investigated cases in the discussion and, given that we can invert the function

$$x(a,b;v) = \frac{1}{b}\text{artanh}\left(1 + \frac{2v}{a}\right)\,, \tag{3.72}$$

we can use it to study Δx.

Superluminal case

Taking $\xi = 1$, the effective horizon will always be located inside the Killing horizon, as such we have to consider the case $v \leq -1$ in condition (3.46)). So let us consider, for a given α, the values of the flow velocity for which the conditions (3.43) and (3.46) are saturated

$$v_1(\alpha) = -\sqrt{\frac{1+\sqrt{1+4\alpha^2}}{2}}\,, \quad \text{and} \quad v_2(\alpha) = -1-\alpha\,. \tag{3.73}$$

Then, after multiplying (3.70) by α and collecting the α-dependence, we can use (3.72) to write

$$\alpha \cdot \Delta x(\alpha) = \frac{\alpha}{b}\left[\operatorname{artanh}\left(1+\frac{2}{a}v_2(\alpha)\right) - \operatorname{artanh}\left(1+\frac{2}{a}v_1(\alpha)\right)\right]. \tag{3.74}$$

Since we are in the superluminal case, particle production occurs only in the supercritical regime, namely for $a \geq 1$. In general, the expression for $\alpha \cdot \Delta x(\alpha)$ is parametrically small, depending on the value of b as follows: if b increases, then v will change rapidly in a very narrow region in x, such that the particles will be produced in a small neighborhood around the Killing horizon. Note that b for $a = 2$ represents exactly the Killing surface gravity, as one can immediately see from (3.51).

At low energies, one can expand (3.74) for $\alpha \simeq 0^+$ obtaining

$$\alpha \cdot \Delta x(\alpha) = -\frac{a\alpha^2}{2b(a-1)} + O(\alpha^3), \tag{3.75}$$

which reveals that (3.70) will be always satisfied at low energies for $a > 1$, independently from the value of b. For $a = 1$, representing the critical behaviour for the flow, (3.75) must be analyzed separately due to the obvious pole. If we set $a = 1$ and then expand for $\alpha \simeq 0$,

$$\alpha \cdot \Delta x(\alpha) = -\frac{\alpha}{2b}\ln\left(\frac{\alpha}{2}\right) + O(\alpha^2), \tag{3.76}$$

which is again perturbatively small and satisfies the bound given by (3.70).

The only point where the approximation fails independently from b, occurs when v is a slightly supercritical flow ($a \gtrsim 1$) such that we can have particle production up to $v_{-\infty}$ for $\alpha \leq 1/2$. This happens only[4] when

$$v_2(\alpha) = -a = v_{-\infty} \iff \alpha = a - 1\,. \tag{3.77}$$

When (3.77) is fulfilled at a finite $\alpha \neq 0$, the product $\alpha \cdot \Delta x(\alpha)$ diverges and we cannot satisfy (3.70). This can be understood, simply because for $\alpha = a-1$, particle production should happen for velocities $v_{-\infty}$, viz. in the point $x = -\infty$.

[4]Notice that $|v_2(\alpha)| > |v_1(\alpha)|$.

Subluminal case

For the subluminal case the discussion resembles the previous one in most parts. By setting $\xi = -1$ while considering that the effective horizon lies outside of the Killing horizon, the breakdown of the approximation, outside and inside the EFH, is destined to happen respectively at

$$v_1(\alpha) = -\sqrt{\frac{1+\sqrt{1-4\alpha^2}}{2}}\,, \quad \text{and} \quad v_2(\alpha) = -1+\alpha\,, \tag{3.78}$$

which yields an expression for $\alpha \cdot \Delta x(\alpha)$ very close to (3.75). In general, this expression changes antiproportionally with b. At low energy, for $a > 1$ (supercritical flow), we find again (3.75) while for the critical case $a = 1$ we recover (3.76). This confirms that the low energy behaviour is well described by our approximant.

Again, here, we violate (3.70) when $\Delta x(\alpha)$ diverges at a finite α, which is at

$$v_2(\alpha) = -a = v_{-\infty} \iff \alpha = 1-a\,. \tag{3.79}$$

This is possible only for the subcritical scenario, since $\alpha > 0$. In this case, we discover again that the approximation breaks down at $x = -\infty$ when particles fulfill $\alpha = a - 1$, then our treatment becomes invalid.

Let us then summarise:

- our approximation is always valid for low energy particles, in the supercritical and critical case, both for super- and subluminal perturbations and independently of the model,
- for a generic value of α, the validity of the approximation depends strongly on the model, namely, the energy scale Λ, the sound speed c_s and the steepness of the profile $v(x)$, [5]
- for a $v(x)$-profile of the $\tanh(x)$-type, there exists an α for the supercritical and superluminal case ($\alpha = a - 1$) and one for the subcritical and subluminal case ($\alpha = 1 - a$), for which our approximation fails.

3.6 Outlook

Let us conclude this Chapter giving an outlook on the found results. We have discussed analogue models as a tool for investigating QFT in curved spacetime. In particular, our focus has been devoted to the Hawking radiation.

Quantum fluids seem to provide a good playground where to probe quantum effects on acoustic geometry. The case of BECs is quite instructive for us, because it offers the possibility to analyze both the effect of the background geometry, together with the possibility to understand the role of the dispersion in superluminal particles. While in a gravitational setting, modified dispersions are allowed only if one invokes

[5] Recently, it has been shown that some polariton models can be engineered in order to tune the steepness without changing the other parameters (such as the asymptotic behaviour of $v(x)$), becoming a good place to test the calculations developed in this chapter [97]

a Lotrentz violation mechanism, in analogue systems this is automatically built-in in the properties of the background, as dispersion arises as soon as one studies the behaviour of the quantum perturbations moving on a condensate.

Departing a bit from the standard techniques, we have investigated the problem of Hawking radiation with dispersion with a tool that offer an intuitive description of it: the tunneling method. This, which is a standard and well-established approach in gravitational settings, has allowed us to explore several different scenarios that may be prevalent in analogue set-ups. That was possible with the introduction of a new concept, the approximant, that interpolates between the two Hawking partners far from the effective horizon.

A first outcome is that, in presence of a sonic horizon, the particle production phenomenon is mainly driven by the standard Hawking effect. Deviations from thermality are there, but they are very mild in the low energy regime: that conclusion confirms once again the robustness of Hawking radiation against the breakdown of Lorentz symmetry.

Secondly, we have analyzed the possibility for an horizonless geometry, to undergo such a phenomenon. We have shown that subluminal particles are emitted also from slightly subcritical case (or very compact objects, from the gravitational viewpoint). This emission is purely non-thermal and it is very suppressed compared with its counterpart in a geometry with an acoustic horizon. This fact, which has previously been noticed in the literature, shows that an horizon works like an anchor for particle production, driving the main part of the emission (i.e. the low energy part of the spectrum).

The quality of the calculation is analyzed and reveals that the approximant is a good tool for computing the production of particles both for low-energy particles and for steep flows. This is given by invoking the Heisenberg indetermination principle and considering produced particles to go on-shell (so to be effectively produced) when their distance is bigger that their de-Broglie wavelength. If the production happen when the two are too close to each other, they cannot be distinguished at the quantum mechanical level.

This last observation gives also an insights about the trans-Planckian problem, since the very same reasoning – which is necessary in the case of MDRs in order to apply the tunneling procedure – can be applied to relativistic dispersions. One may consider the ray tracing of the particle just a mathematical tool: the production of particles physically happens at a finite distance (within which only a quantum soup exists, maybe exiting our QFT-in-curved-spacetime approximation) and no trans-Planckian frequencies can ever be really reached.

A last comment is reserved to the quantum state. We have shown, that the tunneling rate describes a temperature, once the vacuum for the infalling observer is imposed at the horizon (see section 2.3). Throughout the whole discussion – helped by the fact that our metric (3.24) enjoys an asymptotically flat region for $v = 0$ – we have implicitly considered the local vacuum at the EFH in a similar way. However, this requirement is not motivated by anything, if not the analogy with the relativistic case. One can assume that, for supercritical flow, the formation of an horizon will make the system to collapse onto the Unruh state, and in case of MDRs, the almost-thermal character of the spectrum will determine small correction

for the low-energy sector. This is a reasonable assumption for a state described by an adiabatic evolution with an initial vacuum in Minkowski. However, let us stress that the presence of a cut-off energy Λ would also allow for a regular Boulware state, which predicts no radiation at all, even though it would imply an energy firewall of order Λ at the horizon.

However, this last comment points out that the AG-analysis cannot be the end of the story. In the following section we will show how in some gravitational models we can provide a completion to the geometry, allowing the definition of a unique quantum state, also in the case of MDRs. We shall return to the comparison with the result of this Chapter in the conclusions.

Chapter 4

Gravity without Lorentz invariance

In Chapter 3 we have shown how analogue models can provide an extremely useful tool to investigate QFT in curved spacetime. Acoustic geometries can be used to simulate black holes for phonons and to check their radiative properties. The theoretical predictions and the experimental detection of this effect confirm once again that Hawking radiation has nothing to do with gravitodynamics itself, but rather with the kinematics of quantum particles onto a non-flat geometry.

In addition, we have studied the robustness of this effect against violation of the (sonic) Lorentz symmetry, which naturally arises in AG from the fundamental condensed-matter equations.

Albeit AG is an interesting research area *per sè*, we would now like to employ the insights we gained from it in order to learn something more about the gravitational world. While the discover that Hawking's result is not so intimately linked to the invariance under local Lorentz transformations could be seen as surprising, the nature of this robustness makes us expect that similar results should be valid also for gravitational LV-models.

Nonetheless, even though the Lorentz violating behaviour of perturbations has been shown to cut-off the trans-Planckian physics from the analysis, the analogue treatment leaves open some fundamental questions about the structure of the vacuum state. We shall see that, by extending the Lorentz breaking framework to gravity – not anymore limited to be described by the Euler and continuity equations (3.1) – will probe crucial in this and other questions.

Finally, and perhaps most importantly, studying LV gravity can be a step forward in understanding QG. As we shall discuss, dropping local Lorentz invariance will not turn out to be just an academic exercise, but rather a concrete way to address the problem of quantizing gravity.

Hence, in this Chapter we shall direct our efforts in this directions. In what follows we will present an introduction to Lorentz violation in gravity restricting, in particular, to models of gravity with a preferred frame. We will review the causal structure of such geometries, discuss the generalization of black holes within this setting, and explore their interplay with Lorentz breaking matter fields.

4.1 Breaking Lorentz symmetry

Lorentz symmetry has been massively tested throughout the past hundred years [33]. Extremely high-precision measures in high-energy astrophysics leave severely constrained the violation of Lorentz invariance in the Standard Model. However, this is not the case for the gravitational sector, where the experimental accessible energies are lower and allows for some theoretical room where to play.

Mathematically speaking, the non-compactness of the Lorentz group makes impossible to test it uniformly. While this can be actually done for the $SO(3)$ rotation subgroup, that is impossible with the addition of boost transformations [98].

Physically speaking, dropping rotational invariance will break spatial isotropy, while abandoning boost invariance translates into the insertion of a preferred frame, thus dropping the relativity principle [1].

Exploring the presence of a preferred reference frame in gravity can be seen as an interesting problem for several reasons. First of all, preferred frames arise in spacetimes with initial singularities – such as cosmological settings – for which the gradient of the cosmological time represents a preferred time direction [98]. Besides, breakdown of local boost invariance arises in many condensed matter situations, as we saw in Chapter 3, suggesting that similar structures might arise in emergent gravity scenarios.

However, the main theoretical motivation for facing the study of LV theories of gravity boils down to the non-renormalizability of GR [7]. It has been known for long time that the addition of higher derivative (i.e. higher curvature) terms in the gravitational Lagrangian would have cured the renormalizability issue [99, 100]. Unfortunately, the addition of higher derivatives brings, together with itself, the presence of instabilities [101]. In a Lorentz invariant theory, the propagator D for a higher derivative massive field is given by:

$$D(p) \sim \frac{1}{p^2(p^2 - m^2)} = \frac{1}{m^2}\left[\frac{1}{p^2} - \frac{1}{p^2 - m^2}\right], \tag{4.1}$$

where $p^2 = p_a p^a$ and m is the mass of the particle. We can immediately see that the spectrum of D contains two relativistic particles, one of which is a ghost. This problem has been recently faced, in a Lorentz-invariant context, at the perturbative level in [102, 103] and at a non-perturbative analysis is given in [104].

It is clear though that the problems brought by higher derivatives arise because of the presence of higher *temporal* derivatives. Due to Lorentz-invariance, the propagator (4.1) must depend only on p^2, thus admitting as many temporal derivatives as spatial ones in any frame.

Intuitively, this problem can be overcame if one consider a theory which admits only higher *spatial* derivative operators. The Lagrangian becomes power-counting renormalizable, but the absence of higher temporal derivatives prevents the presence of instabilities. This was exactly the observation made by Hořava in 2009 [32][2]. In

[1] The relativity principle enters into the axiomatic derivation of special relativity as the equivalence of all the inertial frames [33]

[2] Previous investigations in the same direction have been made by Anselmi in [105]

this model, the spacetime manifold $\mathcal{M}$ is considered to be factorized:

$$\mathcal{M} \simeq \mathbb{R} \times \Sigma \tag{4.2}$$

with Σ being a co-dimension 1 (spatial) sub-manifold. Therefore, spacetime is foliated with Σ-leaves along the time direction. This automatically introduce a preferred time direction τ which runs over the real line $\tau \in \mathbb{R}$. Gravity becomes a Lifshitz field, because of the anysotropic scaling between τ and the spatial coordinates $\mathbf{x}$ defined over Σ:

$$\mathbf{x} \to \lambda \mathbf{x}\,, \qquad \tau \to \lambda^d \tau\,, \tag{4.3}$$

where d is the dimension of Σ.

It is quite clear that the *à priori* introduction of a foliation onto $\mathcal{M}$ breaks the local Lorentz invariance, giving a preferred notion of time. Within the Arnowitt–Deser–Misner (ADM) decomposition, the time direction is given by the 1-form

$$u = N(\tau, \mathbf{x})\, \mathrm{d}\tau\,, \tag{4.4}$$

called *aether*. N is the lapse function [106], which determines the geometry together with the shift vector N_i and the spatial metric γ_{ij}. The preferred notion of time (4.4) breaks the local boost invariance, therefore it is possible to build a theory with a different number of time and space derivatives. The full *Diff*-invariance breaks down to the subset of transformation which preserve the structure of the foliation, called *FDiff* (foliation-preserving diffeomorphisms):

$$\textit{Diff} \to \textit{FDiff}\,. \tag{4.5}$$

Actually, in order to achieve renormalizability, one *needs* to consider higher spatial derivative terms up to $2d$ [32]. In $(3+1)$ dimensions, we can order the full gravitational Lagrangian in powers of derivatives:

$$\mathcal{L}_{\mathrm{HG}} = \mathcal{L}_2 + \frac{1}{M_*^2}\mathcal{L}_4 + \frac{1}{M_*^4}\mathcal{L}_6\,, \tag{4.6}$$

where M_* is an energy scale at which LV effect becomes sensible and $\mathcal{L}_n$ contains operators with n-derivatives.

The power-counting renormalizability of the theory is quite appealing and makes HG a sensible QG candidate, even though the analysis of the coupling dimensions cannot be directly used to infer directly the perturbative renormalizability, given the absence of Lorentz invariance [107]. We shall discuss about this fact later on, in Chapter 7.

Besides the formal aspects, we emphasize that having an actual QG candidate makes the investigation of such a gravity theory tempting (if not mandatory). Therefore, the rest of the Chapter will be devoted to introduce the phenomenology of gravity with a preferred frame and to analyze its implications.

4.1.1 Gravity with a preferred time direction

In doing phenomenology, we assume that our gravitational sector will describe a geometry well below the energy scale M_*, thus we will restrict our analysis to $\mathcal{L}_2$ of equation (4.6). It is convenient to use a Stükelberg field to recover the full *Diff*-invariance of the Lagrangian. This field, dubbed *khronon*, is nothing else that the function $\tau(x)$ which determines the shape of the foliations thorugh

$$\Sigma = \{\tau(x) = \text{const.}\}. \tag{4.7}$$

Within this parametrization, we abandon the ADM formalism and we recover a metric-aether one with a usual Lorentzian metric tensor g_{ab} and an aether vector field which takes the form:

$$u_a = \frac{\partial_a \tau}{\sqrt{-g^{bc}\partial_b\tau\partial_c\tau}}\,. \tag{4.8}$$

From there we see immediately that the lapse function given in (4.4) is

$$N = (-\partial_a\tau\partial^a\tau)^{-1/2}\,. \tag{4.9}$$

Note that the aether field (4.8) is, by definition, hypersurface orthogonal and always timelike. A quadratic (in derivatives) theory with a preferred, hypersurface orthogonal, timelike vector field, is called *khronometric theory*. At this level, τ enters the Lagrangian only through u

$$\mathcal{L}_{kh} = R + \lambda(\nabla_a u^a)^2 + \beta(\nabla_a u_b)(\nabla^b u^a) + \alpha a_a a^a\,, \tag{4.10}$$

where $a_a = u^b\nabla_b u_a$ is the acceleration of u. The three (dimensionsless) couplings λ, α and β are constrained to be $|\beta| \lesssim 10^{-15}$, $|\alpha| \lesssim 10^{-7}$ with λ unconstrained or $|\alpha| \lesssim 10^{-4}$ with $\lambda \simeq \alpha/(1-2\alpha)$ (in any case $\lambda > 0$ to avoid ghosts) [107–109].

If one relaxes the hypotesis of hypersurface orthogonality of u, so exiting from the realm of low-energy Hořava solutions, one can study a generic quadratic theory of gravity with a preferred frame, called *Einstein-aether (EA)* gravity [98]. Without the constraint on the hypersurface orthogonality, the requirement for u to be unit-timelike normalized is implemented "by hand" with a Lagrange-multiplier. The EA action can be formulated in terms of the irreducible representation of the $SO(3)$-subgroup which leaves u^a invariant:

$$\mathcal{L}_{EA} = R + \frac{1}{3}c_\theta\theta^2 + c_\sigma\sigma_{ab}\sigma^{ab} + c_\omega\omega_{ab}\omega^{ab} + c_a a_a a^a + \Phi(u_a u^a + 1)\,, \tag{4.11}$$

where Φ is the Lagrange multiplier. The expansion θ, the shear σ_{ab}, the twist ω_{ab} and the acceleration a_a are defined as the trace part, symmetric traceless part, and antisymmetric part of $\nabla_a u_b$ [110]:

$$\nabla_a u_b = \frac{1}{3}\theta\gamma_{ab} + \sigma_{ab} + \omega_{ab} + u_a a_b \tag{4.12}$$

with $\gamma_{ab} = g_{ab} + u_a u_b$ being the spatial projector and we have:

$$\begin{aligned} \theta &= \nabla_a u^a \,, \\ \sigma_{ab} &= \nabla_{(a} u_{b)} - \frac{1}{3}\theta\gamma_{ab} - u_{(a} a_{b)} \,, \\ \omega_{ab} &= \nabla_{[a} u_{b]} - u_{[a} a_{b]} \,. \end{aligned} \tag{4.13}$$

The basic difference between the khronometric theory and EA is that, for hypersurface orthogonal aethers, the twist tensor ω_{ab} must vanish due to the Frobenious theorem [1]. Thus, we can recover khronometric theory from EA just by taking the limit $c_\omega \to \infty$. Equations (4.13) gives the relations between the couplings of given in (4.10) and (4.11) [98]:

$$c_a = \alpha \,, \quad c_\sigma = \beta \,, \quad c_\theta = \beta + 3\lambda \,. \tag{4.14}$$

The crucial aspect of those theories of gravity with a preferred frame is that this frame is local and obeys an equation of motion, therefore is dynamical. This is of great importance since it allows to respect general covariance in the theory [98]. Moreover, this highlights an important difference with respect to the case of AG, where the preferred frame was defined without a field equation, but as a comoving frame with the fluid (3.11). In the following, we will see the consequences of this fact.

Given that khronometric theory can be seen as "hypersurface orthogonal EA", one can show that the hypersurface orthogonal solutions of EA gravity are also solutions of the khronometric theory, even if the discussion can hide some subtleties [110, 111].

Both (4.10) and (4.11) can be written as $\mathcal{L}_{\rm EH} + \mathcal{L}_u$, where we disentangle the Einstein-Hilbert term $\mathcal{L}_{\rm EH} = R$ from the parts containing the aether u. The field equations can be written as

$$G_{ab} = 8\pi G T^u_{ab} \,, \tag{4.15}$$

where G_{ab} is the usual Einstein tensor and

$$T^u_{ab} = -\frac{2}{\sqrt{-g}} \frac{\delta \mathcal{S}_u}{\delta g^{ab}} \,, \tag{4.16}$$

where $\mathcal{S}_u$ is the action correspondent to $\mathcal{L}_u$, giving the interpretation to the tensor T^u_{ab} of stress-energy-tensor of the aether, which particular expression differs from EA to khronometric theory [112]. From (4.15) one can us the generalized Bianchi identities [113] to derive the equation of motion[3] for the aether (in the case of EA) or for the khronon (in the khronometric case). Both of them are defined in terms

[3]This means that (4.15) contains already all the information on the dynamics. Working out

$$\frac{\delta S}{\delta u^a} = 0 \tag{4.17}$$

is redundant, if one takes into account the geometrical identities.

of a vector $\mathcal{A}_a$ orthogonal to the aether $\mathcal{A}_a u^a = 0$. In the EA case, these equations are:

$$\mathcal{A}^a = 0\,, \tag{4.18}$$

while for the khronometric case, the equation of motion is given for a scalar field, namely the khronon τ, that returns a scalar equation of motion:

$$\nabla_a(N\mathcal{A}^a) = 0\,. \tag{4.19}$$

It is clear that an aether without twist satisfying $\mathcal{A}^a = 0$, also satisfies this latter equation.

Of course, a matter action can be included, thus entering the field equations (4.15) through its stress energy tensor T^m_{ab} on the right-hand-side of the equation.

4.2 Black holes in LV gravity

Let us now move on describing the causal structures of these kind of spacetimes. This will be of fundamental importance to study black hole geometries.

As already mentioned, the motivation of considering the introduction of a preferred time direction is to be able to insert higher spatial derivative without having Ostrogadski instabilities [101]. This means that dispersion relations for the perturbations will be in general non-relativistic. Generically, they will be of the form

$$\omega(\mathbf{k})^2 = \beta_0\mathbf{k}^2 + \beta_1\frac{\mathbf{k}^4}{\Lambda^2} + \beta_2\frac{\mathbf{k}^6}{\Lambda^4}\,, \tag{4.20}$$

where ω is the energy defined with respect to the preferred time u and $\mathbf{k}_a = \gamma^b_a k_b$ is the spatial projection of the four-momentum and β_i constants. Let us emphasize that this dispersion relation takes the simple form of (4.20) only in the preferred frame, while it can assume a more complicated shape in any other frames (similarly to what happens for (3.19)). In the case of gravitational perturbation, from (4.10), we have the identification $\Lambda = M_*$, but generically, Λ will be considered as a scale at which the non-relativistic modification becomes non-negligible. In (4.20) we stopped to the order $\mathbf{k}^6$ because this is the case for Hořava's model, due to the renormalizability requirement. However, for the phenomelogical's sake we can imagine more general polynomial expression up to $\mathbf{k}^{2n}$, with a generic $n \in \mathbb{N}$.

In principle, this discussion, which is valid in the case of an hypersurface orthogonal aether, can be taken as true also for EA gravity. There, gravitational degrees of freedom propagates at finite speed [114, 115], but the presence of a local preferred frame allows aether-matter couplings that lead to MDRs like (4.20)[4].

The important aspect of (4.20) is that, if $\beta_i > 0$ [116], the dispersion relation becomes superluminal, thus changing the causal structure of the spacetime. The presence of superluminal particles invalidates the usual causal analysis. In particular, Killing horizons cannot anymore be identified as causal boundaries, because particles can classically travel from the inside to the outside, as we already found out in Chapter 3. The prevision of object like black holes is a key feature of GR, therefore let us explain how to extend this concept to LV gravity.

[4]Actually, whether the non-hypersurface orthogonality may or may not lead to ill definiteness in the quantization of the theory would be an interesting question.

4.2.1 Black holes in khronometric theory

Let us start in the hypersurface orthogonal case. In defining the causality we will recall some concept from [117]. We have said that in principle there is no universal finite limiting speed for particles with (4.20). Therefore the only notion of causality for physical particles can be given just by the requirement form them to move forward in the preferred time.

Indeed, considering a world-line $x^a(\lambda)$ parametrized by $\lambda \in \mathbb{R}$, we define it *causal and future (past) directed* if $\dot{x} \cdot u < 0\,(> 0)$ evrywhere, where $\dot{x}^a = \partial_\lambda x^a$. If $x^a(\lambda)$ posses at least one point where $\dot{x} \cdot u = 0$, then it is defined to be *acausal*.

Intuitively, a black hole region will be described by the portion of spacetime from which a causal curve cannot reach the asymptotic region. So, let us be concrete and consider the following situation. Let us take a point $p \in \mathcal{M}$ and let us consider the (unique) leaf Σ_p of constant-khronon which contains p. Let us now imagine to have a notion of spatial infinity, which we will denote as $\mathfrak{i}_p$, where the metric is flat $g_{ab}|_{\mathfrak{i}_p} = \eta_{ab}$ and the aether becomes there the Minkowskian time-translation vector $u^a\partial_a|_{\mathfrak{i}_p} = \partial_t$. Now, the asymptotic region $\mathscr{I}$ for $\mathcal{M}$ is the union of all the $\mathfrak{i}_p$:

$$\mathscr{I} = \bigcup_p \mathfrak{i}_p\,. \tag{4.21}$$

Let us notice that in theories with no limiting speed there is no formal notion of null infinity and spacelike infinity. The asymptotic region is only defined by some properties of the metric-aether couple.

It is possible to interpolate between the relativistic definitions of infinities and this one given in equation (4.21), by considering the conformal boundary for a speed-c metric. For any finite c we will obtain a similar asymptotic structure with respect to the relativistic case. For $c \to \infty$, we recover the definition of $\mathscr{I}$ that we have given in (4.21) (see [117] for more details). However, for the purpose of our discussion, we will skip this discussion here.

The complementary region to the black hole one is defined by "The set of causal curves which reaches $\mathscr{I}$ in the future". Therefore, we can take $\mathscr{I}$ and trace back all the causal curves which future endpoints belong to $\mathscr{I}$. Let us indicate this trace-back with $J^-(\mathscr{I})$. The black hole region $\mathcal{B}$ is defined as:

$$\mathcal{B} = \mathcal{M} \backslash J^-(\mathscr{I})\,. \tag{4.22}$$

This is of course a notion that is as teleological as in GR, since it requires one to know the whole history of spacetime. A more useful notion of black hole region, can be given, as well as in relativistic geometries, if the spacetime is static. Let us see how.

Universal horizon

If the spacetime is stationary, i.e. it admits a Killing vector χ for which

$$\mathcal{L}_\chi u = 0\,, \tag{4.23}$$

and asymptotically flat, namely

$$(u\cdot\chi)|_{\mathscr{I}}=-1\,,\qquad \gamma_{ab}\chi^a\chi^b|_{\mathscr{I}}=0\,, \tag{4.24}$$

then we can define the black hole region with a local statement. The black hole's horizon will be given by the so-called *universal horizon (UH)* which defines the following two conditions:

$$(u\cdot\chi)=0\,,\qquad (a\cdot\chi)\neq 0 \tag{4.25}$$

with a being the acceleration of u. The fact that this object defines an horizon is explained as follows: the condition (4.23) can be employed to show that $\{(u\cdot\chi)=0\}$ is a leaf orthogonal to u^a itself [117]. However, in each point of this leaf, $(u\cdot\chi)\neq -1$ by definition. So, this leaf never reaches the asymptotic region and is compact [117]. This means that, once a particle following a causal curve, crosses this surface inwards, then coming back to the outside is impossible, without going backwords in the preferred time. In this sense, every physical particles, which must go forward in the preferred time, are trapped by the UH.

The condition $(a\cdot\chi)\neq 0$, as we will see, it is tantamount to ask the black hole not to be extremal. In [117] is fundamental to show that the UH is actually a leaf Σ, but can be relaxed in order to define extremal objects [118].

4.2.2 Spherically symmetric universal horizons

The spherically symmetric case is obviously of particular interest, so let us start with that one. The high degree of symmetry in spherical spacetimes constraints the aether to be hypersurface orthogonal [115]. Therefore, EA and khronometric solutions match and we can use the notions developed in section 4.2.1.

In particular, in spherical coordinates $\{t,r,\theta,\varphi\}$ we will consider a spherically symmetric aether $u_a=u_a(r)$ with $u_\theta=u_\varphi=0$. The stationarity is given by $\chi^a\partial_a=\partial_t$ and we have:

$$\mathcal{L}_\chi u_a=0\,,\qquad \mathcal{L}_\chi g_{ab}=0\,. \tag{4.26}$$

One can try to solve (4.15) in this geometry. Let us consider a static spherically symmetric metric in Schwarzschild coordinates [107]

$$\mathrm{d}s^2=-F(r)\mathrm{d}t^2+\frac{B(r)^2}{F(r)}\mathrm{d}r^2+r^2\mathrm{d}\mathbb{S}_2\,, \tag{4.27}$$

and a spherically symmetric aether

$$u_a\mathrm{d}x^a=\frac{1+F(r)A(r)^2}{2A(r)}\mathrm{d}t+\frac{B(r)}{2A(r)}\left(\frac{1}{F(r)}-A(r)^2\right)\mathrm{d}r. \tag{4.28}$$

Here $F(r)$, $B(r)$, and $A(r)$ are arbitrary functions to be determined by the EA field equations, while the normalization of the aether is chosen for convenience, and automatically satisfies the unit norm condition $|u|^2=-1$.

Let us notice that a Killing horizon may be present for $|\chi|^2 = F(r) = 0$. In order to satisfy (4.25) and (4.24) we must have that the Killing vector passes from a timelike behaviour (near $\mathscr{I}$) to a spacelike one (near the UH), therefore becoming null, at some point. In figure 4.1 we give a representation, through a Penrose diagram, of an eternal, spherically symmetric, LV black hole. Therefore a root for $F(r)$ is anyway needed. Asymptotic flatness implies:

$$F(r) \to 1\,, \quad B(r) \to 1\,, \quad A(r) \to -1\,, \tag{4.29}$$

for $r \to \infty$. Solutions of (4.15) of the form (4.28) and (4.27) are present in all the parameter space [112], although in a numerical form. However, two analytical forms are known form some specific values of α, β and λ [107, 119]. Specifically, for both $B(r) = 1$ everywhere and r_0 represents twice the ADM mass of the spacetime:

- **Case $\alpha = 0$:**

$$F(r) = 1 - \frac{r_0}{r} - \beta\frac{r_{\rm ae}^4}{r^4}\,, \quad A(r) = -\frac{1}{F(r)}\left(-\frac{r_{\rm ae}^2}{r^2} + \sqrt{\frac{r_{\rm ae}^4}{r^4} + F(r)}\right) \tag{4.30}$$

  and

$$r_{\rm ae} = \frac{r_0}{4}\left(\frac{27}{1-\beta}\right)^{1/4} \tag{4.31}$$

  is an integration constant which has been chosen in order to keep $A(r) \in \mathbb{R}$. The UH for this solution corresponds to a sphere of radius:

$$r_{\rm UH} = \frac{3r_0}{4}\,. \tag{4.32}$$

- **Case $\beta + \lambda = 0$:**

$$F(r) = 1 - \frac{r_0}{r} - \frac{\mathcal{C}(\mathcal{C}+r_0)}{r^2}\,, \quad A(r) = -\frac{r}{r+\mathcal{C}}\,. \tag{4.33}$$

  and

$$\mathcal{C} = \frac{r_0}{2}\left(\sqrt{\frac{2-\alpha}{2(1-\beta)}} - 1\right) \tag{4.34}$$

  The UH for this solution corresponds to a sphere of radius:

$$r_{\rm UH} = \frac{r_0}{2}\,. \tag{4.35}$$

Solutions (4.30) is compatible with the observational bounds, while (4.33) is compatible only if one impose also $\alpha = \lambda = 0$, thus implying $\beta = 0$ and reducing to GR. However, that branch is interesting because, fixing the couplings in such a way that $\mathcal{C} = 0$, one finds the metric (2.17) with $A = -1$ that implies an aether compatible with the Schwarzschild metric:

$$u_a {\rm d}x^a = -\frac{F(r)+1}{2}{\rm d}t - \frac{1}{2}\left(\frac{1}{F(r)} - 1\right){\rm d}r\,. \tag{4.36}$$

In this highly symmetric situation, we can also generically integrate the shape of the foliation (or *preferred time*) $\tau(t,r)$. If we choose the lapse function

$$-N = u\cdot\chi = u_t\,, \tag{4.37}$$

we can define a preferred timelike coordinate

$$\tau = t + \int^r \frac{u_r}{u_t}\mathrm{d}r\,. \tag{4.38}$$

One can explicitly check that $\tau(r,t)$ is the scalar function entering equation (4.8). Within this choice, the UH can be also defined through $N=0$. Interestingly, the preferred time value blows up while approaching the horizon, since the $r-$component of (4.38) diverges logarithmically while approaching $u_t=0$. However, the aether $u_a\mathrm{d}x^a = N\mathrm{d}\tau$ is integrable and well-defined, crossing smoothly the UH. We shall see the implications of this observation in Chapter 5.

Another convenient choice of coordinates, can be made by considering the spacelike vector s^a orthogonal to u^a (analogously to what we did in (3.25)), defining in the same way a preferred spacelike coordinate $\rho(t,r)$

$$\rho = t + \int^r \frac{s_r}{s_t}\mathrm{d}r\,. \tag{4.39}$$

In the following, the chart $\{\tau,\rho\}$ will be addressed as *preferred frame*.

Within the spherically symmetric geometries, an alternative definition for the UH, which makes use of s^a can be given studying the expansion θ_s:

$$\theta_s = h^{ab}\nabla_a s_b \quad \text{where} \quad h^{ab} = g^{ab} + u^a u^b - s^a s^b \tag{4.40}$$

that defines the UH with the equations $\theta_s=0$, thus recalling the relativistic formalism of Killing horizons with the null expansion coefficients [120].

The metric, written in the $\{\tau,\rho,\theta,\varphi\}$ coordinates, takes the form

$$\begin{aligned}\mathrm{d}s^2 &= (-u_a u_b + s_a s_b)\mathrm{d}x^a\mathrm{d}x^b + r(\tau,\rho)^2\mathrm{d}\mathbb{S}_2\\ &= -N^2\mathrm{d}\tau^2 + V^2\mathrm{d}\rho^2 + r(\tau,\rho)^2\mathrm{d}\mathbb{S}_2\,,\end{aligned} \tag{4.41}$$

where $V = s\cdot\chi$. The definition of these quantities has a direct link with the acoustic geometry. If one, in the $\{t,r\}$ plane, makes the replacements

$$N \longleftrightarrow c_s \quad \text{and} \quad V \longleftrightarrow v \tag{4.42}$$

recovers the geometry (3.4) in (1+1) dimensions [5]. Indeed, the Killing horizon (please, compare to (3.8)) is given by:

$$-F(r) = |\chi|^2 = -(u\cdot\chi)^2 + (s\cdot\chi)^2 = V^2 - N^2 = 0\,. \tag{4.44}$$

[5] Actually, this is not explicit in the preferred frame. However, it is possible to define a coordinate $X(\rho,\tau)$ such that $s^a\partial_a = \partial_X$. In $\{t,X\}$ the aether takes the form $u_a\mathrm{d}x^a = N\mathrm{d}t$ and the line element assumes the Painlevé-Gullstrand form:

$$\mathrm{d}s^2 = -N^2\mathrm{d}t^2 + (\mathrm{d}X + V\mathrm{d}t)^2 \tag{4.43}$$

where the interpretation of N as the sound speed and of V as the flow velocity is explicit [121]

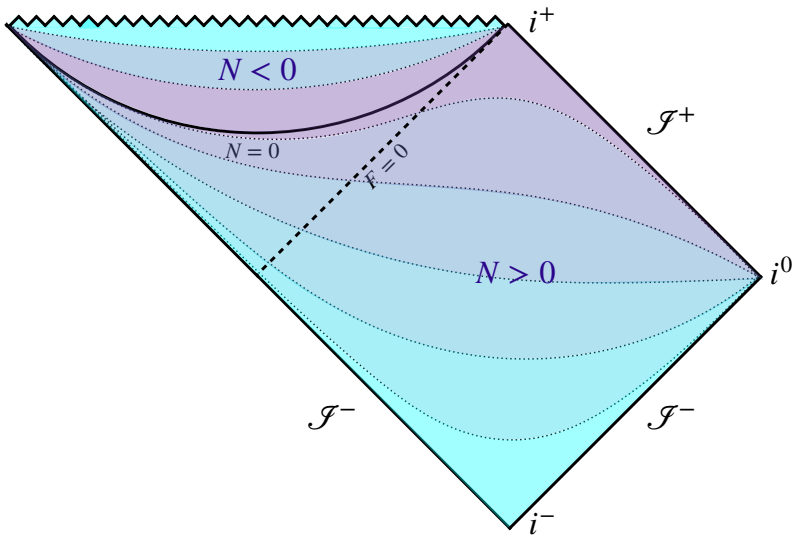

Figure 4.1: Penrose diagram for an EA spherical black hole: the Killing horizon is depicted by the dashed line, while the bold line displays the universal horizon at $N = 0$. Dotted lines mark the individual leafs $\Sigma \perp u$, with the color coding indicating the value of the preferred time (4.38) from an outside observer perspective. Purple indicates large τ, while cyan corresponds to small values of τ. The asymptotic regions can be defined similarly to the relativistic Schwarzschild black hole [117].

Surface gravity

One can associate to UH some analogous properties that horizons have in GR. A notion of surface gravity is well defined [119, 122] and reads

$$\kappa_{\rm UH} = \frac{(a\cdot\chi)}{2}\bigg|_{\rm UH} = \frac{1}{2}u^a\partial_a(u\cdot\chi)\bigg|_{\rm UH}\,. \tag{4.45}$$

Some observations on the definition of $\kappa_{\rm UH}$ are:

- Since $(u\cdot\chi) = 0$ defines a constant-khronon leaf, $\kappa_{\rm UH}$ corresponds to the normal derivative of the function defining the surface. In [122], this quantity has been shown to coincide with the possible alternative definitions of surface gravity for UHs.

- $\kappa_{\rm UH}$ is constant over all the UH [117]. This, from a BH-thermodynamical viewpoint, corresposnds to the so-called *zeroth law* of BH thermodynamics.

- (4.45) implies that the lapse function N must vanish regularly with a well defined derivative. A kink-behaviour like $N \simeq |r-r_{\rm UH}|$ brings to ill-definiteness in the QFT of such spacetime [35].

- The request $a\cdot\chi \neq 0$ contained in (4.25) can be read as a non-vanishing surface gravity. As already mentioned, see [118] for the extremal treatment $(a\cdot\chi) = 0$.

4.2.3 Analogue UH?

At this point, it is quite natural to ask ourselves the following question: given the similarities of the geometries, are there any analogue version of UH?

The problem has been addressed in [83] and the answer is, unfortunately, that there is none. The motivation lies in the fact that the geometries that we can derive from analogue models (3.4) are endowed with a notion of preferred frame (3.11), so with a notion of aether. Nevertheless, this aether vector field is not an additional ingredient to the geometry but can be completely derived from the metric. In LV gravity, however, we can see that u_a contains, even in static, spherically symmetric spacetimes, an additional degree of freedom (the function A) which does not appear in the metric tensor (4.28).

This lack of freedom limits the choice of aether-metric geometries in analogue models to a set of backgrounds which cannot enjoy any UH structure. If one considers additional ingredients – thus increasing the number of degrees of freedom– such as an external magnetic field, it is possible to show that such an horizon can be made of analogue spacetimes [123].

4.3 Digression on axisymmetric solutions

Now that we have described spherically symmetric solutions, the logical extension would be to study rotating objects. However, the existence of rotating black holes is a currently standing problem. In khronometric theory, slowly rotating solutions have been studied numerically [111], but extensions to higher spins and analytical treatments are still lacking.

EA theory seems to offer a more feasible playground where to look for rotating solutions. Actually, numerical rotating geometries have been found [124] for arbitrary high spins, even if those geometries arise without Killing horizons.

A interesting analytical solution has been found in [125]: restricting within the corner of the parameter space correspondent to

$$c_a = c_\sigma = c_\omega = 0\,, \tag{4.46}$$

it is possible to solve the field equations by imposing the Kerr geometry at the metric level and any normalized timelike vector u^a with zero expansion, namely

$$\theta_u = \nabla_a u^a = 0\,. \tag{4.47}$$

The interesting feature of this solution is that it exhibits a possible notion of UH. Indeed, considering the Killing vector for the Kerr geometry, which in Boyer-Lindquist (BL) coordinates [43] takes the form $\chi^a\partial_a = \partial_t$, the solution presented in [125] has a surface correspondent to the condition[6]:

$$\chi_a u^a = 0\,. \tag{4.48}$$

[6]Since the solution is axysimmetric, $u_\varphi = 0$ and the equation (4.48) is satisfied simultaneously by the vector ∂_t and the generator of the Killing horizon $\partial_t + \Omega_{\rm H}\partial_\varphi$, where $\Omega_{\rm H}$ is the angular velocity of the solution

This surface, called quasi-universal horizon (QUH), is in BL coordinates an oblate surface $r = r_{\rm QUH}(\theta)$ which *is not orthogonal to the aether* u^a. This is allowed by the structure of the EA theory and it is a mathematical consequence of the non-vanishing twist $\omega_{ab} \neq 0$ of this solution.

This non-hypersurface orthogonality, however, spoils the analysis of [117], and so the local definition of the UH given in (4.25) does not *à priori* imply any causal property. Therefore, the name QUH. Intuitively, the non-hypersurface orthogonality allows for causal, future-directed trajectories to escape the QUH classically, without going backwards in the preferred time. In the following section, we shall comment on the possibility for (4.48) to define a true horizon and speculate on the possibilities for having rotating solutions.

4.3.1 Rotating UH?

Let us set up the spacetime symmetries. In the following we will consider an aether-metric couple (g_{ab}, u_a), describing our spacetime. We assume that the metric admits two Killing vector fields: χ^a, generating time translations, and ψ^a, generating rotations around an axis; χ^a is assumed to be timelike in a neighbourhood of infinity, while ψ^a, whose orbits are closed, is assumed to be everywhere spacelike. Hence, the metric is assumed to be stationary, but not necessarily static, and axisymmetric. Moreover, we assume that the Killing vectors commute and that the aether obeys the same symmetries as the metric, i.e. we assume it to be Lie-dragged along the Killing vector fields:

$$\mathcal{L}_\chi \psi^a = 0\,, \tag{4.49}$$

$$\mathcal{L}_\chi u^a = 0 \quad \text{and} \quad \mathcal{L}_\psi u^a = 0\,. \tag{4.50}$$

In addition, we assume that

$$u_a\, \psi^a = 0\,. \tag{4.51}$$

This condition, which entails that an observer at rest in the aether frame has zero Killing angular momentum (i.e. it is "ZAMO"), is herein assumed because it greatly simplifies the discussion. Though this does not seem indispensable, it is physically well motivated: indeed, if (4.51) were not satisfied, the integral curves of ψ^a would be causal and closed – thus nullifying the chronology protection conjecture and possibly leading to paradoxes.

It is quite natural to address this problem in the following particular basis for the tangent space: the timelike direction will be u^a. The first spacelike leg can be taken to be

$$\varphi^a = \psi^a / |\psi|\,. \tag{4.52}$$

Then we take a second (unique, up to a sign) spacelike vector θ^a, normalized, and orthogonal to u, χ and φ, namely

$$\theta_a \chi^a = \theta_a u^a = \theta_a \varphi^a = 0\,. \tag{4.53}$$

To complete the basis, we determine s^a as the orthonormal direction to u^a, θ^a and φ^a (but not orthogonal to χ^a). Therefore our basis will be $\{u^a, s^a, \theta^a, \varphi^a\}$. In this basis, the twist tensor

$$\omega_{ab} = \nabla_{[a} u_{b]} + u_{[a} a_{b]} \,, \tag{4.54}$$

where $a^a = u^b \nabla_b u^a$, will have only one independent component[7]. It is quite straightforward to see that ω_{ab} is orthogonal to ψ^a, namely

$$\omega_{ab} \psi^a = 0 \,, \tag{4.56}$$

and, by construction

$$\omega_{ab} u^a = 0 \,, \tag{4.57}$$

therefore the only component that does not vanish trivially is given by $\omega_{ab} s^a \theta^b$ or, equivalently, using χ^a,

$$\omega_{ab} \chi^a \theta^b = (s \cdot \chi) \omega_{ab} s^a \theta^b \,. \tag{4.58}$$

Causal boundary

The definition of a causal boundary for a theory with a preferred frame must be given by the causal structure of the theory. Since, in principle, both in EA and in khronometric theory there is no notion of limiting speed for particles, the causality is determined just by going forward in time. This means that a signal following a causal curve $x^a(\lambda)$ will generically travel along a tangent vector of the form

$$\dot{x}^a = u^a + c_S v^a \,, \tag{4.59}$$

where v^a is a normalized combination of s^a, θ^a and φ^a and c_S is the velocity at which it propagates. Here we have parametrized $x^a(\lambda)$ in such a way that $\dot{x}^a u_a = -1$, so the curve is future directed. Now, let us consider a compact spacelike surface $\mathcal{S}$ and let us call its inward-pointing, normal, timelike vector n^a. In order to escape this surface, c_S has to satisfy:

$$0 < n_a \dot{x}^a = -n_a u^a + c_S n_a v^a \implies c_S > \frac{n \cdot u}{n \cdot v} \,. \tag{4.60}$$

Since c_S is unbounded, apparently we can always tune it in order for the signal to escape $\mathcal{S}$, even if it goes forward in the preferred time. However, if

$$n_a v^a = 0 \tag{4.61}$$

for any spacelike vector v^a this might not be the case. The above condition implies that n^a is parallel to u^a, i.e. u^a is hypersurface orthogonal on $\mathcal{S}$.

[7]Note that here we define the anisymmetric part of a tensor T_{ab} as:

$$T_{[ab]} = \frac{1}{2} (T_{ab} - T_{ba}) \tag{4.55}$$

This surface, in order not to reach the asymptotic region, has to evade the condition (4.24). Therefore, we can consider the surfaces

$$(u \cdot \chi) = \text{const.} \tag{4.62}$$

and define their normal vector:

$$n_a = \nabla_a (u \cdot \chi) \,. \tag{4.63}$$

Note that no surface of this kind can reach the asymptotic region $\mathscr{I}$, since, by definition of $\mathscr{I}$ we have $(u \cdot \chi)|_{\mathscr{I}} = -1$. Working in our basis, we can write down the components of n_a

$$\begin{aligned} n_a = &- \left(a_b \, \chi^b\right) u_a + \left(u_b \, \chi^b\right) \left(a_c \, s^c\right) s_a + \\ &\left[\left(u_b \, \chi^b\right) \left(a_c \, \theta^c\right) + 2 \left(s_b \, \chi^b\right) \left(\theta^c \, \omega_{cd} \, s^d\right)\right] \theta_a \,. \end{aligned} \tag{4.64}$$

In order for a causal trajectory not to escape one of this surface along the s-direction one has to find:

$$(u \cdot \chi) = 0 \,, \tag{4.65}$$

That exactly defines $\mathcal{S}$ as the QUH. One can write n_a, evaluated at $(u \cdot \chi) = 0$

$$n_a|_{\text{QUH}} = \left[- \left(a_b \, \chi^b\right) u_a + \left(s_b \, \chi^b\right) \left(\theta^c \, \omega_{cd} \, s^d\right) \theta_a\right]_{\text{QUH}} \,. \tag{4.66}$$

This makes us conclude that $n^a \propto u^a$ (so ensuring the no-esacping condition also in θ) only if

$$\left(\theta^c \, \omega_{cd} \, s^d\right)_{\text{QUH}} = 0 \iff \omega_{ab}|_{\text{QUH}} = 0 \,. \tag{4.67}$$

Therefore the conclusion, which is quite obvious, is that the QUH is an UH only if the twist vanishes on $(u \cdot \chi) = 0$ (which, unfortunately, is not the case for [125]). Whether this is possible without having complete hypersurface orthogonality – namely, the twist vanishes pointwise on $\mathcal{S}$ only – is not clear and it is material for future work. However, let us stress that, within the EA framework, the requirement $\omega_{ab} = 0$ is highly unstable, since we expect generic perturbation of the aether field δu^a to add also a component $\delta\omega_{ab}$ to the twist, destroying the UH structure.

Chapter 5

Hawking radiation in LV gravity: a tale of two horizons

The presence of black holes in LV contexts, although not obvious, renders the theory viable for their phenomenological investigations. The presence of horizons which are universal for any kind of particle, resembles very closely the relativistic situation, where the horizon is completely detrmined by the causal structure of the theory, *à priori* from the specifics of particles.

In this Chapter, we will probe the QFT effect in such curved backgrounds. Our analysis will focus on spherically symmetric geometries.

We have already pointed out in Chapter 3 that Killing horizons, at least in the low-energy regime, radiate with an (approximate) thermal spectrum. However, the non-thermal deviations of the spectrum are a direct consequence of the dispersive character of perturbations. The main point is to see how MDRs – which also characterize the LV gravity theory – percieve the presence of such a universal surface, which was not considered in the previous chapters.

In the following, we shall study Hawking radiation in the presence of UH and the presented results are mainly based on [36, 38]. We will take the chance to analyze previous calculations [119, 121, 126, 127] and to spot the differences between our results and the ones contained in these previous works.

5.1 On the necessity of universal horizons

Before jumping into the analysis of the QFT with a UH, let us make an observation. From the causal point of view, the motivation which encouraged the search for a surface which can trap universally every kind of signals, comes from spacetimes where no limiting speed is present. If particles enjoy dispersion relations such as (4.20), then an UH is the only way to define a black hole.

Nevertheless, such a surface is needed also in the case of particles travelling at a finite speed – which is the case, for instance, that corresponds to the gravitational perturbations in EA theory [114, 115].

This can be shown with a thermodynamical reasoning [128–130]: let us consider two types of massless particles (type 1 and type 2) which enjoy two different causal

cones, defined by the velocities c_1 and c_2, with $c_2 > c_1$:

$$\omega_1 = c_1|\mathbf{k}_1|\,, \qquad \omega_2 = c_2|\mathbf{k}_2|\,. \tag{5.1}$$

These two particles feel two different horizons, which corresponds to the Killing horizon of the metric capturing their causal structures. In particular, if the energies ω_i in (5.1) are given with respect to a time direction u^a, then the effective metrics describing our particles as objects travelling along null trajectories are:

$$g_{1,ab} = g_{ab} + (1 - c_1^2)u_a u_b\,, \quad g_{2,ab} = g_{ab} + (1 - c_2^2)u_a u_b\,, \tag{5.2}$$

where g_{ab} is the original metric. The surfaces which work as causal boundaries for particles 1 and 2 are given by the Killing horizons of the disfomal transformed metric (5.2).

Those surfaces will radiate, by Hawking effect, with temperatures T_1 and T_2. Note that $c_2 > c_1$ implies $T_2 > T_1$. Now, following [128], let us consider two shells A and B, interacting only with particle 1 and 2, respectively. Let us choose those two shells with temperatures T_A and T_B in such a way that

$$T_B > T_2 > T_1 > T_A\,. \tag{5.3}$$

Given $T_A > T_1$, there will be a flux $\Phi(T_A, T_1) > 0$ of particles of type-1. Conversely, since $T_B < T_2$, the type-2 flux will go on the other direction, namely $\Phi(T_B, T_2) < 0$. So, a net flux of energy is extracted from the surface A and another one is acquired from the shell B. If we fine tune the shells A and B in order for the two flux to compensate:

$$\Phi(T_A, T_1) = -\Phi(T_B, T_2)\,, \tag{5.4}$$

then we will have that the black hole mass will not decrease. From an exterior observer, nothing happens if not a net energy flux from A to B. However, since A is colder than B, this would violate the second law of thermodynamics, thus making possible to build a *perpetuum mobile*.

This construction, pictorially represented in figure 5.1 mrefined later on in [129, 130], tells that multiple limiting speeds are in conflict with thermodynamics.

Subsequent works [131], where it has been proven that this general construction does not apply to spherically symmetric geometries in theories where gravity is attractive, such as EA or Hořava gravity. This may suggest that such a perpetuum mobile is not actually possible in general, but the picture has still to be completed in this direction.

Nevertheless, the introduction of Lorentz invariance violations as a species-dependent geometries can evidently lead to possible paradoxes. On top of that, this may spoil the point of view of the Hawking effect as a kinematical effect, making it depending on the specific of the coupling of perturbation with gravity. This makes the UH an appealing extension as an horizon candidate for theories with a preferred frame.

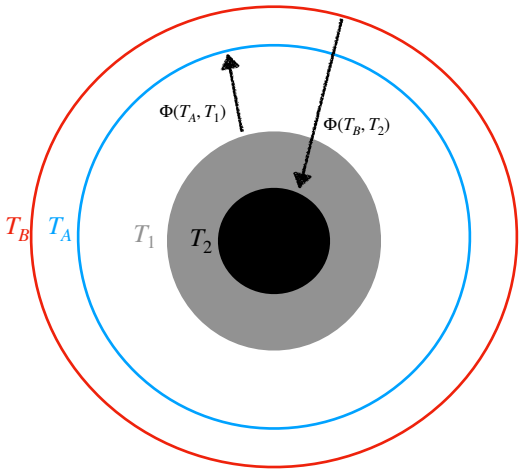

Figure 5.1: Pictorial representation of a perpetuum mobile of the secon kind. An outgoing flux $\Phi(T_1, T_A)$ and an incoming one $\Phi(T_2, T_B)$ creates a net flux from a colder shell A to a hotter one B

5.1.1 Hawking radiation from UH: previous results

As soon as it was realized that UHs exist, the investigation on their radiative properties started [119]. In order to probe the presence of an UH, one should consider a particle which fulfills a MDR like (4.20). Let us consider a spherically symmetric geometry. For phenomenological's sake, one can generically consider, for a generic $n \in \mathbb{N}$, a particle satisfying

$$\omega(k)^2 = k^2 + \sum_{j=2}^{n} \beta_{2j} \frac{k^{2j}}{\Lambda^{2j-2}} \,, \tag{5.5}$$

where ω is the energy with respect to u^a, k is the momentum defined with respect to its orthogonal s^a. In the following, we will avoid subluminal behaviours taking $\beta_{2j} \geq 0$. In general, a particle's trajectory will be defined by the group velocity c_g

$$c_g = \frac{\mathrm{d}\omega}{\mathrm{d}k} = \frac{k}{\omega} \left(1 + \sum_{j=2}^{n} j \beta_{2j} \frac{k^{2j-2}}{\Lambda^{2j-2}} \right) \,, \tag{5.6}$$

and follows the curve:

$$\mathrm{d}\bar{u} = (c_g u_a + s_a) \mathrm{d}x^a = 0 \,. \tag{5.7}$$

As we shall see, in the near-UH limit, the particle undergoes an infinite blueshift, analogously to what happens in GR nearby Killing horizons. This implies that, in equation (5.6), only the highest $j = n$ term in the sum will contribute. Therefore, the near-horizon physics of the group velocity is sensitive to n. Skipping the technical details, which we shall explain better in the following sections, one can study the

trajectory (5.7) and compute the tunneling probability through the UH, finding [126, 127]:

$$T_{\rm UH} = \frac{n}{n-1}\frac{\kappa_{\rm UH}}{\pi}\,. \tag{5.8}$$

Obviously, since $c_g = c_g(n)$, also the temperature will be $n-$dependent. This result, which we will comment, resolves only partially the problem which we presented in section 5.1. In fact, it was noticed in previous works that the solution comes at the price of invoking some UV-completion argument to impose the universality of the exponent n for every LV particle living wihtin our spacetime.

Indeed, one should exclude the case for which different partilcles obey (5.5) for different n. If n is non-unique, say we have $n_1 \neq n_2$, then we could repeat the perpetuum mobile construction with $T_{\rm UH}(n_1)$ and $T_{\rm UH}(n_2)$.

Invoking the universality of n is not a crazy idea, in the context of Hořava gravity: the power-counting renormalisability fixes $n = 3$ for the gravitational sector, and one expect the same argument to hold for matter fields, see cf. [105, 132]. However, in the EA context, it is not clear why we should fix that exponent.

In contrast with these calculations, the literature contains even more puzzling results [121]. In an analogue-inspired calculations, the authors argue that no radiation is emitted by the UH. They find that all the radiative properties are expressed by the Killing horizons, in a similar way to what we have found in Chapter 3. This result is even more astonishing: since the UH is the true causal barrier of foliated spacetimes, the tunnel-out through quantum processes should be there in a way very similar to GR.

In addition, in [119] the authors find a third different result, valid only for the case $n = 2$. That anisotopic scaling does not match the $n = 3$ UV-requirement of Hořava proposal, enhancing the tension contained in the literature.

In what follows we shall revise in details the calculations that drive to the Hawking radiation from UH. We will rederive the temperature and discuss these contrasts, higlighting a possible way to solve the inconsistencies.

5.2 Particles in LV black holes

In order to probe static spherically symmetric UHs we will consider the geometry given in (4.28) and (4.27). If calculations requires specific expressions for the functions $A(r)$, $B(r)$ and $F(r)$ we will specify to:

$$A(r) = -1\,, \quad B(r) = 1\,, \quad F(r) = 1 - \frac{2M}{r}\,, \tag{5.9}$$

which is exactly the solution given in (4.33) for $\mathcal{C} = 0$. For this solution the UH is given by [38]

$$N = -\chi \cdot u = \frac{M}{r} - 1 = 0 \implies r_{\rm UH} = \frac{r_{\rm KH}}{2} = M\,, \tag{5.10}$$

which coincides with (4.35).

Matter fields on this geometry will be taken in order to be able to probe the UH. Therefore we consider the following action for a massless scalar field ϕ:

$$S_{\rm m} = \frac{1}{2}\int_{\mathcal{M}} {\rm d}^4x\,\sqrt{-g}\,\phi\left[\Box + \sum_{j=2}^{n}\frac{\beta_{2j}}{\Lambda^{2j-2}}(-\Delta)^j\right]\phi\,, \tag{5.11}$$

where $\Box\phi = g^{ab}\nabla_a\nabla_b\phi$ is he usual d'Alambert operator and $\Delta\phi = \gamma^{ab}\nabla_a\nabla_b\phi$ is the spatial (in the preferred frame sense) Laplace operator, being $\gamma_{ab} = g_{ab} + u_a u_b$ the projector onto Σ. The ϕ-variation of (5.11) leads to the equation of motion

$$\Box\phi + \sum_{j=2}^{n}\frac{\beta_{2j}}{\Lambda^{2j-2}}(-\Delta)^j\phi = 0. \tag{5.12}$$

Here all the β_i are coupling constants, while n controls the scaling of the equations at large momentum. We have normalized $\beta_{2n} = 1$, which is always possible by rescaling the energy scale Λ. For simplicity, we have also set the infrared speed of the mode to $c = 1$, in order to agree with the GR result in the decoupling limit. We will also assume that all $\beta_i \geq 0$, in order to avoid regions of the parameter space with sub-luminal behavior, as we did in the preliminary discussion below (5.5).

5.2.1 WKB ansatz

Once again, we will focus on a WKB treatment of the solution, like what we did in (2.45). Therefore, we will consider the field ϕ to assume the form

$$\phi_{\rm WKB} = \phi_0 e^{i\mathcal{S}_0}\,, \tag{5.13}$$

where the phase $\mathcal{S}_0$ is the point particle action, so that curves with constant phase are equivalent to trajectories followed by classical rays. It is useful to define the two functions ω and k which satisfy the eigenvalue equations

$$u^a\partial_a\phi = -i\omega\phi \quad \text{and} \quad s^a\partial_a\phi = -ik\phi\,, \tag{5.14}$$

namely the preferred energy and the preferred momentum. Here we have suppressed any angular dependence, thus focusing solely on the s-wave contribution to the solution.

The advantage of this choice is that, as previously discussed, only in the preferred frame the equation of motion reduces to the dispersion relation

$$\omega^2 = k^2 + \sum_{j=2}^{n}\frac{\beta_{2j}}{\Lambda^{2j-2}}k^{2j} + G(\omega,\nabla\omega,k,\nabla k)\,, \tag{5.15}$$

where the function $G(\omega,\nabla\omega,k,\nabla k)$ encodes all the terms which depend on the derivatives of either ω or k. If the evolution is adiabatic, namely $|\nabla k| \ll k^2$ we can neglect $G(\omega,\nabla\omega,k,\nabla k)$ and boil down to (5.5), which corresponds to an eikonal approximation. For now, let us assume adiabaticity and let us discuss it in the following.

Since neither u^a nor s^a are Killing vectors, ω and k are space-time dependent. Similarly to what has happened in Chapter 3, the Killing vector $\chi^a\partial_a = \partial_t$ allows to separate the variables in the (t, r) plane via the eigenvalue equation

$$\chi^a\partial_a\phi_\Omega = -i\Omega\phi_\Omega\,, \tag{5.16}$$

and label the modes ϕ_Ω with constant Killing energy Ω. Rewriting the left hand side of this definition in the preferred frame, we arrive to the identity

$$\Omega = -\omega(u\cdot\chi) + k(s\cdot\chi) = \omega N + kV\,, \tag{5.17}$$

where $V = (s\cdot\chi)$ and $N = -(u\cdot\chi)$, as introduced in Chapter 4. Together, equations (5.5) and (5.17) provide a complete system that can be solved for ω and k, and hence for the monochromatic mode ϕ_Ω.

Getting ω from (5.17) and substituting it into the dispersion relation (5.5), we obtain the following algebraic equation for k

$$\sum_{j=2}^{n}\frac{\beta_{2j}}{\Lambda^{2j-2}}k^{2j} + \left(1-\frac{V^2}{N^2}\right)k^2 + \frac{2\Omega V}{N^2}k - \frac{\Omega^2}{N^2} = 0\,. \tag{5.18}$$

This is a polynomial of degree $2n$ with position dependent coefficients. Note however that all coefficients accompanying powers of k are sign definite for all r – once the sign of Ω is chosen –, except for the term multiplying k^2, which vanishes at the Killing horizon, since $|\chi|^2 = -N^2 + V^2$.

Asymptotic solutions

In the outer region of the Killing horizon, (5.18) will display exactly two real roots, corresponding to positive and negative values of k. Indeed, in the asymptotic region $r \to \infty$, where $N = 1$ and $V = 0$, we get

$$\sum_{j=2}^{n}\frac{\beta_{2j}}{\Lambda^{2j-2}}k^{2j} + k^2 - \Omega^2 = 0\,, \tag{5.19}$$

which has exactly two real roots of opposite sign[1].

Near-UH solutions

In the region inside the Killing horizon instead, the change of sign allows for the number of real roots to potentially grow up to four. Focusing in the near-UH limit, where $N \to 0$, we indeed find four roots [121, 127] – two *hard solutions*, for which k diverges when approaching the UH; and two *soft solutions*, for which k remains finite. The latter two can be obtained straightforwardly by setting $N = 0$ and $V = 1$ in (5.17), obtaining

$$k_s = -\Omega, \quad \omega_s = \pm\Omega\sqrt{1 + \sum_{j=2}^{n}\beta_{2j}\alpha^{2j-2}}, \tag{5.20}$$

[1]These are the same solutions as the one found in (3.41) for $\xi = 1$.

where again $\alpha = \Omega/\Lambda$, as in (3.74).

For hard solutions instead, the radial momentum k diverges at the position of the horizon, with its behavior controlled by the highest power in the dispersion relation. The divergence must be polynomial from (5.5) and the exponent can be found by solving (5.17) at constant Ω:

$$\begin{aligned} k^{\pm}_{h,\text{out}} &= \pm\Lambda\left(-\frac{V}{N}\right)^{\gamma} - \frac{1}{n-1}\frac{\Omega}{V} + O(N)\,, \\ \omega^{\pm}_{h,\text{out}} &= \pm\Lambda\left(-\frac{V}{N}\right)^{n\gamma} + \frac{n}{n-1}\frac{\Omega}{N} + O(N^0)\,, \end{aligned} \tag{5.21}$$

where we have introduced the exponent $\gamma = 1/(n-1)$. The "out" label indicates that these solutions are obtained in the limit $N \to 0^+$, corresponding to the outer near-horizon region. If we look at the inner neighborhood instead, we get

$$k^{\pm}_{h,\text{in}} = \pm\Lambda\left(\frac{V}{N}\right)^{\gamma} - \frac{1}{n-1}\frac{\Omega}{V} + O(N)\,, \tag{5.22}$$

$$\omega^{\pm}_{h,\text{in}} = \mp\Lambda\left(\frac{V}{N}\right)^{n\gamma} + \frac{n}{n-1}\frac{\Omega}{N} + O(N^0)\,. \tag{5.23}$$

At some intermediate point inside the Killing horizon, but not necessarily at its surface, the character of the equation must change and the number of real solutions reduces to two, connecting to the exterior modes. This is exactly the turning point, found also in Chapter 3.

5.2.2 Wavepackets and characteristics

While above we have discussed monochromatic waves, in what follows we focus on the more physical case of a wavepacket. This has a direct link with the modelling of a particle and, as we will see in the following, it allows us to explore the differences induced by the modified dispersion relation (5.15) with respect to the general relativistic case.

As a wavepacket, we will consider a superposition of positive energy modes ϕ_Ω, centered around a frequency ω_0

$$\psi(r) = \int_0^{+\infty} \frac{\mathrm{d}\omega}{\sqrt{2\pi\sigma}}\,\phi_\Omega(r)\,e^{-\frac{(\omega-\omega_0)^2}{2\sigma}} = \int_0^{+\infty} \frac{\mathrm{d}\Omega}{\sqrt{2\pi\sigma}}\frac{\mathrm{d}\omega}{\mathrm{d}\Omega}\,\phi_\Omega(r)\,e^{-\frac{(\omega-\omega_0)^2}{2\sigma}}, \tag{5.24}$$

with standard deviation σ, and where $\mathrm{d}\omega/\mathrm{d}\Omega$ can be computed from the behavior of the modes. This expression satisfies the equations of motion (5.15) as long as the approximations previously introduced – WKB and adiabaticity – hold, since adiabaticity allows us to neglect derivatives of ω. Note that at large radii $\omega \to \Omega$ and ψ describes a Gaussian wavepacket in Killing frequencies.

The wavepacket ψ can be classically thought of as an object travelling with speed determined by its enveloping wave-front, with group velocity $c_g(r,\alpha) = \mathrm{d}\omega/\mathrm{d}k$. This determines the trajectory (5.7) of the particle once one specifies k and ω. In terms of c_g the trajectory reads, in the EFB frame $\{v(r), r\}$ (see (2.26)):

$$\frac{\mathrm{d}v}{\mathrm{d}r} = \frac{c_g + 1}{N c_g + V}, \tag{5.25}$$

or, in the preferred frame $\{\rho, \tau\}$:

$$\dot{\rho} = \frac{\mathrm{d}\rho}{\mathrm{d}\tau} = -\frac{N}{V} c_g \,. \tag{5.26}$$

Equation (5.25) can be integrated in r in order to find the characteristics of the four wavepackets. These are plotted, for the case $n = 2$, in figure 5.2.

Turning point

Analogously to what we have found in Chapter 3, the characteristics enjoy the presence of a turning point. This, as mentioned above, must lie inside the Killing horizon. However, with respect to the analogue gravity case, the presence of an UH admits the possibility of having two turning points: one outside the UH $r_{\mathrm{out}}(\alpha) > r_{\mathrm{UH}}$ and another one inside it at $r_{\mathrm{in}}(\alpha) < r_{\mathrm{UH}}$. Both of them depend on $\alpha = \Omega/\Lambda$ (defined in (3.74)), which also in this case governs the energy dependence of the trajectories. A complete analysis of the turning point location, in the case $n = 2$ is given in Appendix A.

The positions of the turning points are given by (5.25) whenever

$$c_g(r, \alpha) = -\frac{V}{N} \,. \tag{5.27}$$

In figure 5.2 we see explicitly that there are two modes turning back in the $\{v, r\}$ plane: the "orange mode" – which was called "turning mode" in the analogue case – which turns back in the exterior of the UH and the "blue mode" – which was called "regular mode" in Chapter 3 – that turns inside it.

5.2.3 Energy balance

Before moving on to investigate radiative properties of the UH, let us comment on the energy content of the particles that are depicted in figure (5.2). The natural interpretation of these particle must be given in terms of the preferred time direction u^a. Since

$$u^a \partial_a \phi = -i\omega\phi \tag{5.28}$$

then modes with $\omega > 0$ can be interpreted as particles moving forward in the preferred time direction. Therefore, in the following analysis, we will fix $\omega > 0$ for all the particles and see what this tells us for the associated Ω and their direction of propagation.

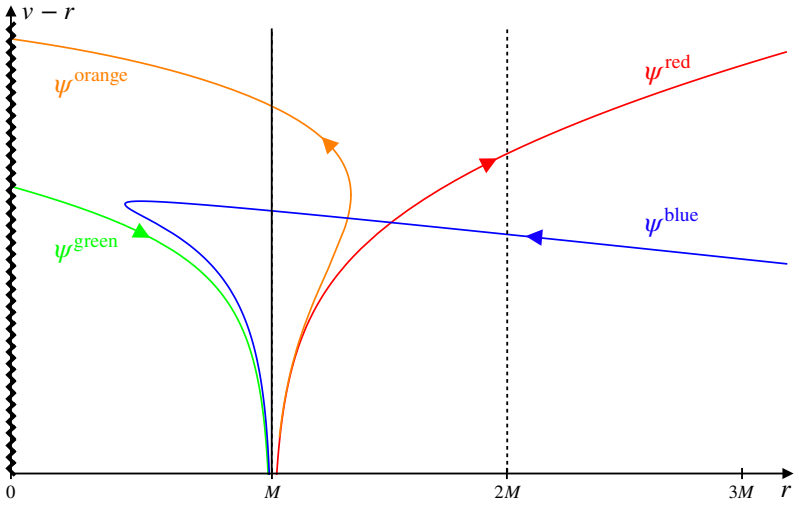

Figure 5.2: Characteristics of all modes for $\alpha = 0.5$ and $n = 2$. Starting from outside the Killing horizon at $r/M = 2$, we see that at fixed r, there are only two possible solution: the red out-going mode and the blue in-going one. In the interior of the Killing horizon we find the turning point $r_{\rm out}(\alpha)$, where the two orange lines meet. For $r_{\rm UH} < r < r_{\rm out}(\alpha)$ we have four real solutions. Inside the UH, the red line and the hard branch of the orange mode leave the stage to the green mode and the hard branch of the blue mode, until they reach $r_{\rm in}(\alpha)$, where the two blue modes' branches are linked. Beyond this point, only the orange and green lines hit the singularity. The arrows represent the direction of propagation of the rays, given by their group velocities c_g. The labels $\{\psi^{\rm red}, \psi^{\rm orange}, \psi^{\rm blue}, \psi^{\rm green}\}$ associated to each ray are the same ones that we refer to along the text.

Outside the horizon

If we focus outside the UH $r > r_{\rm UH}$ we have that the aether flows towards the horizon. Particles living here are analogous to the ones found in Chapter 3 and can be summarized as:

- **The blue mode** $\psi^{\rm blue}$: this is one of the two asymptotic solutions, the ingoing one. It has positive Killing energy and crosses the UH inwards.
- **The red mode** $\psi^{\rm red}$: also this one can be found within the asymptotic solutions as the positive-Ω outgoing one. Tracing it back, we can see that it has support only in the exterior of the UH and shows a hard behaviour like the one given in (5.21), in the branch with positive Ω.
- **The orange mode** $\psi^{\rm orange}$: this mode is a turning mode. It enjoys a hard branch $\psi^{\rm orange}_{\rm hard}$ which peels out from the UH, that is defined only outside by (5.21) and at the leading order in the near-UH limit it share the same trajectory as the red mode. Departing from the horizon it starts to differ from $\psi^{\rm red}$ and eventually turns back, with its upper branch $\psi^{\rm orange}_{\rm soft}$, crossing the UH. Imposing $\omega > 0$ for the orange modes means that it has to carry a negative Killing energy $\Omega < 0$.

	sgn(Ω)	sgn(ω)	Direction
ψ^{red}	+	+	Out
ψ^{blue}	+	+	In
$\psi^{\text{orange}}_{\text{hard}}$	−	+	Out
$\psi^{\text{orange}}_{\text{soft}}$	−	+	In

Table 5.1: Behavior of the modes in the exterior region. The last column indicates the direction of propagation.

Inside the horizon

Inside the horizon the situation is symmetric, at the level of solutions. However, due to the change of sign of the lapse N, inside the UH the aether u^a points inwards and departs from r_{UH} flowing into the singularity $r = 0$. However, we can still study the behaviour of the solutions:

- **The orange mode** ψ^{orange}: this is the smooth continuation of the upper branch $\psi^{\text{orange}}_{\text{soft}}$ that we found outside. It carries a negative-Ω Killing energies towards the singularity.

- **The green mode** ψ^{green}: this is a true novel mode, that was not present in the AG case. This mode carries a negative energy $\Omega < 0$ towards the singularity and it has support only inside the UH. Of course, at costs of employing the CPT symmetry of the equations (5.5) and (5.17):

$$(\Omega, \omega, k) \to (-\Omega, -\omega, -k) \tag{5.29}$$

  it can always be interpreted as a positive-Ω particle travelling towards the UH

- **The blue mode** ψ^{blue}: this mode is the other turning mode. It continues smoothly the trajectory of ψ^{blue} that crosses form outside with a soft behaviour $\psi^{\text{blue}}_{\text{soft}}$. Than, always carrying $\Omega > 0$, it turns back and it approaches the UH

	sgn(Ω)	sgn(ω)	Direction
ψ^{green}	−	+	In
$\psi^{\text{blue}}_{\text{soft}}$	+	+	In
$\psi^{\text{blue}}_{\text{hard}}$	+	+	Out
ψ^{orange}	−	+	In

Table 5.2: Behavior of all modes in the interior region. The last column indicates the direction of propagation.

Let us notice that the condition $\omega > 0$ must hold at any along the trajectory for particle with $\Omega \neq 0$. Otherwise, $\omega = 0$ would imply $k = 0$ through the MDR and consequently $\Omega = 0$. This condition always ensures us that, even if a ray peels at the UH – thus becoming asympotically parallel to a constant-khronon slice – it will always go locally forward in the preferred time direction.

5.3 Tunneling the UH

Armed with our knowledge of the behaviour of particles on a LV black hole, we are ready to compute the radiation given by the UH. Referring to figure 5.2, it is obvious that the wavepacket that interests us is represented by ψ^{red}. That, in the future asymptotic region $\mathscr{I}^+$, will describe the only outgoing radiation, so the one emitted by the black hole. In the following, we shall consider no incoming radiation from $\mathscr{I}^-$, therefore turning off ψ^{blue}, as we did in previous calculation on the AG case.

Once again, we want to apply the tunneling formalism to address this calculation. Therefore, in the same way we did in section 2.2.2, we have to specify the shape of the mode in the near-UH limit

5.3.1 Squeezing the wavepacket

Let us start with the following observation: in the relativistic case, the near-horizon behaviour of outgoing wavepackets and monochromatic waves is exactly the same. Considering a Gaussian superposition of fixed-energy modes ϕ_Ω or a pure Ω-labelled mode does not change the shape of the trajectory followed by the constant phase contours. Indeed, the former is specified by the group velocity c_g and the latter by the phase velocity c_p. In the relativistic case we always have, near the Killing horizon

$$\omega = |k|\,, \tag{5.30}$$

both for massive and massless particle[2]. This implies that:

$$c_p = \frac{\omega}{k} = \frac{\mathrm{d}\omega}{\mathrm{d}k} = c_g \tag{5.32}$$

Therefore, no difference occurs, from the tunneling point of view, between the two cases. Actually, in Chapter 2 we have not even specified if we were considering a wavepacket or a monochromatic wave. However, formally speaking, we have been worked with the fixed-energy modes ϕ_Ω (see (2.52) and below).

In the presence of MDRs, the degenracy between c_g and c_p does not hold anymore. This is clear from:

$$\begin{aligned} c_p = \frac{\omega}{k} &= \pm\sqrt{1+\sum_{j=2}^{n}\beta_{2j}\left(\frac{k}{\Lambda}\right)^{2j-2}} \\ \neq c_g = \frac{\mathrm{d}\omega}{\mathrm{d}k} &= \frac{k}{\omega}\left(1+\sum_{j=2}^{n} j\beta_{2j}\left(\frac{k}{\Lambda}\right)^{2j-2}\right)\,. \end{aligned} \tag{5.33}$$

[2]due to the infinite blueshift a massive particle will behave as:

$$\omega = \sqrt{m^2+k^2} \simeq |k| \tag{5.31}$$

So, which one do we choose? The answer can be derived just by looking at what the hard solutions (5.21) do the wavepacket defined in (5.24).

It is easy to see that the Gaussian distribution, due to the divergence of ω in approaching $N = 0$, squeezes the packet and projects it onto a mochromatic solution ϕ_Ω. We have, from (5.21)

$$\frac{\mathrm{d}\omega}{\mathrm{d}\Omega} = \frac{n}{n-1}\frac{1}{N}\,, \qquad \omega - \omega_0 = \frac{n}{n-1}\frac{\Omega-\Omega_0}{N}\,. \tag{5.34}$$

In this limit, the distribution in (5.24) hence becomes a delta distribution, given the identity

$$\lim_{N\to 0^+} \frac{n}{n-1}\frac{1}{\sqrt{2\pi\sigma}N}\, e^{-\frac{n^2(\Omega-\Omega_0)^2}{2\sigma N^2(n-1)^2}} = \delta(\Omega-\Omega_0)\,. \tag{5.35}$$

What we observe here, is nothing else than a huge blueshift which erases the details of the wavepacket when traced back to the UH. In this limit, the wavepacket experiences infinite squeezing, such that it eventually degenerates to a monochromatic mode ϕ_{Ω_0} near the UH, i.e.

$$\lim_{r\to r^+_{\mathrm{UH}}} \psi^{\mathrm{red}} = \phi_{\Omega_0}\,. \tag{5.36}$$

5.3.2 Signal velocity as a notion of causality

The projection of our wavepacket onto a monochromtic wave comes with no surprise, due to the infinite blueshift of ω. The problem is that no notion of group is now associated anymore to our particle. So, which kind of signal does ϕ_Ω represent? A nice treatment is given in [133]: whenever the frequency diverges, the function ϕ_Ω represents a signal which travel with the phase velocity c_p. This can easily be seen as a general feature, i.e. for any kind of dispersion relation $\omega(k)$. Indeed, locally, one can always recast our WKB solution of energy Ω as [133]:

$$\phi^m_\Omega(R,T) = \lim_{\varepsilon\to 0^+}\int_{-\infty}^{+\infty} d\omega \frac{e^{-i\omega T + ik_m(\omega)R}}{\Omega + \omega(u\cdot\chi) - k(s\cdot\chi) + i\varepsilon} \tag{5.37}$$

where the index m refers to one of the branches that invert the relation $\omega = \omega(k)$. The imaginary part $i\varepsilon$ has been put in order to shift the pole – which implements the constraint equation (5.17) for Ω – from the real axis. Note that integral (5.37) is computed at fixed points in the spacetime and we have set locally $u^a\partial_a = \partial_T$, $s^a\partial_a = \partial_R$ [3].

The implementation of the constraint at fixed Ω in the integral (5.37) can be understood via the Sokhotski-Plemelj theorem [84, 85] for a function of form $f(x)/(x-x_o)$ after a complexification around the pole x_o

$$\lim_{\varepsilon\to 0}\int_a^b \frac{f(x)}{x - x_o + i\varepsilon}\mathrm{d}x = -i\pi f(x_o) + \mathcal{P}\left(\int_a^b \frac{f(x)}{x-x_o}\mathrm{d}x\right) \tag{5.39}$$

[3] This can be done at any fixed point (τ_0,ρ_0) just by defining:

$$dT = u_a(\tau_0,\rho_0)dx^a\,, \quad \text{and} \quad dR = s_a(\tau_0,\rho_0)dx^a\,. \tag{5.38}$$

with $\mathcal{P}$ denoting the Cauchy principal value.

With the help of the Cauchy theorem [134], we can compute the integral since

$$\exp\left[-i\omega T + ik_m(\omega)R\right] \tag{5.40}$$

is analytical in the upper half of the ω-complex plane. When the exponential is dumped, namely:

$$\lim_{|\omega|\to\infty}(k_m(\omega) - \omega\theta) > 0\,, \tag{5.41}$$

with $\theta = T/R$, we have that the contour on the upper-half plane vanishes and therefore $\phi^m_\Omega(R,T) = 0$. So, (5.37) represents a signal which is not causally connected with the region outside the causal cone defined by the infinite limit speed of the group velocity. Therefore, the causal connection for $\phi^m_\Omega(R,T)$ is represented by a cone for which the edges are given by [133]:

$$R(T) = T \cdot \left(\lim_{|\omega|\to\infty} c_p\right)\,. \tag{5.42}$$

In other words, if we set $\phi^m_\Omega(R_0,T_0) \neq 0$ on a single point (R_0,T_0), the function $\phi^m_\Omega(R,T)$ will vanish outside the future cone, centered in (R_0,T_0), defined by (5.42).

In our case, the causal meaning captures exactly the structure of the foliation. Let us change coordinates, passing from the preferred frame to the $\{t,r\}$ one:

$$\begin{aligned} k_r(\omega,k) &= -\omega u_r + k s_r \\ \Omega(\omega,k) &= -\omega u_t + k s_t\,. \end{aligned} \tag{5.43}$$

In this case the infinite-frequency limit of the phase velocity for a dispersion relation (5.5) takes the form:

$$\lim_{|\omega|\to\infty}\frac{k_r}{\Omega} = \lim_{|\omega|\to\infty}\frac{-\omega u_r + k s_r}{-\omega u_t + k s_t} = \frac{u_r}{u_t} \tag{5.44}$$

which tells us that:

$$k_r = \Omega\frac{u_r}{u_t}\,, \tag{5.45}$$

that can be integrated in r find the effective null coordinate determining the causal cone

$$\bar{u} = \left(t + \int^r \frac{k_r}{\Omega}\mathrm{d}r\right) = \left(t + \int^r \frac{u_r}{u_t}\mathrm{d}r\right) = \tau\,, \tag{5.46}$$

with τ defined in (4.38) as the khronon. So, in the case at hand, an infinitely blueshifted signal will travel along the constant τ lines.

This analysis captures exactly the causal horizon, so the black hole region, which can be thought as the surface where the causal cone alignes with a surface that does not touch $\mathscr{I}$. Therefore, a signal moving closeby the black hole horizon will be a function of $\bar{u}$ (or, equivalently, of τ) only

$$\phi^{\mathrm{UH}}(r,t) = \phi^{\mathrm{UH}}(\tau) \tag{5.47}$$

similarly to what happens in the relativistic case, where the near-horizon outgoing signals become function of the retarded time $u = t - r_*$ (see (2.29)). If we label these modes with constant Killing energy Ω, imposing $\partial_t \phi_\Omega^{\rm UH} = -i\Omega \phi_\Omega^{\rm UH}$, this defines for us the set of outgoing modes near the UH

$$\phi_\Omega^{\rm UH} = e^{-i\Omega\tau} \,. \tag{5.48}$$

This result makes completely sense, a posteriori. From (5.5) we see that the infinite-frequency limit of the phase velocity is infinite in the preferred frame. An infinite-speed signal, in our theory, is exactly defined to move along a constant τ slice. This is also expected to happen for outgoing modes near the black hole horizon, as they must get infinitely blueshifted in order to escape the gravitational potential.

Let us comment that, from this analysis, the same result can also be derived generically for a wavepacket [133]. If one consider a generic superposition

$$\psi = \int \mathrm{d}\Omega \, \Gamma(\Omega) \phi_\Omega^m \tag{5.49}$$

one can repeat the same analiticity argument and find again (5.41). This tells us that, nearby the black hole horizon, all the details about the matter-aether coupling that we considered in (5.11) are washed out and the behaviour of the modes become universal. Note that this discussion shows also that the angular momentum of the mode plays no role, in the near horizon physics, as in the relativistic case.

No group velocity

Following the same treatment, we can also show that no propagation with the group velocity is possible. Let us consider

$$\frac{c_g}{c_p} = \frac{1 + \sum_{j=2}^n j \beta_{2j} \left(\frac{k}{\Lambda}\right)^{2j-2}}{1 + \sum_{j=2}^n \beta_{2j} \left(\frac{k}{\Lambda}\right)^{2j-2}} \,. \tag{5.50}$$

Taking the infinite-frequency limit we have

$$\lim_{|\omega| \to \infty} \frac{c_g}{c_p} = n > 1 \,. \tag{5.51}$$

Therefore, a ray-tracing of high-frequency signals cannot be made with c_g, since the ray would travel outside the causal cone defined by (5.42). In particular, this rules out the near-horizon analysis with c_g for any mode at a given energy Ω. Therefore the results which claim a n-dependent horizon peeling, that leads to a n-dependent Hawking temperature (5.8), violates these causal analysis.

In general, the converse may happen as well: it is also possible that the c_g-propagation becomes slower as we increase the frequencies. In [93, 94] it has been shown that in slow light experiments [59] it is possible to arbitrarily tune down the group velocity, in order to artificially form a "group horizon" that may play the role of a causal boundary. However, the same works analyze the fact that this notion of horizon cannot really be used for setting up particle production phenomena. In order to have those, a mode-mixing mechanism is needed, therefore a "phase

horizon" must exists. As already commented in Chapter 3, one can work this out from the conservation equation. (5.17) tells us that $\Omega < 0$ are allowed for

$$c_p = \frac{\omega}{k} < -\frac{V}{N}\,. \tag{5.52}$$

The equality $c_p = -V/N$ is satisfied exactly at the UH, which is also the high-frequency limit of the phase velocity, thus capturing the causal meaning of the horizon.

Alternative derivation

Let us present here an alternative derivation for the trajectory of the ray nearby $u \cdot \chi = 0$. Let us emphasize that, with respect to what contained in [38], this presentation is more general and will be useful also to speculate on the axisymmetric black hole case.

Let us consider the conservation equation (5.17). Whenever $k = s_a k^a$ diverges approaching the UH, we must have that ω diverges as well, in order to compensate for keeping Ω constant. This, in turn, implies the n-dependent hard behaviour (5.21). However, without specifying the degree of divergence of ω and k, this gives us the information on the phase velocity

$$c_p = \frac{\omega}{k} = -\frac{s \cdot \chi}{u \cdot \chi}\,, \tag{5.53}$$

which exactly reproduces the behaviour found in the previous section. The effective trajectory followed by our ray is then

$$\mathrm{d}\bar{u} = (c_p u_a + s_a) dx^a = 0\,, \tag{5.54}$$

therefore, the relative displacements along u^a and along s^a are given, near $u \cdot \chi = 0$, by

$$\frac{s_a \mathrm{d}x^a}{u_a \mathrm{d}x^a} = -c_p = \frac{s \cdot \chi}{u \cdot \chi}\,. \tag{5.55}$$

Equation (5.55) has an advantage: it does not strongly rely on the form of τ, which diverges at the UH, but instead provide a formula using the aether, which is regular at the UH and does not require our spacetime to be foliated (in poor words, it applies in principle also to EA non-hypersurface orthogonal, solutions). Now, let us take a parametrization λ for the curve $x^a(\lambda)$ which defines our particle's trajectory. Without loss of generality, we require that the parameter λ is finite at the UH, such that the curve "reaches" the UH for $\lambda|_{\mathrm{UH}} = \bar{\lambda} \in \mathbb{R}$.

Let us define:

$$dT = -(u_a \dot{x}^a)\mathrm{d}\lambda\,, \tag{5.56}$$

where $\dot{x}^a = \mathrm{d}x^a(\lambda)/\mathrm{d}\lambda$. Since u^a is regular everywhere in a neighborhood of the UH we can safely normalize $(\dot{x}^a u_a) = -1$ such that $\lambda = T$ represents the aether time. Similarly, we can define

$$dR = (s_a \dot{x}^a)\mathrm{d}\lambda\,. \tag{5.57}$$

Therefore we can rewrite (5.55) as

$$\frac{\mathrm{d}R}{\mathrm{d}T} = -c_p(\lambda) = \frac{s\cdot\chi}{u\cdot\chi}\,. \tag{5.58}$$

This equation can be locally integrated around $u\cdot\chi = 0$. Around that point, we can expand

$$u_a\chi^a = (n_a\dot{x}^a)|_{\mathrm{UH}}(\lambda-\bar{\lambda}) + \mathcal{O}((\lambda-\bar{\lambda})^2)\,, \tag{5.59}$$

where only the component of $\dot{x}^a$ along the normal n^a counts, since $(u\cdot\chi)$ is constant (i.e. it vanishes) along the surface. In the hypersurface orhotogonal case we have $n^a \propto u^a$ and, plugging (5.56) and (5.59) into (5.58) we get in the near-UH limit

$$\mathrm{d}R = \frac{s\cdot\chi}{u\cdot\chi}\mathrm{d}T = -\left.\frac{(s\cdot\chi)(u_a\dot{x}^a)}{(n_a\dot{x}^a)}\right|_{\mathrm{UH}}\frac{\mathrm{d}\lambda}{\lambda-\bar{\lambda}}\,. \tag{5.60}$$

In the hypersurface orthogonal case equation (5.59) transforms into

$$(u\cdot\chi)(\lambda) = \dot{x}^a\partial_a(u\cdot\chi)|_{\mathrm{UH}}(\lambda-\bar{\lambda}) = -(\dot{x}\cdot u)u^a\partial_a(u\cdot\chi)|_{\mathrm{UH}}(\lambda-\bar{\lambda})\,, \tag{5.61}$$

so that:

$$n_a\dot{x}^a|_{\mathrm{UH}} = -(a\cdot\chi)u_a\dot{x}^a|_{\mathrm{UH}}\,, \tag{5.62}$$

that makes us conclude, in the hypersurface orthogonal case that

$$n^a|_{\mathrm{UH}} = -(a\cdot\chi)u^a|_{\mathrm{UH}} \tag{5.63}$$

as we expected from (4.66). Therefore we have, from (5.60)

$$R(\lambda) = \left.\frac{(s\cdot\chi)}{(a\cdot\chi)}\right|_{\mathrm{UH}}\log(\lambda-\bar{\lambda})\,. \tag{5.64}$$

Since (5.56) is locally invertible, we can write:

$$\lambda-\bar{\lambda} = \frac{T-\bar{T}}{\dot{T}(\bar{\lambda})}\,, \tag{5.65}$$

where $\bar{T} = T(\bar{\lambda})$ and $\dot{T} = \partial_\lambda T$. Thus we conclude that, up to a constant

$$R(T) = \left.\frac{(s\cdot\chi)}{(a\cdot\chi)}\right|_{\mathrm{UH}}\log(T-\bar{T})\,. \tag{5.66}$$

In the spherically symmetric case we have, by definition that near the UH

$$\mathrm{d}R = s_a dx^a = s_t\mathrm{d}t\,, \qquad \mathrm{d}T = u_a dx^a = u_r\mathrm{d}r\,, \tag{5.67}$$

so that

$$t(r) = \left.\frac{1}{(a\cdot\chi)}\right|_{\mathrm{UH}}\log(r-r_{\mathrm{UH}}) = \frac{1}{2\kappa_{\mathrm{UH}}}\log(r-r_{\mathrm{UH}})\,. \tag{5.68}$$

We can see immediately that (5.68) recovers exactly the log-type divergence of the Killing time with respect to the radial coordinate, as it happens for the near-horizon modes in relativistic case (2.29). That behaviour corresponds exactly with a $\{\tau = \text{const.}\}$ surface for $r \simeq r_{\mathrm{UH}}$, as a consistency check with what we found in (5.46). Moreover, this approach tells us some additional things:

- In the near horizon limit, equations adjust in order to preserve the constancy of the Killing energy. The condition for the phase velocity is given without the specifics of the MDR. This confirms, once again, that the Hawking effect is a consequence of the fields kinematics in a curved background.
- This happens at $u \cdot \chi = 0$ any time the components k along s^a diverges. In principle this is the case also for non-hypersuface orthogonal aether, with small modifications, as we shall see.
- The pre-factor of the logarithm in the expression for $t(r)$ is given by the normal derivative of $u \cdot \chi$. This coincides with the usual definition of surface gravity, given also for sonic horizons (3.9). When $u^a \propto n^a$, this matches exactly twice the surface gravity given in (4.45).

5.3.3 Radiation from the universal horizon

Now we are ready to compute the tunneling rate through the UH. Our particle action will be obtained considering the point particle action

$$\mathcal{S} = -\Omega\tau\,, \tag{5.69}$$

which describes the phase of ϕ_Ω. As we have described in section 5.2.2, the hard red solution has support only outside and it has a symmetric partner inside the UH: the green mode ψ^{green}. Therefore we can evaluate $\text{Im}(\mathcal{S})$ tunneling from the green (inside) to the red (outside) trajectories.

UH temperature

Equation (5.68) tells us how the monochromatic waves have to peel at the UH in order to preserve the constancy of Ω, therefore the tunneling amplitude, between the green and the red trajectories can be given by considering the imaginary part of:

$$\text{Im}(\mathcal{S}) = \text{Im}(-\Omega\tau) = \lim_{\varepsilon\to 0^+} \text{Im}\left[-\Omega t - \int_{r_{\text{UH}}-\varepsilon}^{r_{\text{UH}}+\varepsilon} \frac{dr}{2\kappa_{\text{UH}}(r-r_{\text{UH}})}\right] \tag{5.70}$$

where the shape of $\tau(r,t)$ is given in equation (4.38) and near the UH assumes the form:

$$\text{d}\tau \simeq \text{d}t + \frac{\text{d}r}{2\kappa_{\text{UH}}(r-r_{\text{UH}})}\,. \tag{5.71}$$

So, for a regular crossing path $t(r)$ (even $\{t = \text{const.}\}$) we get[4]

$$\text{Im}(\mathcal{S}) = \lim_{\varepsilon\to 0^+} \text{Im}\left[-\int_{r_{\text{UH}}-\varepsilon}^{r_{\text{UH}}+\varepsilon} \frac{dr}{2\kappa_{\text{UH}}(r-r_{\text{UH}})}\right] = \frac{\pi\Omega}{2\kappa_{\text{UH}}}\,. \tag{5.72}$$

[4]unlike the relativistic calculation, at the UH, the coordinate t is well behaved, therefore taking this path is a well-defined procedure

Therefore we can compute the tunneling rate

$$\Gamma_{\rm UH} = e^{-\Omega/T_{\rm UH}}\,, \qquad T_{\rm UH} = \left.\frac{(a\cdot\chi)}{2\pi}\right|_{\rm UH} = \frac{\kappa_{\rm UH}}{\pi}\,. \tag{5.73}$$

As already mentioned in Chapter 2, this can be equivalently computed with the Bogolybov coeffients approach, just analytically continuing the logarithm in (5.68), thus building the analytical combinations $\Phi^{\pm}_{\Omega}$:

$$\Phi^{\pm}_{\Omega} = \mathcal{C}^{\pm}\left[\psi^{\rm red} + e^{\mp\frac{\Omega\pi}{2\kappa_{\rm UH}}}(\psi^{\rm green})^*\right], \tag{5.74}$$

and, repeating the same steps that led to (2.38) in Chapter 2 we arrive to [38]

$$\int \frac{{\rm d}\bar{\Omega}}{2\pi}|\beta_{\Omega\bar{\Omega}}|^2 = -\mathcal{C}^{-} = \frac{1}{e^{\pi\Omega/\kappa_{\rm UH}}-1}\,, \tag{5.75}$$

obtaining the same UH-temperature.

5.3.4 Effective metric: UH radiation from thermal time

In Chapter 2 we have also shown that the Hawking temperature can be derived as the required periodicity to give to the Euclidean time, in order to avoid the conical singularity at the horizon. Let us show here that the discussion can be generalized to spacetimes with arbitrary signal velocities. Let us take a matter field ϕ which obeys some dispersion relation $\omega(k)$ in the preferred frame. We have shown that the causal structure felt by the field is given by the quantity (the so-called *signal velocity* or sometimes *front velocity*):

$$c_f = \lim_{|\omega|\to\infty}\frac{\omega}{k(\omega)}\,. \tag{5.76}$$

Let us now consider this velocity as an arbitrary parameter in a (1+1) spacetime (or a spherically symmetric one) which enjoys a timelike Killing symmetry $\chi^a\partial_a = \partial_t$. Let us choose the frame spanned by $\{u, s\}$ (where s is the orthogonal to u in the $\{u,\chi\}$ space) and consider therein a generalized null-ray with propagation speed c_f such that:

$$u_a{\rm d}x^a = \pm\frac{s_a{\rm d}x^a}{c_f}. \tag{5.77}$$

This ray can be interpreted as moving on the causal cone of the effective metric

$$g^{(c_f)}_{{\rm eff},ab}{\rm d}x^a{\rm d}x^b = -\left(u_t^2 - \frac{1}{c_f^2}s_t^2\right){\rm d}t^2 + \left(u_r^2 - \frac{1}{c_f^2}s_r^2\right){\rm d}r^2. \tag{5.78}$$

where r is the other coordinate which spans the $\{u,\chi\}$ space. This metric enjoys a Killing horizon at:

$$|\chi|^2 = \left(u_t^2 - \frac{1}{c_f^2}s_t^2\right) = 0\,. \tag{5.79}$$

The idea behind this calculation, where the horizon for a c_f-speed causal cone is given as a Killing horizon of some effective metric, has also been developed in a similar context in [135].

Relativistic case

If $c_f^2 = 1$, then (5.78) becomes:

$$g^{(1)}_{\text{eff},ab}\mathrm{d}x^a\mathrm{d}x^b = -\left(u_t^2 - s_t^2\right)\mathrm{d}t^2 + \left(u_r^2 - s_r^2\right)\mathrm{d}r^2\,. \tag{5.80}$$

and the Killing horizon becomes the relativistic one:

$$|\chi|^2 = \left(u_t^2 - s_t^2\right) = (u\cdot\chi)^2 - (s\cdot\chi)^2 = 0\,. \tag{5.81}$$

This Killing horizon exactly coincides with the usual one provided by the Lorentz invariant treatment, just described in a different basis $\{u, s\}$. Therefore, we recover the interpretation of the Hawking temperature as the one given in section 2.4.

UH case

If instead we send $c_f^2 \to \infty$ our effective metric becomes

$$g^{(\infty)}_{\text{eff},ab}\mathrm{d}x^a\mathrm{d}x^b = -u_t^2\mathrm{d}t^2 + u_r^2\mathrm{d}r^2\,. \tag{5.82}$$

The Killing horizon occours at

$$|\chi|^2 = u_t^2 = (u\cdot\chi)^2 = 0\,, \tag{5.83}$$

which corresponds to the definition of the UH. Performing a near-horizon expansion

$$u_t^2 = -(\partial_r u_t)^2|_{r_{\text{UH}}}(r - r_{\text{UH}})^2\mathrm{d}t^2\,, \tag{5.84}$$

so that

$$g^{(\infty)}_{\text{eff},ab}\mathrm{d}x^a\mathrm{d}x^b = -(\partial_r u_t)^2|_{r_{\text{UH}}}(r - r_{\text{UH}})^2\mathrm{d}t^2 + (u_r)^2|_{r_{\text{UH}}}\mathrm{d}r^2\,. \tag{5.85}$$

Defining $\rho = u_r|_{\text{UH}}(r - r_{\text{UH}})$ we get

$$g^{(\infty)}_{\text{eff},ab}\mathrm{d}x^a\mathrm{d}x^b = -\left.\frac{(\partial_r u_t)^2}{u_r^2}\right|_{r_{\text{UH}}}\rho^2\mathrm{d}t^2 + \mathrm{d}\rho^2\,, \tag{5.86}$$

which, after a Wick rotation in the Euclidean time we get

$$g^{(\infty)}_{\text{E},ab}\mathrm{d}x^a\mathrm{d}x^b = \left.\frac{(\partial_r u_t)^2}{u_r^2}\right|_{r_{\text{UH}}}\rho^2\mathrm{d}\tau^2 + \mathrm{d}\rho^2\,. \tag{5.87}$$

Similarly to what we have done in the relativistic case, we can get rid of the conical singularity just by imposing the periodicity on τ with

$$\beta = \left.\frac{2\pi u_r}{\partial_r u_t}\right|_{r_{\text{UH}}} \implies T_{\text{UH}} = \left.\frac{\partial_r u_t}{2\pi u_r}\right|_{r_{\text{UH}}}\,. \tag{5.88}$$

therefore we obtain, as a function of u_a and its derivatives, the temperature of the UH. We can enforce the normalization condition in (5.86):

$$u^t u_t + u^r u_r = -1 \implies u_r(r_{\text{UH}}) = -\frac{1}{u^r(r_{\text{UH}})}\,, \tag{5.89}$$

and get the known result

$$T_{\rm UH} = \left.\frac{u^r \partial_r u_t}{2\pi}\right|_{r_{\rm UH}} = \frac{\kappa_{\rm UH}}{\pi}\,. \tag{5.90}$$

Therefore, the temperature of the UH is something which can be derived by the causal structure, just imposing the presence of an absolute time for everyone, very much likely the relativistic case.

5.3.5 Comparison with previous results

Throughout the previous discussion, we have commented about the tension between our result and previous calculations contained in the literature. Let us sum up the differencies here.

- In [126, 127] the group velocity c_g has been used top trace the trajectory up to the UH. This, as we have stressed, is in conflict with causality. The group velocity of an infinite blueshifted ray defines a trajectory which cannot be allowed by the causal structure of the theory. This can be seen from equation (5.51), which tells us that for $n > 1$ the c_g-ray would travel faster than the single surface of simultaneity. More explicitly, in the case of a ray propagating with the phase velocity c_p, the trajectory in the preferred frame is given by:

  $$\left.\frac{\mathrm{d}\rho}{\mathrm{d}\tau}\right|_{\rm c_p,UH} = 1\,. \tag{5.91}$$

  The same computation using c_g returns

  $$\left.\frac{\mathrm{d}\rho}{\mathrm{d}\tau}\right|_{\rm c_g,UH} = n\,. \tag{5.92}$$

  Since we have seen in section 5.3.2 that the c_p-propagation leads to a ray travelling on a constant τ surface, the c_g propagation clearly violates the causality fixed by the preferred frame.

- The derivation contained in [121] computes the particle production through the Bogolyubov coefficients between $(\psi^{\rm red}, \psi^{\rm orange})$. This makes the authors to conclude that the Killing horizon gives a non-vanishing contribution, while the UH does not play any role. As we shall see in the following of this Chapter, the interplay between $\psi^{\rm red}$ and $\psi^{\rm orange}$ will be the source of a contribution from the Killing horizon, in a very similar fashion to what we have computed in Chapter 3 for the analogue case. However, it is clear from our analysis of the characteristics that the contribution given by the UH has to be computed by the Bogolyubov between $(\psi^{\rm red}, \psi^{\rm green})$, thus obtaining our result.

- The discrepancy between us and [119] is more difficult to explain. At a careful reading, one can see that the discrepancy of their treatment with ours consists in the fact that they consider

  $$\mathcal{S}_\Lambda = \int (\omega u_a + k s_a)\mathrm{d}x^a \tag{5.93}$$

which by construction satisfy the definition of preferred momentum k and energy ω for the field ϕ given in (5.14). They compute the tunneling amplitude by considering the r-component of the action $\mathcal{S}_\Lambda$ using the hard solutions (5.21). This gives, at the leading order:

$$\mathcal{S}_\Lambda = \Lambda \int \left[\left(-\frac{V}{N} \right)^{n\gamma} u_r - \left(-\frac{V}{N} \right)^{\gamma} k s_r \right] \mathrm{d}r \,. \tag{5.94}$$

This formula contains a non-integer pole of degree $n\gamma = n/(n-1)$. This contribution can be analytically continued around $N = 0$ only in the case $n = 2$, namely for integer values of $n\gamma$, which is the one considered by the authors. However, this action loses its Ω-dependence, since the most-divergent part of ω and k is only Λ-dependent and there is no memory of Ω anymore.

One may (correctly) argue that considering the next-to-leading contribution given in (5.21) this dependence could be recovered[5], having

$$\mathcal{S}_\Lambda = -\Omega t + \int \left[\Lambda \left(-\frac{V}{N} \right)^{n\gamma} u_r - \Lambda \left(-\frac{V}{N} \right)^{\gamma} s_r + \frac{n}{n-1} \frac{\Omega}{N} \right] \mathrm{d}r \,. \tag{5.95}$$

Nonetheless, also this approach presents some problematic features. First of all, it requires considering a sub-leading order, which in principle should be negligible very close to the horizon. Secondly, and maybe most importantly, the constant-phase contour defined by $\mathcal{S}_\Lambda$ is

$$\mathrm{d}t = \left[\frac{\Lambda}{\Omega} \left(-\frac{V}{N} \right)^{n\gamma} u_r - \frac{\Lambda}{\Omega} \left(-\frac{V}{N} \right)^{\gamma} s_r + \frac{n}{n-1} \frac{1}{N} \right] \mathrm{d}r \,, \tag{5.96}$$

which is a trajectory describing an object which travels "faster" than a signal on a surface of simultaneity, namely (note that $s_r \to 0$ linearly at the UH)

$$\left. \frac{\mathrm{d}t}{\mathrm{d}r} \right|_{\mathrm{d}\mathcal{S}_\Lambda = 0, \mathrm{UH}} = \frac{\Lambda}{\Omega} \left(-\frac{V}{N} \right)^{n\gamma} u_r + \frac{n}{n-1} \frac{1}{N} > \frac{1}{2\kappa_{\mathrm{UH}}} \frac{1}{N} = \left. \frac{\mathrm{d}t}{\mathrm{d}r} \right|_{\mathrm{d}\tau = 0, \mathrm{UH}} . \tag{5.97}$$

This cannot be possible, just by a simple causality reasoning. In particular, one can directly read off k_r from $\mathcal{S}_\Lambda$

$$k_r^\Lambda = \Lambda \left(-\frac{V}{N} \right)^{n\gamma} u_r + \Omega \frac{n}{n-1} \frac{1}{N} \tag{5.98}$$

and see that (5.97) compares with (5.44):

$$\frac{k_r^\Lambda}{\Omega} = \frac{\Lambda}{\Omega} \left(-\frac{V}{N} \right)^{n\gamma} u_r + \frac{n}{n-1} \frac{1}{N} > \frac{u_r}{u_t} \,. \tag{5.99}$$

So, a ray defined by $\mathcal{S}_\Lambda$ does not define a signal in the sense of [133], thus the propagation cannot happen along the constant-$\mathcal{S}_\Lambda$ phase contours.

[5] This is exactly what has been done in [119]

Concluding, let us state what we have found in the following way: the fact that the constant-phase contour of the near-horizon modes coincides with a surface of simultaneity should be viewed as a ray travelling "as fast as possible" in order to escape the gravitational well of the black hole. This is analogous to what we found in Chapter 2 for the outoging modes near the Killing horizon: any particle that escapes the potential should travel along a null trajectory which is the fastest way allowed in GR by causality. In the same way, once we have found that $\phi = \phi(\tau)$ near UH, the assignment of a conserved Killing energy Ω fixes uniquely the shape of the function.

5.4 Towards the Killing horizon

We have shown that the behaviour of the rays nearby the UH is universal, and it is given by the shape of the foliation. This happens because a wavepacket stops travelling with the group velocity, due to the infinite blueshift, and starts travelling with the phase velocity, which diverges as it approaches $r = r_{\rm UH}$. Far from it, the packet will be peaked in energy, thus following the trajectory defined with c_g (5.25), here in EFB coordinates:

$$\frac{\mathrm{d}v}{\mathrm{d}r} = -\frac{c_g u_r + s_r}{c_g u_v + s_v}\,. \tag{5.100}$$

A particle with energy Ω will thus minimize the action:

$$\mathcal{S}_0 = -\Omega v - \Omega \int^r \frac{c_g u_r + s_r}{c_g u_v + s_v}\,. \tag{5.101}$$

Let us recall that the group velocity is energy-dependent, i.e. $c_g = c_g(r, \alpha)$, so it does the trajectory. Equation (5.101) has the same feature that we have found for particles in the analogue case of Chapter 3. This particle does not enjoy an infinite peeling at the Killing horizon, but, the lower the energy, the bigger is the intensity of the lingering, as shown by figure 5.3.

Exactly in the same way as it happens for analogue geometries, one can do a perturbative analysis around $\alpha = 0$ and compute the tunneling amplitude between the outside branch of $\psi^{\rm red}$ lingering mode and the soft branch of the turning mode $\psi^{\rm orange}$.

In principle one can repeat the analysis made for the analogue case with superluminal dispersion and supercritical flows, specifying to $n = 2$. As a generical feature, namely for any n, it is possible to extract the first correction, since for any n the first term appearing in the dispersion relation (5.5) is of order $\mathcal{O}(k^2/\Lambda^2)$. Since the solution depends on the geometry, for this calculation we specify to (5.9), thus getting[6]:

$$c_g^{\rm red}(r, \alpha) = 1 + \frac{3r^2}{2(r-2M)^2}\alpha^2 + \mathcal{O}(\alpha^3)\,. \tag{5.102}$$

[6]Here we have set the coefficient $\beta_4 = 1$. Keeping that parameter free, one must rescale $\alpha^2 \to \beta_a \alpha^2$.

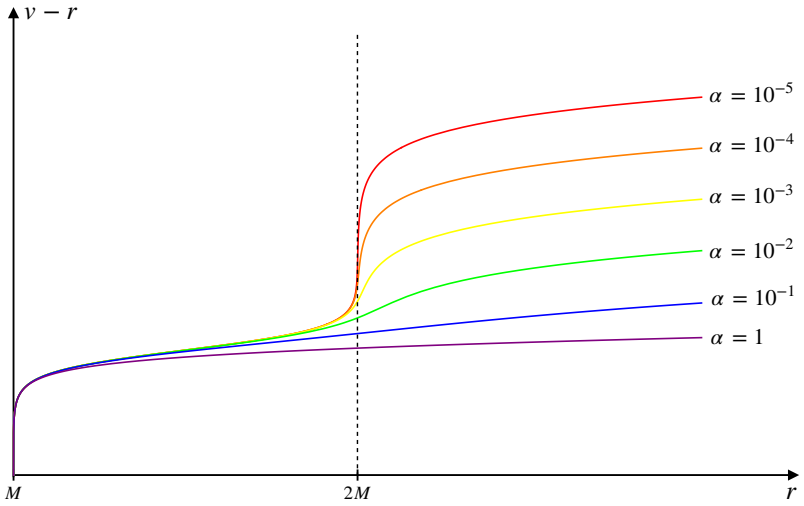

Figure 5.3: Classical trajectories for ψ^{red}, evaluated at different values of α in the case $n = 2$. Each value of α is reported next to the correspondent ray. We observe a lingering behaviour at the Killing horizon (dashed line) for low-energy modes. The UH is at $r_{\text{UH}} = M$.

Plugging this into $\mathcal{S}_0$ and evaluating the imaginary part we get:

$$\text{Im}(\mathcal{S}_0) = \frac{\Omega\pi}{\kappa_{\text{KH}}}(1 - 3\alpha^2) + \mathcal{O}(\alpha^3)\,. \tag{5.103}$$

that leads to

$$T(\alpha) = T_{\text{H}}\frac{1}{1 - 3\alpha^2} + \mathcal{O}(\alpha^3) = T_{\text{H}}(1 + 3\alpha^2 + \mathcal{O}(\alpha^3))\,, \tag{5.104}$$

where $T_{\text{H}} = \kappa_{\text{KH}}/2\pi$ is the Hawking temperature (2.39). As in (3.55), we perturbatively obtain a slightly hotter temperature with respect to the relativistic one. The coefficient of the correction does not match because of the difference of the two geometries.

5.4.1 WKB condition

Since all of our analysis is based on a WKB approximation of the field, let us now spend a few lines in trying to see the validity of this assumption. The WKB approach, as mentioned in Chapter 2, is based on the validity of the adiabaticity condition:

$$\left|\frac{\dot{\omega}}{\omega^2}\right| \ll 1\,. \tag{5.105}$$

Equation (5.105) tells us that, if the phase of the field does not vary to much, we can locally define a basis of "plane waves" $\{e^{i\mathcal{S}_0}\}$ with action (5.101). This tells us that, whenever we have such a basis, we can perform our QFT calculations within our twofold interpretation of mode and particle of the function $e^{i\mathcal{S}_0}$. Therefore, the

field operator decomposition given in equation 2.7 holds and a vacuum state can be defined instantaneously as $\hat{a}_\Omega|0\rangle = 0$.

A more intuitive interpretation of (5.105) can be the following: whenever that condition is fulfilled, the single-energy modes adapt to the variation of ω, which is small compared to ω itself. This means that we are able to ray trace the mode, following its evolution in the spacetime. Therefore, the tunneling applies correctly. Whenever this approximation breaks down, we cannot identify the single-energy mode anymore. Therefore, the place where the WKB is broken, is usually identified as the point where the particle production happens [51, 96][7]. This, in terms of Bogolyubov coefficients has a direct interpretation: if the adiabaticity condition is satisfied at $\mathscr{I}$ and at the horizon, we can compare the two basis, and compute the particle production, which happens where the two basis are not anymore a good way to define a vacuum state in terms of $\hat{a}_\Omega$ and $\hat{a}^\dagger_\Omega$.

In the analysis of (5.105) it is crucial to specify the evolution parameter, namely who is the "dot" applied to ω in the numerator. This is, as underlined in [86], an observer-dependent statement. In GR, we would have taken the time defined by the freely-falling observer, who is the one that has to define the vacuum at the horizon. In LV case, the analougus of the free-falling observer is not automatically given. Therefore, we will chose to follow the trajectory of the infalling solution ψ^{blue}. If ψ^{blue} is taken with small α, the world-line of our observer will be very close to those of a GR observer. We choose to label the trajectory using the $\bar{u}$ coordinate for the out-going red mode, that thus defines our clock. This yields

$$\dot{\omega} = \frac{\mathrm{d}\omega(r(\bar{u}),\alpha)}{\mathrm{d}\bar{u}} = \frac{\mathrm{d}r(\bar{u})}{\mathrm{d}\bar{u}}\omega' \,, \tag{5.106}$$

where $\omega' = \partial_r\omega$. If we work within (5.9), the relation between $\bar{u}$ and r is given by

$$\frac{\mathrm{d}\bar{u}}{\mathrm{d}\lambda} = \frac{\mathrm{d}t}{\mathrm{d}\lambda} + \frac{c_g^{\text{red}}(r,\alpha)u_r + s_r}{c_g^{\text{red}}(r,\alpha)u_t + s_t}\frac{\mathrm{d}r}{\mathrm{d}\lambda} = \left(\frac{c_g^{\text{red}}(r,\alpha)u_r + s_r}{c_g^{\text{red}}(r,\alpha)u_t + s_t} - \frac{r}{r-2M}\right)\frac{\mathrm{d}r}{\mathrm{d}\lambda} \,, \tag{5.107}$$

where λ parametrizes the infalling world-line. The derivation of this formula is given in Appendix B, together with an alternative derivation of $T(\alpha)$.

Let us rewrite the group velocity as

$$c_g(r,\alpha) = \frac{\partial\omega}{\partial k} = \frac{\partial_r\omega}{\partial_r k} = \frac{\omega'}{k'} \,, \tag{5.108}$$

where also $k' = \partial_r k$. Differentiating (5.17) with respect to r yields

$$0 = (\omega + k)N' + N\omega' + Vk' \,, \tag{5.109}$$

where we used that $N' = V'$, which holds true for (5.9). Combining the previous two expressions we thus get

$$\omega' = -\frac{c_g N'(\Omega + k)}{N(c_g N + V)} \implies \frac{\omega'}{\omega^2} = -\frac{c_g N N'(\Omega + k)}{(\Omega - kV)^2(c_g N + V)} \,. \tag{5.110}$$

[7] Incidentally, this happens at $r \simeq 3M$ for the relativistic case.

Therefore:

$$\frac{\dot{\omega}}{\omega^2} = \frac{\mathrm{d}r(\bar{u})}{\mathrm{d}\bar{u}}\frac{\omega'}{\omega^2} = -\left(\frac{c_g U_r + S_r}{c_g N + V} - \frac{r}{r-2M}\right)^{-1} \frac{c_g N N'(\Omega + k)}{(\Omega - kV)^2(c_g N + V)}\,. \tag{5.111}$$

This expression can be plotted in function of r, as we did in figure 5.4. As one can see, the adiabaticity holds perfectly at the UH, due to the divergence of k, for any α. Moreover, the modes conserves the adiabatic structure if sufficiently low energy. One can show that, in the case $n = 2$, ψ^{red} enjoy a behaviour of the type $k \sim 1/\alpha$ for $\alpha \ll 1$. This implies also $c_g \sim 1/\alpha$, thus implying

$$\lim_{\alpha\to 0^+} \frac{\dot{\omega}}{\omega^2} = 0 \quad \text{for} \quad r \in [M, 2M]\,. \tag{5.112}$$

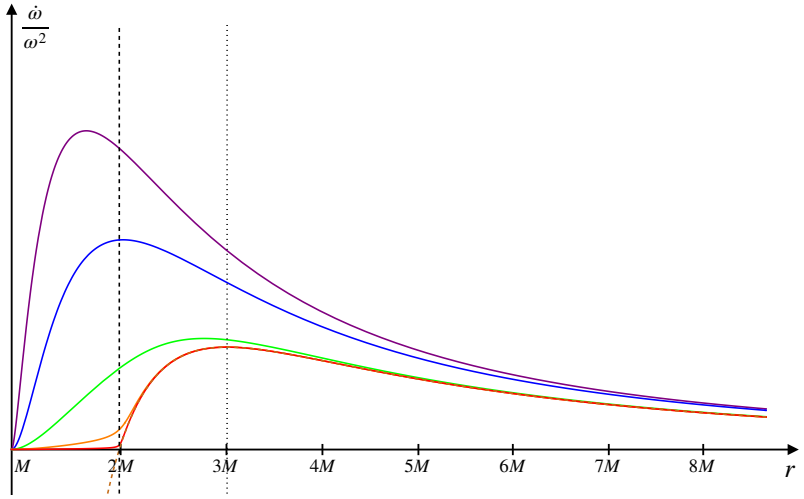

Figure 5.4: Adiabatic condition for modes $\psi^{\mathrm{red}}_{\Omega}$ with different α: $\alpha = 10$ (purple), $\alpha = 1$ (blue), $\alpha = 10^{-1}$ (green), $\alpha = 10^{-2}$ (orange), $\alpha = 10^{-3}$ (red). The dashed orange line represent the checking of the WKB condition for the relativistic case. The vertical lines are at the Killing horizon $r = 2M$ (dashed) and $r = 3M$ (dotted), where the relativistic-WKB breaks down. All lines are computed with $\Omega = 1.6 \times 10^{-1}$, laying close to the peak of the emission from the UH, which sits at $\Omega = 1/(2\pi M)$.

In conclusion: the UH treatment is exact within the WKB approximation, thus the emission at T_{UH} remains. For low energy modes, the adiabaticity is preserved in the region between the Killing and the universal horizons, thus rendering the tunneling treatment valid and it breaks down closeby the relativistic $r = 3M$. That calculation, however, cannot be applied to the high-energy modes, for which the adiabaticity is violated and the maximum violation of the WKB condition happens before the KH.

5.4.2 Quantum state

The result (5.104) was expected from the analysis of the analogue case. Besides the specifics of the geometry, in both cases we have faced the problem of describing

superluminal particles in the presence of a Killing horizon, and we have obtained the same result.

However, in contrast to what we had in the AG case, for an LV black hole, an UH is present. What does it imply for the quantum state of ϕ?

In section 5.3, we have learned that the causal properties of the spacetime make all the modes to exponentially peel at the horizon surface $r = r_{\rm UH}$ in the same way. Due to the infinite blueshift, the infalling observer would see an infinite-energy barrier if the field is not set to be in vacuum. Actually, setting the vacuum at the horizon in GR, is exactly what tells us that the state percieved on $\mathscr{I}^+$ is thermal, due to the Bogolyubov relation between the basis.

Similarly, here we will take our near-UH basis $\{e^{-i\Omega\tau}\}$ and define, through the associated creation-annihilation operators $\hat{a}_\Omega$ and $\hat{a}^\dagger_\Omega$, the vacuum $|0_{\rm UH}\rangle$ as

$$\hat{a}_\Omega|0_{\rm UH}\rangle = 0\,. \tag{5.113}$$

It is in this way that the UH completes the picture with respect to the AG case of Chapter 3. In section 3.6, we have mentioned the absence of a sensible way to define the vacuum state for the field ϕ. Here we have a preferred choice, which follows closely the GR analysis, due to the infinite divergence of the modes at the UH, defining a LV version of the Unruh state.

Nevertheless, our computation for low-energy rays at the Killing horizon holds and predicts an almost-Hawking spectrum in its low-energy part. However, as already mentioned, this would imply to set the local vacuum state at any effective horizon, as defined in equation (3.48). If ϕ is not in this state, an infalling observer would perceive the lingering as a sort of energy-Λ firewall which, even if not infinite, would imply a huge energy barrier nearby the EFH. A possible solution to get rid of it maintaining the regularity of the state at the UH would be to have compatibility of the two state; namely if it would exist a quantum state $|\phi\rangle$ which looks like vacuum on the UH and vacuum on the EFH, no firewalls appear.

The compatibility of the two states is exactly what it is shown by the adiabaticity condition analysis of the previous section. We have seen that the low energy part of the spectrum satisfy the adiabatic condition. This means that the same basis $\{e^{i\mathcal{S}_0}\}$ is valid in the whole region between the UH and the EFH. The adiabaticity allows to say that the low energy particle content of $|0_{\rm UH}\rangle$ is the same as $|0_{\rm EFH}\rangle$ in between the two horizons. Therefore, once one has set the vacuum $|0_{\rm UH}\rangle$, he is also ensured to find vacuum at the EFH, for low α, thus explaining the compatibility between the two conditions.

The resulting spectrum will be something which interpolates between a thermal distribution with $T_{\rm UH}$ for the high-α modes, and a distribution following $T(\alpha)$ at low-α. We shall come back to this point in the conclusion.

5.5 Axisymmetric solutions

The fact that, in the near-horizon limit, rays travel along a spacelike hypersurface is a consequence of the infinite blueshift character of the near-horizon solutions. However, as we already pointed out in section 5.3.2, this fact can be derived in a

pretty generic way as a behaviour of a particle, obeying a MDR nearby $(u \cdot \chi) = 0$. Let us take the expression for Ω

$$\Omega = -\omega(u \cdot \chi) - k_s(s \cdot \chi)\,, \tag{5.114}$$

where the subscript "s" has been introduced to underline the fact that it indicates the momentum along s^a. In the spherically symmetric analysis, this component of the momentum is the only one which can diverge, due to the rotational invariance. However, let us consider a geometry like the one given in [125], which has been analysed in section 4.3. This solution, although not endowed with an UH, enjoy a surface for which $(u \cdot \chi) = 0$, named QUH. However any signal defined here will be able also to travel along θ^a (as defined in section 4.3), without the constraint of spherical symmetry. This is exactly what makes the QUH to fail being an horizon: any ray can escape from it, if it travels along θ^a fast enough.

Note that, unlike the spherically symmetric case, where the symmetries plus the MDR combined with the conservation of Ω allows us for a complete description of the WKB solution, in the less-symmetric rotating case, this is no longer possible. The rotational invariance along the azimuthal angle φ, the conservation of Ω and the MDR remains, but we lose the constraint on k_θ, which now becomes another incognita of our system.

However, let us point out that the constraint (5.114) still admits for solutions which diverge nearby the QUH. Actually, the treatment made in section 5.3.2 can be adapted quite easily for a generic trajectory which travels with the phase velocity c_p.

Whenever $|k_s| \to +\infty$ as approaching the QUH, equation (5.114) tells us that, near $(u \cdot \chi) = 0$

$$\frac{\omega}{k_s} = -\frac{s \cdot \chi}{u \cdot \chi}\,. \tag{5.115}$$

We can then consider the MDR for a divergent $|\mathbf{k}|$

$$\omega^2 \simeq \frac{|\mathbf{k}|^{2n}}{\Lambda^{2n-2}}\,. \tag{5.116}$$

In the case of divergent ω – namely if at least one of the components k_s, k_θ blows up – the motion is given in terms of the phase velocity, as we explained in section 5.3. Let us define the spatial direction as

$$v^a = \frac{\mathbf{k^a}}{|\mathbf{k}|}\,, \tag{5.117}$$

such that the trajectory is locally determined by

$$(c_p u_a + v_a)\mathrm{d}x^a = 0\,, \quad \text{where} \quad c_p = \frac{\omega}{|\mathbf{k}|}\,. \tag{5.118}$$

If $|k_s/k_\theta| \to \infty$ at the QUH, we have

$$v^a|_{\mathrm{QUH}} = s^a\,. \tag{5.119}$$

Therefore, we recover exactly the spherically symmetric computation. The (non-normalized) tangent vector to the trajectory is

$$\dot{x}^a = u^a + c_p v^a \tag{5.120}$$

such that, since $n \cdot s = 0$ at the QUH from (4.66), we get

$$(n \cdot \dot{x}) = (a \cdot \chi) \tag{5.121}$$

and, after the same steps, we recover exactly the formula given in (5.68), thus reproducing the logarithmic peeling. This seems to tell us that the surface $(u \cdot \chi) = 0$, even if it does not represent, purely speaking, an UH, it defines a surface where trajectories with an exponential peeling solve the field equations at constant Ω. However, this happen only for those motions which happen in the $\{u, s\}$ plane in a neighborhood of the QUH. Whenever the ray enjoys a near-QUH nontrivial θ component, the product $(n \cdot \dot{x})$ assumes the form:

$$(n \cdot \dot{x}) = (a \cdot \chi) + (n \cdot \theta)(v \cdot \theta) c_p \tag{5.122}$$

which contains a divergent contribution given by c_p, and the trajectory does not longer show any logarithmic behaviour.

Additionally, the peeling factor of the k_s-dominated trajectories

$$\kappa_{\text{QUH}} = \frac{a \cdot \chi}{2}\,, \tag{5.123}$$

cannot automatically shown to be constant on the whole surface $u \cdot \chi = 0$, but instead it will be a θ-dependent function. This would mean that, from the thermodynamical point of view, even if this surface would start to radiate, it would not be in equilibrium, since it would not have a constant temperature.

Let us conclude commenting that in this axisymmetric case, the possible way to clarify the kinematic of the field are the following two:

- One finds that $(u \cdot \chi) = 0$ is an actual UH: if one manages to find an aether field u^a with a vanishing twist on the QUH, then, this surface becomes orthogonal to the aether itself – therefore $n^a \propto u^a$ – and the logarithmic behaviour is recovered for all the outgoing trajectories.

- One finds out a way to close the system of equations. Indeed, a WKB field ϕ in the rotating case is determined completely by the three functions ω, k_s and k_θ. However, only two equations – the MDR $\omega = \omega(|\mathbf{k}|)$ and the conservation of Ω – are given, as far as we know. The integrability of the GR geodesics in a Kerr geometry is given by the conservation of the so-called Carter's constant [136], determined through a Killing tensor, which in our case is not conserved anymore (or at least, not in general, as one can verify for the solution of [125]). Let us underline that, the notion of a second conserved quantity, will allow us to determine whether the outgoing peeling trajectory with $k_s \to \infty$ are actual physical solution or just a feature of the underdetermination of the system of the equations.

5.6 Outlook

As a summary of this Chapter, let us go through its main results. The analysis of the causal structure of a LV black hole has been performed considering a field with a (superluminal) MDR on top of this geometry.

The universal horizon, which represents the main difference between this Chapter and Chapter 3, radiates with a constant temperature, proportional to its surface gravity $T_{\rm UH} = \kappa_{\rm UH}/\pi$. The analysis of the causal behaviour for the modes tells us that a species-dependent result is not possible, because those modes have to propagate onto a constant-khronon surface, when they get infinitely blueshifted. The study of the modes in section 5.2.2 gives also a picture on the energy balance of the LV-Hawking process. The appearance of a negative-energy mode with support only inside the UH – namely $\psi^{\rm green}$ – allows the pair production at the horizon in the usual way. This was not considered in [121], where the analysis was performed considering the interplay $\psi^{\rm red}$ and $\psi^{\rm orange}$ which gives no contribution at the UH.

However, this contribution turns out to be of great importance in the analysis of the (α-dependent) propagation of the rays. The Killing horizon acts on those as a prism, differently for each α. This allows us to recover the analysis made in the analogue case at the acoustic horizon.

The combination of these two effects returns a global, coherent picture. The UH serves as an anchor to fix a vacuum state for the infalling observer, which turns out to be compatible, at low energy, with the relativistic Unruh state, determining vacuum at the Killing horizon. At the phenomenological level, it implies a spectrum at infinity which low-energy parts are dominated by the Killing horizon – therefore by the Hawking temperature (plus α-corrections) – and which the high-energy sector are determined by $T_{\rm UH}$.

However, the full spectrum is still to be derived, probably with the help of semi-analytical or full fledged numerical methods. Also, this is just a first step in understanding the thermodynamics of black holes in Lorentz violating theories, in particular if the four laws of black hole thermodynamics can be extended to them (see e.g. [137, 138]). We will come back on this in the conclusions.

Chapter 6

Unruh effect without Lorentz invariance

As we have discussed in Chapter 1, the duality between gravity and acceleration encoded in the equivalence principle makes the Hawking effect and the Unruh effect two sides of the same coin. Actually, at the local level there is no difference between an observer hovering at constant r near a large black hole Killing horizon in a Schwarzschild geometry and a constantly accelerating one on a flat background, since the apparent horizon perceived by the latter can be mapped into the Killing one.

The Hawking temperature $T_{\rm H} = \kappa/(2\pi)$ of equation (2.39) is the temperature perceived by an observer sitting at $r = +\infty$. In general, a constant-r observer will detect the black hole radiation with the Hawking temperature rescaled by the Tolman factor [139]:

$$T_{\rm obs} = \frac{T_{\rm H}}{|\chi|} = T_{\rm H}\left(1 - \frac{r_s}{r}\right)^{-1/2} , \tag{6.1}$$

where $\chi = \partial_t$ is the time translation invariance. Hence, as anticipated, $T_{\rm H} = \lim_{r\to\infty} T_{\rm obs}$.

In a near-Killing horizon limit, the constant-r observer is mathematically equivalent to an accelerated one in the Rindler wedge of Minkowski spacetime: a constant-r trajectory becomes an integral line of the boost Killing vector $\chi = \partial_\eta$ and an observer living there feels the temperature given by its proper acceleration [41]

$$T_{\rm obs} = \frac{a_p}{2\pi} . \tag{6.2}$$

The magnitude of a_p depends on the particular χ-orbit followed by the observer. Since its proper time τ_p on a particular orbit is given by

$$\mathrm{d}\tau_p = \sqrt{-g_{\eta\eta}}\mathrm{d}\eta = |\chi|\mathrm{d}\eta , \tag{6.3}$$

then one can write a_p as

$$a_p = \frac{a}{|\chi|} , \tag{6.4}$$

where a is a bookkeping parameter. Therefore, we have

$$T_{\rm obs} = \frac{a_p}{2\pi} = \frac{a}{2\pi}\frac{1}{|\chi|}\,. \tag{6.5}$$

If one defines the $T_{\mathscr{R}} = a/(2\pi)$ as the temperature of the Rindler wedge, then the relation resembles closely the one in (6.1), where the observed temperature is rescaled by the norm of the Killing vector.

The fact that this equivalence could hold also without Lorentz invariance is a matter of debate. Since LV gravity as we discussed here drops the local boost invariance, the equivalence between the two effect can be spoiled at the fundamental level.

Indeed, even if the robustness of Hawking radiation is common wisdom within this framework, the same cannot be told for what regards for the Unruh effect [140–142].

The different fate of the two phenomena when dealing just with ultraviolet Lorentz-breaking matter can be readily understood in terms of separation of scales: while the Hawking effect is characterized by an objective scale provided by the surface gravity of the black hole, which in turns is determined by the conserved charges of the black hole solution (e.g. mass and angular momentum for a Kerr black hole), no such scale is present in the Unruh effect, as the Rindler wedge temperature $T_{\mathscr{R}}$ of (6.2) can always be rescaled to be $1/2\pi$ [143], being a a bookkeeping parameter. The absence of an intrinsic scale (akin to the black hole surface gravity κ) to be contrasted to the UV Lorentz breaking scale, say Λ, is what prevents the scale separation ($\kappa \ll \Lambda$) so crucial in preserving the Hawking effect for example in analog models of gravity.

So it was no surprising that a stream of papers on the subject concluded that the question concerning the robustness of Unruh radiation in the presence of UV Lorentz breaking matter had to be answered in the negative [140–142]. Note that technically, the main culprit of such an apparent wipe out of the effect can be traced down to the breakdown of the KMS condition of the Wightman function [142, 144].

However, we have already seen that the presence of an UH may serve as an anchor for preserving the KMS structure of the state, by providing the usual conical singularity, in the Euclidean patch. The presence of such a surface cannot be found in the relativistic Rindler wedge, which is limited by the Killing horizon. However, as we shall see, such a thing is possible if the Rindler spacetime is extended in order to contain an aether field u^a, that has to be dynamical, satisfying the gravitational field equations (4.15). We will show that this consideration is crucial, because it will insert a physical scale in the problem, that will provide the aforementioned separation of scales. Within this treatment, the analogy between the Unruh and the Hawking effect can be restored also in LV settings.

In this Chapter, we will describe how to make this construction, basing our treatment mostly on [39]. We will describe the LV-Rindler wedge, solving for a compatible aether and then we will compute the Unruh effect in two ways. The first one will rely on a Bogolyubov transformation and the other one on the Unruh-De Witt detector, accompanying our accelerated observer.

6.1 Geometrical set up: the Rindler wedge

Let us start by briefly reviewing the relativistic Rindler wedge to extract its internal geometrical logic which can then be utilized to identify an according patch of space-time in LV gravity. For more details on the relativistic case see [41, 145].

The relativistic Rindler space-time $(\mathscr{R}, g_{\mathscr{R}})$ is a subset of Minkowski space-time, the intersection of the future and the past of the worldline of a uniformly accelerated observer. In Rindler coordinates, its metric takes the form

$$g_{\mathscr{R}} = e^{2a\xi}(-\mathrm{d}\eta^2 + \mathrm{d}\xi^2) + \mathrm{d}\mathbb{E}_2 \tag{6.6}$$

where lines of constant ξ correspond to an accelerated observer's worldline, and a is a bookkeeping parameter with the dimension of an acceleration. For all our purposes, the problem at hand effectively reduces to a two-dimensional problem, and therefore we can relinquish the Euclidean plane $\mathbb{E}_2$ in our subsequent analysis focusing on the (1+1) dimensional spacetime $\{\eta, \xi\}$.

The metric $g_{\mathscr{R}}$ is static and admits a globally timelike Killing vector $\chi = \partial_\eta$ which in Minkowski space-time can be easily recognized to be the boost Killing vector $\chi = a(x\partial_t + t\partial_x)$.

Because of the relativistic causal structure, an accelerated observer is in this case in causal contact only with a limited region, i.e. $g_{\mathscr{R}}$ where $|t| < x$, of the full Minkowski space-time $g_{\mathscr{M}}$. The two metrics are related by the coordinate transformation

$$\eta(t,x) = \frac{1}{a}\mathrm{artanh}\left(\frac{t}{x}\right), \quad \xi(t,x) = \frac{1}{2a}\ln\left(a^2(x^2 - t^2)\right) \tag{6.7}$$

The coordinates (η, ξ) are adapted to an observer on an orbit of the boost Killing vector in flat space-time, and they are only defined on a restricted region due to their logarithmic nature. Indeed, it is easy to see that in Minkowski coordinates, the trajectory of an observer at $\{\xi = \mathrm{const}\}$ is $\{x^2 - t^2 = a_{\mathrm{p}}^{-2}\}$, i.e. a hyperbolic trajectory with proper acceleration $a_{\mathrm{p}} = a\, e^{-a\xi}$.

Since the Rindler space-time is just a section of Minkowski, it is Riemann-flat and its asymptotic regions correspond to the future null infinity $\mathscr{I}^+$, and past null infinity $\mathscr{I}^-$, because the space-time is asymptotically simple and empty. Hence, the Penrose diagram for the Rindler dissection of Minkowski space-time – cf. figure 6.1 – comprises of four regions, the left and right wedges, $\mathscr{R}$ and $\mathscr{L}$, and a future and past wedge, $\mathscr{F}$ and $\mathscr{P}$. Those regions are separated by a Killing horizon, that is, a bifurcating, non-degenerate, null 3-surface defined by the Killing vector χ becoming null. In the coordinate patch (6.6), this condition holds at

$$|\chi|^2 = 0 \quad \Leftrightarrow \quad g_{00}\chi^0\chi^0 = -e^{2a\xi} \to 0 \quad \Leftrightarrow \quad \xi \to -\infty, \tag{6.8}$$

such that the horizon creates an asymptotic boundary and, therefore, determines the closure of the Rindler wedge. The feature that a coordinate patch asymptotes to the Killing horizon is familiar from Schwarzschild space-time in tortoise coordinates.

After analyzing the construction of the relativistic Rindler patch, we extract the following properties: the Rindler patch is a globally hyperbolic Riemann-flat space-time that admits a boost Killing vector. These conditions will serve as a blueprint to construct the Rindler patch in a Lorentz breaking setting.

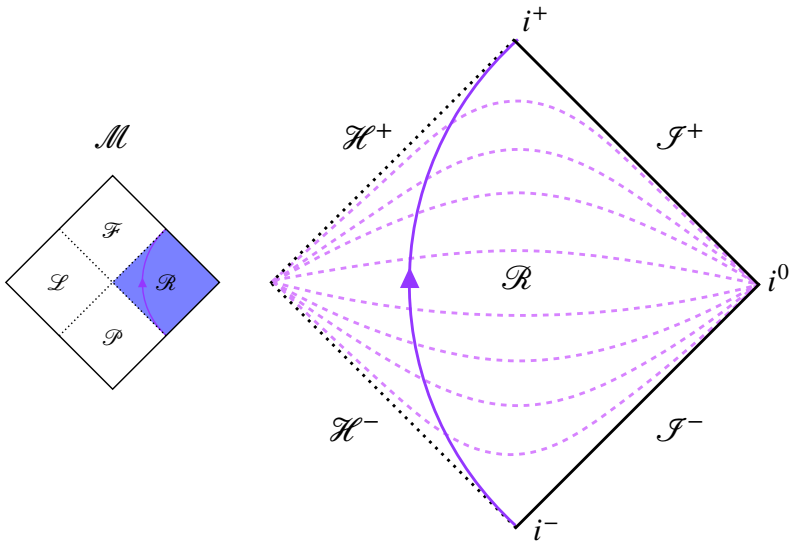

Figure 6.1: Penrose diagram for the right Rindler wedge $\mathscr{R}$ (colored area in the Penrose diagram of the full Minkowski manifold $\mathscr{M}$) with the hyperbolic trajectory of the relativistic accelerated observer ranging from i^- to i^+ and rapidity $a\eta$. The future and past horizons $\mathscr{H}^+$ and $\mathscr{H}^-$ determine the closures of the part of the manifold that borders to $\mathscr{F}$ and $\mathscr{P}$. Each point in this figure represents a Euclidean flat plane.

6.1.1 The non-relativistic Rindler patch

In contrast to the general relativistic case, in Lorentz-breaking theories we face a Newtonian causal structure, in which the Killing horizon, as a null surface, becomes permeable in both ways for signals that travel with propagation speed $c_S > 1$. Hence, the non-relativistic version of the Rindler wedge should be larger than the corresponding relativistic one, and include the latter. However, the foliated Rindler patch $\mathbb{R}$ will be a subset of the foliated Minkowski manifold $\mathbb{M}$ and will fail to cover it completely, as we will see.

The LV geometry is defined by a space-time triplet $(\mathbb{R}, g_{\mathbb{R}}, u_{\mathbb{R}})$. We begin demanding the following properties to be satisfied by a non-relativistic version of the Rindler wedge

- Boost invariance: $\mathcal{L}_\chi g_{\mathbb{R}} \equiv 0$, and $\mathcal{L}_\chi u_{\mathbb{R}} = \mathcal{L}_\chi s_{\mathbb{R}} \equiv 0$
- Riemann flatness: Riem $= 0$

It is important to highlight the relevance of the first condition[1], as it ensures the existence of stationary orbits, in the non-relativistic Rindler patch, consistent with standard Rindler orbits. This condition is crucial because, without it, no equilibrium state could be associated with these orbits. Consequently, it would be unclear how our investigation would relate to the standard Unruh effect.

Moreover, we demand the pair $(g_{\mathbb{R}}, U_{\mathbb{R}})$ to solve the equations of motion of EA gravity [98]. Since the spacetime is Riemann-flat from the metric point of view, the

[1] as usual, s^a is the spacelike vector orthonormal to u^a

equations of motion for the aether are given by (4.15) and (4.18):

$$T^u_{ab} = 0\,, \qquad \mathcal{A}^a = 0\,. \tag{6.9}$$

Let us note that the $(1+1)$-dimensional EA formulation with a timelike Killing symmetry have the same degrees of freedom as the $(3+1)$-dimensional spherically symmetric one, namely, a single-variable function determining the metric tensor and another one determining the aether. Therefore, the solution will be hypersurface orthogonal. This can be proven just by taking the twist tensor ω_{ab} and recalling that

$$\omega_{ab}u^b = 0\,. \tag{6.10}$$

Therefore, the only possible contraction in the $\{u, s\}$ basis is $\omega_{ab}s^a s^b$, which vanishes because of the antisymmetry of the twist. The expression for the two tensors in (6.9) is given in [109, 111]:

$$\begin{aligned} T^u{}_{ab} =& \nabla_c(g^{cd}u_{(b}F_{a)d} - g^{cd}F_{d(a}u_{b)} - F_{(ab)}u^c) + c_a a_a a_b \\ &+ (u_d\nabla_c F^{cd} - c_a a_c a^c)u_a u_b + \frac{1}{2}g_{ab}\mathcal{L}_{\mathrm{EA}} + 2\mathcal{A}_{(a}u_{b)}\,, \end{aligned} \tag{6.11}$$

where $\mathcal{L}_{\mathrm{EA}}$ is the Lagrange density of (4.11) and

$$\begin{aligned} F_{ab} &= c_\theta\theta g_{ab} + c_\sigma\nabla_b u_a + c_a a_b u_a\,, \\ \mathcal{A}_a &= \gamma_{ab}(\nabla_c F^{cb} - c_a a_c\nabla^b u^c)\,. \end{aligned} \tag{6.12}$$

Finding the geometry

Now, we can use the properties attributed to the relativistic Rindler space-time $(\mathscr{R}, g_{\mathscr{R}})$ in order to construct the Lorentz-violating space-time $(\mathbb{R}, g_{\mathbb{R}}, U_{\mathbb{R}})$. A sketch of the computation is reported below but we refer to Appendix C for explicit calculations.

Let us focus on the aether equation of motion $\mathcal{A}^a = 0$. Since all relevant physics takes place in a $(1+1)$-dimensional submanifold, we adopt the following ansatz to determine our spacetime's building blocks

$$g_W = W^2(\tau,\rho)(-\mathrm{d}\tau^2 + \mathrm{d}\rho^2), \qquad u_W = W(\tau,\rho)\mathrm{d}\tau, \tag{6.13}$$

with $W(\tau,\rho)$ a conformal factor. This ansatz reflects the dimensionality of the physical setup: since the observer's trajectory is embedded in a $(1+1)$-dimensional submanifold spanned by u and s, we use an adapted coordinate system $\{\tau,\rho\}$ such that u assumes the form in (6.13) and $s = W(\tau,\rho)\mathrm{d}\rho$. This is complemented with the statement that all two-dimensional metrics are conformally flat. Hence, the $(1+1)$-dimensional submanifold containing the trajectory of the observer can be decomposed into the $\{u, s\}$ orthonormal basis as

$$g_{ab} = -u_a u_b + s_a s_b \tag{6.14}$$

Imposing boost invariance and Riemann flatness, the aether equation of motion leads to the solution (and its time correspondent reversal used later on)

$$W_{\pm}(\tau,\rho)=\frac{1}{\bar{a}(\rho\pm\tau)}, \tag{6.15}$$

which we can insert into (6.13) to arrive at

$$g_W=\frac{-\mathrm{d}\tau^2+\mathrm{d}\rho^2}{\bar{a}^2(\rho\pm\tau)^2}, \qquad u_W=\frac{\mathrm{d}\tau}{\bar{a}(\rho\pm\tau)}\,. \tag{6.16}$$

Note, we display here both solutions for the sake of completeness but specify in the following analysis to the '+-branch' while we refer to the lower sign later in the article.

As required, this solution is Lie dragged with respect to the Killing vector $\chi=\tau\partial_\tau+\rho\partial_\rho$, that is, the boost Killing vector[2], see below. In (6.15), $\bar{a}$ arises as an integration constant, but it is straightforward to see that it encodes a geometrical meaning, corresponding to the norm of the aether acceleration $\|a\|=\bar{a}$, as well as to its expansion $\theta=\nabla_a u^a=\bar{a}$.

The metric (6.16) is Riemann flat, and therefore it is always possible to introduce a coordinate change $(\tau,\rho)\to(t,x)$ to the Minkowski metric

$$g_{ab}\mathrm{d}x^a\mathrm{d}x^b=-\mathrm{d}t^2+\mathrm{d}x^2 \tag{6.17}$$

taking the form

$$\tau(t,x)=\frac{x-t}{2}+\frac{1}{2\bar{a}^2(t+x)}, \quad \text{and} \quad \rho(t,x)=\frac{t-x}{2}+\frac{1}{2\bar{a}^2(t+x)}\,. \tag{6.18}$$

In the chart parametrized by (t,x), the Killing vector $\chi=\tau\partial_\tau+\rho\partial_\rho$ becomes, as anticipated, the usual boost generator $\chi=\bar{a}(x\partial_t+t\partial_x)$. From that, the aether can be easily deduced given the shape of $W(\tau(t,x),\rho(t,x))$.

To draw a closer comparison between this non-relativistic Rindler manifold $\mathbb{R}$ and the relativistic $\mathscr{R}$, it is convenient to perform the coordinate transformation (6.7) to the chart (η,ξ), in which the metric is given by (6.6). The resulting geometry is

$$g_{\mathbb{R}}=e^{2\bar{a}\xi}(-\mathrm{d}\eta^2+\mathrm{d}\xi^2)\,, \qquad u_{\mathbb{R}}=-\frac{e^{2\bar{a}\xi}+1}{2}\mathrm{d}\eta+\frac{e^{2\bar{a}\xi}-1}{2}\mathrm{d}\xi\,. \tag{6.19}$$

Note that for the left Rindler patch $\mathbb{L}$ the metric tensor $g_{\mathbb{L}}$ as well as the aether $U_{\mathbb{L}}$ assume the exact same form as their siblings in $\mathbb{R}$ while the boost generator becomes $\chi=\partial_\eta$ in $\mathbb{R}$ and $\chi=-\partial_\eta$ in $\mathbb{L}$; the corresponding Killing horizons are, therefore, located at $\xi\to\mp\infty$. As we shall see, this space-time incorporates the usual Rindler wedge fully.

However, its different causal structure allows for trajectories crossing the Killing horizon in both ways and, as such, the foliation extends into the neighboring regions of $\mathscr{R}$. Here, we stress again the role of the parameter $\bar{a}$. While it is usually just a bookkeeping parameter, in this case, it represents a physical scale which arises from the gravitational background, associated with the expansion and acceleration of the aether.

[2]Note that such solution admits an additional pair of Killing vectors where $K^{\mathrm{p}}=\partial_\tau+\partial_\rho$ generates the past and $K^{\mathrm{f}}=\partial_\tau-\partial_\rho$ the future Killing horizons.

Rindler wedge as a near-horizon limit

An alternative derivation of this geometry can be performed in the following way: it is well-known that the near-Killing horizon approximation of a Schwarzschild black hole is represented by the Rindler metric of the form of $g_{\mathbb{R}}$. So, accompanying this near-horizon expansion with the same one applied to a compatible aether, we should recover a perturbative solution of (6.9). In other words, let us consider (4.33) with (5.9), namely

$$g_{\mathbb{S}} = -\left(1-\frac{2M}{r}\right)\mathrm{d}t^2 + \frac{\mathrm{d}r^2}{1-\frac{2M}{r}} + r^2\mathrm{dS}_2\,, \qquad u_{\mathbb{S}} = \left(1-\frac{M}{r}\right)\mathrm{d}t + \frac{M}{r-2M}\mathrm{d}r\,, \tag{6.20}$$

where dS_2 is the line-element of the two sphere. Retaining the leading order in an $(r-2M)$-expansion, and relabelling afterwards $r-2M = 2Me^{2\bar{a}\xi}$ and $t=\eta$, then (6.20) becomes

$$g_{\mathbb{S}} = e^{2\bar{a}\xi}(-\mathrm{d}\eta^2+\mathrm{d}\xi^2) + 4M^2\mathrm{dS}_2\,, \qquad u_{\mathbb{S}} = -\frac{e^{2\bar{a}\xi}+1}{2}\mathrm{d}\eta + \frac{e^{2\bar{a}\xi}-1}{2}\mathrm{d}\xi \tag{6.21}$$

which reduces to (6.19) in the large mass limit, that implies $\mathrm{S}_2 \to \mathbb{E}_2$.

6.1.2 Causal structure

Let us now analyze the causal structure of the spacetime we have just found. Coming back to (6.19), we introduce at this point a change of variables through

$$2\bar{a}\epsilon(\xi) = e^{2\bar{a}\xi}\,, \tag{6.22}$$

in order to cover the region beyond the Killing horizon $\mathscr{F}$ as well, finding

$$g_{\mathbb{R}} = 2\bar{a}\epsilon(-\mathrm{d}\eta^2+\mathrm{d}\xi^2)\,, \qquad U_{\mathbb{R}} = -\frac{2\bar{a}\epsilon+1}{2}\mathrm{d}\eta + \frac{2\bar{a}\epsilon-1}{2}\mathrm{d}\xi, \tag{6.23}$$

The extension from $\mathscr{R}$ into $\mathscr{F}$ thus requires a sign change in ϵ

$$2\bar{a}\epsilon(\xi) = \begin{cases} +e^{2\bar{a}\xi} & \text{in} \quad \mathscr{R}, \\ -e^{2\bar{a}\xi} & \text{in} \quad \mathscr{F}. \end{cases} \tag{6.24}$$

To determine the extent of this manifold into the region $\mathscr{F}$, it is convenient to regard ϵ as a spatial coordinate.

Universal horizon

Our solution allows for an UH, located at

$$(\chi\cdot u) = -\frac{1+2\bar{a}\epsilon_{\mathrm{UH}}}{2} = 0, \tag{6.25}$$

which admits the solution $\epsilon_{\mathrm{UH}} = -1/(2\bar{a})$. Associated to the universal horizon, we also compute its surface gravity

$$\kappa_{\mathrm{UH}} = \left.\frac{(a\cdot\chi)}{2}\right|_{\mathrm{UH}} = \frac{\bar{a}}{2}, \tag{6.26}$$

which is again characterized by the æther's acceleration $\bar{a}$, being the only scale in the problem.

Foliation

Since $\epsilon_{\rm UH} < 0$, the UH lies in $\mathscr{F}$, which means in turn that the foliation of $\mathscr{R}$ extends into the relativistic wedge $\mathscr{F}$ – since the previous condition can never be met in $\mathscr{R}$. To substantiate this result, we solve (4.8) for the khronon field coordinating the foliation in both patches, $\mathbb{R}$ and $\mathbb{L}$, in Minkowski coordinates – foliation leafs corresponding to constant khronon surfaces. We find[3],

$$\tau_{\mathbb{R}}(t,x) = -\frac{1}{\bar{a}}\ln\left(\frac{\bar{a}^2(x^2-t^2)+1}{\bar{a}(x+t)}\right), \quad \tau_{\mathbb{L}}(t,x) = -\frac{1}{\bar{a}}\ln\left(-\frac{\bar{a}^2(x^2-t^2)+1}{\bar{a}(x+t)}\right). \tag{6.27}$$

The khronon leafs accumulate exactly at the hyperbola

$$t^2 - x^2 = 1/\bar{a}^2\,, \tag{6.28}$$

which corresponds to the location of the universal horizon. The first observation to emphasize here is the existence of two solutions that constitute the foliation of the right and the left Rindler patches ($\mathbb{R}$ and $\mathbb{L}$, respectively) until the universal horizon, as well as the future and past patches ($\mathbb{F}$ and $\mathbb{P}$). Second, due to the sign difference in the argument of the logarithm, both foliations are oriented in opposite directions. If, for instance, $\tau_{\mathbb{R}}$ is future oriented, then $\tau_{\mathbb{L}}$ is past oriented, and vice versa. More colloquially speaking, the clock $\tau_{\mathbb{R}}$ ticks in opposite direction with respect to $\tau_{\mathbb{L}}$. Since the lapse of the foliation $N_{\mathbb{R}} = -(\chi\cdot u)$ flips sign across the universal horizon, $\mathbb{F}$ is foliated according to $\tau_{\mathbb{L}}$ and $\mathbb{P}$ with respect to $\tau_{\mathbb{R}}$. As can be seen in figure 6.2, foliation leafs accumulate from both sides at the universal horizon, describing a natural closure that limits the Rindler patches.

Additionally, from (6.27) it is straightforward to show that the lapse function N assumes an opposite sign between the two regions $\mathbb{R}$ and $\mathbb{L}$. Indeed, since $\mathrm{d}\tau_{\mathbb{R}} = \mathrm{d}\tau_{\mathbb{L}}$ we have $u_{\mathbb{R}} = u_{\mathbb{L}}$. However the boost Killing vector $\chi = x\partial_t + t\partial_x$ flips sign between the two regions that gives us $N_{\mathbb{R}} = -N_{\mathbb{L}}$

Figure 6.2 also shows that the accelerated aether cuts the space-time into four pieces. We observe that the foliation of $\mathbb{R}$ extents into the region $\mathscr{F}$, yielding a very particular form of the right patch that resembles the shape of the exterior foliation of an EA-Schwarzschild black-hole [38]. Similar to the black hole interior, the change of sign in $(\chi\cdot u)$ ensures that the manifold is $\mathcal{C}^2(\mathbb{R})$ across the horizon [35].

It should be emphasized that the space-time, and thus the foliation, are invariant under the action of the boost vector χ. For foliated manifolds, this implies that the aether itself is invariant. As a consequence, $(\chi\cdot u)$ is independent of the time coordinate η and the aether is Lie dragged with respect to ∂_η. This determines our foliation uniquely and constitutes the Rindler patch.

An analog patch $\mathbb{L}$ can be found by considering the outside red part in figure 6.2 with adjacent region $\mathbb{P}$ given by the lower green part. Altogether, these four parts cover all of Minkowski space-time like in the relativistic scenario. The corresponding Penrose diagram for $\mathbb{R}$ can be seen in figure 6.3.

As a final remark, let us point out that the structure depicted by the foliation (6.27) represents the unique $(1+1)$-dimensional spacetime with a boost-invariant

[3]The same spacetime was found, in an independent manner in [146]

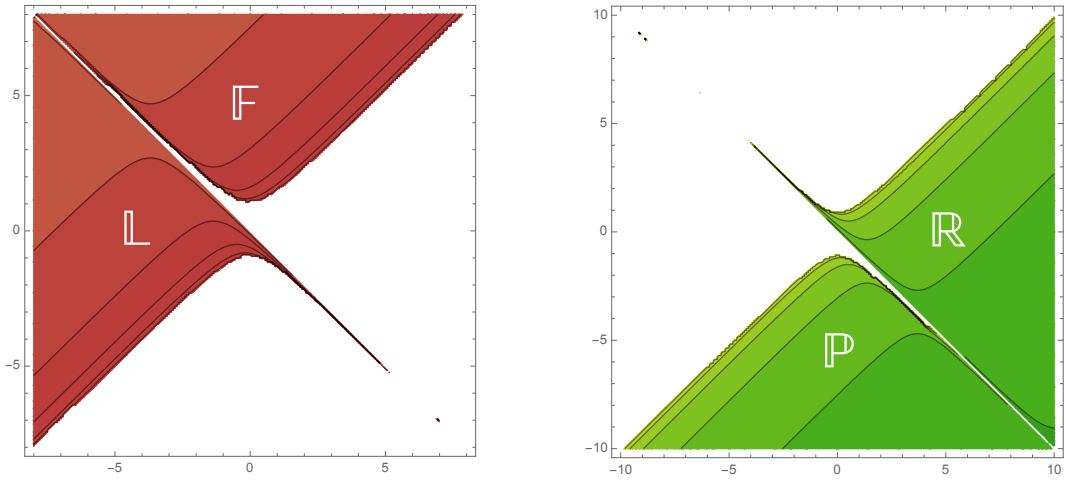

Figure 6.2: Foliated area of Minkowski space-time through an accelerated aether. The right, green panel shows the lines of constant $\tau_{\mathbb{R}}$, which generate a future directed aether $u_{\mathbb{R}}$ and charts $\mathbb{R}$ and $\mathbb{P}$. The left, red panel depicts the folium generated by constant $\tau_{\mathbb{L}}$ lines, and covers the regions $\mathbb{L}$ and $\mathbb{F}$. The corresponding aether $u_{\mathbb{L}}$ is past-directed with respect to $u_{\mathbb{R}}$.

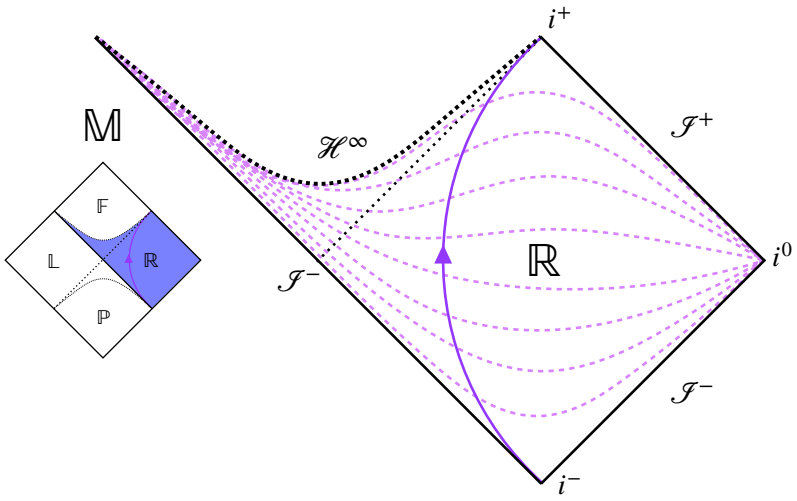

Figure 6.3: Penrose diagram for the right Rindler patch $\mathbb{R}$ (colored area in $\mathbb{M}$) with hyperbolic trajectory of the relativistic accelerated observer ranging from i^{-} to i^{+} with rapidity $\bar{a}\eta$. The future universal horizon $\mathscr{H}^{\infty}$ determines the closures of the part of the manifold that borders to $\mathbb{F}$. The Killing horizon is displayed by the dotted null line while the constant khronon leafs are the dashed purple lines. It is visible that $\mathscr{R} \subset \mathbb{R}$ for identical hyperbolae. The left Rindler patch $\mathbb{L}$ can be obtained by reflecting $\mathbb{R}$ at the point where $\mathscr{I}^{+}$ meets the Killing horizon.

preferred time. Considering a usual uniformly accelerated observer, which follows an orbit of χ up to i^+, our Rindler wedge defines the portion of Minkowski which is causally connected with him. This construction becomes a crucial difference in the study of the Unruh effect for LV physicis with respect to previous investigations [142] which limit their analysis to the relativistic wedge.

6.2 The Unruh effect: Bogolyubov approach

The Unruh effect consists in the detection of a thermal bath by a uniformly accelerated (Rindler) observer in Minkowski vacuum. Its derivation usually follows from the confrontation of the vacuum associated to an inertial observer in Minkowski with that associated to the second quantization of the field in a basis of modes appropriated for the Rindler observer.

More specifically, let us consider a massless relativistic field obeying the usual Klein Gordon equation [13, 145]

$$\Box\phi(x,t) = (-\partial_t^2 + \partial_x^2)\phi(x,t) = 0 \tag{6.29}$$

which space of solutions can be labelled by the modes

$$u_k = \frac{1}{\sqrt{2\pi|k|}} e^{-i|k|t+ikx}\,, \tag{6.30}$$

thus defining the energy $\omega = |k|$ with respect to the Minkowskian time ∂_t. This mode-decomposition allows to define the Mikowski vacuum as

$$\hat{a}_k|0\rangle_{\mathscr{M}} = 0\,, \tag{6.31}$$

being $\hat{a}_k$ the annihilation operator for a mode with energy $\omega(k) = |k|$. This vacuum will be the vacuum for any inertial observer in Minkowski, being a Poincarè invariant state.

On the other hand, (6.29) can be solved in the Rindler patches (6.6), i.e. for $\{x > |t|\}$ and $\{x < -|t|\}$. This is a particularly simple task for a massless scalar field, since the field equation is conformal invariant and the metric is conformally flat:

$$\Box\phi(\xi,\eta) = e^{-2a\xi}(-\partial_\eta^2 + \partial_\xi^2)\phi(\xi,\eta) = 0 \tag{6.32}$$

that admits again a mode decomposition of the form

$$v_p = \frac{1}{\sqrt{2\pi|p|}} e^{-i|p|\eta+ip\xi}\,, \tag{6.33}$$

with $\Omega(p) = |p|$ being the energy of the mode defined with respect to the boost Killing vector ∂_η. Those modes are associated with another couple of creation and annihilation operators $\hat{b}_p^\dagger$ and $\hat{b}_p$. As already discussed, these functions are not analytical at the Killing horizon and it is possible to build an analytical combination of only positive and only negative Minkowski modes [13]:

$$\psi_p^\pm(\eta,\xi) = v_{\mathscr{R},p}(\eta,\xi) + e^{\mp\frac{\pi\omega}{a}} v^*_{\mathscr{L},-p}(\eta,\xi)\,, \tag{6.34}$$

where the subscripts $\mathscr{L}$ and $\mathscr{R}$ refer to the left and right Rindler wedge. From (6.34), one can work out the Bogolyubov coefficients as described in Chapter 2 and in particular the mean value of the particle number operator $\hat{N}_p = \hat{b}_p^\dagger \hat{b}_p$ onto the Minkowski vacuum [41]:

$$\langle \hat{N}_p \rangle_{\mathscr{M}} = \frac{1}{e^{\frac{2\pi\Omega}{a}} - 1} \,. \tag{6.35}$$

The resulting Bose-Einstein distribution tells us that the Minkowski vacuum looks like a thermal state for the accelerated observer. That defines the wedge temperature as:

$$T_{\mathscr{R}} = \frac{a}{2\pi} \,. \tag{6.36}$$

As a final remark, let us notice that $T_{\mathscr{R}}$ is exclusively governed by the horizon $\mathscr{H}^+$, but not by the particular observer. In fact, the bookkeeping parameter a can always be set to one in (6.7) without loss of generality. However, the proper temperature measured by an accelerated observer, travelling along a specific hyperbola of constant ξ, can be derived from the wedge temperature by the appropriate Tolman factor

$$T_{\rm p} = \frac{T_{\mathscr{R}}}{\sqrt{-g_{00}}} = \frac{a e^{a\xi}}{2\pi} = \frac{a_{\rm p}}{2\pi} \,. \tag{6.37}$$

We hence see that the observed temperature of a given Rindler observer depends on its proper acceleration $a_{\rm p}$, and coincides with $T_{\mathscr{R}}$ on the special hyperbola $\xi = 0$.

6.2.1 Rindler modes in Lorentz-violating gravity

Let us now consider a dispersive field in the (boost invariant) LV geometry that we described in section 6.1.1. As usual we will take a field ϕ of the form of (5.11) with field equation

$$\left[\Box - \sum_{j=2}^{n} \frac{\beta_{2j}}{\Lambda^{2j-2}} (-\Delta)^j \right] \phi = 0, \tag{6.38}$$

where $\Delta = \gamma^{ab} \nabla_a \nabla_b$ is the usual Laplace operator. One can define the preferred energy and momentum as we did previously in this thesis. Within a WKB ansatz

$$\phi_{\rm WKB} = \phi_0 e^{i\mathcal{S}_0} \,, \tag{6.39}$$

one can set

$$u^a \partial_a \phi = -i\omega\phi \quad \text{and} \quad s^a \partial_a \phi = -ik\phi \,. \tag{6.40}$$

The equation of motion becomes a modified dispersion relation:

$$\omega^2 = k^2 + \sum_{j=2}^{n} \frac{\beta_{2j}}{\Lambda^{2j-2}} k^{2j} \,, \tag{6.41}$$

accompained with the conserved quantity connected with the boost invariance

$$\Omega = -\omega(u\cdot\chi) - k(s\cdot\chi) = \omega N - kV\,. \tag{6.42}$$

Let us emphasize that the mathematics is exactly the same as the one found in Chapter 5. The modes which solve (5.15) do not completely decouple due to the dispersion. Actually, the massless, $(1+1)$-dimensional relativistic case is the only case where right-going and left-going modes decouple completely [147]. In general, the propagation of the modes is affected from the geometry and the dispersion, which also is the cause of the greybody factor. This computation is thus more similar to the black hole case then to the Unruh computation for the massless field.

However, in addition to the UH analysis we will have to investigate the shape of the modes also nearby the juction $\{x+t=0\}$, since the goal will be to combine the modes in the left and right Rindler patches in such a way to build an analogous of (6.34) and compare with the Minkowski vacuum.

Near horizon modes

Indeed, even if the computation of the full form of the modes in the whole spacetime is quite involved an perhaps impossible for generic n, we are interested in the near-UH limit of the solution. There, we find a behaviour of divergent ω and k in complete analogy to what we found in Chapter 5. This again gives the phase velocity (readable directly from (6.42))

$$c_p = \frac{\omega}{k} = -\frac{V}{N}\,. \tag{6.43}$$

The (divergent) phase velocity, defines the constant-phase contours of the right-going modes through

$$\mathrm{d}\bar{u} = (c_p u_a + s_a)\mathrm{d}x^a = 0\,. \tag{6.44}$$

Following the same steps given in Chapter 5, one see that the near-UH, right-going modes in the right Ringler patch are given by:

$$\phi_\Omega = e^{-i\Omega\tau}\,, \quad \text{where} \quad \tau = \eta - \frac{1}{\bar{a}}\log(1+2\bar{a}\epsilon)\,, \tag{6.45}$$

where the energy has been fixed with respect to $\chi = \partial_\eta$.

Near $x+t=0$

The other point where we have to look is the surface $\{x+t=0\}$ where the constant khronon leaves accumulate in the infinite past. The situation can be analyzed in a similar fashion. Let us introduce a set of null coordinate to describe the $\{u\,,s\}$ plane:

$$\bar{V} = t+x\,, \qquad \bar{U} = t-x\,, \tag{6.46}$$

in which we have

$$u = -\frac{1}{2}\left(\frac{\mathrm{d}\bar{V}}{\bar{a}\bar{V}} + \bar{a}\bar{V}\mathrm{d}\bar{U}\right), \qquad s = \frac{1}{2}\left(\frac{\mathrm{d}\bar{V}}{\bar{a}\bar{V}} - \bar{a}\bar{V}\mathrm{d}\bar{U}\right). \tag{6.47}$$

Closeby the surface $\bar{V} = 0^+$ the conservation of Ω (6.42) can be easily evaluated as

$$\Omega = \frac{\omega - k}{2}\,, \tag{6.48}$$

that, together with (6.41) allows to determine the shape of the WKB mode ϕ, just by evaluating the classical action of (6.39) in the limit $(x + t) \to 0^+$:

$$\phi_\Omega = e^{-i\frac{\Omega}{\bar{a}}\log(\bar{V})}\,. \tag{6.49}$$

6.2.2 Analytical continuation

Give the non-analiticities of the modes both at the UH and at $\bar{V} = 0$ we can build the following combinations between the $\mathbb{L}$ and $\mathbb{R}$ modes:

$$\Phi^{\pm}_\Omega(\eta, \epsilon) = \phi_{\mathbb{L},\Omega}(\eta, \epsilon) + e^{\mp\frac{\pi\Omega}{\bar{a}}}(\phi_{\mathbb{R},\Omega}(\eta, \epsilon))^*\,. \tag{6.50}$$

Surprisingly, the factor $e^{\mp\frac{\pi\Omega}{\bar{a}}}$ cures the non-analyticities both at the horizon and at $\bar{V} = 0$. Hence the set $\{\Phi^{\pm}_\Omega\}$ describes modes at fixed Ω which are well defined in the whole Minkowski space-time.

The Bogolyubov coefficients can be computed again in the usual way giving the following number of created particles

$$\langle\hat{N}_\Omega\rangle_{\mathbb{M}} = \int \mathrm{d}\bar{\Omega}\,|\beta^{\mathbb{R}}_{\bar{\Omega}\Omega}|^2 = \frac{1}{e^{\frac{2\pi\Omega}{\bar{a}}} - 1} \tag{6.51}$$

where we have defined the particle number operator $\hat{N}_\Omega = \hat{b}^\dagger_\Omega \hat{b}_\Omega$, and the expectation value has been evaluated within the Minkowski vacuum state. We find that the number of measured particles follows a Bose-Einstein distribution from which we can read off the associated patch-temperature

$$T_{\mathbb{R}} = \frac{\bar{a}}{2\pi} = \frac{\kappa_{\mathrm{UH}}}{\pi}. \tag{6.52}$$

Note, we identified $\bar{a} = 2\kappa_{\mathrm{UH}}$ where κ_{UH} is the surface gravity calculated from the expansion, which is related to the peeling surface gravity [122] at the universal horizon.

Again, the above temperature is purely set on the basis of geometrical considerations related to the universal horizon induced by the aether flow of the Rindler patch. In this sense, we derived the equivalent of the Rindler wedge temperature $T_{\mathscr{R}} = a/2\pi$. However, this is not the temperature that an observer will detect while moving on a specific orbit of the boost Killing vector, the equivalent of (6.37) for our case.

One might contemplate applying the usual Tolman factor to get the proper acceleration, but this would not do: indeed the Tolman factor is purely metric dependent and would not capture the relevance of the observer motion with respect to the preferred frame set by the aether. The important question, we need to address here, is, what would an observer on a Rindler trajectory (along ξ =const.) actually detect in a realistic, thus simplified, measurement process. Therefore, let us now push further

our investigation (and double check the above results) by considering the response of a uniformly accelerated Unruh-DeWitt detector. We shall see in what follows that this will not only corroborate our previous analysis but will also enlighten where the imprints of the LV physics can be found in spite of the insensitivity of the found temperature (6.52) on the details of the modified dispersion relation.

6.3 Unruh-De Witt detector

In order to understand what an actual Rindler observer would measure, we consider a simple model describing a point-like Unruh-DeWitt detector [148]. We will again work within the $(1+1)$-dimensional submanifold that contains the world-line of the detector. This treatment is in line with [145], which also shows the generalization to the full $(1+3)$-dimensional setup.

The detector is composed out of a Hermitian operator $\hat{\mu}$ which acts on a two-dimensional Hilbert space $\mathcal{H}_\mu \simeq \mathbb{C}^2$ spanned by the orthonormal basis $\{|E_0\rangle, |E_1\rangle\}$ where $|E_0\rangle$ denotes the ground-state and $|E_1\rangle$ the excited state. These states are designed to be the eigenstates of the free Hamilton operator $\hat{H}_\mu$, that is, they fulfill

$$\hat{H}_\mu |E_{0/1}\rangle = E_{0/1}|E_{0/1}\rangle \quad \text{with} \quad E_0 < E_1 \,. \tag{6.53}$$

To detect field excitations, we couple the detector to a scalar field $\hat{\phi}$ via the interaction term [145, 148, 149]

$$\hat{W} = b \int_{-\infty}^{\infty} \mathrm{d}\tau \; \chi(\tau) \hat{\mu}(\tau) \hat{\phi}[y(\tau)] \tag{6.54}$$

with coupling strength $b \in \mathbb{R}$, and switching function $\chi(\tau)$, that has support only on the time interval of the measurement [140]. The evolution parameter τ is always adapted to the Cauchy problem; and it is typically chosen to be the proper time of the detector on its world-line. Here, we choose τ to be the preferred time of the foliation, dictated by the khronon. This aligns the Hamiltonian flow with the direction of the preferred clock and yields a consistent Schrödinger evolution.

Since our detector is constantly accelerated, its domain of dependence will only cover the right Rindler patch $\mathbb{R}$, as previously argued, whose khronon is given by (6.27). The Hamiltonian flow must then be tangent to u and the Schrödinger operator $i\mathcal{L}_u - \hat{H}_\mu$ acquires an additional dependence on the lapse. Colloquially speaking, the detector evolution is determined by the preferred time rescaled by the lapse as

$$\hat{\mu}(s) = e^{-iN\hat{H}_\mu \tau(s)} \hat{\mu}_0 \, e^{iN\hat{H}_\mu \tau(s)}. \tag{6.55}$$

Note that we have introduced the proper time of the detector s via $\tau(s) = s e^{\bar{a}\xi}$ so that we can relate our result to the relativistic Unruh setup that is naturally parametrized by s, the detector clock.

The Hamilton operator [148] that acts on states in the Hilbert space $\mathcal{H}_\phi$ is given by

$$\hat{H}_\phi(\tau) = \int_{\Sigma_\tau} \mathrm{d}^3 y \sqrt{-\det(\gamma)} \, \left\{ \hat{\Pi}(\tau, \vec{y}) \, u^a \partial_a \hat{\phi}(\tau, \vec{y}) - \mathcal{L}[\hat{\phi}, \nabla\hat{\phi}](\tau, \vec{y}) \right\}, \tag{6.56}$$

where the Lagrange density $\mathcal{L}[\hat{\phi}, \nabla\hat{\phi}](\tau, \vec{y})$ is given by (5.11). As usual, $\hat{\Pi}(\tau, y)$ denotes the canonical momentum conjugated to the field $\hat{\phi}(\tau, y)$. Then the total Hilbert space is $\mathcal{H} = \mathcal{H}_\mu \otimes \mathcal{H}_\phi$ and the total Hamilton operator takes the form

$$\hat{H} = \hat{H}_\mu \otimes \hat{\mathrm{id}}_\phi + \hat{\mathrm{id}}_\mu \otimes \hat{H}_\phi + \hat{W}\,, \tag{6.57}$$

where $\hat{\mathrm{id}}$ represents the identity operator. In order to avoid infrared divergences [145], we introduce a regularization scale m that can be interpreted as a fiducial mass for the field, which then obeys

$$\left(\Box - \sum_{j=2}^{n} \frac{\beta_{2j}}{\Lambda^{2j-2}}(-\Delta)^j - m^2\right)\phi = 0. \tag{6.58}$$

Also, by doing this the comparison with the relativitic case as discussed in [145] becomes immediate. Note that the quantum field $\hat{\phi}$ must be evaluated on the detector's trajectory $y(s)$ such that $\hat{\phi}(\tau, \vec{y}) \to \hat{\phi}[y(s)]$. As an operator, $\hat{\phi}$ is represented through a positive frequency basis, such that

$$\hat{\phi}(y) = \int_{\mathbb{R}} \frac{\mathrm{d}k}{2\pi}\left\{\hat{a}_k u_k(y) + \hat{a}_k^\dagger u_k^*(y)\right\} \tag{6.59}$$

where $u_k(y)$ is a solution to the equations of motion and $\hat{a}_k|0\rangle = 0$ the destruction operator annihilating the vacuum state of the quantum field $|0\rangle$.

In general, the outcome of a measurement is given by acting with $\hat{W}$ onto a given state. This can either be the ground state $|\mathfrak{o}\rangle$, or the corresponding excited state $|\mathfrak{1}\rangle$, respectively

$$|\mathfrak{o}\rangle = |0\rangle \otimes |E_0\rangle \quad \text{and} \quad |\mathfrak{1}\rangle = |k\rangle \otimes |E_1\rangle\,, \tag{6.60}$$

which describes a particle with momentum k that has excited the detector – a clicking event. With this,

$$\hat{W} = \int_{\mathbb{R}} \mathrm{d}s\, \{\hat{\mathrm{id}} \otimes \hat{\mu}(s) + \hat{\phi}[y(s)] \otimes \hat{\mathrm{id}}\}\,, \tag{6.61}$$

since the total Hilbert space is given by a tensor product, and we can define the excitation rate over a probing-time interval Δs as

$$\mathcal{R} = \frac{1}{\Delta s}\int_{\mathbb{R}} \mathrm{d}k\, |\mathcal{A}_k|^2, \tag{6.62}$$

where

$$\mathcal{A}_k = i\langle \mathfrak{1}|\hat{W}|\mathfrak{o}\rangle \quad \text{and} \quad \Delta s = \int_{-\infty}^{\infty} \chi(s)\mathrm{d}s\,. \tag{6.63}$$

Note that we tacitly assumed k to be conserved. This is not true in the Lorentz violating case, but let us assume it so for the moment. We will come back to this point later when we particularize the setup to our Gedankenexperiment (for a general discussion, cf. [145]).

6.3.1 Temperature

Here, we are interested in the question of what a detector in Minkowski vacuum measures on a uniformly accelerated trajectory. Let us start with the solution space to (6.38) in a foliated Minkowski vacuum – hence with a homogeneous aether. We find for the mode

$$u_k[y(s)] = \frac{e^{ik[y(s)]}}{\sqrt{2\omega_\Lambda(k)}}, \tag{6.64}$$

where $k[y(s)] = \omega_\Lambda(k)t(s) - kx(s)$ and $\omega_\Lambda(k) = \sqrt{m^2 + k^2 + \frac{k^4}{\Lambda^2}}$ denotes the dispersion relation in Minkowski space-time.

In the (foliated) Minkowski space-time, the hyperbola described by the accelerated detector can be parametrized as usual

$$t(s) = \frac{1}{a_{\rm p}}\sinh(a_{\rm p}s), \qquad x(s) = \frac{1}{a_{\rm p}}\cosh(a_{\rm p}s), \tag{6.65}$$

where $a_{\rm p}$ is the proper acceleration. Using the mode (6.64), we find that the amplitude in (6.62) factorizes as follows

$$\begin{aligned}\langle \mathfrak{1}|\hat{W}|\mathfrak{o}\rangle &= \int_{\mathcal{I}} \mathrm{d}s\, \langle E_1| \otimes \langle k|\hat{\mu}(s)\hat{\phi}[y(s)]|0\rangle \otimes |E_0\rangle \\ &= \int_{\mathcal{I}} \mathrm{d}s\, \langle E_1|\hat{\mu}(s)|E_0\rangle \int_{\mathbb{R}} \frac{\mathrm{d}k}{\sqrt{8\pi^2\omega_\Lambda(k)}}\, e^{\frac{i}{a_{\rm p}}(k\cosh(a_{\rm p}s) - \omega_\Lambda(k)\sinh(a_{\rm p}s))},\end{aligned} \tag{6.66}$$

where $\mathcal{I} = [-s_0, s_0]$ is the time-interval of the measurement determined by the indicator function $\chi(s)$, here taken symmetric for simplicity. The first of these factors depends on the specifics of the detector, while the second, usually called the response function, describes how the field is perceived on the hyperbola.

The evaluation of $\hat{\mu}(s)$ requires to consider the Hamiltonian flow. From the coordinate transformations (6.7), we derive the function $\tau(s)$ on a fixed ξ trajectory from (6.27) to be $\tau(s) = e^{-\bar{a}\xi}s$. Note how, via this relation, the aether acceleration just came into play. The consequences for the rate are immediate. Considering (6.55) and the fact that $|E_{0/1}\rangle$ form a basis of $\mathcal{H}_\mu$, we find that

$$\langle E_1|\hat{\mu}(s)|E_0\rangle = q\, e^{iN\Delta E\tau(s)} \tag{6.67}$$

where we defined $q = \langle E_1|\hat{\mu}_0|E_0\rangle$, and $\Delta E = E_1 - E_0$.

After squaring the amplitude, we are thus facing the following integral for the rate

$$\mathcal{R} = \frac{|q|^2}{4\pi a_{\rm p}\Delta s}\int_{-\infty}^{\infty}\frac{\mathrm{d}k}{\omega_\Lambda(k)}\int_{\mathcal{I}}\mathrm{d}s\int_{\mathcal{I}}\mathrm{d}s'\left[e^{iNe^{-\bar{a}\xi}\Delta E(s-s')}e^{i\Phi(s,s',k)}\right], \tag{6.68}$$

where $\Phi(s, s', k)$ is defined as

$$\Phi = \frac{\omega_\Lambda(k)}{a_{\rm p}}\left[\sinh\left(a_{\rm p}s\right) - \sinh\left(a_{\rm p}s'\right)\right] + \frac{k}{a_{\rm p}}\left[\cosh\left(a_{\rm p}s'\right) - \cosh\left(a_{\rm p}s\right)\right]. \tag{6.69}$$

Let us now define $\sigma = s - s'$ and $2\zeta = s + s'$. We can rewrite Φ as

$$\Phi(\sigma, \zeta, k) = \frac{2}{a_{\rm p}} \sinh\left(\frac{a_{\rm p}\sigma}{2}\right) \left[\omega_\Lambda(k) \cosh(a_{\rm p}\zeta) - k \sinh(a_{\rm p}\zeta)\right]. \tag{6.70}$$

The expression for $\mathcal{R}$ becomes then

$$\mathcal{R} = \frac{|q|^2}{2\pi a_{\rm p} \Delta s} \int_{-\infty}^{\infty} \frac{{\rm d}k}{\omega_\Lambda(k)} \int {\rm d}\sigma \int {\rm d}\zeta \left\{ e^{iNe^{-\bar{a}\xi}\Delta E \sigma} e^{i\Phi(\sigma,\zeta,k)} \right\}, \tag{6.71}$$

where $\sigma \in [-2s_0, 2s_0]$ and $\zeta \in [-s_0, s_0]$ and we omitted the extrema of integration for compactness. The σ-integral can be transformed into a soluble form after another change of variables $\lambda = \exp(a_{\rm p}\sigma/2)$ – thus $\lambda \in [e^{-s_0 a_{\rm p}}, e^{s_0 a_{\rm p}}]$ – so that we find Φ to be

$$\Phi(\lambda, \zeta, k) = \frac{1}{a_{\rm p}} \left(\lambda - \frac{1}{\lambda}\right) \left[\omega_\Lambda(k) \cosh(a_{\rm p}\zeta) - k \sinh(a_{\rm p}\zeta)\right] \tag{6.72}$$

and

$$\mathcal{R} = \frac{|q|^2}{2\pi a_{\rm p} \Delta s} \int_{-\infty}^{\infty} \frac{{\rm d}k}{\omega_\Lambda(k)} \int {\rm d}\zeta \int \frac{{\rm d}\lambda}{\lambda} \left\{ \lambda^{\frac{i2Ne^{-\bar{a}\xi}}{a_{\rm p}}\Delta E} e^{i\Phi(\lambda,\zeta,k)} \right\}. \tag{6.73}$$

If we want our observer to experience the whole curve we have to send $s_0 \to +\infty$. In this way, the λ-integral becomes within the range $[0, +\infty)$ while the ζ one runs all over the real line $\zeta \in (-\infty, +\infty)$. At the same time also the normalization $\Delta s = 2s_0$ blows up. The λ integration can be faced easily[4]:

$$\begin{aligned} &\int_0^{\infty} \frac{{\rm d}\lambda}{\lambda} \left\{ \lambda^{\frac{i2Ne^{-\bar{a}\xi}}{a_{\rm p}}\Delta E} e^{i\Phi(\lambda,\zeta,k)} \right\} = \\ &e^{-\pi\nu} K_{i\nu}\left(\frac{2\left[\omega_\Lambda(k)\cosh(a_{\rm p}\zeta) - k\sinh(a_{\rm p}\zeta)\right]}{a_{\rm p}} \right). \end{aligned} \tag{6.75}$$

where we have defined

$$\nu = \frac{2Ne^{-a\xi}}{a_{\rm p}} \Delta E \tag{6.76}$$

and $K_{i\nu}(x)$ is a modified Bessel function of the second kind [151]. Since

$$K_{i\nu}\left(\frac{2\left[\omega_\Lambda(k)\cosh(a_{\rm p}\zeta) - k\sinh(a_{\rm p}\zeta)\right]}{a_{\rm p}} \right). \tag{6.77}$$

is limited in ζ, the following ζ-integration

$$\frac{1}{\Delta s} \int {\rm d}\zeta \, K_{i\nu}\left(\frac{2\left[\omega_\Lambda(k)\cosh(a_{\rm p}\zeta) - k\sinh(a_{\rm p}\zeta)\right]}{a_{\rm p}} \right), \tag{6.78}$$

[4]To solve this integral explicitly, we used the subsequent identity [150]

$$\int_0^{\infty} {\rm d}x \, x^{\nu-1} \exp\left(\frac{i\mu}{2}\left(x - \frac{\beta^2}{x}\right)\right) = 2\beta^\nu e^{\frac{i\pi\nu}{2}} K_\nu(\beta\mu). \tag{6.74}$$

is finite, as the divergence of the integral is compensated by the divergence of Δs in the denominator. Namely, the limit

$$\lim_{s_0\to+\infty}\frac{1}{2s_0}\int_{-s_0}^{s_0}\mathrm{d}\zeta\; K_{i\nu}\left(\frac{2\left[\omega_\Lambda(k)\cosh(a_{\mathrm{p}}\zeta)-k\sinh(a_{\mathrm{p}}\zeta)\right]}{a_{\mathrm{p}}}\right)<+\infty\,. \tag{6.79}$$

We can thus define the total response of the detector $\mathfrak{R}$

$$\mathfrak{R}=\frac{|q|^2}{2\pi a_{\mathrm{p}}\Delta s}\int_{-\infty}^{\infty}\frac{\mathrm{d}k}{\omega_\Lambda(k)}\int\mathrm{d}\zeta\; K_{i\nu}\left(\frac{2\left[\omega_\Lambda(k)\cosh(a_{\mathrm{p}}\zeta)-k\sinh(a_{\mathrm{p}}\zeta)\right]}{a_{\mathrm{p}}}\right)\,. \tag{6.80}$$

In other words, we have the excitation rate to be

$$\mathcal{R}=e^{-\frac{\pi N e^{-\bar{a}\xi}}{a_{\mathrm{p}}}\Delta E}\times\mathfrak{R}\,. \tag{6.81}$$

To extract the temperature from this calculation, we need to compute also the de-excitation rate. While (6.73) is given by the k-integral of $|\mathcal{A}_k|^2$, where $\mathcal{A}_k$ is the matrix element $\mathcal{A}_k=i\langle\mathfrak{1}|\hat{W}|\mathfrak{o}\rangle$ given in (6.63), the de-excitation rate $\bar{\mathcal{R}}$ is given by the probability of the inverse process to occur

$$\bar{\mathcal{R}}=\frac{1}{\Delta s}\int_{\mathbb{R}}\mathrm{d}k\;|\bar{\mathcal{A}}_k|^2\,. \tag{6.82}$$

where $\bar{\mathcal{A}}_k=i\langle\mathfrak{o}|\hat{W}|\mathfrak{1}\rangle$.

In practical terms, this requires to compute the de-excitation probability of the detector

$$\langle E_0|\hat{\mu}(s)|E_1\rangle=q^*\;e^{-iN\Delta E\tau(s)}\,, \tag{6.83}$$

where $q^*=\langle E_0|\hat{\mu}_0|E_1\rangle$ is the complex conjugate of q. Additionally we need to compute the $|k\rangle\to|0\rangle$ matrix element of $\hat{\phi}[y(s)]$ which is given by

$$\begin{aligned}\langle 0|\hat{\phi}[y(s)]|k\rangle&=\int_{\mathbb{R}}\frac{\mathrm{d}k}{\sqrt{8\pi^2\omega_\Lambda(k)}}\,e^{-\frac{i}{a_{\mathrm{p}}}(k\cosh(a_{\mathrm{p}}s)-\omega_\Lambda(k)\sinh(a_{\mathrm{p}}s))}\\&=\Big(\langle k|\hat{\phi}[y(s)]|0\rangle\Big)^*\,.\end{aligned} \tag{6.84}$$

The computation now goes along the same lines as that previously shown for $\mathcal{R}$. We arrive to

$$\bar{\mathcal{R}}=\frac{1}{\Delta s}\int_{\mathbb{R}}\mathrm{d}k\;|\bar{\mathcal{A}}_k|^2=e^{\frac{\pi N e^{-\bar{a}\xi}}{a_{\mathrm{p}}}\Delta E}\times\mathfrak{R}\,, \tag{6.85}$$

where $\mathfrak{R}$ is the same response function, containing the remaining ζ-integral, appearing in (6.80). Using (6.73) and (6.85) we can see that the ratio

$$\frac{\mathcal{R}}{\bar{\mathcal{R}}}=e^{-2\frac{\pi N e^{-\bar{a}\xi}}{a_{\mathrm{p}}}\Delta E}\,, \tag{6.86}$$

is a Boltzmann factor which then allows us to read off the temperature that is measured by the detector [145]

$$T_{\mathrm{UDW}}=\frac{a_{\mathrm{p}}e^{\bar{a}\xi}}{2\pi N}=\frac{\bar{a}}{2\pi N}=\frac{1}{N}T_{\mathbb{R}}\,. \tag{6.87}$$

This turns out to have the same value as in the relativistic version of the Unruh effect, albeit being rescaled by the factor $Ne^{-a\xi}$.

Alternatively, one can interpret (6.87) as the wedge temperature rescaled by N instead of $\sqrt{-g_{00}}$. In hindsight, this is not a surprising result. Indeed, the conversion factor linking the Rindler patch temperature to the observed one on a given hyperbola is nothing else that the rescaling factor between the preferred and the Killing time. In the relativistic case, one can get (6.37) from the wedge temperature just by looking at the proportionality factor between the proper time s of the observer and the Killing time η: on a $\xi = \text{const.}$ hyperbola we have $\mathrm{d}s = \sqrt{-g_{00}}\,\mathrm{d}\eta$, telling us the different rates at which the two times pass. Similarly, if one computes the same quantity for the preferred time τ on the same hyperbola, one gets $u_a \mathrm{d}x^a = N\,\mathrm{d}\eta$. From that, we can directly read the new proportionality factor – corresponding to the lapse N – which we have found in (6.87). Note that, similarly to the relativistic case, on the hyperbola $\xi = 0$, the detector temperature corresponds to the wedge one (6.2).

6.3.2 Response function: the effect of dispersion

In the previous section, we have seen that an accelerated observer will detect particles with a rate determined by T_{UDW}. The scale factor which determines the hyperbola at which the observer is located is given by the lapse function of the foliation, coherently with the choice of the clock for the detector, i.e. the preferred time.

As one may immediately note, the relativistic limit $\Lambda \to \infty$ is quite easy to recover. In that case $\omega_\Lambda \to \sqrt{k^2 + m^2}$ and the response (6.80) can be integrated analitically in ζ, recovering the relativistic result of [145]. With a finite Λ, there is no analytical expression for $\mathfrak{R}$. Moreover, it is possible to show that the relativistic result is not dependent on the range of ζ within which the integral is performed. In our case, this is not true, since the dispersion is sensitive to the time of detection, as we discuss below. This does not spoil the form of T_{UDW} but it changes the response. However, for $k \ll \Lambda$ we should be able to recover the relativistic response, at least approximately. In order to investigate this question, let us define $\mathfrak{A}_k$ as

$$\mathfrak{R} = \int_{-\infty}^{+\infty} \mathfrak{A}_k \mathrm{d}k\,. \tag{6.88}$$

Here $\mathfrak{A}_k$ describes the momentum distribution that determines the rate when integrated over the full k-space. We plotted this quantity evaluated on the central hyperbola for several values of the LV scale Λ in figure 6.4.

As it can be seen, the maximum coincides for all distributions, and in particular with that of the relativistic limit $\Lambda \to \infty$ (in blue). However, while the latter decays monotonically towards larger values of k, the rest of the distributions show an oscillatory tail, connected to the zeros of the Bessel function, that starts earlier for lower values of Λ. This behavior seems to point to the emergence of Lorentz symmetry at low energies. As long as the condition $k \ll \Lambda$ can be trusted, the effect of the Lorentz-violating operators, and thus the oscillatory behavior, can be safely

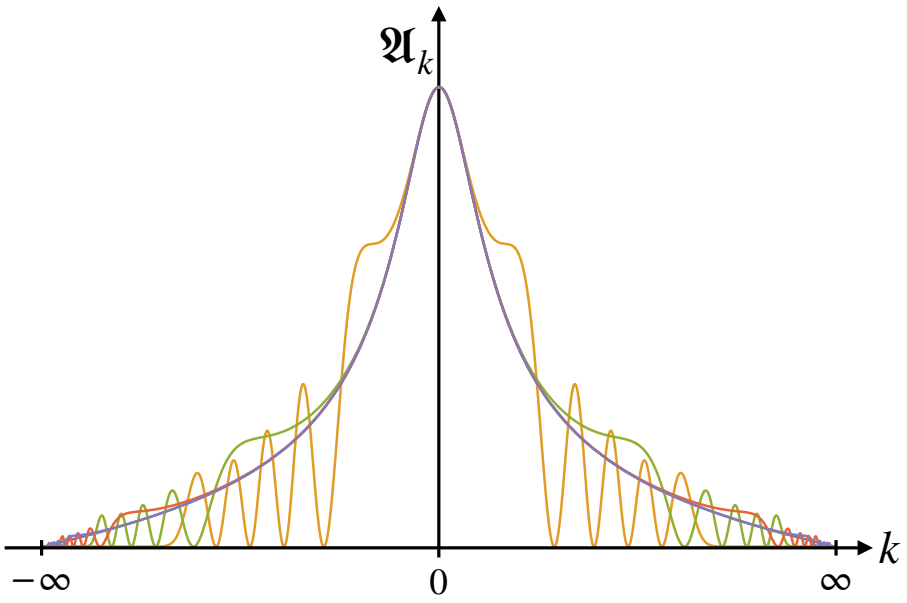

Figure 6.4: The distribution $\mathfrak{A}_k$ in the response function integral $\mathfrak{R}$ for different values of Λ: the Lorentz breaking amplitudes are shown for different values of $\Lambda \in \{10, 10^2, 10^3, 10^4\}$ (in units of $\bar{a}$) in orange, green, red, and purple, while the relativistic result obtained from the integral in [145] is indistinguishable from the purple curve (but shows no oscillations whatsoever). We have set the particular hyperbola for which $a_p = \bar{a}$ for this plot, and identified the mass in the result of [145] to equal m. We have furthermore chosen $m = \bar{a}$.

neglected. Once the approximation breaks down, we start observing modifications in $\mathfrak{A}_k$ that differ from the relativistic case.

Shape of $\mathfrak{A}_k$

To develop a deeper understanding of what happens when Lorentz-symmetry is reinstated, let us discuss the behavior of $\mathfrak{A}_k$ in the non-relativistic case further. First of all, we place the observer onto the hyperbola where $a_p = 1$ for simplicity and rewrite

$$\begin{aligned}\mathfrak{A}_k \propto \int_{-\infty}^{\infty} \mathrm{d}\zeta \, \frac{K_{i\nu}(2\{\omega_\Lambda(k)\cosh(\zeta) - k\sinh(\zeta)\})}{\omega_\Lambda(k)} = \\ \int_{-\infty}^{\infty} \mathrm{d}\zeta \, \frac{K_{i\nu}\big([\omega_\Lambda(k) - k]e^{\zeta} + [\omega_\Lambda(k) + k]e^{-\zeta}\big)}{\omega_\Lambda(k)} \,.\end{aligned} \tag{6.89}$$

Now, with a change of variable $\zeta \to \zeta + \ln(\omega_\Lambda(k) - k)$, which is valid for any $k \in \mathbb{R}$, we get

$$\mathfrak{A}_k \propto \int_{-\infty}^{\infty} \mathrm{d}\zeta \, \frac{K_{i\nu}\big(e^{\zeta} + [\omega_\Lambda^2(k) - k^2]e^{-\zeta}\big)}{\omega_\Lambda(k)} \,. \tag{6.90}$$

Eq. (6.90) is illuminating in several aspects. First of all, it is clear that a relativistic dispersion relation will decouple the ζ-integration and the k-integration in (6.73) as

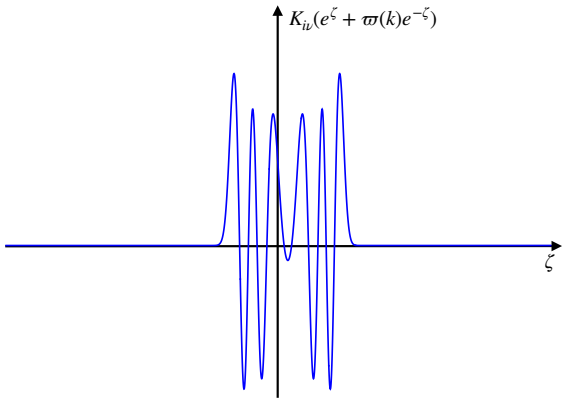

Figure 6.5: Shape of $K_{i\nu}(e^{\zeta} + \varpi(k)e^{-\zeta})$ for $\varpi(k) = 2$ and $\nu = 4\pi$ as a function of ζ

already observed in [145]. Since in the relativistic case we have

$$\mathfrak{A}_k \propto \int_{-\infty}^{\infty} \mathrm{d}\zeta \, \frac{K_{i\nu}\big(e^{\zeta} + m^2 e^{-\zeta}\big)}{\sqrt{k^2 + m^2}} \,, \tag{6.91}$$

where m is the mass of the field, it becomes obvious that the two integrals factorize. Then, the shape of $\mathfrak{A}_k$ will be controlled by the $\sqrt{k^2 + m^2}$ in the denominator. Let us point out that this fact is intimately linked with the boost invariance of the dispersion relation. This can be deduced by noticing that the argument of the Bessel function in (6.89) is just the result of a boost of $(\omega_\Lambda(k), k)$ with rapidity ζ. In [145] it has been shown that a change of variable $k \to k'(k, \zeta)$ in the k-integration of (6.80) while applying the inverse boost, leaves the measure unchanged (so $\mathrm{d}k'/\omega' = \mathrm{d}k/\omega$ for the relativistic case), thus factorizing the ζ- and k-integrals.

Without this symmetry, however, we cannot disentangle the two integrals, since the coefficient $(\omega_\Lambda^2(k) - k^2)$ remains k-dependent. This explains why, for $k = 0$, the relativistic and non relativistic values of $\mathfrak{A}_k$ both give

$$\mathfrak{A}_0 \propto \int_{-\infty}^{\infty} \mathrm{d}\zeta \, \frac{K_{i\nu}\big(e^{\zeta} + m^2 e^{-\zeta}\big)}{m} \,, \tag{6.92}$$

while they depart for other values of k. In other words, in the infrared region, our detector enjoys the same response function regardless of Lorentz-symmetry while high energy measurements differ significantly. In fact, in the deep ultraviolet region, where $k \to \infty$, we notice that the non-relativistic $\mathfrak{A}_k$ is strongly suppressed with respect to the relativistic one. This is a consequence of the ultraviolet behavior of $\omega_\Lambda(k)$. While in the latter case $\omega \propto |k|$ at large k, the former case leads to $\omega \propto |k|^n/\Lambda^{n-1}$, so that $\mathfrak{A}_k$ is suppressed by a power law. Let us define for convenience the quantity

$$\varpi(k) = \omega_\Lambda^2(k) - k^2 \,. \tag{6.93}$$

In the intermediate region, we notice the presence of a finite number of oscillations in the non-relativistic $\mathfrak{A}_k$. Mathematically this can be explained by looking at the shape of $K_{i\nu}(e^{\zeta} + \varpi(k)e^{-\zeta})$ before the ζ-integration, at fixed k, as shown in figure 6.5. There, we observe a finite number of oscillations, while the tails decay very

rapidly[5]. Note that for large values of $\varpi(k)$, the Bessel function stops oscillating [152]. The same happens for the value of the mass, which acts here as an IR regulator effectively cutting-off the distribution at low energies. In particular, since $\varpi(k) = \omega_\Lambda^2(k) - k^2 \geq m^2$, we can show, by computing its minimum, that

$$e^\zeta + \varpi(k)e^{-\zeta} \geq 2\sqrt{\varpi(k)} \geq 2m\,, \tag{6.94}$$

and the number of zeros of $K_{i\nu}$ is governed by m and ΔE. For large values of the mass m, no oscillation is present, and no bumps appear in $\mathfrak{A}_k$.

It should be mentioned that the detector still couples to the aether even in the decoupling limit of the field $\Lambda \to \infty$. Due to this, the previous limit will not impact the value of the temperature in (6.87).

Therefore we observe actually a real thermal spectrum without modifications in the perceived temperature, the only modifications appear in the response function, and additionally the temperature is dictated by the universal horizon's surface gravity. As we shall see, this is an evidence for an existing KMS state within this setup. As explained in Chapter 2, this can be inferred by checking the periodicity of the Euclidean time of the metric. This has been already shown in a very similar fashion in Chapter 5 for the black hole temperature $T_{\rm UH}$.

6.4 Euclidean effective metric and thermal state

Similarly to what we have said in section 5.3.4, in a (1+1) dimensional LV spacetime with a timelike symmetry $\chi = \partial_\eta$, it is possible to build an effective metric that captures the causal structure of the spacetime:

$$g^{(c_f)}_{{\rm eff},ab}\mathrm{d}x^a\mathrm{d}x^b = -\left(u_\eta^2 - \frac{1}{c_f^2}s_\eta^2\right)\mathrm{d}\eta^2 + \left(u_\xi^2 - \frac{1}{c_f^2}s_\xi^2\right)\mathrm{d}\xi^2\,, \tag{6.95}$$

where $c_f = \lim_{|\omega|\to+\infty} c_p$ is the signal velocity, capturing the causality perceived by a field.

When $c_f = +\infty$, the steps of the calculations are the same as the ones performed in Chapter 5, and the Eucliedan version of $g^{(c_f)}_{{\rm eff},ab}$ (i.e. after the complex rotation $\eta \to i\eta$) enjoys a conical singularity solved by a periodicity

$$\beta = \left.\frac{2\pi u_\xi}{\partial_\xi u_\eta}\right|_{\rm UH}, \quad \text{such that} \quad T_{\mathbb{R}} = \left.\frac{\partial_\xi u_\eta}{2\pi u_\xi}\right|_{\rm UH} = \frac{\kappa_{\rm UH}}{\pi} \tag{6.96}$$

providing the wedge temperature. This tells us that the quantization of a field ϕ onto a LV Rindler wedge will describe a thermal state with a temperature $T_{\mathbb{R}}$.

6.4.1 Invitation: EA equations from thermodynamics

Let us conclude this Chapter with some speculative ideas. The derivation of the thermal properties of the Rindler wedge via the effective metric $g^{(c_f)}_{{\rm eff},ab}$ seems to

[5]For large values of the argument, we have $K_{i\nu}(x) \sim e^{-x}/\sqrt{x}$ [151]

suggest that the geometry described by that metric feels the causal properties of a speed-c_f signal in the $\{u, s\}$ frame in a relativistic way. In other words, $g^{(c_f)}_{\text{eff},ab}$ describes the UH as an edge of its null cone, and characterizes it as a Killing horizon.

The similarities are so strong that one may wonder if they can be pushed further. In particular, the effective metric $g^{(c_f)}_{\text{eff},ab}$ can be taken as the true geometry felt by the c_f-speed matter living on the Rindler spacetime. In [14], Jacobson derived the Einstein field equations, by invoking the notion of causality given by the Rindler metric (that can be written also as $g^{(1)}_{\text{eff},ab}$) and the energy flux of the matter content across its (local) Killing horizon.

More explicitly, if $\mathcal{H}$ is the local Killing horizon, defined by the local Killing vector which generates boosts, one has that the Killing energy flowing across generates a heat flow of

$$\delta Q = \int_{\mathcal{H}} T_{ab}\chi^a \mathrm{d}\Sigma^b \,, \tag{6.97}$$

where $\mathrm{d}\Sigma^b$ is the surface element of $\mathcal{H}$. Making the assumption that the variation of the horizon's entropy is given by the variation of its area times a constant α, we have:

$$\mathrm{d}S = \alpha\, \delta\mathcal{A}_{\mathrm{H}} = \alpha \int_{\mathcal{H}} \theta \mathrm{d}\lambda \mathrm{d}\mathcal{A} \tag{6.98}$$

where θ is the expansion of the – affinely parametrized – geodesic tangent to $\mathcal{H}$, determining the variation of the horizon's area [14]. Since matter is in a thermal state, heat and entropy are related by the Clausius relation

$$\delta Q = T_{\mathrm{U}} \mathrm{d}S \,. \tag{6.99}$$

After some algebra and invoking the Raychaudury equation to understand the rate of change of $\mathcal{A}_{\mathrm{H}}$, the Einstein equations comes as a general consequence of the Clausius relation.

As pointed out in Chapter 1, this derivation, and the subsequent refinements to more general cases (see, cf. [153, 154]), is completely agnostic from the gravitational action. Its main ingredients are:

1. A Lorentzian geometry, given by a metric g_{ab}. Any metric can be locally diagonalized to the flat one η_{ab}, choosing the appropriate reference frame (for instance, using Riemann normal coordinates [43]). Therefore it admits a local boost invariance χ in that system of coordinates.

2. The Unruh effect, which tells us that the quantization with respect to the boost invariance gives a thermal character to the Minkowskian vacuum state for matter fields. This encodes a notion of horizon and of the causal structure felt by matter.

3. The assumption that the horizon has an associated entropy defined by its area[6].

[6]This assumption holds for GR, while for more general metric theories, this assumption may have to be adapted [154]

Within these assumptions, one can argue that, in order to respect the thermodynamical equilibrium, the geometry must adjust to compensate the heat flow, following the Clausius relation.

Let us now come back to the LV case, where a notion of preferred time u^a is part of the local geometry, together with g_{ab}. In this case the causality felt by LV matter includes the UH, as emphasized in this Chapter. As we have observed, this horizon comes out automatically if one considers the causality perceived by a a signal travelling at infinite-speed in the preferred frame, namely by $g^{(\infty)}_{\text{eff},ab}$. Remarkably, as shown in section 5.3.4, the UH, which is a spacelike surface if described by the "true" metric g_{ab}, assumes a null characterization from the point of view of $g^{(\infty)}_{\text{eff},ab}$, becoming its Killing horizon. This can easily be explained just by noticing that the effective metric adapts the suprluminal signal to travel on the edges on its causal cone. Most importantly, that metric contains the information about the aether field encoded within itself. We have seen how the thermal character of the quantum matter state could be derived directly form $g^{(\infty)}_{\text{eff},ab}$.

On top of that, previous result has been argued that the UH possesses in fact an entropy, which is proportional to its area [137], pointing towards the formulation of a first thermodynamical law for LV black holes. This feature pushes the analogy with the relativistic case.

In summary: the effective metric $g^{(\infty)}_{\text{eff},ab}$ seems to fit the assumptions behind the Jacobson's derivation. In particular, it is a metric which enjoys the boost invariance, whose Killing horizon defines the boundary of the Rindler wedge. That horizon has an associated temperature, that defines the local matter fields to live in a thermal state. In addition, this horizon seems to have an entropy defined by its area. Given the striking analogy, it is quite tempting to try to ask ourselves if it would be possible to reproduce the EA-field equations just by thermodynamical arguments.

Let us clarify that the discussion of the present section is purely speculative and unfortunately it is not supported by any calculations yet. However, the author of this thesis hopes to be able to tackle this question in the near future.

6.5 Outlook

Let us now sum up the main results of this Chapter. We started from questioning the existence of the Unruh effect without Lorentz invariance. As already explained, this has been a debated topic in the literature, where it has been claimed the breakdown of this effect, while arguing the robustness of its "gravitational counterpart", the Hawking effect [142]. The fact that the Hawking effect can provide an intrinsic scale in the problem – the black hole's surface gravity κ – makes possible to compare it with the UV scale Λ and show the presence of Hawking radiation by Killing horizons for $\kappa \ll \Lambda$. This cannot be done just by considering LV matter fields within the relativistic Rindler wedge. The latter does not provide any intrinsic scale, since the Unruh temperature can always be rescaled to $1/(2\pi)$, forbidding to treat in the same way as the Hawking effect.

Additionally, in Chapter 5, we have proven that the Lorentz-violating version of the black hole radiation is determined through the true causal boundary of the theory, the universal horizon, which is linked to a true thermal emission governed

by its surface gravity, and not by the Killing horizon. This enforces the argument that no true thermality is possible, for LV matter, without a UH. This horizon is clearly absent in the relativistic Rindler patch.

The starting point of our discussion lies exactly here: a new notion of Rindler patch is needed in order for the field to experience the LV causal structure. Inspired by the black hole case we have worked out the unique $(1+1)$, flat, boost invariant, Lorentz violating geometry, solving the equations of motion.

Note that our solution is valid at all times, therefore eternal, and so it is the accelerated observer that we take in the Unruh-De Witt detector part. As in the relativistic case, this cannot correspond to any physical situation, but instead we use this solution as a proxy for the late-time behaviour of the spacetime foliation. In other words, the physical case will be a Minkowskian foliation, which then starts bending, coinciding with our solutions at late times. It is worth mentioning the fact that, an observer-aether coupling can be used in order to make the aether itself to bend (see [155] for a cosmological example), aligning with the observer itself. However, the description of this mechanism goes beyond the scope of our discussion.

Our LV-Rindler wedge does two main things: it provides a bipartition of the Minkowskian manifold in two patches, through the presence of an universal horizon. Secondly, it defines a physical scale, correspondent to the aether acceleration, and defines the wedge temperature $T_{\mathbb{R}} = \bar{a}/(2\pi)$, that now cannot be arbitrarily rescaled, restoring the aforementioned separation of scales.

The LV modes near the UH enjoy a very similar shape with respect to the ones near the black hole horizon in Chapter 5. Therefore, the analytical arguments work the same way, bringing the value for $T_{\mathbb{R}} = \bar{a}/(2\pi)$. The Unruh effect is restored, even without Lorentz invariance.

It is worth mentioning that, in the $(1+1)$ dimensional relativistic massless case, the left- and right-going branches of the modes decouples completely, therefore there is no greybody factor, unlike in the $(3+1)$ dimensional case with the Hawking effect. This can be seen by the conformal structure of the $(1+1)$ spacetime and the conformal invariance of the massless relativistic fields. However, this simplification happens only in this particular case, as pointed out in [147]. In our case, the effect of dispersion is given by the Λ-suppressed term in the matter field equations.

This is clear from the analysis of the Unruh-De Witt detector, made in section 6.3. There we take into account the case of a detector with a monopole coupling. We show that the temperature – defined through the excitation-deexcitation ratio – coincides exactly with the one found with the Bogolyubov coefficients.

However, the detector gives additional hindsights with its response function. First of all, unlike in the relativistic case, the time of detection has a nontrivial impact[7], since the MDR for the Minkowski modes is not invariant under η-translation. Secondly, the sensivitity of the detector to the different frequencies k assumes a peculiar non-relativistic taste: while approaching the GR result at small frequencies, the high-k part of $\mathfrak{A}_k$ has completely different shape, showing a series of bumps, which number is governed by a nontrivial interplay of the detector's energy gap ΔE, the field's mass m and the LV scale Λ. In the far high-k part, $\mathfrak{A}_k$ drops faster

[7]The dependence from Δs is evident from (6.71) that, in our calculation, we send to $+\infty$

than the relativistic case, accordingly to the high-energy behaviour of the dispersion relation $\omega_\Lambda(k) \simeq k^n/\Lambda^{n-1}$ ($n = 2$ in the present Chapter).

The particular shape of $\mathfrak{A}_k$ may also have interesting experimental consequences. In our treatment, we considered a detector which sensitivity is uniform in the whole real line $k \in \mathbb{R}$. However, taking a detector with a different sensitivity, say with some high-energy peaked distribution $P(k)$, will give a completely different outcome with respect to the relativistic case. Moreover, it would be interesting to adapt this calculation to the so-called "circular Unruh effect": a proposal within the analogue setting to measure the Unruh effect in a $(2 + 1)$-dimensional system, for which the accelerated observer follows a circular orbit [156, 157]. This would limit the experimental issues given by the linear acceleration. Our shape of $\mathfrak{A}_k$, will affect the spectrum in case of LV matter that, as we have seen in Chapter 3, is commonplace within analogue systems.

The energy-independent wedge temperature, fixed by the universal horizon, seems to be linked to the causal structure of the spacetime through the imaginary periodicity of η within the effective metric $g^{(\infty)}_{\text{eff},ab}$. This is a strong hint for the KMS structure of the matter quantum state, as emphasized in section 2.4. This would explain, by standard treatment, why we have obtained such a temperature even without Lorentz invariance.

The effective metric turns out to be a nice tool also in order to describe another feature. It is well-known that the wedge temperature is not the actual temperature felt by the observer. In fact, an observer on a specific $\xi = \text{const.}$ hyperbola, will perceive the wedge temperature rescaled by the Tolman factor

$$|\chi| = \sqrt{-g_{00}}. \tag{6.100}$$

In the LV case, the Tolman factor is given by the lapse N, which is constant on any hyperbola, given the symmetries of our Rindler wedge. This, in our treatment, is a clear outcome if one defines the Hamiltonian flow accordingly to the preferred time direction τ. However, this can be interpreted also as the usual Tolman factor $|\chi|$ built with the effective metric $g^{(\infty)}_{\text{eff},ab}$, namely

$$|\chi|^{(\infty)}_{\text{eff}} = \sqrt{-g^{(\infty)}_{\text{eff},00}} = N\,. \tag{6.101}$$

This is quite appealing if one wonders about recovering the relativistic behaviour from our calculation. Intuitively, the speed-c_f signal effectively feels the spacetime described by $g^{(c_f)}_{\text{eff},ab}$. In other words, $g^{(c_f)}_{\text{eff},ab}$ captures the causal structure felt by a matter field which travels at speed c_f in the preferred frame. Since the causal structure is what determines the thermal character of the state, one can imagine to compute the temperature associated to the perturbation of the c_f-speed modes, detected by an accelerated observer. This, for any value of c_f, gives a one-parameter family of Tolman factors

$$|\chi|^{(c_f)}_{\text{eff}} = \sqrt{-g^{(c_f)}_{\text{eff},00}} = \sqrt{u_\eta^2 - \frac{s_\eta^2}{c_f^2}} \tag{6.102}$$

which interpolates between the standard result, with $c_f = 1$ and the EA case where $c_f \to +\infty$. So, even if at first sight the choice of τ in the Hamiltonian flow seems not

continuously connected with the relativistic choice of η[8], the effective metric offers an heuristic way to make this limit in a smooth way.

As a final remark, we emphasize that the rescue of the Unruh effect from the breaking of local Lorentz invariance, gives also the opportunity for further analogies between spacetime and thermodynamics, such as the Jacobson's derivation of the gravitational field equations as equations of state.

[8]Actually, this point has been raised exactly in [39], emphasazing the apparent discontinuity between the choice of η and the choice of τ.

Chapter 7

Towards QG: ultraviolet aspects of Hořava gravity

As a final Chapter, let us conclude our journey talking about quantum gravity. Throughout the previous Chapters, we have analyzed the behaviour of quantum perturbations on top of a classical background. As mentioned in Chapter 1, this treatment is valid in a range of energies well below the QG scale. Namely below the energies at which quantum gravitational perturbations become tangible. However, renormalizability of gravity has to do with the ultraviolet structure of the theory. Indeed, a theory of QG should be under control at any scale and should be able to give theoretical predictions at all the energies at which the experiments are performed.

General relativity is unable to satisfy this theoretical requirement, at least at the perturbative level. The presence of a negative-dimensional coupling $G = M_p^{-2}$ allows for the construction of higher derivative operators in the gravitational Lagrangian that scales in powers of (Gp^2), where p^2 represents the energy of the propagating quantum perturbation. It is possible to show that all these operators appear in a perturbative loop expansion and the number of new divergencies to cure through renormalization increases at every order[1], making the theory to loose predictivity [158–160]. GR as a quantum field theory can be considered only an effective field theory well-below the Planck's energy [161].

In a Lorentz invariant theory, the dimensional analysis of the coupling constants appearing in the Lagrangian is enough to argue renormalizability [159], since every propagator must be a function of Lorentz-invariant quantities, that, at high energy, it means that propagators are function of p^2 only. Knowing the divergence of propagators and the dimension of the couplings, the behaviour of every Feynman diagram can be analyzed in the UV. As explained, the negative mass-dimension of G allows to build infinitely many vertices with higher p^2-scaling, while this is not possible in renormalizable Lorentz-invariant theories, where the couplings are at most dimensionsless (if not even with positive mass-dimension) and no such construction takes place.

An option to cure this problem would be to increase the number of derivatives, leading to quadratic gravity (or, more in general, higher derivative gravity). However, this approach leads to the presence of Ostrogadsky insitabilities, as discussed

[1]This is not true at one-loop for a pure-gravity Lagrangian [7, 8]

in Chapter 4.

Hořava gravity [32] is a ghost-free alternative to this approach. Containing only two temporal derivatives, it allows for perturbations with MDRs, instead of ghosts [107], thus abandoning Lorentz-invariance. As already mentioned, the set of transformation that leaves the theory invariant are the so-called *FDiff* (foliation-preserving diffeomorphisms), that leave untouched the shape of the spacetime foliation. Basically, given our absolute time τ and a set of spatial coordinates $\{x^i\}$, scaling as (4.3), onto a constant-τ leaf Σ we have:

$$FDiff = \{(\tau, x^i) \to (\tilde{\tau}(\tau)\,, \tilde{x}^i(x^j, \tau))\}\,. \tag{7.1}$$

Due to the anisotropic scaling (4.3) between τ and x^i, the spacetime is assumed to have a factorized topology between time and space as in (4.2). Therefore it is convenient to write the theory in the ADM decomposition in the preferred foliation. The dynamical fields are the lapse N, the shift N_i and the spatial metric γ_{ij}. The 4-dimensional line element takes the form [107]

$$\mathrm{d}s^2 = (N^2 - N_i N^i)d\tau^2 - \gamma_{ij}\left(\mathrm{d}x^i + N^i d\tau\right)\left(\mathrm{d}x^j + N^j d\tau\right)\,. \tag{7.2}$$

Under an *FDiff* (7.1), the fields transform as

$$\begin{aligned} N &\to \tilde{N} = \frac{\mathrm{d}\tau}{\mathrm{d}\tilde{\tau}} N\,, \\ N^i &\to \tilde{N}^i = \frac{\mathrm{d}\tau}{\mathrm{d}\tilde{\tau}}\left(N^j \frac{\mathrm{d}\tilde{x}^i}{\mathrm{d}x^j} - \frac{\mathrm{d}\tilde{x}^i}{\mathrm{d}t}\right)\,, \\ \gamma_{ij} &\to \tilde{\gamma}_{ij} = \gamma_{kl} \frac{\mathrm{d}x^k}{\mathrm{d}\tilde{x}^i} \frac{\mathrm{d}x^l}{\mathrm{d}\tilde{x}^j}\,. \end{aligned} \tag{7.3}$$

In the rest of the Chapter, we will discuss HG from the point of view of a QFT. We will review the state of art, and we will make some speculation on the further developments. Technical details will be sometimes omitted, being not instructive for the purpose of this treatment, in order to give priority to a physical understanding of the situation. Let us now see how the theory is formulated, at the Lagrangian level.

Notation of this Chapter

Within this chapter, and solely for this one, we are going to adapt the following notations:

- The signature of the metric is the one commonly used in particle physics, namely the mostly minus. I.e. the 4-dimensional flat spacetime will be identified by the Minkowski metric $\eta = \mathrm{diag}(+,-,-,-)$ as we already did in (7.2).
- The indices $(i, j, k, l \dots)$ will identify the spatial directions, unless differently specified
- The Riemann tensor R_{ijkl}, the Ricci tensor R_{ij} and the Ricci scalar R will be the ones built with the spatial metric γ_{ij}, namely only the spatial ones, unless differently specified.

7.1 Lagrangian formulation

The Lagrangian formulation of the theory proposed in [32] involves the objects which transform covariantly under (7.3). The kinetic term can be built with the extrinsic curvature K_{ij}

$$K_{ij} = \frac{1}{2}\mathrm{D}_t\gamma_{ij} = \frac{\dot{\gamma}_{ij} - 2\nabla_{(i}N_{j)}}{2N} \tag{7.4}$$

where we defined a "covariant time derivative" [162]

$$\mathrm{D}_t := \frac{1}{N}\left(\partial_t - \mathcal{L}_{N^i}\right) . \tag{7.5}$$

One can see from (7.4) that the terms built with K_{ij} contain time derivatives. Therefore a generic kinetic term up to 2 time derivatives takes the form:

$$\mathcal{L}_{\mathrm{kin}} = \frac{1}{16\pi G}\left(K^{ij}K_{ij} - \lambda K^2\right) , \tag{7.6}$$

where λ is a dimensionless coupling and $K = K^i_i$.

Besides the kinetic part, the most generic Lagrangian compatible with (7.3) contains all the terms allowed with the symmetry. In general, we have, in d spatial dimensions

$$\mathcal{S}_{\mathrm{HG}} = \frac{1}{16\pi G}\int_{\mathcal{M}} N\mathrm{d}\tau\,\sqrt{|\gamma|}\mathrm{d}^dx\,\left(K^{ij}K_{ij} - \lambda K^2 - \mathcal{V}\right) . \tag{7.7}$$

The shape of the potential $\mathcal{V}$ depends on d [107], but in general it contains all the possible terms without time derivatives. The case

$$\lambda = 1 \quad \text{and} \quad \mathcal{V} = R - 2\Lambda\,, \tag{7.8}$$

corresponds to the ADM decomposition of the Einstein-Hilbert action [106]. Looking at equation (7.7), one can immediately see that, given the different scaling dimensions of τ and x^i:

$$[\tau] = d\,, \qquad [x^i] = 1\,, \tag{7.9}$$

and the corresponding one for the fields:

$$[\gamma_{ij}] = 0\,, \qquad [N_i] = d - 1\,, \qquad [N] = 0 \tag{7.10}$$

the coupling G becomes dimensionsless

$$[G] = 0\,. \tag{7.11}$$

In the original proposal [32], the potential $\mathcal{V}$ was taken to contain only the possible contraction made with the spatial Riemann tensor R_{ijkl} up the the scaling dimensions of $2d$. The number of possible terms increases as one increases d.

In [163, 164], it was recognized that, if $\mathcal{V}$ is built only with the spatial Riemann tensor, the infrared behaviour of perturbations around flat spacetime contains an

unstable scalar mode. A "healthy" version of the theory can be build considering the co-vector

$$a_i = \nabla_i \log(N)\,, \tag{7.12}$$

which transforms covariantly with respect to (7.1) and adding it to the Lagrangian. Note that, inserting the aether vector field u^a with a Stückelberg trick, the vector a^i corresponds exactly to its acceleration.

In particular, the lowest energy term containing two derivatives

$$\alpha a_i a^i\,, \tag{7.13}$$

is needed to ensure a low-energy well-behaved dispersion relation for the perturbations [163]. Specifically, it is possible to show that, without such a term, recovering GR at low energies is not possible [116][2].

With such a potential $\mathcal{V}$ one can compute the superficial degree of divergence for an L-loop Feynman diagram, which is:

$$D_g = 2d - 2L[G] = 2d\,. \tag{7.14}$$

The theory with $[G] = 0$ is therefore power-counting renormalizable because the counterterms will affect operators with scaling dimensions up to $2d$ [107].

7.1.1 Projectable HG

The symmetries of HG allow for a simplified version of the theory, called *projectable HG*. That is defined by the requirement that the lapse function N will depend only on the preferred time τ

$$N = N(\tau)\,. \tag{7.15}$$

This automatically implies that the acceleration a_i vanishes[3]. This fact, for the previous discussion tells us that this projectable version possesses infrared instabilities, thus not phenomenologically viable [116]. However, condition (7.15) serves as a great simplification of the theory. This simplified treatment allows for impressive results that render the projectable version of HG worth mentioning.

The projectable condition (7.15) allows to fix $N = 1$ with an appropriate rescaling of time, so that the action become

$$\mathcal{S}_{\rm pHG} = \frac{1}{16\pi G}\int_{\mathcal{M}} \mathrm{d}\tau \mathrm{d}^d x\, \sqrt{|\gamma|}\left(K^{ij}K_{ij} - \lambda K^2 - \mathcal{V}\right)\,. \tag{7.16}$$

where $\mathcal{V}$ is now an expression built only with the Riemann tensor R_{ijkl}. Note that if $d = 3$, $\mathcal{V}$ can be built with the Ricci tensor R_{ij} alone and in $d = 2$ there is only the Ricci scalar R.

[2]To be precise, in [116] it has been shown that one never recovers GR, because a small amount of Lorentz violation is always present. However, with "recover GR" we mean having an approximation reproducing the same phenomenology

[3]The careful reader will note that this condition implies that there is no solution within the projectable branch of HG which can describe a stationary black hole in the sense of Chapter 4. This is evident from the UH definition (6.25).

The theory enjoys two propagating degrees of freedom: a scalar mode and the usual transverse-traceless mode that also characterizes general relativity. In $d = 3$, their UV behaviour is well-defined (i.e. ghost-free) if [163]

$$\frac{3\lambda - 1}{1 - \lambda} > 0\,. \tag{7.17}$$

These modes show a dispersion relation of the form [107, 165]:

$$\begin{aligned} \omega_{TT}^2 &= \eta k^2 + \mu_2 k^4 + \nu_5 k^6\,, \\ \omega_S^2 &= \frac{1-\lambda}{1-3\lambda}(-\eta k^2 + (8\mu_1 + 3\mu_2)k^4 + (8\nu_4 + 3\nu_5)k^6)\,. \end{aligned} \tag{7.18}$$

where the labels "TT" and "S" refer to the transverse-traceless and scalar mode, respectively, and η, μ_1, μ_2, ν_4 e ν_5 are couplings contained in $\mathcal{V}$ which refers to the interactions:

$$-\eta R\,, \quad \mu_1 R^2\,, \quad \mu_2 R_{ij}R^{ij}\,, \quad \nu_4 \nabla_i R \nabla^i R\,, \quad \nu_5 \nabla_i R_{jk} \nabla^i R^{jk}\,. \tag{7.19}$$

From (7.18) one can immediately see the problem of a vanishing a_i. Setting $\eta > 0$ in order to recover the relativistic behaviour of the TT-mode, implies that the infrared dispersion relation for the S-mode defines an imaginary sound speed [163, 164]

$$c_S^2 = -\eta \frac{\lambda - 1}{3\lambda - 1} < 0\,, \tag{7.20}$$

which is the source of the instability.

7.1.2 Non-projectable HG

The non-projectable version of HG is the general version of the theory. The lapse function is allowed to have a spatial-dependence

$$N = N(\tau, x^i) \tag{7.21}$$

and it cannot be gauged away by fixing the time reparametrization. The spatial-dependence generically implies a non-vanishing acceleration a^i. The action reads

$$\mathcal{S}_{\text{npHG}} = \frac{1}{16\pi G} \int_{\mathcal{M}} \mathrm{d}\tau \mathrm{d}^d x\, N \sqrt{|\gamma|} \left(K^{ij} K_{ij} - \lambda K^2 - \mathcal{V} \right)\,. \tag{7.22}$$

The potential at low energy – i.e. at the lowest order in spatial derivatives – contains the two terms

$$\mathcal{V} = \eta R + \alpha a_i a^i + \text{higher orders}\,. \tag{7.23}$$

The low-energy interaction modifies the infrared behaviour of the propagating modes [107, 163, 165][4]:

$$\begin{aligned} \omega_{\text{TT}}^2 &= k^2 + \mathcal{O}(k^4)\,, \\ \omega_{\text{S}}^2 &= \frac{1-\lambda}{1-3\lambda}\left(\frac{2}{\alpha} - 1\right) k^2 + \mathcal{O}(k^4)\,. \end{aligned} \tag{7.24}$$

[4]Here we have set $\eta = 1$ for simplicity. This, in pure gravity is always possible up to a spatial rescaling.

which now represent a stable perturbation if

$$0 < \alpha < 2\,. \tag{7.25}$$

Note that the limit in which the projectable case is recovered is $\alpha \to \infty$, in order to decouple the lapse perturbations from the Lagrangian.

Noticeably, the phenomenology of non-projectable HG predicts analogous results to the low energy GR, recovering the Newton's law with gravitational constant [163]

$$G_N = \frac{1}{8\pi M_p^2(1-\alpha/2)}\,, \tag{7.26}$$

where G_N is the effective Newton's constant, determining the low-energy gravitational potential, and M_p is the Planck mass.

7.2 Towards renormalization: HG in the UV

Now that we have settled down the Lagrangian formulation of the theory, it is time to talk about renormalizability. It is important to stress that, unlike the Lorentz-invariant cases, in HG the perturbative renormalizability cannot be argued directly from the dimensions of the coupling constants.

In presence of Lorentz symmetry, the dependence of the propagators from the momenta can take place only thorugh the 4-dimensional modulus squared of the 4-momentum $p_a p^a = p^2 = \omega^2 - k^2$. This fact, together with the scaling of the vertices, allows to infer pertubative renromalizability if the couplings have positive mass dimensions or if they are dimensionless [159, 160].

This argument, which is based on the scaling of the propagators in the UV, seems to be applicable also in Hořava gravity. The HG propagators for the perturbations scales in the ultraviolet as ω^{-2} or, equivalently k^{-2d}. What forbids us to recycle the same Lorentz-invariant argument is that, due to the time-space separation, propagators in HG may occur in the form

$$D(\omega,k) \sim \frac{1}{\omega^2}\,, \quad \text{or} \quad D(\omega,k) \sim \frac{1}{k^{2d}}\,. \tag{7.27}$$

The suppression of the propagators only in the frequency ω or in the momentum k, even if ensures the right scaling of the propagator, generates non-local divergencies either along all the time axis or a spatial leaf. Namely, the inverse Fourier transform of ω^{-2} gives [107, 166]

$$\frac{1}{\omega^2} \xrightarrow{\mathcal{F}^{-1}} |\tau|\delta^d(\mathbf{x})\,, \tag{7.28}$$

which is divergent at all-times. The problem of renormalizability of HG can be then reformulated in the problem of how to treat these non-local divergencies.

7.2.1 Renormalizability of the projectable case

With no small suprise, in 2016, Barvinski and collaborators managed to tame the projectable version of the theory, showing its perturvative renormalizability [166] and, immediately after, its asymptotic freedom behaviour in the $(2+1)$-dimensional case [167].

The key point of their treatment, was to find a way to get rid of those non-local terms, by choosing the appropriate way to gauge-fix the spatial diffeomorphisms – while the time-reparametrization invariance has beeen used to identify $N = 1$ – in the Lagrangian (7.16).

In the projectable case only one of the two possible irregular behaviours (7.27) – the $D \sim \omega^{-2}$ one – arises. Expanding the perturbation at the quadratic level around a background $\{\tilde{\gamma}_{ij}, \tilde{N}_i\}$:

$$\gamma_{ij} = \tilde{\gamma}_{ij} + h_{ij}\,, \qquad N_i = \tilde{N}_i + n_i\,, \tag{7.29}$$

such that

$$\tilde{\mathrm{D}}_t := \partial_t - \mathcal{L}_{\tilde{N}^i}\,. \tag{7.30}$$

From the structure of the kinetic term $K_{ij}K^{ij} - \lambda K^2$ we see that the quadratic Lagrangian (that is the Lagrangian at the quadratic level in the perturbations n_i and h_{ij}) contains the term [107, 166]

$$\tilde{\mathrm{D}}_t n_i \partial_j h^{ij}\,. \tag{7.31}$$

This term, when computing the propagators, is responsible for the irregular one, which in turn appears in the $\langle hh \rangle$ part, as we shall see.

Case $d = 2$

Let us, for the following calculations, specialize to $d = 2$ in order to simplify the treatment. In this case we have [166]:

$$\langle h_{ij} h_{kl} \rangle = (\delta_{ik}\delta_{jl} + \delta_{il}\delta_{jk} - 2\delta_{ij}\delta_{kl})\,\frac{16\pi i G}{\omega^2} + \text{regular propagators}\,. \tag{7.32}$$

So, we see the $1/\omega^2$ irregular behaviour.

The way out to solve this issue has been found in [166] when the authors realized that there was possible to fix the gauge of the spatial dieffeomorphisms

$$x^i \to \tilde{x}^i(\tau, x^j) \tag{7.33}$$

in such a way to get rid of the term (7.31) in the gauge-fixed Lagrangian. The gauge fixing condition F_i is a vector and must scale homogenously [166]. If we want it to include the term $\tilde{\mathrm{D}}_t n_i$, which scales as:

$$[\tilde{\mathrm{D}}_t n_i] = 2d - 1 = 3 \tag{7.34}$$

we will have to add h-terms with three spatial derivatives. Therefore we have to consider a possible contraction of the tensor $\tilde{\nabla}_i \tilde{\nabla}_j \tilde{\nabla}_k h_{lm}$. The n_i-h_{ij} terms (7.31)

come from the kinetic part of the Lagrangian in which h_{ij} appears through the combination

$$\tilde{\nabla}_k h^k_j - \lambda \tilde{\nabla}_j h \,. \tag{7.35}$$

So, in order to cancel those terms, we need F_i to contain h_{ij} through (7.35). Therefore, we need to construct F_i by suitably applying a generic operator with two $\tilde{\nabla}_i$ to (7.35). In particular we can parametrize it with

$$\mathcal{O}_{ij} = \tilde{\gamma}_{ij}\tilde{\Delta} + \xi \tilde{\nabla}_i \tilde{\nabla}_j \tag{7.36}$$

where ξ is a gauge parameter. The gauge-fixing condition F_i, which is required to scale homogeneously, thus become [166]

$$F_i = \tilde{\mathrm{D}}_t n_i + \frac{1}{2\sigma}\mathcal{O}_{ij}\left(\tilde{\nabla}_k h^{kj} - \lambda \tilde{\nabla}^j h\right) , \tag{7.37}$$

and σ is a second gauge parameter. The turning point with respect to the usual treatment in the gauge fixing procedure, was to recognize that the gauge-fixing Lagrangian $\mathcal{L}_{\mathrm{gf}}$ can be generically written as a quadratic form of F_i which is not necessarily given by $F_i F^i$. Actually, the gauge-fixing term that regularize the propagators is given by [166, 167]

$$\mathcal{L}_{\mathrm{gf}} = \frac{\sigma}{2G}\sqrt{\tilde{\gamma}}\, F^i (\mathcal{O}^{-1})_{ij} F^j \tag{7.38}$$

where $\mathcal{O}^{-1}$ is given by the inverse of (7.36). The resulting $\mathcal{L}_{\mathrm{gf}}$ is then

$$\begin{aligned}\mathcal{L}_{\mathrm{gf}} =& \frac{\sigma}{2G}\sqrt{\tilde{\gamma}}\Bigg[\tilde{D}_t n^i (\mathcal{O}^{-1})_{ij}\tilde{D}_t n^i + \frac{(\tilde{D}_t n^i)(\tilde{\nabla}_k h^k_i - \lambda\tilde{\nabla}_i h)}{\sigma} + \\ & \frac{(\tilde{\nabla}_k h^k_i - \lambda\tilde{\nabla}_i h)\mathcal{O}^{ij}(\tilde{\nabla}_l h^l_j - \lambda\tilde{\nabla}_j h)}{4\sigma^2}\Bigg] .\end{aligned} \tag{7.39}$$

The second term in (7.39) exactly compensates for (7.31) in the original action. At first sight, this gauge fixing procedure introduce a non-local term given by

$$\tilde{D}_t n^i (\mathcal{O}^{-1})_{ij}\tilde{D}_t n^i \,. \tag{7.40}$$

However, one can get rid of it just by introducing an auxiliary field π^i – a sort of conjugated variable to n_i – and "integrate it in" in the path integral [166, 167]:

$$\begin{aligned}&\exp\left[i\int \mathrm{d}^2x\mathrm{d}\tau\sqrt{\tilde{\gamma}}\,\frac{\sigma}{2G}\tilde{D}_t n^i (\mathcal{O}^{-1})_{ij}\tilde{D}_t n^i\right] \\ &\propto \int \mathcal{D}[\pi]\exp\left[i\int \mathrm{d}^2x\mathrm{d}\tau\sqrt{\tilde{\gamma}}\,\left(-\frac{G}{2\sigma}\pi_i\mathcal{O}^{ij}\pi_j + \pi_i\tilde{D}_t n^i\right)\right] ,\end{aligned} \tag{7.41}$$

where we have used the following identity for Gaussian functional integrals [160]:

$$\int \mathcal{D}[\phi]\exp\left[\frac{i}{2}\phi^T\cdot A\cdot\phi + iJ\cdot\phi\right] \propto (\det(A))^{-1/2}\exp\left[-\frac{i}{2}J\cdot A^{-1}\cdot J\right] \tag{7.42}$$

for a generic matrix A_{ij} and vectors ϕ^i and J^i. therefore, we end up with a local gauge fixing term in the action which is:

$$\begin{aligned}\mathcal{L}_{\rm gf} = \frac{\sigma}{2G}\sqrt{\tilde{\gamma}}\Bigg[-\frac{G^2}{\sigma^2}\left(\pi^i\tilde{\Delta}\pi_i + \xi\pi^i\tilde{\nabla}_i\tilde{\nabla}_j\pi^j\right) + \frac{2G}{\sigma}\pi^i(\tilde{D}_t n_i) + \\ \frac{(\tilde{D}_t n_i)(\tilde{\nabla}_j h^{ij} - \lambda\tilde{\nabla}^i h)}{\sigma} + \frac{\tilde{\nabla}_k h^{ik} - \lambda\tilde{\nabla}_i h}{4\sigma^2}\times \\ \times\left(\tilde{\Delta}(\tilde{\nabla}_j h_i^j - \lambda\tilde{\nabla}^i h) + \xi\tilde{\nabla}_i\tilde{\nabla}_j(\tilde{\nabla}_l h^{jl} - \lambda\tilde{\nabla}^j h)\right)\Bigg].\end{aligned} \tag{7.43}$$

As usual, after having fixed the gauge, we get a couple of Faddeev-Popov ghosts [159, 160], namely a couple of anti-commuting vectors c_i and $\bar{c}_i$, which enters the action through [166]

$$\begin{aligned}\mathcal{L}_{\rm gh} = \frac{\sqrt{\tilde{\gamma}}}{G}\Bigg[- \tilde{D}_t\bar{c}^i\tilde{D}_t c_i - \bar{c}^i\Bigg(-\frac{1}{2\sigma}(\tilde{\Delta}^2 c_i + \tilde{\Delta}\tilde{\nabla}_k\tilde{\nabla}_i c^k - 2\lambda\tilde{\Delta}\tilde{\nabla}_i\tilde{\nabla}_k c^k \\ + \xi(\tilde{\nabla}_i\tilde{\nabla}_k\tilde{\Delta}c^k + \tilde{\nabla}_i\tilde{\nabla}_j\tilde{\nabla}_k\tilde{\nabla}^j c^k - 2\lambda\tilde{\nabla}_i\tilde{\Delta}\tilde{\nabla}_k c^k)\Bigg)\Bigg].\end{aligned} \tag{7.44}$$

All the resulting propagator are regular, therefore the theory results perturbatively renormalizable via standard arguments, also in $d = 3$[5], showing that all the divergencies (which now are local) can be reabsorbed into the terms already contained in (7.16), see cf. [166].

This result is of great importance if one thinks to that in this way: the projectable version of HG is an ultraviolet complete quantum theory of gravity! Given the scarcity of QG theories, this statement is quite remarkable.

However, as we already explained, this QG candidate is not in agreement with the phenomenology at low energies. At high energy, as already mentioned, the case $d = 2$ has been show to be asymptotically free [167].

7.2.2 Non projectable case: constraints

In the same work where the projectable version of the theory has been proved to be perturbatively renormalizable, it has been pointed out that the non projectable case hides additional subtleties. Even if the gauge-fixing of the spatial diffeomorphism can be done the same way as in the projectable version, problems arise with the time-reparametrization invariance.

At current times, the problem is mathematically understood within the Hamiltonian formalism. The spatial-dieffeomorphism invariance, which we discussed in the projectable case, corresponds, in a canonical approach to the quantization of the theory, to a first-class constraint. First-class constraint can be usually identified with the generator of the gauge symmetries in the Lagrangian formalism [168].

[5] In the case $d = 3$ we have to take $\mathcal{O}_{ij}$ of the form:

$$\mathcal{O}_{ij} = \tilde{\Delta}\left(\tilde{\gamma}_{ij}\tilde{\Delta} + \xi\tilde{\nabla}_i\tilde{\nabla}_j\right). \tag{7.45}$$

However, the implementation within the Lagrangian formalism of the second-class ones is less clear. The quantization of a second-class constraint necessities of Dirac brackets and an adapted formalism developed by Batalin, Vilkovisky, Fradkin and Fradkina [169–171], known as Batalin-Fradkin-Vilkovisky (BFV) quantization. This formalism seems to fit the implementation of the second-class constraint of HG [172, 173]. Let us briefly describe it.

Hamiltonian formalism

Within the Hamiltonian formalism we associate to each field its conjugated variable, forming the couples (N, π_N), (N_i, π_i) and (γ_{ij}, π_{ij}). Following [173], the second-class constraints are

$$\theta_1 = N\mathcal{H}_0 - \nabla_i \left(\sqrt{\gamma} N \frac{\delta \mathcal{V}}{\delta a_i} \right) = 0 \,, \qquad \theta_2 = \pi_N = 0 \,, \tag{7.46}$$

where $\mathcal{H}_0$ is the classical Hamiltonian defined as the Legendre transform of the Lagrangian

$$\pi^A \Phi_A - \mathcal{L} = \mathcal{H}_0 = \left(\frac{\pi_{ij}\pi^{ij}}{\gamma} + \bar{\sigma}\frac{\pi^2}{\gamma} + \mathcal{V} \right) \tag{7.47}$$

where Φ_A represents the fields and π_A the corresponding conjugated momenta. The unique first class constraint is

$$\mathcal{H}_i = -2\gamma_{ij}\nabla_k \pi^{jk} = 0 \,. \tag{7.48}$$

The implementation of the second-class constraint in the BFV formalism leads to the construction of the following path integral [173]:

$$Z = \int \mathcal{D}[\phi_A] \delta(\theta_1)\delta(\theta_2) \det\{\theta_1, \theta_2\} \exp\left[i \int \mathcal{L} \right] , \tag{7.49}$$

where ϕ_A serves as a proxy for all the fields and their conjugated momenta, $\{\theta_1, \theta_2\}$ is the Poisson bracket between the second-class constraints and $\mathcal{L}$ is the Lagrangian density already implemented with the spatial-diffeomorphism gauge fixing (namely with the first-class constraint). Note that, since $\theta_2 = \pi_N$ we have

$$\{\theta_1, \theta_2\} = \frac{\delta \theta_1}{\delta N} \,. \tag{7.50}$$

This has a clear intuitive meaning in terms of functional integral measure. The vanishing of the second class constraint restricts the space of configurations available for N. Namely, let us assume that $\bar{N}$ is a root of the equation $\theta_1 = 0$[6]. Then, we can rewrite:

$$\delta(\theta_1) = \frac{\delta(N - \bar{N})}{\det \frac{\delta \theta_1}{\delta N}|_{\theta_1 = 0}} \,. \tag{7.51}$$

[6]Here, we assume also that the solution $\bar{N}$ is unique, for simplicity

Therefore, the implementation of the constraint through the combination

$$\delta(\theta_1)\det\{\theta_1,\theta_2\} = \delta(N-\bar{N}) \tag{7.52}$$

should be equivalent to integrate over only the configurations of the lapse which solve $\theta_1 = 0$. One can implement the constraints adding auxiliary fields in (7.49), namely a Lagrange multiplier $\mathcal{A}$ and a couple of Grassmann variables $(\bar{\eta},\eta)$ so that [173]:

$$\delta(\theta_1)\det\{\theta_1,\theta_2\} \propto \int \mathcal{D}[\mathcal{A}]\mathcal{D}[\bar{\eta}\eta]\,\exp\left[i\int\left(\mathcal{A}\theta_1 - \bar{\eta}\frac{\delta\theta_1}{\delta N}\eta\right)\right], \tag{7.53}$$

while the other second class constraint – $\pi_N = 0$ – can be implemented directly in $\mathcal{L}$ setting to 0 the conjugated momentum to N. At this point, one remains with local operators involving the fields $\{N, N_i, \pi_i, \gamma_{ij}, \pi_{ij}, c_i, \bar{c}_i, \mathcal{P}_i, \bar{\mathcal{P}}_i, \mathcal{A}, \bar{\eta}, \eta\}$, where c_i and $\bar{c}_i$ are the ghosts given from the spatial-diffeomorphism gauge-fixing and the couple $(\mathcal{P}_i, \bar{\mathcal{P}}_i)$ represents their conjugated momenta. It is then clear that this approach, involving 12 fields, will be computationally quite involved.

Note that this implementation of the constraint, understood as a sort of "equation of motion" for the lapse N, implies to solve $\theta_1 = 0$ at some fixed time and then preserve it with a Lagrange multiplier at all times and it was already suggested in earlier studies on the Hamiltonian structure of the theory in [174].

7.2.3 Non projectable case: Lagrangian formulation

Although referring to very preliminary and speculative results, we can try to reformulate the problem within a Lagrangian approach. The advantage of the Hamiltonian formalism is to make us understand which field configurations for N have to be taken into account in the path integral. On the other hand, working in the Hamiltonian approach means to face an action containing more fields and interaction with respect to the ones given within the Lagrangian formulation. Therefore, it is worth trying to understand if we can reformulate the problem in this latter setting.

A first trial would be to consider the Lagrangian with the direct implementation of the constraints, through a Lagrange multiplier as in equation (7.53). In this way we take the action (7.22), armed with the gauge-fixing terms of the spatial-diffeos and we consider a total Lagrangian:

$$\mathcal{L}_{\rm tot} = \mathcal{L}_{\rm npHG} + \mathcal{L}_{\rm gf} + \mathcal{L}_{\rm gh} + \mathcal{A}\theta_1 - \bar{\eta}\frac{\delta\theta_1}{\delta N}\eta\,. \tag{7.54}$$

The path integral is given by

$$Z = \int \mathcal{D}[\Phi_A]\exp\left[i\int\mathcal{L}_{\rm tot}\right], \tag{7.55}$$

where $\{\Phi_A\} = \{N, N_i, \gamma_{ij}, \pi_i, c_i, \bar{c}_i, \mathcal{A}, \eta, \bar{\eta}\}$ and π_i is the auxiliary field introduced in (7.41) in order to make the gauge-fixing Lagrangian local. Note that the resulting $\mathcal{L}_{\rm tot}$ is local Lagrangian where we have implemented the constraint θ_1. So, in principle it is possible to proceed with the usual calculation of diagrams.

Irregular propagators

Let us take the same $d = 2$ case as we did for the projectable case. The potential in this case reads [173]:

$$\begin{aligned}\mathcal{V} = &- \beta R - \alpha a^2 + \mu_1 R^2 + \mu_2 a^4 + \mu_3 a^2 R + \mu_4 a^2 \nabla_i a^i \\ &+ \mu_5 R \nabla_i a^i + \mu_6 \nabla_i a^j \nabla^i a_j + \mu_7 (\nabla_i a^i)^2\end{aligned} \tag{7.56}$$

In order to compute propagators we expand around a flat background, namely

$$N = 1 + n\,, \qquad N_i = 0 + n_i\,, \qquad \gamma_{ij} = \delta_{ij} + h_{ij}\,, \tag{7.57}$$

and all the other fields already represents perturbations, having a vanishing classical value. The quadratic Lagrangian in the $\xi\sigma$-gauge $\mathcal{L}^{(2)}_{\text{flat}}$ is:

$$\begin{aligned}\mathcal{L}^{(2)}_{\text{flat}} = &-\frac{\mu_{67}}{2G} n \Delta^2 n - \frac{1-2\lambda}{4G} N^i \partial_{ij} N^j - \frac{1}{4G} N^i \Delta N_i + \frac{1}{8G} \dot{h}_{ij} \dot{H}^{ij} \\ &- \frac{\lambda}{8G} \dot{h}^2 + \dot{N}_i \pi^i - \frac{G\xi}{2\sigma} \pi^i \partial_{ij} \pi^j - \frac{G}{2\sigma} \pi^i \Delta \pi_i - \frac{1}{2G} \frac{1}{\sigma} \bar{c}^i (\Delta^2 c_i - \Delta \partial_i \partial_j c_j) \\ &+ \frac{\lambda\xi}{4G\sigma} h^{ij} \partial_{ij} \Delta h - \frac{\xi}{8G\sigma} h^{ij} \partial_{ijkl} h^{kl} - \frac{\lambda^2 \xi}{8G\sigma} h \Delta^2 h - \frac{1}{8G\sigma} h^{ij} \partial_{jk} \Delta h^k_i \\ &- \frac{\mu_1}{2G} h^{ij} \partial_{ijkl} h^{kl} + \frac{\lambda}{4G\sigma} h^{ij} \partial_{ij} \Delta h + \frac{\mu_1}{G} h^{ij} \partial_{ij} \Delta h - \frac{\mu_1}{2G} h \Delta^2 h \\ &- \frac{\lambda^2}{8G\sigma} h \Delta^2 h + \frac{\mu_5}{2G} n (\Delta^2 h - \Delta \partial_{ij} h^{ij}) + \frac{\mu_5}{2G} \mathcal{A} (\partial_{ij} \Delta h^{ij} - \Delta^2 h) \\ &+ \frac{\mu_{67}}{G} \mathcal{A} \Delta^2 n - \frac{\mu_{67}}{G} \bar{\eta} \Delta^2 \eta + \frac{1}{G} \dot{\bar{c}}^i \dot{c}_i - \frac{1}{G} \frac{(1+\xi)(1-\lambda)}{\sigma} \bar{c}^i \partial_{ij} \Delta c^j\,,\end{aligned} \tag{7.58}$$

where the notation $\partial_{ij} = \partial_i \partial_j$ and similarly for more indices. From the quadratic Lagrangian we can compute the propagators in flat spacetime. Using our compact notation for the fields, we can write generically

$$\mathcal{L}^{(2)}_{\text{flat}} = \frac{1}{2} \Phi_A O^{AB} \Phi_B \tag{7.59}$$

and the propagators are simply given by the inverse matrix $D_{AB} = O^{-1}_{AB}$ (see cf. [159, 160]).

The form of the propagators consists in a series of quite long expressions. The important part to notice is the presence of irregular propagators involving n, $\mathcal{A}$, η and $\bar{\eta}$, namely, in Fourier space:

$$\langle n\mathcal{A} \rangle = \langle \mathcal{A}\mathcal{A} \rangle = \frac{iG}{(\mu_6 + \mu_7) k^4} = \langle \bar{\eta}\eta \rangle = -\langle \eta\bar{\eta} \rangle\,, \tag{7.60}$$

which exactly corresponds to the type of divergence reported in (7.27). Note that this result, derived in the Lagrangian context, matches the one of [173, 175].

It is clear that these irregular propagators arise together with the implementation of the constraint, involving $\mathcal{A}$, η and $\bar{\eta}$. In principle, as already explained, they may spoil the perturbative renormalizability, leading to non-local counterterms. However, this does not seem to be the case for HG. Let us see how.

7.2.4 Non projectable case: cancellation of non-localities

Even if it is true that irregular propagators arise from the calculations, the shape with which they come into the game it is not casual. In particular, remarkably we have

$$\langle n\mathcal{A}\rangle = \langle \mathcal{A}\mathcal{A}\rangle = \langle \bar{\eta}\eta\rangle. \tag{7.61}$$

This symmetric behaviour reflects inevitably on the diagrammatic computation. At one-loop this can be seen explicitly. Let us make an example, following what has been done in the projectable case [167]. In order to compute the running of the coupling constants we have to choose a non-trivial background and treat it as a classical source in the loops. In our case, let us pick the flat background with some non-trivial background shift

$$\gamma_{ij} = \delta_{ij} + h_{ij}\,, \qquad N = 1 + n \qquad N_i = \bar{N}_i + n_i\,. \tag{7.62}$$

Expanding the Lagrangian at the quadratic order in the perturbation and considering the interaction with the classical source $\bar{N}_i$, we get the Feynman rules for the vertices. In particular, working with a non-trivial background shift vector allows for the computation of the running of G and λ. However, for our discussion here we just need to specify the interaction terms that generates diagrams with irregular propagators, since the complete expression for the Lagrangian is extremely long and not particularly instructive for what regards this section. Let us assign a graphic notation to each field:

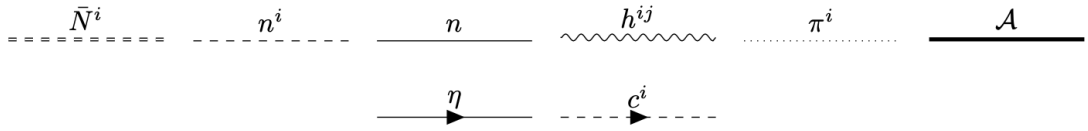

Figure 7.1: Graphic notation for the propagators

The interaction which interst us are defined by the following vertices:

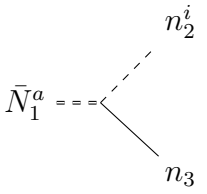

$$= \frac{k_1^i k_2^a + \delta^{ai}(k_1\cdot k_2) - 2\lambda k_1^a k_2^i}{2G} \tag{7.63}$$

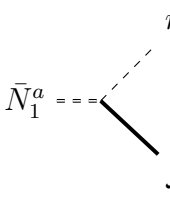

$$= -\frac{k_1^i k_2^a + \delta^{ai}(k_1\cdot k_2) - 2\lambda k_1^a k_2^i}{2G} \tag{7.64}$$

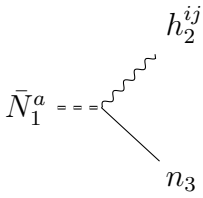

$$= \frac{\omega_2}{2} \frac{\delta^{ai} k_1^j + \delta^{aj} k_1^i - 2\lambda \delta^{ij} k_1^a}{2G} \tag{7.65}$$

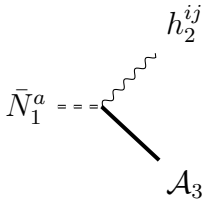

$$= -\frac{\omega_2}{2} \frac{\delta^{ai} k_1^j + \delta^{aj} k_1^i - 2\lambda \delta^{ij} k_1^a}{2G} \tag{7.66}$$

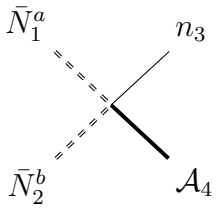

$$= -\frac{-k_1^i k_2^a - \delta^{ai}(k_1 \cdot k_2) + 2\lambda k_1^a k_2^i}{2G} \tag{7.67}$$

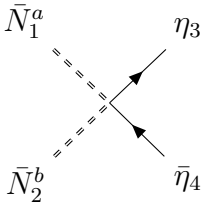

$$= \frac{-k_1^b k_2^a + 2\lambda k_1^a k_2^b - \delta^{ab}(k_1 \cdot k_2)}{2G} \tag{7.68}$$

Where the vertices are defined by [160]:

$$V[\Phi_1 \Phi_2 \cdots \Phi_n] = \frac{\delta^n \mathcal{L}}{\delta\Phi_1 \delta\Phi_2 \cdots \delta\Phi_n} \,. \tag{7.69}$$

Note that the vertices listed above have two by two the same structure up to a global sign. Namely the expression (7.63) has opposite sign with respect to (7.64) and similarly for the couples (7.65)-(7.66) and (7.67)-(7.68). This means that the diagrams that can be build with those vertices with $\bar{N}_i$ as an external source, *cancel exactly*. That implies that, for this one-loop computation, the non-local divergencies will not generate any counterterm. Therefore the renormalization will proceed as usual in QFT and so the computation of the beta-functions.

In order to be more explicit, let us take the vertices (7.67) and (7.68). These will contribute to the renormalization of the 2-point function $\langle \bar{N}_a \bar{N}_b \rangle$ with the two diagrams:

We have:

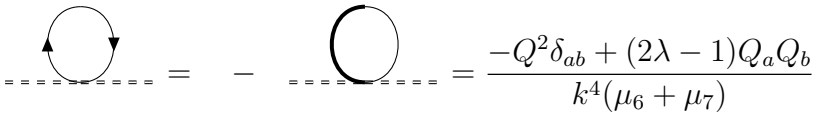

$$= \quad - \quad = \frac{-Q^2\delta_{ab} + (2\lambda - 1)Q_a Q_b}{k^4(\mu_6 + \mu_7)}$$

where Q^a is the external momentum of $\bar{N}_a$ and k^a is the internal one, which runs in the loop: the two diagrams sum exactly to 0, as anticipated. An identical cancellation takes place for the other contributions.

This nice cancellation seems to strongly push towards the definitve conclusion of the perturbative renormalizability of the non projectable version of HG. Let us emphasize that the relation between the vertices, which ensures the cancellation, strongly relies on the particular shape of the $\mathcal{A}$-$\eta\bar{\eta}$ sector of the Lagrangian

$$\mathcal{A}\theta_1 - \bar{\eta}\{\theta_1, \theta_2\}\eta\,. \tag{7.70}$$

The last step towards the final proof of renormalizability would be to show that the structure of the terms given in (7.70) is preserved by the renormalization procedure. The most natural way to do it would be to find some BRST symmetry, as it has been done for the spatial-diffeomorphisms in the projectable version [163]. However, so far the problem remains unsolved.

7.3 Outlook

In this Chapter we have revised the status of Hořava gravity as a candidate to be a quantum theory of gravity. The related investigations are quite involved, since the power-counting renormalizability does not represent a sufficient condition for a non-Lorentz invariant theories to be perturbatively renormalizable. However, even if the standard arguments do not hold, the theoretical advancements in the study of HG are quite impressive.

The first remarkable result is that HG *is* an ultraviolet- complete theory of spacetime, in its projectable version. Although non-phenomenologically viable in the infrared, this is the only known example where a perturbative-renormalization technique can be applied to gravity to make prediction at any energy as it happens for the Standard Model.

Besides that, the same ideas developed within the projectable setting, in order to prove renormalizability, can be transferred directly to the non-projectble case, where the generalized gauge-fixing condition (7.38) manages to cure the irregular propagators of the form $1/\omega^2$, fixing the spatial-diffeomorphism invariance.

The non-projectable version of HG has been shown to be viable and well-behaved phenomenologically.

Its UV aspects, however, are trickier. The implementation of the symmetry given by the reparametrization of time can be rigorously done within the BFV Hamiltonian formulation, as an imposition of a second-class constraint in the action. Once implemented in the path integral, this constraint implies the presence of other irregular propagators of the kind $1/k^{2d}$, implying non-local divergencies.

Interestingly, and somehow magically, these nonlocalities in the action seems to not contribute to the counterterms, therefore to the renormalization procedure.

Within this Chapter an explicit example, based on preliminaries calculations, has been made in order to show how this happens. The main point now is to show that this behaviour is encoded in the symmetries of the theory and it is not spoiled by the renormalization procedure. Although not yet completed, the proof of HG renormalizability seems now closer then ever.

Chapter 8

Conclusions

In this thesis we have analyzed the impact of Lorentz invariance violation in gravity. Such a choice has been motivated, on one side, by the existence of a quantum gravity proposal, Hořava gravity, that seems to show well-behaved ultraviolet properties. On the other side, laboratory-based experiments of QFT in curved spacetimes undoubtedly share the presence of Lorentz breaking features for phonons, as in the case of analogue models of gravity.

This latter setting has been the starting point of our journey. In Chapter 3 we have revised how the analogue framework could provide a suitable playground for the detection of the (sonic) black hole radiation. This has allowed us to revise and confirm the resilience of the Hawking effect in the presence of non-Lorentz invariant perturbations. Within the Chapter, we have developed a new technique, based on the definition of an approximant ray. This ray has the utility to describe the Hawking pair far from the horizon, while enjoying a peeling behaviour closeby an effective horizon, which location depends on the energy of the ray. Since Lorentz breaking particles do not enjoy any pure horizon-peeling behaviour, the approximant turns out to be particularly useful in simplifying the problem.

In addition, it provides interesting hindsights about the physics behind the Hawking radiation. First of all, the energy conservation: we understood that the energy balance is led by the phase velocity and that particle production is possible only when ω/k switches sign. This fact allows also the possibility for horizonless object to emit particles, in the case of subluminal dispersion, even if not in a thermal way.

Secondly, the approximant makes us understand that the horizon's particle production is not an ultralocal process: the actual effect takes place when the Hawking couple has departed at least a de Broglie wavelength from the horizon, in order to respect the Heisenberg indetermination principle. This interpretation justifies the introduction of the approximant ray and explains why such an emission process can happen in nonrelativistic settings.

This brings us directly to Chapter 5. Since sonic black holes emit particles, one may wonder if the same effect extends to the gravitational case. In Chapter 4, black holes are defined in the context of Lorentz-violating gravity, such as in Einstein-aether and khronometric theory. The built-in presence of superluminal signals within LV gravity allows for a similar treatment of the Killing horizon particle production: modes at low Killing energy (with respect to the LV scale Λ) are produced by that

surface with an energy-dependent rate $T(\alpha)$.

However, LV gravitational black holes offer a completion of the picture left by the analogue analysis. In a spacetime which admits superluminal particles, a Killing horizon does not provide a true boundary, thus being unable to determine a black hole region, from the causal point of view. Therefore, an additional notion, corresponding to the universal horizon, is needed. This surface is able to trap any possible physical signal, regardless its speed.

In khronometric theory, this horizon is determined by a compact constant-khronon leaf. The aether vector field is orthogonal to this surface, thus forbidding particles, which always move forward in time, to escape it. The possibility of having axisymmetric solution is analyzed and the requirement for the aether to be orthogonal to the UH seems mandatory: if the normal to any surface misaligns with the time direction, one can always find a fast-enough signal which can exit it. This in turn implies, for the EA case, that the twist tensor has to vanish locally. This latter condition seems quite unstable, from the point of view of EA theory, since a generic perturbation will destroy the horizon itself.

In a static, spherically symmetric case, where Einstein-aether and khronometric theories match, the UH is a sphere, enclosed in the Killing horizon. We have investigated the UH as a source of particle production and we have found its behaviour to resemble the relativistic Killing horizon's one. The outgoing modes share an universal peel-out, together with an infinite blueshift. In the near-horizon limit, these signals have infinite speed, so that they follow a surface of simultaneity, which approaches logarithmically the UH with a coefficient defined by its surface gravity κ_{UH}.

Note that this behaviour is universal – so energy-independent – and the emission from the UH is purely thermal, peaked at T_{UH}. This conclusion, although logical, appears to be in contrast with several previous treatments. The root of the tension has to be found in a more involved modes structure which LV dispersions imply. First of all, Lorentz invariance violation breaks the relativistic degeneracy which occurs between the notion of phase and group velocity in Lorentz-invariant theories. We have shown that near-horizon modes must be described by the phase velocity, which leads to the aforementioned universal peeling behaviour and not by the group velocity, which would result in a species-dependent horizon temperature $T_{\mathrm{UH}}(n)$.

Additionally, the presence of a larger set of modes with respect to the relativistic case has as a consequence a two-step calculation: at the UH the energy balance is ensured by identifying the Hawking couple as the $(\psi^{\mathrm{green}}, \psi^{\mathrm{red}})$ couple of figure 5.2, while the Killing horizon emission is governed by the $(\psi^{\mathrm{orange}}, \psi^{\mathrm{red}})$ couple, as in the AG case. However, no $(\psi^{\mathrm{orange}}, \psi^{\mathrm{red}})$ can be found at the UH. This explains why in [121] only the Killing horizon contribution appears.

The UH also saves the day in terms of quantum state. The infinite blueshift experienced by near-horizon modes fix the state at the UH, just by imposing the regularity for the infalling observer. This condition, together with an analysis of the WKB condition for the modes, turns out to be compatible with the almost-relativistic behaviour that low-energy rays show at the Killing horizon. Therefore the quantum state, a LV version of the relativistic Unruh state, describes a spectrum at infinity governed by the Hawking temperature T_{H} at low energies and by T_{UH} at

high energies.

Remarkably, this completes the picture of the analogue calculation, where the notion of UH is missing and no fixed prescription for choosing the vacuum is given. The absence of such a structure in analogue black holes boils down to the lack of a sufficient number of degrees of freedom to determine the background geometry. In gravity, the aether and the metric tensor are two independent entities, while this is not true in AG. Actually, it has been shown that the possible geometries within the analogue frameworks – if not endowed with external fields – do not allow any UH [123].

The presence of Hawking radiation by UHs is a strong hint for a formulation of black hole thermodynamics in LV theories, which is currently lacking. Finalizing this picture, besides being a matter of completeness, would definitely establish that thermodynamics can be more fundamental than Lorentz invariance itself.

Chapter 6 enforces the link between geometry and thermodynamics. There we show that, despite a controversial debate in the literature, the Unruh effect can be rescued from the breakdown of Lorentz invariance. The presence of a dynamical aether makes us to define a novel LV-Rindler wedge, extended with respect to the relativistic one, which enjoys the boost invariance, thus being suitable for describing an uniformly accelerated observer.

This geometry, that can be also seen as a near-Killing horizon black hole approximation, contains an universal horizon, determined by a physical scale, namely the aether acceleration $\bar{a}$. Given the spacetime symmetries, the analysis of the modes goes pretty much as for the black hole case, making us to identify the wedge temperature through a standard Bogolyubov approach as $T_{\mathbb{R}} = \bar{a}/(2\pi)$. Note that $\bar{a}$ is not anymore a bookkeping parameter, as in GR, thus it cannot be absorbed away by a suitable coordinate rescaling.

An independent analysis with an accelerated Unruh-De Witt detector gives the same result. As expected, and in analogy with the relativistic case, the wedge temperature is not the one perceived by the observer. From the detector's calculation, the observer instead measures the wedge temperature rescaled by the foliation lapse $T_{\rm obs} = T_{\mathbb{R}}/N$. This is a consequence of the definition of the Hamiltonian flow with respect to the preferred time direction.

An additional, independent calculation can be carried following Hawking's Euclidean approach: the thermal character of a spacetime can be deduced by finding the right periodicity that the Euclidean Killing time must have in order to get rid of a conical singularity at the horizon. This, both for the black hole's UH and for the Rindler's UH, tells us that the Euclidean time right periodicity is given by $1/T_{\rm UH}$ ($1/T_{\mathbb{R}}$ in the Rindler's case), thus recovering our result. In order to perform this calculation, we have built an effective metric, which is able to describe the infinite-speed signals as null rays, thus capturing the LV causal structure of the spacetime in a relativistic language.

The rediscovery of the Unruh effect within a LV setting also opens a window onto the thermodynamical treatment of the Einstein-aether field equations *à la* Jacobson. An interesting future perspective for this field would be to see the viability of this idea.

In the last part, namely in Chapter 7, we have focused in Hořava gravity as

a candidate for quantum gravity, investigating its ultraviolet properties. We have described the two possible branches of the theory: the projectable and the non-projectable one. The former, while not viable at the phenomenological level, turns out to be a perturbatively renormalizable theory. This makes the projectable HG an ultraviolet complete theory of quantum gravity.

The non-projectable branch seems to describe a quite appealing phenomenology: it agrees with observations in the Newtonian limit and it allows – in the low-energy regime – for black hole solutions, as the ones we described in Chapter 4. These solutions are absent in the projectable case, where the aether's acceleration vanishes everywhere.

However, the UV properties of the non-projectable version of HG are not completely understood yet. As we have shown, the unavoidable presence of irregular propagators seems to threaten the possibility of the theory to be renormalizable. Surprisingly, the strange divergences originated by these propagators give the impression not to contribute to the renormalization procedure.

The definitive proof of perturbative renormalizability, where these divergences are tamed, is a clear perspective of great importance for future research.

Therefore, a coherent path – from the lab to the UV – emerges from our discussion. Lorentz violating phenomenology seems to be smoothly connected with the relativistic one. That implies a robustness of Hawking and Unruh effect. At the same time, the breakdown of such a fundamental symmetry has made us rethink fundamental notions, such as the causal structure of spacetime. Some hidden relativistic degeneracies have been spoiled, like the different roles of group and phase velocity, teaching us a lesson about the physics behind the behaviour of quantum fields on a curved spacetime.

In conclusion, we feel that this exploration exemplifies the profound insights that can be gained by pushing the boundaries of our theoretical frameworks. Violation of Lorentz invariance might or might not be realized in nature, but its interplay in showing the resilience of thermodynamical aspects of gravity has surely still much to teach us about the intimate nature of spacetime.

Appendix A

Turning point

In this appendix we will give an additional analysis on the characteristics of Chapter 5. In particular, we will analyze the position of the turning point for the case $n = 2$.

As already said, the turning point is defined as the point $r_{\rm tp}$ where the polynomial (5.18) admits a solution with algebraic multiplicity 2. In other words, whenever that polynomial have two degenerate roots.

The treatment for $n = 2$ is meaningful both at the technical level – because for a $4^{\rm th}$-order polynomial the shape of the roots is known exactly as a function of the coefficients – and at the phenomenological level, since a perturbative theory in k/Λ will be described at the leading order by the $n = 2$ case of (5.5), which corresponds to the lowest order in the effective field theory expansion for a CPT-even Lorentz violating theory [33].

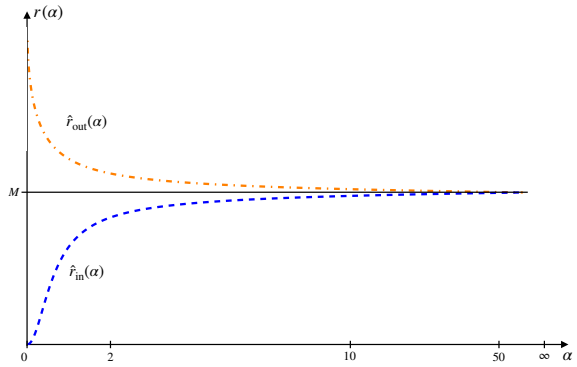

Figure A.1: Position of the roots $\hat{r}_{\rm out}(\alpha)$ (in orange, dash-dotted) and $\hat{r}_{\rm in}(\alpha)$ (in blue, dashed) in terms of $\alpha > 0$. The solid black line represent the UH radius.

The degeneracy of the roots of a polynomial (5.18) can be studied through its discriminant $\Delta(r, \alpha)$[1]:

$$\begin{aligned}\Delta(r,\alpha) = &\left(4\alpha^2+1\right)^2 \hat{r}^4 - 2\left(16\alpha^4+16\alpha^2+3\right)\hat{r}^3 + \\ &4\left(4\alpha^4+17\alpha^2+3\right)\hat{r}^2 - 8\left(9\alpha^2+1\right)\hat{r} + 27\alpha^2\,,\end{aligned} \tag{A.1}$$

[1]The discriminant Δ of a polynomial $\mathcal{P}(x, b_i)$ with real coefficients $\{b_i\}$ is a real function of the coefficients $\Delta[\mathcal{P}](b_i)$. Its vanishing indicates degeneracy of at least two of the solutions, while a change of sign in Δ implies that two real solutions become complex conjugate.

where $\hat{r} = r/M$. Remarkably, $\Delta(r, \alpha)$ displays two real roots $\{\hat{r}_{\rm out}(\alpha), \hat{r}_{\rm in}(\alpha)\}$, one on each side of the UH, and whose positions depend on α, as it can be seen in figure A.1. They correspond to the turning point for $\psi^{\rm orange}$ and for $\psi^{\rm blue}$, respectively. Note that for $\alpha \to 0$, the outer solution approaches the Killing horizon, moving inwards as we increase the value of α. The inner one, instead, starts from the singularity and moves towards the UH for large α.

Appendix B

Effective temperature function

As a second alternative derivation of (5.104), we introduce now the concept of "Effective Temperature Function (ETF)". Defined in [20], the ETF measures the degree of peeling of a ray with respect to a given surface. This notion is particularly useful in the case of quasi-horizons [20], and in situations in which event horizons are not yet formed, but the situation is close enough to its final state so that most of the dynamics will approach the latter under certain conditions.

The ETF is defined through the relation $U_+ = p^{-1}(U_-)$, which relates the light-cone coordinates at $\mathscr{I}^+$ and $\mathscr{I}^-$, thus connecting the choice of the vacuum state with the coordinate followed locally by the modes. The ETF is then defined as [20]

$$\kappa(U_+) := -\frac{\mathrm{d}^2 U_-}{\mathrm{d}U_+^2}\left(\frac{\mathrm{d}U_-}{\mathrm{d}U_+}\right)^{-1} = -\frac{\ddot{p}(U_+)}{\dot{p}(U_+)}. \tag{B.1}$$

In the particular case where $p(U_+)$ takes an exponential form, this captures exactly the peeling surface gravity $\kappa(U_+) = \kappa_{\text{peeling}}$. In a general case instead, and even if the peeling behaviour is not perfectly exponential, one can start having Hawking radiation if the variation of κ remains adiabatic [20]

$$\left|\frac{\dot{\kappa}(U_+)}{\kappa(U_+)^2}\right| \ll 1 \tag{B.2}$$

which implies the approximated constancy of $\kappa(U_+)$ over the time scale associated with the typical period of Hawking quanta – since the peak frequency of the spectrum is $\omega_{\text{peak}} \sim \kappa(U_+)$.

Let us then apply this idea to the case discussed throughout this paper, by treating the Killing horizon as a quasi-horizon, following [139]. It is not an event horizon for rays of arbitrary α, but satisfies the previous conditions, and thus rays peel off it, for small α. The role of the light-cone coordinates U_+ and U_- is played here respectively by the adapted null coordinate for the outgoing (red) modes $\bar{u}$ and its equivalent one for in-going ones $\bar{U}$ (blue mode). Note that at $\mathscr{I}^-$ one has $\bar{U} = U_-$.

Let us now consider the variation of $\bar{u}$ as perceived by an infalling observer along a blue mode trajectory. For concreteness, we take such an observer to have Killing energy well below Λ at $\mathscr{I}^-$, so it will be approximately relativistic all along its path

while infalling into the Killing horizon. Indeed, for low-energy blue modes, for which $k_{\rm blue}(r,\alpha) \ll 1$, we have that the trajectory can be described by a parameter λ as

$$\frac{\mathrm{d}t}{\mathrm{d}\lambda} = -\frac{r}{r-2M}\left[1+\frac{3}{2}\frac{k_{\rm blue}^2}{\Lambda^2}\left(\frac{2M}{r}-1\right)\right]\frac{\mathrm{d}r}{\mathrm{d}\lambda}\,, \tag{B.3}$$

which near the Killing horizon coincides exactly with the relativistic null observer along $\mathrm{d}v = 0$. Since we will be interested in that region, in the following we will neglect the subleading term in (B.3). Then, using eq.(B.3) and (5.26), we can label a constant $\bar{U}$ line with $\bar{u}$ getting

$$\frac{\mathrm{d}\bar{u}}{\mathrm{d}\lambda} = \frac{\mathrm{d}t}{\mathrm{d}\lambda} + \frac{c_g^{\rm red}(r,\alpha)U_r + S_r}{c_g^{\rm red}(r,\alpha)U_t + S_t}\frac{\mathrm{d}r}{\mathrm{d}\lambda} = \left(\frac{c_g^{\rm red}(r,\alpha)U_r + S_r}{c_g^{\rm red}(r,\alpha)U_t + S_t} - \frac{r}{r-2M}\right)\frac{\mathrm{d}r}{\mathrm{d}\lambda}\,. \tag{B.4}$$

This relation – formula (5.107) in the main text – describes exactly the situation depicted in figure B.1, corresponding to an observer travelling along a $\bar{U} = \bar{U}_0 =$ const. line crossing the outgoing red trajectories.

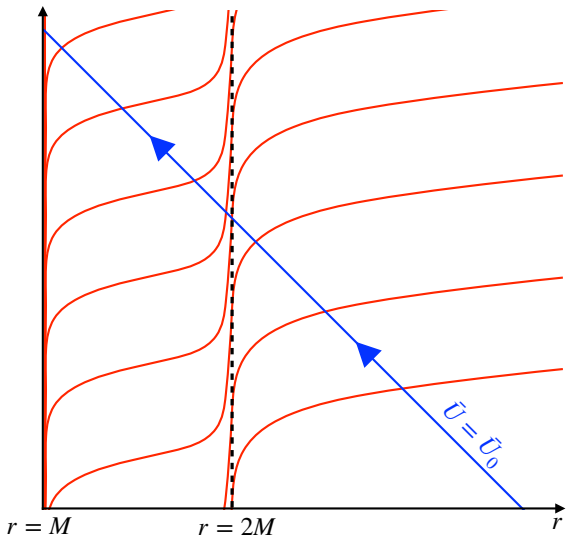

Figure B.1: Constant $\bar{U} = \bar{U}_0$ observer (in blue) which crosses a congruence of $\bar{u} =$ const. lines (in red).

Let us now make a convenient choice that simplifies the computation, i.e. we label points along a $\bar{U}$=const. trajectory using their radius (this is always allowed as long as the relation between λ and r is monotonic, as in our case). This is tantamount to choosing a parameter λ so that coinciding with the radial coordinate. In this case we have $\partial_\lambda r = 1$ and, expanding (B.4) using (5.102), we obtain

$$\frac{\mathrm{d}\bar{u}}{\mathrm{d}\bar{U}} = \frac{\mathrm{d}\bar{u}}{\mathrm{d}r} = -\frac{2r}{r-2M} + \frac{3\alpha^2\left(4M^2+4Mr+r^2\right)}{2(r-2M)^2} + O\left(\alpha^3\right)\,, \tag{B.5}$$

that we can integrate to

$$\bar{u}(r) = \frac{1}{2}\left(-\frac{48\alpha^2M^2}{r-2M} + 8M\left(3\alpha^2-1\right)\log(r-2M) + \left(3\alpha^2-4\right)r\right)\,. \tag{B.6}$$

Neglecting the terms which are finite for $r \to 2M$, we can invert the expression above getting finally the relation $\bar{U}(\bar{u})$

$$\bar{U}(\bar{u}) = r(\bar{u}) = 2M + M\frac{6\alpha^2}{3\alpha^2-1}\frac{1}{W\left(\frac{6\alpha^2}{3\alpha^2-1}e^{-\frac{1}{4M(3\alpha^2-1)}\bar{u}}\right)}\,, \tag{B.7}$$

where the function $W(x)$ is the (principal branch of the) Lambert function[1]. Let us notice that, when $\alpha \to 0^+$, the expression for $\bar{U}(\bar{u})$ matches, as expected, the one for the Kruskal–Szekeres null coordinates plus $\mathcal{O}(\alpha^2)$ corrections,

$$\lim_{\alpha\to 0^+}\bar{U}(\bar{u}) = Me^{-\bar{u}/4M}\left(1 - 3\alpha^2\frac{\bar{u}}{4M} + \mathcal{O}(\alpha^4)\right), \tag{B.8}$$

thus recovering exactly the relativistic peeling with $\kappa = (4M)^{-1}$.

With these ingredients, we are ready to compute the ETF and expand it at small α

$$\begin{aligned}\kappa(\bar{u}) &= -\frac{\mathrm{d}^2\bar{U}}{\mathrm{d}\bar{u}^2}\left(\frac{\mathrm{d}\bar{U}}{\mathrm{d}\bar{u}}\right)^{-1} \\ &= \frac{1}{4M(1-3\alpha^2)}\frac{1+2W\left(\frac{6\alpha^2}{3\alpha^2-1}e^{-\frac{1}{4M(3\alpha^2-1)}\bar{u}}\right)}{\left[1+W\left(\frac{6\alpha^2}{3\alpha^2-1}e^{-\frac{1}{4M(3\alpha^2-1)}\bar{u}}\right)\right]^2} = \frac{1}{4M}(1+3\alpha^2+\cdots)\,,\end{aligned} \tag{B.9}$$

which is constant up to corrections of order $\mathcal{O}(\alpha^4)$, hence automatically satisfying the adiabatic condition. The result obtained in (B.9) leads to the same temperature in (5.104).

As a final interesting observation, let us note that the same result displayed here can be obtained by taking the limit in which the observer approaches the Killing horizon. In (B.6), this corresponds in $\bar{u}$ to the limit $\bar{u} \to -\infty$. In the ETF, this corresponds to

$$\lim_{\bar{u}\to-\infty}\kappa(\bar{u}) = \frac{1}{4M(1-3\alpha^2)}, \tag{B.10}$$

which can be interpreted as the rays departing the Killing horizon with a constant α-dependent exponent.

[1]The Lambert function is defined as the solution of the equation $W(x)e^{W(x)} = x$ [176].

Appendix C

Derivation of the Rindler wedge

C.1 Geometry

Here we give a detailed derivation of the solution (6.15) to the equation of motion (4.19). We will assume invariance under boosts and local flatness – i.e. Riem = 0. For the ease of notation, we work with the $(1+1)$-dimensional submanifold of the metric in (6.13), thus neglecting the sub-manifold $\mathbb{E}_2$, which will not contribute in any case.

Let us start with the first condition, that is that the aether as well as the metric are Lie dragged with respect to the boost vector. To this aim we have to find out the explicit form of the Killing vector which obeys $\mathcal{L}_\chi g = 0$. Using the conformal metric, we find the following set of equations

$$\begin{aligned}
\partial_\tau\chi_\tau - \chi_\tau\partial_\tau \ln(W(\tau,\rho)) - \chi_\rho\partial_\rho \ln(W(\tau,\rho)) &= 0, &\text{(C.1)}\\
\partial_\rho\chi_\rho - \chi_\tau\partial_\tau \ln(W(\tau,\rho)) - \chi_\rho\partial_\rho \ln(W(\tau,\rho)) &= 0, &\text{(C.2)}\\
\chi_\rho\partial_\rho \ln(W(\tau,\rho)) + W(\tau,\rho)\partial_\tau \ln(\chi_\tau W(\tau,\rho)) &= 0 &\text{(C.3)}
\end{aligned}$$

which leads immediately to the relation $\partial_\tau\chi_\tau = \partial_\rho\chi_\rho$. Moreover, the space-time should not depend on the time associated to the timelike Killing vector field, such that $\mathcal{L}_\chi g(U,\chi) = 0$ and $\mathcal{L}_\chi g(S,\chi) = 0$ respectively. Together with the Killing equation we find that the components of the Killing vector read

$$\chi_\tau = f_1(\tau)W^2(\tau,\rho) \quad \text{and} \quad \chi_\rho = f_2(\rho)W^2(\tau,\rho) \tag{C.4}$$

with until now, arbitrary functions $f_1(\tau)$ and $f_2(\rho)$. Using again the space-time independence of the Killing time, and plugging in the above components, we find that $\partial_\tau f_1(\tau) = \partial_\rho f_2(\rho)\ \forall\tau,\rho$ which implies that the derivatives must equal to a constant c_0 so that the arbitrary functions f_1 and f_2 take the form

$$f_1(\tau) = c_0\tau + c_1, \quad \text{and} \quad f_2(\rho) = c_0\rho + c_2. \tag{C.5}$$

Now, using the equations above, we can find a functional relation between $W(\tau,\rho)$ and $f_1(\tau)$ and $f_2(\rho)$

$$W(\tau,\rho) = \frac{h\left(\frac{f_1(\tau)}{f_2(\rho)}\right)}{f_1(\tau)} \tag{C.6}$$

where h is a function to determine. We do this by imposing local flatness through Riem $= 0$. Being a bi-dimensional geometry, it is sufficient to ask for our geometry to have a vanishing scalar curvature [41]. We cast the two-dimensional Ricci scalar curvature in the (τ, ρ) coordinate system and find

$$R = -2(-\partial_\tau^2 + \partial_\rho^2)W(\tau,\rho) + 2\frac{(\partial_\rho W(\tau,\rho))^2 - (\partial_\tau W(\tau,\rho))^2}{W(\tau,\rho)} = 0, \tag{C.7}$$

which leads to the following solution

$$W(\tau,\rho) = F_1(\tau+\rho)F_2(\tau-\rho), \tag{C.8}$$

with, again, arbitrary functions F_1 and F_2.

To simplify $f_1(\tau)$ and $f_2(\rho)$, we impose the coordinate shift

$$\tau \to \tau - \frac{c_1}{c_0} \quad \text{as well as} \quad \rho \to \rho - \frac{c_2}{c_0} \tag{C.9}$$

such that

$$f_1(\tau) = c_0\tau \quad \text{and} \quad f_2(\rho) = c_0\rho\,. \tag{C.10}$$

Relating the two forms (C.6) and (C.7) for the conformal factor and their τ- and ρ-derivatives we arrive at

$$1 + \tau\partial_\tau \ln(F_1(\tau+\rho)) - \tau\partial_\tau \ln(F_2(\tau-\rho)) + \rho\partial_\rho \ln(F_1(\tau+\rho)) + \rho\partial_\rho \ln(F_2(\tau-\rho)) = 0. \tag{C.11}$$

Since we find a differential equation for the functions $F_1(\tau+\rho)$ and $F_2(\tau-\rho)$, we find a unique family of solutions for both that lead to the following conformal factor

$$W(\tau,\rho) = \left(\frac{\rho+\tau}{\rho-\tau}\right)^\alpha \frac{C}{\rho+\tau} \tag{C.12}$$

whith the integration constants $C, \alpha \in \mathbb{R}$.

To determine α we need to fulfill the equation (6.27). However, since our solution is hypersurface orthogonal, the equations of motion of khronometric gravity coincide with those of in EA gravity. This implies that we can proceed to solve the simpler equation $\mathcal{A}^a = 0$ with $\mathcal{A}$ given in (4.18) instead of (4.19), and hypersurface orthogonality will ensure the equivalence of solutions. Inserting our ansatz for g_W, we find that for $\mathcal{A}^a$ to vanish, every individual term in $\mathcal{A}^a$ has to be zero independently, since the couplings are arbitrary. From this, it follows that $\mathcal{L}_S\theta = 0$, which simplifies to $\partial_\rho\theta = 0$. Since $\theta = \nabla_a u^a = \partial_\tau W^{-1}(\tau,\rho)$ we have $\partial_\tau\partial_\rho W^{-1}(\tau,\rho) = 0$, which is solved by

$$W(\tau,\rho) = \frac{1}{A(\tau)+B(\rho)}, \tag{C.13}$$

for two generic functions $A(\tau)$ and $B(\rho)$. This restricts the coefficient $\alpha \in \{0,1\}$, and after setting $C = \frac{1}{\bar{a}}$ for convenience, we find the two solutions

$$W_\pm(\tau,\rho) = \frac{1}{\bar{a}(\rho\pm\tau)}. \tag{C.14}$$

as given in (6.15). Let us notice that the conformal patch we used here is only the easiest way for deriving the solution. However, it is easy to see that the two-dimensional problem of finding a flat boost-invariant solution of (4.19) is anyway overdetermined. One could have proceeded in the following way: the flatness of the solution ensures that the metric can be written as the Minkowski metric, in the right system of coordinates. Then, the normalization condition for a two dimensional vector u links the two components through the relation $|u|^2 = -1$. Finally, boost-invariance makes the problem one-dimensional, transforming (4.19) into an ODE for one of the two components of the aether vector, which leads to the same the solution found through the conformal method.

C.2 Stress energy tensor

The metric-aether solution that we have shown represents the natural extension of the rindler wedge with an everywhere timelike, hypersurface orthogonal, vector (see also [146]).

In particular, as we proved, this solution can be also obtained as a near-Killing horizon limit of a LV-Schwarzschild black hole. This, of course, ensures that the aether equation of motion

$$\frac{\delta S_{\rm EA}}{\delta u^a} = 0 \iff \mathcal{A}^a = 0 \tag{C.15}$$

which is linear in the vector field u^a, is automatically satisfied at the first order in $\epsilon = r - 2M$. In addition, we have seen that this solution is Lie-dragged by the boost generator $\chi = \partial_\eta$ and Riemann flat.

Nevertheless, we have to note that the same reasoning cannot be applied to the gravitational field equations

$$\frac{\delta S_{\rm EA}}{\delta g^{ab}} = 0 \iff G_{ab} = 8\pi G T^u_{ab}\,. \tag{C.16}$$

In a flat manifold the Einstein tensor vanishes $G_{ab} = 0$, so that the EA equations lead to

$$T^u_{ab} = 0\,. \tag{C.17}$$

One can explicitly check that, for general couplings c_θ, c_a and c_σ the stress-energy tensor of the aether does not vanish. Mathematically, this has to do with the quadratic dependence of u^a that T^u_{ab} enjoys: this does not allow to recover the solution perturbatively in ϵ from the black hole geometry. However, in the case of the relativistic Rindler wedge $\mathscr{R}$, we face a very similar issue regarding the space-time geometry sourced by the stress-energy tensor. If one assumes matter fields in $\mathscr{R}$, their stress-energy tensor is found to admit a nonzero vacuum expectation value [177]. This apparent tension is resolved when considering the stress-energy tensor in the left Rindler wedge $\mathscr{L}$ as well. Then, one can show that the value of the stress-energy tensor in $\mathscr{R}$ is exactly compensated by the one in $\mathscr{L}$. The key point of the argument is based on the reverse of the orientation between the two

patches. Namely, on the right side the boost generator ∂_η "flows upwards" in the right Rindler wedge, while it "flows downwards" on the left side.

In the LV case, this has an impact on the sign of the lapse, since

$$(u \cdot \chi)_{\mathbb{R}} = N_{\mathbb{R}} = -N_{\mathbb{L}} = -(u \cdot \chi)_{\mathbb{L}} \,. \tag{C.18}$$

This tells us that the two patches are opposite-oriented, since the spatial constant-τ submanifold Σ are the same on the two sides. Therefore, similarly to what happen for a standard matter field in relativistic settings, the total energy balance is satisfied between $\mathbb{L}$ and $\mathbb{R}$.

This discussion tells us that the left patch is a necessary ingredient in order to describe a solution without any gravitational source.

Bibliography

[1] Robert M. Wald. *General Relativity*. Chicago, USA: Chicago Univ. Pr., 1984. DOI: 10.7208/chicago/9780226870373.001.0001.

[2] Clifford M. Will. "The Confrontation between General Relativity and Experiment". In: *Living Rev. Rel.* 17 (2014), p. 4. DOI: 10.12942/lrr-2014-4. arXiv: 1403.7377 [gr-qc].

[3] Clifford M. Will. *Theory and Experiment in Gravitational Physics*. Cambridge University Press, Sept. 2018. ISBN: 978-1-108-67982-4, 978-1-107-11744-0.

[4] Roger Penrose. "Gravitational collapse and space-time singularities". In: *Phys. Rev. Lett.* 14 (1965), pp. 57–59. DOI: 10.1103/PhysRevLett.14.57.

[5] Stephen Hawking. "The occurrence of singularities in cosmology. III. Causality and singularities". In: *Proc. Roy. Soc. Lond. A* 300 (1967), pp. 187–201. DOI: 10.1098/rspa.1967.0164.

[6] G. F. R. Ellis and Stephen Hawking. "The Cosmic black body radiation and the existence of singularities in our universe". In: *Astrophys. J.* 152 (1968), p. 25. DOI: 10.1086/149520.

[7] Gerard 't Hooft and M. J. G. Veltman. "One loop divergencies in the theory of gravitation". In: *Ann. Inst. H. Poincare A Phys. Theor.* 20 (1974), pp. 69–94.

[8] Steven Weinberg. "Ultraviolet divergences in quantum theories of gravitation". In: *General Relativity: an Einstein Centenary Survey, by Stephen Hawking , W. Israel, Cambridge, UK: Cambridge University Press, 2010* (Mar. 1979), pp. 790–831.

[9] Jiro Murata and Saki Tanaka. "A review of short-range gravity experiments in the LHC era". In: *Class. Quant. Grav.* 32.3 (2015), p. 033001. DOI: 10.1088/0264-9381/32/3/033001. arXiv: 1408.3588 [hep-ex].

[10] James M. Bardeen, B. Carter, and S. W. Hawking. "The Four laws of black hole mechanics". In: *Commun. Math. Phys.* 31 (1973), pp. 161–170. DOI: 10.1007/BF01645742.

[11] Stephen W Hawking. "Particle creation by black holes". In: *Communications in mathematical physics* 43.3 (1975), pp. 199–220.

[12] Jacob D. Bekenstein. "Generalized second law of thermodynamics in black hole physics". In: *Phys. Rev. D* 9 (1974), pp. 3292–3300. DOI: 10.1103/PhysRevD.9.3292.

[13] W. G. Unruh. "Notes on black hole evaporation". In: *Phys. Rev. D* 14 (1976), p. 870. DOI: 10.1103/PhysRevD.14.870.

[14] Ted Jacobson. "Thermodynamics of space-time: The Einstein equation of state". In: *Phys. Rev. Lett.* 75 (1995), pp. 1260–1263. DOI: 10.1103/PhysRevLett.75.1260. arXiv: gr-qc/9504004.

[15] Claus Kiefer. "Quantum gravity - an unfinished revolution". In: Feb. 2023. arXiv: 2302.13047 [gr-qc].

[16] W. G. Unruh. "Experimental black hole evaporation". In: *Phys. Rev. Lett.* 46 (1981), pp. 1351–1353. DOI: 10.1103/PhysRevLett.46.1351.

[17] Stefano Liberati, Giovanni Tricella, and Andrea Trombettoni. "The information loss problem: an analogue gravity perspective". In: *Entropy* 21.10 (2019), p. 940. DOI: 10.3390/e21100940. arXiv: 1908.01036 [gr-qc].

[18] T. A. Jacobson. "Black-hole evaporation and ultrashort distances". In: *Phys. Rev. D* 44 (1991), pp. 1731–1739. DOI: 10.1103/PhysRevD.44.1731.

[19] Antonin Coutant, Renaud Parentani, and Stefano Finazzi. "Black hole radiation with short distance dispersion, an analytical S-matrix approach". In: *Phys. Rev. D* 85 (2012), p. 024021. DOI: 10.1103/PhysRevD.85.024021. arXiv: 1108.1821 [hep-th].

[20] Carlos Barcelo et al. "Hawking-like radiation from evolving black holes and compact horizonless objects". In: *JHEP* 02 (2011), p. 003. DOI: 10.1007/JHEP02(2011)003. arXiv: 1011.5911 [gr-qc].

[21] Don N. Page and C. D. Geilker. "Indirect Evidence for Quantum Gravity". In: *Phys. Rev. Lett.* 47 (1981), pp. 979–982. DOI: 10.1103/PhysRevLett.47.979.

[22] Daniel Carney, Philip C. E. Stamp, and Jacob M. Taylor. "Tabletop experiments for quantum gravity: a user's manual". In: *Class. Quant. Grav.* 36.3 (2019), p. 034001. DOI: 10.1088/1361-6382/aaf9ca. arXiv: 1807.11494 [quant-ph].

[23] Raúl Carballo-Rubio et al. "On the viability of regular black holes". In: *Journal of High Energy Physics* 2018.7 (July 2018). ISSN: 1029-8479. DOI: 10.1007/jhep07(2018)023. URL: http://dx.doi.org/10.1007/JHEP07(2018)023.

[24] *Approaches to Quantum Gravity: Toward a New Understanding of Space, Time and Matter*. Cambridge University Press, 2009.

[25] J. Polchinski. *String theory. Vol. 2: Superstring theory and beyond*. Cambridge Monographs on Mathematical Physics. Cambridge University Press, Dec. 2007. ISBN: 978-0-511-25228-0, 978-0-521-63304-8, 978-0-521-67228-3. DOI: 10.1017/CBO9780511618123.

[26] Abhay Ashtekar and Eugenio Bianchi. "A short review of loop quantum gravity". In: *Reports on Progress in Physics* 84.4 (Mar. 2021), p. 042001. ISSN: 1361-6633. DOI: 10.1088/1361-6633/abed91. URL: http://dx.doi.org/10.1088/1361-6633/abed91.

[27] Daniele Oriti. *Group Field Theory and Loop Quantum Gravity*. 2014. arXiv: 1408.7112 [gr-qc]. URL: https://arxiv.org/abs/1408.7112.

[28] Daniele Oriti. *Hydrodynamics on (mini)superspace, or a non-linear extension of quantum cosmology*. 2024. arXiv: 2403.10741 [gr-qc]. URL: https://arxiv.org/abs/2403.10741.

[29] R Loll. "Quantum gravity from causal dynamical triangulations: a review". In: *Classical and Quantum Gravity* 37.1 (Dec. 2019), p. 013002. ISSN: 1361-6382. DOI: 10.1088/1361-6382/ab57c7. URL: http://dx.doi.org/10.1088/1361-6382/ab57c7.

[30] Roberto Percacci. "Asymptotic Safety". In: (Sept. 2007), pp. 111–128. arXiv: 0709.3851 [hep-th].

[31] Alberto Salvio. "Quadratic Gravity". In: *Frontiers in Physics* 6 (Aug. 2018). ISSN: 2296-424X. DOI: 10.3389/fphy.2018.00077. URL: http://dx.doi.org/10.3389/fphy.2018.00077.

[32] Petr Horava. "Quantum Gravity at a Lifshitz Point". In: *Phys. Rev. D* 79 (2009), p. 084008. DOI: 10.1103/PhysRevD.79.084008. arXiv: 0901.3775 [hep-th].

[33] Stefano Liberati. "Tests of Lorentz invariance: a 2013 update". In: *Class. Quant. Grav.* 30 (2013), p. 133001. DOI: 10.1088/0264-9381/30/13/133001. arXiv: 1304.5795 [gr-qc].

[34] F. Girelli, S. Liberati, and L. Sindoni. "Planck-scale modified dispersion relations and Finsler geometry". In: *Physical Review D* 75.6 (Mar. 2007). ISSN: 1550-2368. DOI: 10.1103/physrevd.75.064015. URL: http://dx.doi.org/10.1103/PhysRevD.75.064015.

[35] Francesco Del Porro et al. "Time orientability and particle production from universal horizons". In: *Phys. Rev. D* 105.10 (2022), p. 104009. DOI: 10.1103/PhysRevD.105.104009. arXiv: 2201.03584 [gr-qc].

[36] F. Del Porro et al. "Gravitational tunneling in Lorentz violating gravity". In: *Phys. Rev. D* 106.6 (2022), p. 064055. DOI: 10.1103/PhysRevD.106.064055. arXiv: 2207.08848 [gr-qc].

[37] M. Schneider et al. "On the Resilience of Black Hole Evaporation: Gravitational Tunneling through Universal Horizons". In: *J. Phys. Conf. Ser.* 2531.1 (2023), p. 012013. DOI: 10.1088/1742-6596/2531/1/012013. arXiv: 2303.14235 [gr-qc].

[38] F. Del Porro et al. "Hawking radiation in Lorentz violating gravity: a tale of two horizons". In: *JHEP* 12 (2023), p. 094. DOI: 10.1007/JHEP12(2023)094. arXiv: 2310.01472 [gr-qc].

[39] F. Del Porro et al. "Rescuing the Unruh Effect in Lorentz Violating Gravity". In: (Dec. 2023). arXiv: 2312.03070 [gr-qc].

[40] Francesco Del Porro, Stefano Liberati, and Marc Schneider. "Tunneling method for Hawking quanta in analogue gravity". In: (June 2024). arXiv: 2406.14603 [gr-qc].

[41] Nicholas David Birrell and Paul Charles William Davies. "Quantum fields in curved space". In: (1984).

[42] Ted Jacobson. *Introduction to Quantum Fields in Curved Spacetime and the Hawking Effect*. 2003. DOI: 10.48550/ARXIV.GR-QC/0308048. URL: https://arxiv.org/abs/gr-qc/0308048.

[43] Eric Poisson. *A Relativist's Toolkit: The Mathematics of Black-Hole Mechanics*. Cambridge University Press, 2004.

[44] Maulik K. Parikh and Frank Wilczek. "Hawking radiation as tunneling". In: *Phys. Rev. Lett.* 85 (2000), pp. 5042–5045. DOI: 10.1103/PhysRevLett.85.5042. arXiv: hep-th/9907001.

[45] L Vanzo, G Acquaviva, and R Di Criscienzo. "Tunnelling methods and Hawking's radiation: achievements and prospects". In: *Classical and Quantum Gravity* 28.18 (2011), p. 183001.

[46] Cecilia Giavoni and Marc Schneider. "Quantum effects across dynamical horizons". In: *Class. Quant. Grav.* 37.21 (2020), p. 215020. DOI: 10.1088/1361-6382/abb576. arXiv: 2003.11095 [gr-qc].

[47] Kenichi Konishi and Giampiero Paffuti. In: *Quantum Mechanics: A New Introduction*. Oxford University Press, Mar. 2009. ISBN: 9780199560264. DOI: 10.1093/oso/9780199560264.003.0001. URL: https://doi.org/10.1093/oso/9780199560264.003.0001.

[48] José M. M. Senovilla and Ramón Torres. "Particle production from marginally trapped surfaces of general spacetimes". In: *Class. Quant. Grav.* 32.8 (2015). [Erratum: Class.Quant.Grav. 32, 189501 (2015)], p. 085004. DOI: 10.1088/0264-9381/32/8/085004. arXiv: 1409.6044 [gr-qc].

[49] James B Hartle and Stephen W Hawking. "Wave function of the universe". In: *Euclidean quantum gravity*. World Scientific, 1983, pp. 310–325.

[50] Gary W Gibbons and Stephen W Hawking. "Cosmological event horizons, thermodynamics, and particle creation". In: *Euclidean quantum gravity*. World Scientific, 1993, pp. 281–294.

[51] Ramit Dey et al. "Black hole quantum atmosphere for freely falling observers". In: *Phys. Lett. B* 797 (2019), p. 134828. DOI: 10.1016/j.physletb.2019.134828. arXiv: 1906.02958 [gr-qc].

[52] Benito A. Juárez-Aubry and Jorma Louko. "Quantum fields during black hole formation: How good an approximation is the Unruh state?" In: *JHEP* 05 (2018), p. 140. DOI: 10.1007/JHEP05(2018)140. arXiv: 1804.01228 [gr-qc].

[53] Ivan Agullo, Anthony J. Brady, and Dimitrios Kranas. "Event horizons are tunable factories of quantum entanglement". In: *Int. J. Mod. Phys. D* 31.14 (2022), p. 2242008. DOI: 10.1142/S0218271822420081. arXiv: 2209.09980 [gr-qc].

[54] G. W. Gibbons and S. W. Hawking. "Action Integrals and Partition Functions in Quantum Gravity". In: *Phys. Rev. D* 15 (1977), pp. 2752–2756. DOI: 10.1103/PhysRevD.15.2752.

[55] Alessio Baldazzi, Roberto Percacci, and Vedran Skrinjar. "Wicked metrics". In: *Class. Quant. Grav.* 36.10 (2019), p. 105008. DOI: 10.1088/1361-6382/ab187d. arXiv: 1811.03369 [gr-qc].

[56] S. A. Fulling and S. N. M. Ruijsenaars. "Temperature, periodicity and horizons". In: (Aug. 1987), pp. 135–176. DOI: 10.1016/0370-1573(87)90136-0.

[57] T. A. Jacobson. "Black hole radiation in the presence of a short distance cutoff". In: *Phys. Rev. D* 48 (1993), pp. 728–741. DOI: 10.1103/PhysRevD.48.728. eprint: hep-th/9303103.

[58] W. G. Unruh. "Sonic analog of black holes and the effects of high frequencies on black hole evaporation". In: *Phys. Rev. D* 51 (1995), pp. 2827–2838. DOI: 10.1103/PhysRevD.51.2827. arXiv: gr-qc/9409008.

[59] Carlos Barcelo, Stefano Liberati, and Matt Visser. "Analogue gravity". In: *Living Rev. Rel.* 8 (2005), p. 12. DOI: 10.12942/lrr-2005-12. arXiv: gr-qc/0505065.

[60] L. D. Landau and E. M. Lifshitz. *Fluid Mechanics, Second Edition: Volume 6 (Course of Theoretical Physics)*. 2nd ed. Course of theoretical physics / by L. D. Landau and E. M. Lifshitz, Vol. 6. Butterworth-Heinemann, Jan. 1987. ISBN: 0750627670. URL: http://www.worldcat.org/isbn/0750627670.

[61] P. K. Townsend. "Black holes: Lecture notes". In: (July 1997). arXiv: gr-qc/9707012.

[62] L. J. Garay et al. "Black holes in Bose-Einstein condensates". In: *Phys. Rev. Lett.* 85 (2000), pp. 4643–4647. DOI: 10.1103/PhysRevLett.85.4643. arXiv: gr-qc/0002015.

[63] L. J. Garay et al. "Sonic black holes in dilute Bose-Einstein condensates". In: *Phys. Rev. A* 63 (2001), p. 023611. DOI: 10.1103/PhysRevA.63.023611. arXiv: gr-qc/0005131.

[64] Franco Dalfovo et al. "Theory of Bose-Einstein condensation in trapped gases". In: *Rev. Mod. Phys.* 71 (1999), pp. 463–512. DOI: 10.1103/RevModPhys.71.463. arXiv: cond-mat/9806038.

[65] R. Brout et al. "Hawking radiation without transPlanckian frequencies". In: *Phys. Rev. D* 52 (1995), pp. 4559–4568. DOI: 10.1103/PhysRevD.52.4559. arXiv: hep-th/9506121.

[66] Steven Corley and Ted Jacobson. "Hawking spectrum and high frequency dispersion". In: *Phys. Rev. D* 54 (1996), pp. 1568–1586. DOI: 10.1103/PhysRevD.54.1568. arXiv: hep-th/9601073.

[67] Steven Corley. "Computing the spectrum of black hole radiation in the presence of high frequency dispersion: An Analytical approach". In: *Phys. Rev. D* 57 (1998), pp. 6280–6291. DOI: 10.1103/PhysRevD.57.6280. arXiv: hep-th/9710075.

[68] Yoshiaki Himemoto and Takahiro Tanaka. "A Generalization of the model of Hawking radiation with modified high frequency dispersion relation". In: *Phys. Rev. D* 61 (2000), p. 064004. DOI: 10.1103/PhysRevD.61.064004. arXiv: gr-qc/9904076.

[69] Hiromi Saida and Masa-aki Sakagami. "Black hole radiation with high frequency dispersion". In: *Phys. Rev. D* 61 (2000), p. 084023. DOI: 10.1103/PhysRevD.61.084023. arXiv: gr-qc/9905034.

[70] William G. Unruh and Ralf Schutzhold. "On the universality of the Hawking effect". In: *Phys. Rev. D* 71 (2005), p. 024028. DOI: 10.1103/PhysRevD.71.024028. arXiv: gr-qc/0408009.

[71] Jeff Steinhauer. "Observation of self-amplifying Hawking radiation in an analog black hole laser". In: *Nature Phys.* 10 (2014), p. 864. DOI: 10.1038/NPHYS3104. arXiv: 1409.6550 [cond-mat.quant-gas].

[72] Jeff Steinhauer. "Observation of quantum Hawking radiation and its entanglement in an analogue black hole". In: *Nature Phys.* 12 (2016), p. 959. DOI: 10.1038/nphys3863. arXiv: 1510.00621 [gr-qc].

[73] Juan Ramón Muñoz de Nova et al. "Observation of thermal Hawking radiation and its temperature in an analogue black hole". In: *Nature* 569.7758 (2019), pp. 688–691. DOI: 10.1038/s41586-019-1241-0. arXiv: 1809.00913 [gr-qc].

[74] L. P. Euvé et al. "Observation of noise correlated by the Hawking effect in a water tank". In: *Phys. Rev. Lett.* 117.12 (2016), p. 121301. DOI: 10.1103/PhysRevLett.117.121301. arXiv: 1511.08145 [physics.flu-dyn].

[75] Carla R. Almeida and Maxime J. Jacquet. "Analogue gravity and the Hawking effect: historical perspective and literature review". In: *Eur. Phys. J. H* 48.1 (2023), p. 15. DOI: 10.1140/epjh/s13129-023-00063-2. arXiv: 2212.08838 [physics.hist-ph].

[76] Antonin Coutant and Silke Weinfurtner. "The imprint of the analogue Hawking effect in subcritical flows". In: *Physical Review D* 94.6 (2016). ISSN: 2470-0029. DOI: 10.1103/physrevd.94.064026. URL: http://dx.doi.org/10.1103/PhysRevD.94.064026.

[77] Silke Weinfurtner et al. "Classical aspects of Hawking radiation verified in analogue gravity experiment". In: *Lect. Notes Phys.* 870 (2013). Ed. by Daniele Faccio et al., pp. 167–180. DOI: 10.1007/978-3-319-00266-8_8. arXiv: 1302.0375 [gr-qc].

[78] Antonin Coutant and Silke Weinfurtner. "Low-frequency analogue Hawking radiation: The Bogoliubov-de Gennes model". In: *Physical Review D* 97.2 (2018). ISSN: 2470-0029. DOI: 10.1103/physrevd.97.025006. URL: http://dx.doi.org/10.1103/PhysRevD.97.025006.

[79] S Finazzi and R Parentani. "On the robustness of acoustic black hole spectra". In: *Journal of Physics: Conference Series* 314 (Sept. 2011), p. 012030. ISSN: 1742-6596. DOI: 10.1088/1742-6596/314/1/012030. URL: http://dx.doi.org/10.1088/1742-6596/314/1/012030.

[80] M. Isoard and N. Pavloff. "Departing from thermality of analogue Hawking radiation in a Bose-Einstein condensate". In: *Phys. Rev. Lett.* 124.6 (2020), p. 060401. DOI: 10.1103/PhysRevLett.124.060401. arXiv: 1909.02509 [cond-mat.quant-gas].

[81] Carlos Barceló et al. "Causal structure of analogue spacetimes". In: *New Journal of Physics* 6 (Dec. 2004), 186–186. ISSN: 1367-2630. DOI: 10.1088/1367-2630/6/1/186. URL: http://dx.doi.org/10.1088/1367-2630/6/1/186.

[82] Ralf Schützhold and William G Unruh. "Origin of the particles in black hole evaporation". In: *Physical Review D* 78.4 (2008), p. 041504.

[83] Bethan Cropp et al. "Ray tracing Einstein-Æther black holes: Universal versus Killing horizons". In: *Physical Review D* 89.6 (Mar. 2014). ISSN: 1550-2368. DOI: 10.1103/physrevd.89.064061. URL: http://dx.doi.org/10.1103/PhysRevD.89.064061.

[84] IM Gelfand and GE Shilov. *Generalized Functions*. Vol. 1. Academic Press, 1964.

[85] Lars Hörmander. *The analysis of linear partial differential operators I: Distribution theory and Fourier analysis*. Springer, 2015.

[86] R. Schützhold and W. G. Unruh. "Hawking radiation with dispersion versus breakdown of the WKB approximation". In: *Physical Review D* 88.12 (2013). ISSN: 1550-2368. DOI: 10.1103/physrevd.88.124009. URL: http://dx.doi.org/10.1103/PhysRevD.88.124009.

[87] Saulo Albuquerque et al. "Inverse problem of analog gravity systems". In: *Physical Review D* 108.12 (2023), p. 124053.

[88] Saulo Albuquerque et al. "Inverse problem of analog gravity systems II: rotation and energy-dependent boundary conditions". In: (2024). arXiv: 2406.16670.

[89] Silke Weinfurtner et al. "Measurement of stimulated Hawking emission in an analogue system". In: *Phys. Rev. Lett.* 106 (2011), p. 021302. DOI: 10.1103/PhysRevLett.106.021302. arXiv: 1008.1911 [gr-qc].

[90] Léo-Paul Euvé et al. "Wave blocking and partial transmission in subcritical flows over an obstacle". In: *Phys. Rev. D* 91.2 (2015), p. 024020. DOI: 10.1103/PhysRevD.91.024020. arXiv: 1409.3830 [gr-qc].

[91] Florent Michel and Renaud Parentani. "Probing the thermal character of analogue Hawking radiation for shallow water waves?" In: *Phys. Rev. D* 90 (4 2014), p. 044033. DOI: 10.1103/PhysRevD.90.044033. URL: https://link.aps.org/doi/10.1103/PhysRevD.90.044033.

[92] Florent Michel and Renaud Parentani. "Mode mixing in sub- and transcritical flows over an obstacle: When should Hawking's predictions be recovered?" In: *14th Marcel Grossmann Meeting on Recent Developments in Theoretical and Experimental General Relativity, Astrophysics, and Relativistic Field Theories*. Vol. 2. 2017, pp. 1709–1717. DOI: 10.1142/9789813226609_0173. arXiv: 1508.02044 [gr-qc].

[93] W. G. Unruh and R. Schützhold. "On slow light as a black hole analogue". In: *Physical Review D* 68.2 (2003). ISSN: 1089-4918. DOI: 10.1103/physrevd.68.024008. URL: http://dx.doi.org/10.1103/PhysRevD.68.024008.

[94] Mário Novello, Matt Visser, and Grigori Volovik. *Artificial Black Holes*. WORLD SCIENTIFIC, 2002. DOI: 10.1142/4861. eprint: https://www.worldscientific.com/doi/pdf/10.1142/4861. URL: https://www.worldscientific.com/doi/abs/10.1142/4861.

[95] Steven B. Giddings. "Hawking radiation, the Stefan–Boltzmann law, and unitarization". In: *Physics Letters B* 754 (Mar. 2016), 39–42. ISSN: 0370-2693. DOI: 10.1016/j.physletb.2015.12.076. URL: http://dx.doi.org/10.1016/j.physletb.2015.12.076.

[96] Ramit Dey, Stefano Liberati, and Daniele Pranzetti. "The black hole quantum atmosphere". In: *Physics Letters B* 774 (Nov. 2017), 308–316. ISSN: 0370-2693. DOI: 10.1016/j.physletb.2017.09.076. URL: http://dx.doi.org/10.1016/j.physletb.2017.09.076.

[97] Kévin Falque et al. "Polariton Fluids as Quantum Field Theory Simulators on Tailored Curved Spacetimes". In: (Nov. 2023). arXiv: 2311.01392 [cond-mat].

[98] Ted Jacobson and David Mattingly. "Gravity with a dynamical preferred frame". In: *Phys. Rev. D* 64 (2001), p. 024028. DOI: 10.1103/PhysRevD.64.024028. arXiv: gr-qc/0007031.

[99] K.S. Stelle. "Renormalization of Higher Derivative Quantum Gravity". In: *Phys. Rev. D* 16 (1977), pp. 953–969. DOI: 10.1103/PhysRevD.16.953.

[100] E.S. Fradkin and Arkady A. Tseytlin. "Renormalizable asymptotically free quantum theory of gravity". In: *Nucl. Phys. B* 201 (1982), pp. 469–491. DOI: 10.1016/0550-3213(82)90444-8.

[101] Richard P. Woodard. "Ostrogradsky's theorem on Hamiltonian instability". In: *Scholarpedia* 10.8 (2015), p. 32243. DOI: 10.4249/scholarpedia.32243. arXiv: 1506.02210 [hep-th].

[102] Damiano Anselmi and Marco Piva. "The ultraviolet behavior of quantum gravity". In: *Journal of High Energy Physics* 2018.5 (2018). ISSN: 1029-8479. DOI: 10.1007/jhep05(2018)027. URL: http://dx.doi.org/10.1007/JHEP05(2018)027.

[103] Damiano Anselmi and Marco Piva. "A new formulation of Lee-Wick quantum field theory". In: *Journal of High Energy Physics* 2017.6 (2017). ISSN: 1029-8479. DOI: 10.1007/jhep06(2017)066. URL: http://dx.doi.org/10.1007/JHEP06(2017)066.

[104] Diego Buccio and Roberto Percacci. "Renormalization group flows between Gaussian fixed points". In: *JHEP* 10 (2022), p. 113. DOI: 10.1007/JHEP10(2022)113. arXiv: 2207.10596 [hep-th].

[105] Damiano Anselmi and Milenko Halat. "Renormalization of Lorentz violating theories". In: *Phys. Rev. D* 76 (2007), p. 125011. DOI: 10.1103/PhysRevD.76.125011. arXiv: 0707.2480 [hep-th].

[106] Éric Gourgoulhon. "3+1 Decomposition of Einstein Equation". In: *3+1 Formalism in General Relativity: Bases of Numerical Relativity*. Berlin, Heidelberg: Springer Berlin Heidelberg, 2012, pp. 73–99. ISBN: 978-3-642-24525-1. DOI: 10.1007/978-3-642-24525-1_5. URL: https://doi.org/10.1007/978-3-642-24525-1_5.

[107] M. Herrero-Valea. "The status of Hořava gravity". In: *Eur. Phys. J. Plus* 138.11 (2023), p. 968. DOI: 10.1140/epjp/s13360-023-04593-y. arXiv: 2307.13039 [gr-qc].

[108] Nicola Franchini, Mario Herrero-Valea, and Enrico Barausse. "Relation between general relativity and a class of Hořava gravity theories". In: *Phys. Rev. D* 103.8 (2021), p. 084012. DOI: 10.1103/PhysRevD.103.084012. arXiv: 2103.00929 [gr-qc].

[109] Oscar Ramos and Enrico Barausse. "Constraints on Hořava gravity from binary black hole observations". In: *Physical Review D* 99.2 (Jan. 2019). ISSN: 2470-0029. DOI: 10.1103/physrevd.99.024034. URL: http://dx.doi.org/10.1103/PhysRevD.99.024034.

[110] Ted Jacobson. "Undoing the twist: The Hořava limit of Einstein-aether theory". In: *Physical Review D* 89.8 (Apr. 2014). ISSN: 1550-2368. DOI: 10.1103/physrevd.89.081501. URL: http://dx.doi.org/10.1103/PhysRevD.89.081501.

[111] Enrico Barausse and Thomas P. Sotiriou. "Slowly rotating black holes in Hořava-Lifshitz gravity". In: *Physical Review D* 87.8 (Apr. 2013). ISSN: 1550-2368. DOI: 10.1103/physrevd.87.087504. URL: http://dx.doi.org/10.1103/PhysRevD.87.087504.

[112] Enrico Barausse, Ted Jacobson, and Thomas P. Sotiriou. "Black holes in Einstein-aether and Hořava-Lifshitz gravity". In: *Physical Review D* 83.12 (June 2011). ISSN: 1550-2368. DOI: 10.1103/physrevd.83.124043. URL: http://dx.doi.org/10.1103/PhysRevD.83.124043.

[113] Ted Jacobson. "Initial value constraints with tensor matter". In: *Classical and Quantum Gravity* 28.24 (Dec. 2011), p. 245011. ISSN: 1361-6382. DOI: 10.1088/0264-9381/28/24/245011. URL: http://dx.doi.org/10.1088/0264-9381/28/24/245011.

[114] Jacob Oost, Shinji Mukohyama, and Anzhong Wang. "Constraints on Einstein-aether theory after GW170817". In: *Phys. Rev. D* 97.12 (2018), p. 124023. DOI: 10.1103/PhysRevD.97.124023. arXiv: 1802.04303 [gr-qc].

[115] Christopher Eling and Ted Jacobson. "Black Holes in Einstein-Aether Theory". In: *Class. Quant. Grav.* 23 (2006). [Erratum: Class.Quant.Grav. 27, 049802 (2010)], pp. 5643–5660. DOI: 10.1088/0264-9381/23/18/009. arXiv: gr-qc/0604088.

[116] Diego Blas, Oriol Pujolas, and Sergey Sibiryakov. "Models of non-relativistic quantum gravity: The Good, the bad and the healthy". In: *JHEP* 04 (2011), p. 018. DOI: 10.1007/JHEP04(2011)018. arXiv: 1007.3503 [hep-th].

[117] Jishnu Bhattacharyya, Mattia Colombo, and Thomas P. Sotiriou. "Causality and black holes in spacetimes with a preferred foliation". In: *Class. Quant. Grav.* 33.23 (2016), p. 235003. DOI: 10.1088/0264-9381/33/23/235003. arXiv: 1509.01558 [gr-qc].

[118] Nicola Franchini, Mehdi Saravani, and Thomas P. Sotiriou. "Black hole horizons at the extremal limit in Lorentz-violating gravity". In: *Phys. Rev. D* 96.10 (2017), p. 104044. DOI: 10.1103/PhysRevD.96.104044. arXiv: 1707.09283 [gr-qc].

[119] Per Berglund, Jishnu Bhattacharyya, and David Mattingly. "Mechanics of universal horizons". In: *Physical Review D* 85.12 (June 2012). ISSN: 1550-2368. DOI: 10.1103/physrevd.85.124019. URL: http://dx.doi.org/10.1103/PhysRevD.85.124019.

[120] Raúl Carballo-Rubio et al. "Geodesically complete black holes in Lorentz-violating gravity". In: *Journal of High Energy Physics* 2022.2 (2022). DOI: 10.1007/jhep02(2022)122. URL: https://doi.org/10.1007%2Fjhep02%282022%29122.

[121] Florent Michel and Renaud Parentani. "Black hole radiation in the presence of a universal horizon". In: *Physical Review D* 91.12 (June 2015). ISSN: 1550-2368. DOI: 10.1103/physrevd.91.124049. URL: http://dx.doi.org/10.1103/PhysRevD.91.124049.

[122] Bethan Cropp, Stefano Liberati, and Matt Visser. "Surface gravities for non-Killing horizons". In: *Class. Quant. Grav.* 30 (2013), p. 125001. DOI: 10.1088/0264-9381/30/12/125001. arXiv: 1302.2383 [gr-qc].

[123] Bethan Cropp, Stefano Liberati, and Rodrigo Turcati. "Analogue black holes in relativistic BECs: Mimicking Killing and universal horizons". In: *Phys. Rev. D* 94.6 (2016), p. 063003. DOI: 10.1103/PhysRevD.94.063003. arXiv: 1606.01044 [gr-qc].

[124] Alexander Adam et al. "Rotating black holes in Einstein-aether theory". In: *Classical and Quantum Gravity* 39.12 (May 2022), p. 125001. ISSN: 1361-6382. DOI: 10.1088/1361-6382/ac5053. URL: http://dx.doi.org/10.1088/1361-6382/ac5053.

[125] Edgardo Franzin, Stefano Liberati, and Jacopo Mazza. "Kerr black hole in Einstein–Æther gravity". In: *Physical Review D* 109.8 (Apr. 2024), p. 084028. ISSN: 2470-0010, 2470-0029. DOI: 10.1103/PhysRevD.109.084028. arXiv: 2312.06891.

[126] Chikun Ding and Changqing Liu. "Dispersion relation and surface gravity of universal horizons". In: *Sci. China Phys. Mech. Astron.* 60.5 (2017), p. 050411. DOI: 10.1007/s11433-017-9012-8. arXiv: 1611.03153 [gr-qc].

[127] Mario Herrero-Valea, Stefano Liberati, and Raquel Santos-Garcia. "Hawking Radiation from Universal Horizons". In: *JHEP* 04 (2021), p. 255. DOI: 10.1007/JHEP04(2021)255. arXiv: 2101.00028 [gr-qc].

[128] S. L. Dubovsky and S. M. Sibiryakov. "Spontaneous breaking of Lorentz invariance, black holes and perpetuum mobile of the 2nd kind". In: *Phys. Lett. B* 638 (2006), pp. 509–514. DOI: 10.1016/j.physletb.2006.05.074. arXiv: hep-th/0603158.

[129] Christopher Eling et al. "Lorentz violation and perpetual motion". In: *Phys. Rev. D* 75 (2007), p. 101502. DOI: 10.1103/PhysRevD.75.101502. arXiv: hep-th/0702124.

[130] Ted Jacobson and Aron C. Wall. "Black Hole Thermodynamics and Lorentz Symmetry". In: *Found. Phys.* 40 (2010), pp. 1076–1080. DOI: 10.1007/s10701-010-9423-5. arXiv: 0804.2720 [hep-th].

[131] Robert Benkel et al. "Dynamical obstruction to perpetual motion from Lorentz-violating black holes". In: *Physical Review D* 98.2 (July 2018). ISSN: 2470-0029. DOI: 10.1103/physrevd.98.024034. URL: http://dx.doi.org/10.1103/PhysRevD.98.024034.

[132] Matt Visser. "Lorentz symmetry breaking as a quantum field theory regulator". In: *Physical Review D* 80.2 (July 2009). ISSN: 1550-2368. DOI: 10.1103/physrevd.80.025011. URL: http://dx.doi.org/10.1103/PhysRevD.80.025011.

[133] R. Fox, C. G. Kuper, and S. G. Lipson. "Faster-than-light group velocities and causality violation". In: *Proc. Roy. Soc. Lond. A* 316 (1970), pp. 515–524. DOI: 10.1098/rspa.1970.0093.

[134] Raghavan Narasimhan and Yves Nievergelt. *Complex Analysis in One Variable*. Jan. 2001. ISBN: 978-1-4612-6647-1. DOI: 10.1007/978-1-4612-0175-5.

[135] Bethan Cropp. "Strange Horizons: Understanding Causal Barriers Beyond General Relativity". Other thesis. Nov. 2016. arXiv: 1611.00208 [gr-qc].

[136] Brandon Carter. "Global Structure of the Kerr Family of Gravitational Fields". In: *Phys. Rev.* 174 (5 1968), pp. 1559–1571. DOI: 10.1103/PhysRev.174.1559. URL: https://link.aps.org/doi/10.1103/PhysRev.174.1559.

[137] Costantino Pacilio and Stefano Liberati. "First law of black holes with a universal horizon". In: *Phys. Rev. D* 96.10 (2017), p. 104060. DOI: 10.1103/PhysRevD.96.104060. arXiv: 1709.05802 [gr-qc].

[138] Costantino Pacilio and Stefano Liberati. "Improved derivation of the Smarr formula for Lorentz-breaking gravity". In: *Phys. Rev. D* 95.12 (2017), p. 124010. DOI: 10.1103/PhysRevD.95.124010. arXiv: 1701.04992 [gr-qc].

[139] Luis C. Barbado, Carlos Barcelo, and Luis J. Garay. "Hawking radiation as perceived by different observers". In: *AIP Conf. Proc.* 1458.1 (2012). Ed. by Jose Beltran Jimenez et al., pp. 363–366. DOI: 10.1063/1.4734435. arXiv: 1203.5407 [gr-qc].

[140] Viqar Husain and Jorma Louko. "Low Energy Lorentz Violation from Modified Dispersion at High Energies". In: *Phys. Rev. Lett.* 116 (6 2016), p. 061301. DOI: 10.1103/PhysRevLett.116.061301. URL: https://link.aps.org/doi/10.1103/PhysRevLett.116.061301.

[141] Reza Rashidi et al. "Unruh's detector in the presence of Lorentz symmetry breaking". In: *Astrophysics and Space Science* 310 (Aug. 2007), pp. 333–337. DOI: 10.1007/s10509-007-9554-0.

[142] David Campo and Nathaniel Obadia. "Why does the Unruh effect rely on Lorentz invariance, while Hawking radiation does not?" In: (2010). DOI: 10.48550/ARXIV.1003.0112. URL: https://arxiv.org/abs/1003.0112.

[143] Ted Jacobson. "Black holes and Hawking radiation in spacetime and its analogues". In: *Lect. Notes Phys.* 870 (2013). Ed. by Daniele Faccio et al., pp. 1–29. DOI: 10.1007/978-3-319-00266-8_1. arXiv: 1212.6821 [gr-qc].

[144] Golam Mortuza Hossain and Gopal Sardar. "Violation of the Kubo-Martin-Schwinger Condition along a Rindler Trajectory in Polymer Quantization". In: *Phys. Rev. D* 92.2 (2015), p. 024018. DOI: 10.1103/PhysRevD.92.024018. arXiv: 1504.07856 [gr-qc].

[145] Luís C. B. Crispino, Atsushi Higuchi, and George E. A. Matsas. "The Unruh effect and its applications". In: *Reviews of Modern Physics* 80.3 (2008), pp. 787–838. DOI: 10.1103/revmodphys.80.787. URL: https://doi.org/10.1103%2Frevmodphys.80.787.

[146] Karl-Peter Marzlin. "The physical meaning of Fermi coordinates". In: *General Relativity and Gravitation* 26.6 (June 1994), 619–636. ISSN: 1572-9532. DOI: 10.1007/bf02108003. URL: http://dx.doi.org/10.1007/BF02108003.

[147] Stefano Finazzi and Renaud Parentani. "Hawking radiation in dispersive theories, the two regimes". In: *Phys. Rev. D* 85 (2012), p. 124027. DOI: 10.1103/PhysRevD.85.124027. arXiv: 1202.6015 [gr-qc].

[148] William G Unruh and Robert M Wald. "What happens when an accelerating observer detects a Rindler particle". In: *Physical Review D* 29.6 (1984), p. 1047.

[149] Bruno Arderucio Costa, Yuri Bonder, and Benito A Juárez-Aubry. "Are inertial vacua equivalent in Lorentz-violating theories? Does it matter?" In: *Annals of Physics* 453 (2023), p. 169303.

[150] Izrail Solomonovich Gradshteyn and Iosif Moiseevich Ryzhik. *Table of integrals, series, and products*. Academic press, 2014.

[151] F. Bowman. *Introduction to Bessel Functions*. Dover Books on Mathematics. Dover Publications, 1958. ISBN: 9780486604626. URL: https://books.google.it/books?id=_k6iJN5QabUC.

[152] Erasmo M. Ferreira and Javier Sesma. "Zeros of the Macdonald function of complex order". In: *Journal of Computational and Applied Mathematics* 211.2 (2008), pp. 223–231. DOI: 10.1016/j.cam.2006.11.014. URL: https://doi.org/10.1016%2Fj.cam.2006.11.014.

[153] Christopher Eling, Raf Guedens, and Ted Jacobson. "Non-equilibrium thermodynamics of spacetime". In: *Phys. Rev. Lett.* 96 (2006), p. 121301. DOI: 10.1103/PhysRevLett.96.121301. arXiv: gr-qc/0602001.

[154] Goffredo Chirco, Christopher Eling, and Stefano Liberati. "Reversible and Irreversible Spacetime Thermodynamics for General Brans-Dicke Theories". In: *Phys. Rev. D* 83 (2011), p. 024032. DOI: 10.1103/PhysRevD.83.024032. arXiv: 1011.1405 [gr-qc].

[155] Isaac Carruthers and Ted Jacobson. "Cosmic alignment of the aether". In: *Physical Review D* 83.2 (Jan. 2011). ISSN: 1550-2368. DOI: 10.1103/physrevd.83.024034. URL: http://dx.doi.org/10.1103/PhysRevD.83.024034.

[156] A. Retzker et al. "Methods for Detecting Acceleration Radiation in a Bose-Einstein Condensate". In: *Physical Review Letters* 101.11 (Sept. 2008). ISSN: 1079-7114. DOI: 10.1103/physrevlett.101.110402. URL: http://dx.doi.org/10.1103/PhysRevLett.101.110402.

[157] Steffen Biermann et al. "Unruh and analogue Unruh temperatures for circular motion in 3 + 1 and 2 + 1 dimensions". In: *Phys. Rev. D* 102 (8 2020), p. 085006. DOI: 10.1103/PhysRevD.102.085006. URL: https://link.aps.org/doi/10.1103/PhysRevD.102.085006.

[158] John F. Donoghue. "General relativity as an effective field theory: The leading quantum corrections". In: *Physical Review D* 50.6 (Sept. 1994), 3874–3888. ISSN: 0556-2821. DOI: 10.1103/physrevd.50.3874. URL: http://dx.doi.org/10.1103/PhysRevD.50.3874.

[159] Damiano Anselmi. *Renormalization*. Independently published, May 2019. ISBN: 978-1-0990-5067-1.

[160] Michael E. Peskin and Daniel V. Schroeder. *An Introduction to quantum field theory*. Reading, USA: Addison-Wesley, 1995. ISBN: 978-0-201-50397-5, 978-0-429-50355-9, 978-0-429-49417-8. DOI: 10.1201/9780429503559.

[161] Cliff P. Burgess. "Quantum Gravity in Everyday Life: General Relativity as an Effective Field Theory". In: *Living Reviews in Relativity* 7.1 (Apr. 2004). ISSN: 1433-8351. DOI: 10.12942/lrr-2004-5. URL: http://dx.doi.org/10.12942/lrr-2004-5.

[162] Andrei O. Barvinsky et al. "Heat kernel methods for Lifshitz theories". In: *JHEP* 06 (2017), p. 063. DOI: 10.1007/JHEP06(2017)063. arXiv: 1703.04747 [hep-th].

[163] D. Blas, O. Pujolàs, and S. Sibiryakov. "Consistent Extension of Hořava Gravity". In: *Physical Review Letters* 104.18 (May 2010). ISSN: 1079-7114. DOI: 10.1103/physrevlett.104.181302. URL: http://dx.doi.org/10.1103/PhysRevLett.104.181302.

[164] Thomas P Sotiriou, Matt Visser, and Silke Weinfurtner. "Quantum gravity without Lorentz invariance". In: *Journal of High Energy Physics* 2009.10 (Oct. 2009), 033–033. ISSN: 1029-8479. DOI: 10.1088/1126-6708/2009/10/033. URL: http://dx.doi.org/10.1088/1126-6708/2009/10/033.

[165] Andrei O. Barvinsky. *Hořava models as palladium of unitarity and renormalizability in quantum gravity*. 2023. arXiv: 2301.13580 [hep-th]. URL: https://arxiv.org/abs/2301.13580.

[166] Andrei O. Barvinsky et al. “Renormalization of Hořava gravity”. In: *Physical Review D* 93.6 (Mar. 2016). ISSN: 2470-0029. DOI: 10.1103/physrevd.93.064022. URL: http://dx.doi.org/10.1103/PhysRevD.93.064022.

[167] Andrei O. Barvinsky et al. “Hořava Gravity is Asymptotically Free in (2+1) Dimensions”. In: *Physical Review Letters* 119.21 (Nov. 2017). ISSN: 1079-7114. DOI: 10.1103/physrevlett.119.211301. URL: http://dx.doi.org/10.1103/PhysRevLett.119.211301.

[168] A. Wipf. “Hamilton’s formalism for systems with constraints”. In: *Canonical Gravity: From Classical to Quantum*. Springer Berlin Heidelberg, 1993, 22–58. ISBN: 9783540486657. DOI: 10.1007/3-540-58339-4_14. URL: http://dx.doi.org/10.1007/3-540-58339-4_14.

[169] E. S. Fradkin and G. A. Vilkovisky. “QUANTIZATION OF RELATIVISTIC SYSTEMS WITH CONSTRAINTS”. In: *Phys. Lett. B* 55 (1975), pp. 224–226. DOI: 10.1016/0370-2693(75)90448-7.

[170] I.A. Batalin and G.A. Vilkovisky. “Relativistic S-matrix of dynamical systems with boson and fermion constraints”. In: *Physics Letters B* 69.3 (1977), pp. 309–312. ISSN: 0370-2693. DOI: https://doi.org/10.1016/0370-2693(77)90553-6. URL: https://www.sciencedirect.com/science/article/pii/0370269377905536.

[171] E.S. Fradkin and T.E. Fradkina. “Quantization of relativistic systems with boson and fermion first- and second-class constraints”. In: *Physics Letters B* 72.3 (1978), pp. 343–348. ISSN: 0370-2693. DOI: https://doi.org/10.1016/0370-2693(78)90135-1. URL: https://www.sciencedirect.com/science/article/pii/0370269378901351.

[172] Jorge Bellorín and Byron Droguett. “BFV quantization of the nonprojectable (2+1)-dimensional Hořava theory”. In: *Physical Review D* 103.6 (Mar. 2021). ISSN: 2470-0029. DOI: 10.1103/physrevd.103.064039. URL: http://dx.doi.org/10.1103/PhysRevD.103.064039.

[173] Jorge Bellorín, Claudio Bórquez, and Byron Droguett. “Cancellation of divergences in the nonprojectable Hořava theory”. In: *Physical Review D* 106.4 (2022). DOI: 10.1103/physrevd.106.044055. URL: https://doi.org/10.1103%2Fphysrevd.106.044055.

[174] William Donnelly and Ted Jacobson. “Hamiltonian structure of Hořava gravity”. In: *Physical Review D* 84.10 (Nov. 2011). ISSN: 1550-2368. DOI: 10.1103/physrevd.84.104019. URL: http://dx.doi.org/10.1103/PhysRevD.84.104019.

[175] Jorge Bellorin, Claudio Borquez, and Byron Droguett. “Effective action of the Hořava theory: Cancellation of divergences”. In: *Phys. Rev. D* 109.8 (2024), p. 084007. DOI: 10.1103/PhysRevD.109.084007. arXiv: 2312.16327 [hep-th].

[176] Manuel Bronstein et al. “Algebraic properties of the Lambert W function from a result of Rosenlicht and of Liouville”. In: *Integral Transforms and Special Functions - INTEGRAL TRANSFORM SPEC FUNCT* 19 (Oct. 2008), pp. 709–712. DOI: 10.1080/10652460802332342.

[177] D. W. Sciama, P. Candelas, and D. Deutsch. “Quantum Field Theory, Horizons and Thermodynamics”. In: *Adv. Phys.* 30 (1981), pp. 327–366. DOI: 10.1080/00018738100101457.